SYNTHESIS AND CHARACTERIZATION OF POLYELECTROLYTES AND AQUEOUS LATICES

By

XIAO YU WU

A thesis

Submitted to the School of Graduate Studies

in Partial Fulfilment of Requirements

for the Degree

Doctor of Philosophy

McMaster University

SYNTHESIS AND CHARACTERIZATION OF POLYELECTROLYTES AND AQUEOUS LATICES

DOCTOR OF PHILOSOPHY (1993)

McMASTER UNIVERSITY

(Chemical Engineering)

Hamilton, Ontario, Canada

TITLE:	Synthesis and Characterization of Polyelectrolytes and Aqueous Latices
AUTHOR:	Xiao Yu Wu, M. Eng. & Sci. (East China University of Chemical Technology, Shanghai, China)
SUPERVISORS:	Professors R.H. Pelton, A.E. Hamielec, and D.R. Woods
NUMBER OF PAGES:	xxiii, 253

ABSTRACT

Methods for molecular weight characterization of polyelectrolytes, poly(acrylamide-co-sodium acrylate) by viscometry and gel permeation chromatography have been developed based on the use of fractionated polyacrylamide with known average molecular weights. A set of Mark-Houwink equations for the copolymer with various acrylate content has been established. With the viscosity measurements, these equations can be used to calculate the molecular weights of the copolymer with known composition, and to estimate the acrylate content when the weight average molecular weight of the polymer is known. The universal calibration method has been proven valid for poly(acrylamide-co-sodium acrylate) using nonionic polyacrylamide standards. The correlation of elution volume shift with the content of ionic groups has been found, from which the molecular weight of the copolymer can be estimated by gel permeation chromatography.

Heterogeneous free-radical polymerization of N-isopropylacrylamide (NIPAM) and NIPAM with N,N'-methylene bisacrylamide (BAM) has been conducted in aqueous media in the presence of low levels of sodium dodecyl sulfate (SDS). The influence of temperature, BAM level, SDS level, pH and ionic strength on the polymerization rate, particle size and size distribution, and particle concentration has been investigated. Studies on the formation mechanism of latex particles of poly(NIPAM) and poly(NIPAM/BAM) have been carried out by measuring the kinetics of polymerization and the micro-structure of the particles. A mechanism of homogeneous nucleation (dispersant-limited agglomeration) and dispersion polymerization has been proposed.

The microstructure of the latex particles has been studied from the swelling extent of the particles at various conversion. It is found that the particles have lowest swelling at early stage and have higher swelling at later stage. This has been interpreted as that the cross-linking density changes along the radius of the particles. In addition to the heterogeneity within the particles, the density distribution among the particles has been observed from the comparison of the particle size distribution by dynamic light scattering and that by disk centrifuge.

The interaction of NIPAM polymers with SDS has been investigated by conductometry and turbidimetry. It has been found that the critical micelle concentration (CMC) of SDS increases with the concentration of NIPAM polymers, and that the cloud point of aqueous solutions of NIPAM polymers is elevated in the presence of SDS.

ACKNOWLEDGEMENTS

I wish to express my sincerest appreciation to the group of my supervisors: Professors R.H. Pelton, A.E. Hamielec, and D.R. Woods, for their constant advise, criticism, and encouragement throughout the course of this thesis.

I also wish to thank the following people for their contributions to this thesis:

A member of my supervisory committee: Professor R. Epand

The members of the water-soluble polymer group: Wolfgang Baade, Vlado Hruska, Tony Neppel, and Hidetaka Tobita.

Dr. David Hunkeler for his cooperation on the project of characterization of polyelectrolytes, and especially for his help and friendship which have been so important to a foreign student.

Drs. Theodora Kourti, Paul Gossen, and Hassan Mousa for their technical assistance in the characterization of poly(NIPAM)/poly(NIPAM/BAM) latex particles, and for their friendship.

Wayne McPhee for his sharing his knowledge and information about the preparation of poly(NIPAM)/poly(NIPAM/BAM) latices, and for letting me use some of his samples for the analysis of SDS effects.

Dr. K.C. Tam for his cooperation on studies of rheological properties of NIPAM polymers and their interaction with SDS, and for his friendship.

Douglas Keller for his help in many things. His broad knowledge about instruments, suppliers, analytical methods, etc., has been and will continue to be a precious resource.

Lisa Morine for her careful operation of GPC measurements.

Dean Anderson for his assistance in the preliminary experiments of rheological properties of poly(NIPAM/BAM) latices, and for his friendship.

My colleagues in MIPPT and Department of Chemical Engineering: Paul Gloor, Stienna Thomas, Mary Ann Barban, Kris Kostanski, Henryk Zacharewicz, Bill Warriner, Gordon Slater, and Justyna Derkach. Their assistance and friendship have been always available when needed.

Funding for this research is from grants from National Science and Engineering Research Council.

Finally, a special thanks to my family for their understanding and support through the duration of this study.

PUBLICATIONS BASED ON THIS RESEARCH

In refereed journals:

1. X.Y.Wu, D. Hunkeler, A.E. Hamielec, R.H. Pelton and D.R. Woods, "Molecular Weight characterization of Poly(acrylamide-co-sodium acrylate) I. Viscometry, J. Appl. Polym. Sci., **42**, 2081-2093 (1991)

2. D. Hunkeler, X.Y. Wu and A.E. Hamielec, "Molecular Weight Characterization of Poly(acrylamide-co-sodium acrylate) II. Light Scattering, J. Appl. Polym. Sci., **46**, 649-657 (1992)

3. K.C. Tam, X.Y. Wu and R.H. Pelton, "Viscometry - A useful Tool for Studying Conformational Changes of Poly(N-isopropylacrylamide) in Solutions", Polymer Communications, **33**(2), 436-438 (1992)

4. X.Y. WU, R.H. Pelton, K.C.Tam, D.R. Woods, and A.E. Hamielec, "Poly(N-isopropylacrylamide) 1: Interaction with sodium dodecyl sulfate measured by conductivity", J. Polym. Sci., in press

5. K.C. Tam, X.Y. Wu, and R.H. Pelton, The Preparation and Characterization Poly(N-isopropylacrylamide) Latex", J. Polym. Sci., in press

Book contribution:

6. D. Hunkeler, X.Y. Wu and A.E. Hamielec, "Characterization of Polyelectrolytes", in Polyelectrolyte Gels, ACS Symposium series **480**, 53-79 (1992)

Published conference proceedings:

7. X.Y. Wu, D. Hunkeler, A.E. Hamielec and R.H. Pelton, "Molecular Weight Characterization of Polyelectrolytes", Polymeric Materials: Science and Engineering, 58, 792-795 (1988)

Papers submitted for publication

8. X.Y. Wu, R.H. Pelton, A.E. Hamielec, D.R. Woods, and W. McPhee, "The Kinetics of Poly(N-isopropylacrylamide) Micrgel Latex Formation", Colloid and Polym. Sci., submitted, Oct. 1992

9. X.Y. Wu, D. Hunkeler, A.E. Hamielec, R.H. Pelton, and D.R. Woods, "Molecular Weight Characterization of Poly(acrylamide-co-sodium acrylate) III. Size Exclusion Chromatography", J. Appl. Polym. Sci., to be submitted, 1992

10. R.H. Pelton, X.Y. Wu, W. McPhee, and K.C. Tam, "The Preparation and Characterization of PolyNIPAM Latexes", in "Colloid Stability", Academic Press, submitted, June 1992

TABLE OF CONTENTS

LIST OF FIGURES

PART A

Page

Page

Page

Appendix

LIST OF TABLES

PART A

PART B

Appendix

PART A

MOLECULAR WEIGHT CHARACTERIZATION OF POLY(ACRYLAMIDE-CO-SODIUM ACRYLATE)

CHAPTER 1 INTRODUCTION TO PART A

MOLECULAR WEIGHT CHARACTERIZATION OF POLY(ACRYLAMIDE-CO-SODIUM ACRYLATE)

Polyelectrolytes are the water-soluble polymers with charged groups. They have found many applications including water treatment, enhanced oil recovery, as retention aids of pulp and filler in papermaking, in electrical conduction, and for controlled drug release. One important issue in the area of polyelectrolytes is the difficulty in determining accurately the molecular weight. The presence of charged groups cause the hydrodynamic volume of the polymer molecules to vary significantly with the conditions, such as, the salt concentration, polymer concentration and the charge density. The molecular weight of polyelectrolytes is a crucial piece of knowledge for polymers since the molecular weight affects the viscosity of the solution, the flocculation and retention capability and the drug release rate. Therefore, it is important to characterize the polyelectrolyte carefully using valid analytical methods.

Part A of this thesis addresses this problem for one particular polyelectrolyte - poly(acrylamide-co-sodium acrylate).

Over the past ten years, a new polymer, poly(N-isopropylacrylamide), has appeared with exciting new properties and applications, including the enzyme immobilization, controlled release of catalyst, and drug delivery. To date, all the knowledge about this revolutionary polymer has focused on large scale "gel" behaviour (as opposed to the increasingly important submicron behaviour of particles) and on the bulk properties (as opposed to learning how to tailor - make this important polymer). This thesis, in Part B, provides insight as to the reaction mechanisms and behaviour of nanoparticles of poly(N-isopropylacrylamide).

This work develops a valid methodology for the molecular weight characterization of poly(acrylamide-co-sodium acrylate). In order to minimize the heterogeneity in charge density and molecular weight, a series of hydrolysed polyacrylamide (HPAM) samples with narrow molecular weight distribution were synthesized and used as model polymers.

The second chapter of Part A investigates the validity of viscometry for molecular weight characterization of HPAM. Polyacrylamide (PAM) samples with narrow molecular weight distribution were prepared by solution precipitation fractionation and then hydrolysed to various degrees of hydrolysis. Intrinsic viscosity and weight average molecular weight of these samples were determined, and Mark-Houwink equations were established for both PAM and HPAM. The effects of charge density and molecular weight on the intrinsic viscosity and thus on the parameters in the Mark-Houwink equation were studied. The molecular weight of HPAM was calculated using the established equations and then compared with the values determined by light scattering and by stoichiometric calculations.

The third chapter of this part involves study of the validity of gel permeation chromatography for molecular weight characterization of HPAM. The relationship between hydrodynamic size and elution volume was investigated for both PAM and HPAM, and the universal calibration for HPAM using nonionic polymer PAM was evaluated for its validity. The influence of charge density on the elution volume of HPAM was studied and a correlation was developed to predict the shift of peak elution volume with charge density. The molecular weight and intrinsic viscosity predicted using this methodology were compared with experimental data.

CHAPTER 2

MOLECULAR WEIGHT CHARACTERIZATION OF POLY(ACRYLAMIDE-CO-SODIUM ACRYLATE) BY VISCOMETRY

2.1 INTRODUCTION

The molecular weight characterization of polyelectrolytes is difficult, since variations in copolymer composition alter the electrostatic environment and hence the size or even the structure of the polymer chain. Hydrolysed polyacrylamide (HPAM) is often used for methods development since it has a random distribution of charged groups along the backbone, provided alkaline hydrolysis is performed under mild conditions,[1,2,3] and because the molecular weights of the parent PAM can be estimated by conventional techniques. Many studies have been reported on the solution properties and the molecular weight characterization of HPAM,[4,5,6,7,8,9,10,11,12,13,14] but only one study was done using fractionated polyacrylamide (PAM) with narrow molecular weight distributions.[14] Using fractionated PAM of molecular weight range 1.0×10^6 - 6.0×10^6, and polydispersity 1.4 - 2, Schwartz and François[14] established two sets of Mark-Houwink parameters for average hydrolysis degrees $\overline{HD}$ at ~ 22% (hydrolysis degree (HD) range 21.6 - 23.2) and ~ 28% (HD range 23.2 - 31.3%). The parameters for $\overline{HD}$ = 37% (HD range 30.1 - 42.7) reported were the same as for $\overline{HD}$ = 28%. These data are, however, insufficient to develop a valid methodology for the molecular weight characterization of poly(acrylamide-co-sodium acrylate) (poly(AM/NaAA) over a wide range of molecular weight and composition.

The objective of this study was to develop valid methods for the molecular weight characterization of HPAM or poly(AM/NaAA) over the composition range of commercial interest (HD = 0 - 30%). A series of fractionated and well-characterized PAM samples have been hydrolysed under mild alkaline conditions. The intrinsic viscosities and weight average molecular weights were measured. In anticipation that the results of these studies could be applied to GPC calibration, an aqueous Na_2SO_4 solution (0.2 M) was used as a solvent for polymers in these measurements and the molecular weight (MW) range of PAM fractions was chosen from 1.4×10^4 to 1.2×10^6 g/mol. Since most commercial HPAM is of hydrolysis degree (HD), 10 - 30%, we have mainly used HPAM samples with the HD in this range.

2.2 EXPERIMENTAL

Polymer preparation

Nonionic polyacrylamides with broad molecular weight distribution (MWD) used for fractionation were synthesized on a pilot scale, except for the sample of Mw 62,000 which was provided by NALCO CANADA (Burlington, Ontario, Canada). The polymerizations were carried out in aqueous solution at 55 - 60 °C with $K_2S_2O_8$ (BDH, 99% purity) as initiator and ethanol mercaptan (BDH) as the chain transfer agent (see Appendix A-1 for details).

Fractionation

Precipitational fractionation was performed at room temperature (~ 25 °C) using water as a solvent, acetone and methanol as non-solvents. The small scale fractionation was carried out in 25 mL bottles and in 2000 mL three-necked flask to find proper ratio of non-solvent to solvent. The non-solvent was added to the polymer solution dropwise, and the turbid point at which the polymer starts to precipitate from the solution was determined visually as well as by tubidity measurement (see Appendix A-2 for the details). The large scale fractionation was conducted in a 50 L plastic tank equipped with a turbine stirrer.

Gel permeation chromatography

The molecular weight distribution of PAM fractions was measured in 0.2 M Na_2SO_4 with a 5000 Liquid Chromatograph (Varian Canada Inc.) equipped with TSK PW 3K, 5K, 6K columns (Toya Soda). A molecular weight calibration was done using universal calibration with seven narrow polyethyleneoxide standards (Toya Soda Manufacturing Co., Ltd.) and two broad MWD PAM samples. Peak broadening corrections were performed using standard methods.[15,16]

Hydrolysis

PAM in aqueous solution was weighed into a 3-neck flask of 500 mL and kept in 30^{0}C water bath for at least 1 hour. Amounts of 4N NaOH and deionized water (making the concentration of PAM 4 wt.% and NaOH 0.5 N) were added to the flask under vigorous agitation. After the addition, gentle stirring was applied to prevent degradation of the polymer. Samples were withdrawn at predetermined times and poured into excess methanol (70-100 times the volume). The precipitated HPAM was purified by repeated washing with methanol. For low molecular weight samples centrifugation at 5,000 rpm for half an hour was performed to recover the fine particles of HPAM. The solid HPAM was dried in a vacuum oven at about 60 °C for at least 16 hours, and weighed for analysis immediately after being cooled to room temperature under vaccum.

Analysis of hydrolysis degree

(a) Elemental C, N, H measurements were done by Guelph Chemical Lab. Ltd.(Ontario, Canada). The amount of Na was determined using atomic absorption spectroscopy (Perkin Elmer 2380).

(b) Carboxyl groups were measured by conductometric and potentiometric titration. The titrations were carried out at constant temperature (20 °C) under N2 atmosphere with 0.01 N NaOH as a titrant. In a typical analysis, 0.02 - 0.07 g HPAM sample was dissolved in 100 mL 2.6×10^{-3} M KCl (the amount of HPAM was determined from the estimation of hydrolysis degree so that the volume of titrant consumed was within the range of 18 - 25 mL). The pH of the polymer solutions was first adjusted to 3.2 - 3.3 with 1 N HCl before it was titrated with 0.01 N NaOH. The amount of carboxyl groups was determined, (1) in potentiometric titration from the peak of the derivative of pH to titrant volume $\Delta pH/\Delta v$; (2) in conductometric titration from the plateau of the plot of conductivity versus titrant volume.

Viscometry

The intrinsic viscosities of polymers in 0.2 M Na_2SO_4 were obtained from the quadratic form as well as the conventional form of Huggins equation by a least square technique.[17,18] The solution viscosities were measured with a #75 Cannon-Ubbelohde semi-micro dilution viscometer at 25 ± 0.05 °C.

Light scattering

The refractive index increment dn/dc measurements were performed with a Chromatix KMX-16 laser differential refractometer at 632.8 nm and 23 °C. The weight-average molecular weights were determined with a low angle laser light scattering photometer (Chromatix KMX-6) in 0.02 M (for PAM) and 0.2 M Na_2SO_4 (for HPAM) at room temperature (~ 23 °C). All of the HPAM samples were dialyzed in the same solvent for 120 hours before measurement. The details are given elsewhere.[19]

2.3 RESULTS AND DISCUSSION

2.3.1 CHARACTERIZATION OF POLYACRYLAMIDE

Eight PAM fractions with polydispersity indices 1.2 - 2.0 and molecular weight range 1.4×10^4 - 1.2×10^6 were obtained by fractionation (Table 2.1). Their reduced specific viscosities η_{sp}/c, when plotted versus concentrations, gave straight lines with regression coefficients of 0.999 ~ 0.9999 (see Figure 2.1). The intrinsic viscosities from the quadratic equation were slightly different from those from the conventional equation with an average deviation of 0.46%.

Table 2.1 $\overline{M_w}$, PDI and $[\eta]$ of PAM fractions

Sample	F1	F2	F3	F4	F5	F6	F7	F8
$\overline{M_w}\times10^{-4}$	124.4	99.0	40.1	20.1	9.90	3.60	2.69	1.39
PDI	1.8	2.0	1.8	1.7	1.6	1.5	1.3	1.2
$[\eta]$ dL/g	3.804	3.555	1.733	1.096	0.6502	0.3220	0.2741	0.1754

The Mark-Houwink constants k and α were estimated by the Error-In-Variables method,[20,21] in which the variance of $\log_{10}\overline{M_w}$ were evaluated from Hunkeler's data,[22] while those of $\log_{10}[\eta]$ were calculated from the data of this work using Chee's equation[17] without consideration of the variance in concentrations. The resulting Mark-Houwink equation for PAM in 0.2 M Na_2SO_4 at 25 ± 0.05 °C is:

$$[\eta] = k\,\overline{M_w}^{\alpha} = 2.43\times10^{-4}\,\overline{M_w}^{0.69} \qquad (2.1)$$

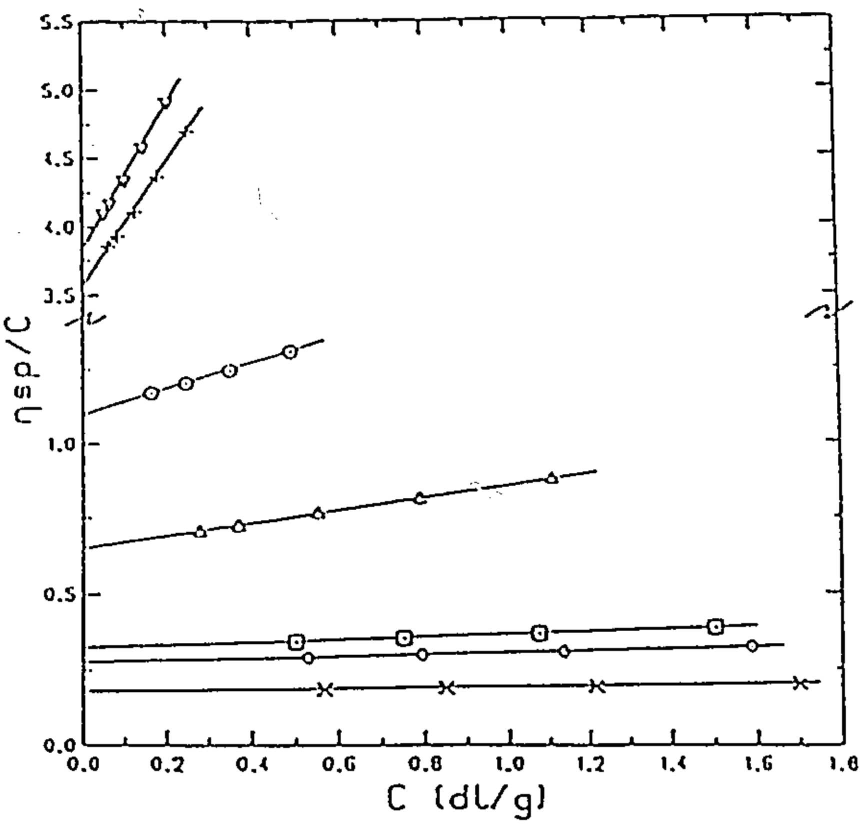

Figure 2.1 Plot of reduced specific viscosity vs concentration of PAM

(X): Mw = 13900, (◊): Mw = 26900, (⊡): Mw = 36000, (Δ): Mw = 99000, (⊙): Mw = 201000, (+): Mw = 990000, (∇): Mw = 1244000

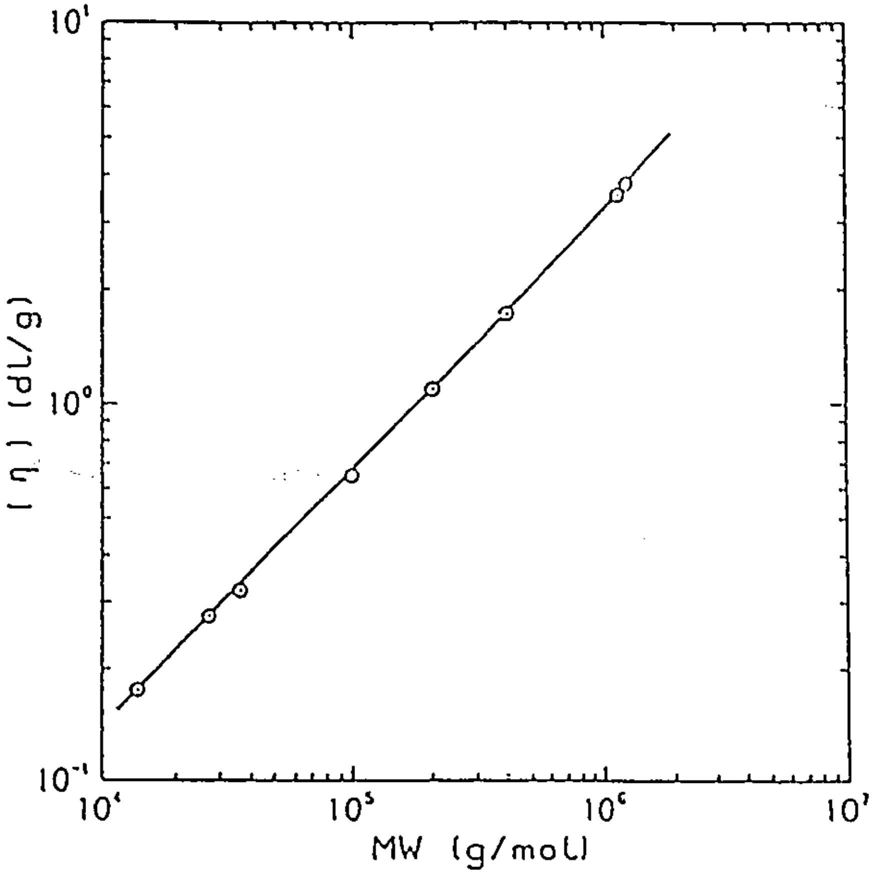

Figure 2.2 Plot of $\log_{10}[\eta]$ vs $\log_{10}Mw$ for PAM in 0.2 M Na_2SO_4 at 25 °C

The 95% confidence intervals for parameters k and α are

$$k = 2.43\times10^{-4} \pm 0.36\times10^{-4} \quad [\mathrm{mol.dL/g^2}]$$

$$\alpha = 0.69 \pm 0.014$$

The log-log plot of $[\eta]$ versus $\overline{M_w}$ is given in Figure 2.2. The α value is consistent with that obtained by Kulicke[23] in 0.1 M Na_2SO_4 which was 0.7.

2.3.2 RATE OF HYDROLYSIS OF POLYACRYLAMIDE

Fractionated PAM (molecular weights from 3×10^5 to 1.2×10^6) was hydrolysed with NaOH. The hydrolysis degree versus reaction time is given in Figure 2.3. The data points for different molecular weights can be correlated by a single curve, i.e., no systematic deviation of reaction rate due to molecular weight was observed.

2.3.3 CHARACTERIZATION OF HYDROLYSED POLYACRYLAMIDE

(1) ANALYSIS OF HYDROLYSIS DEGREE

The hydrolysis degree of HPAM was determined by atomic adsorption spectroscopy (AAS) and titration. A preliminary study of the appropriateness of two methods suggested that for this system titration gave better reproducibility and reliability since AAS is sensitive to the carboxyl forms (H^+ or Na^+), and to the viscosity of the polymer solution.[24] Therefore the hydrolysis data reported in this work were obtained from titration. Conductometry is, however, preferred to potentiometry due to its better reproducibility or smaller standard deviation: 0.4 ~ 2.0%, compared with 1.0 ~ 4.0% for the latter.

(2) VISCOSITY AND THE SQUARE ROOT LAW

As shown by the straight lines of η_{sp}/c vs concentration c in Figure 2.4, HPAM in 0.2

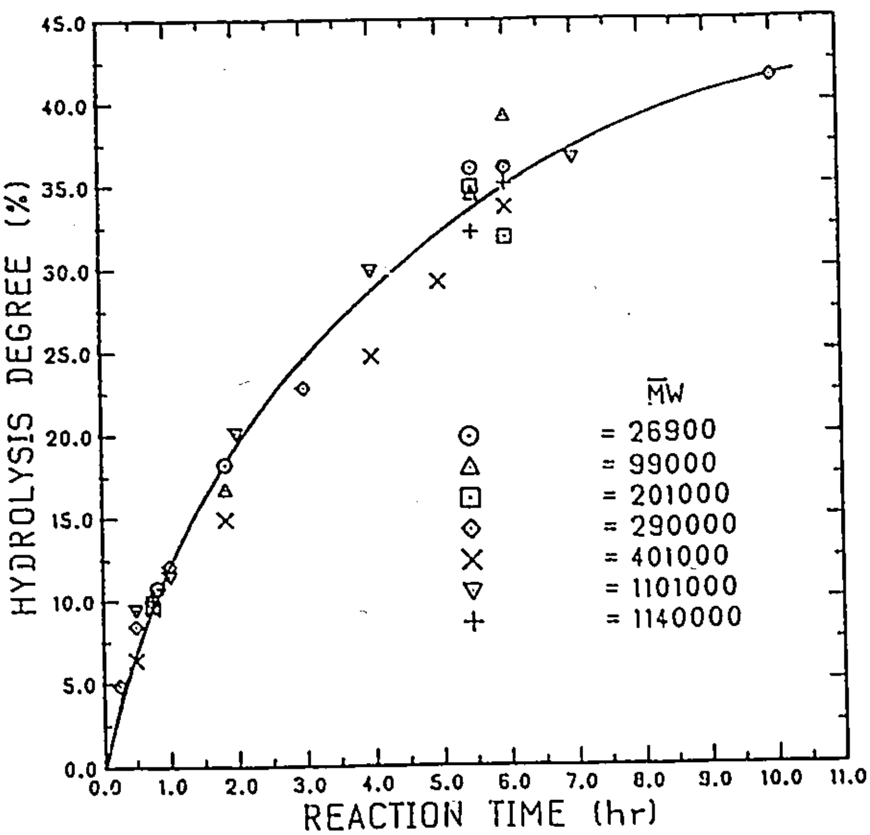

Figure 2.3 Hydrolysis degree versus reaction time

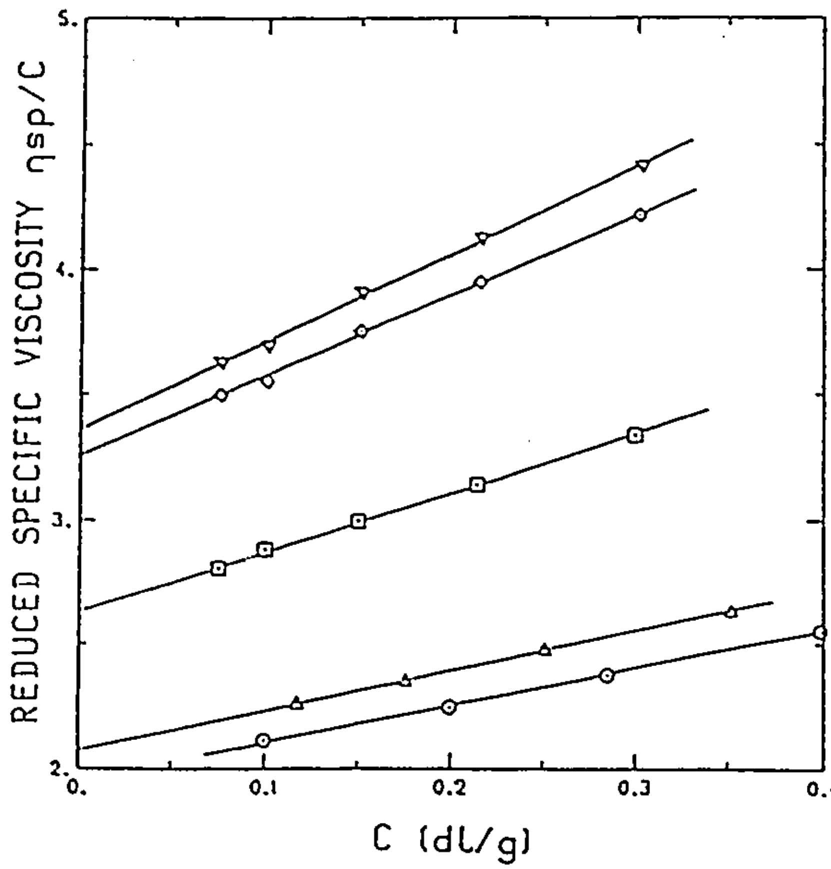

Figure 2.4 Reduced specific viscosity vs concentration of F3HY in 0.2 M Na_2SO_4

(⊙): HD = 6.4%, (△): HD = 9.5%, (⊡): HD = 14.9%,
(◇): HD = 23.0%, (▽): HD = 26.0%

M Na_2SO_4 behaves like a nonionic polymer. However, the intrinsic viscosity of polyelectrolytes with different compositions should be a function of M_w, composition of polymer x and concentration of added salt, C_s:

$$[\eta] = f(M_w, x, C_s)$$

In our case, C_s is constant, HD represents the composition, so

$$[\eta] = f(M_w, HD)$$

For an HPAM sample of given M_w, $[\eta]$ will change with HD only.

The experimental work has supported the preceding analysis.[4,5-9,11,25] The plots of $[\eta]$ vs HD are bell-shaped with a maximum $[\eta]$ at about HD = 40 ~ 50%. Kulkarni et al.[5] plotted $[\eta]$ vs $HD^{1/2}$ and obtained straight lines in the HD range of 10 ~ 35%.

From our own data (Figure 2.5), a square root law has been found:

$$[\eta] = A * HD^{1/2} + B \tag{2.2}$$

where A and B are slope and intercept of plot $[\eta]$ vs $HD^{1/2}$ respectively. Table 2.2 has sumarized the values of parameters A and B for the HPAM of various molecular weights, together with the intrinsic viscosities of their parent PAM samples ($[\eta]_0$). Although they are constant for a series of HPAM samples from the same parent PAM, the A and B will vary with the M_w of parent PAM.

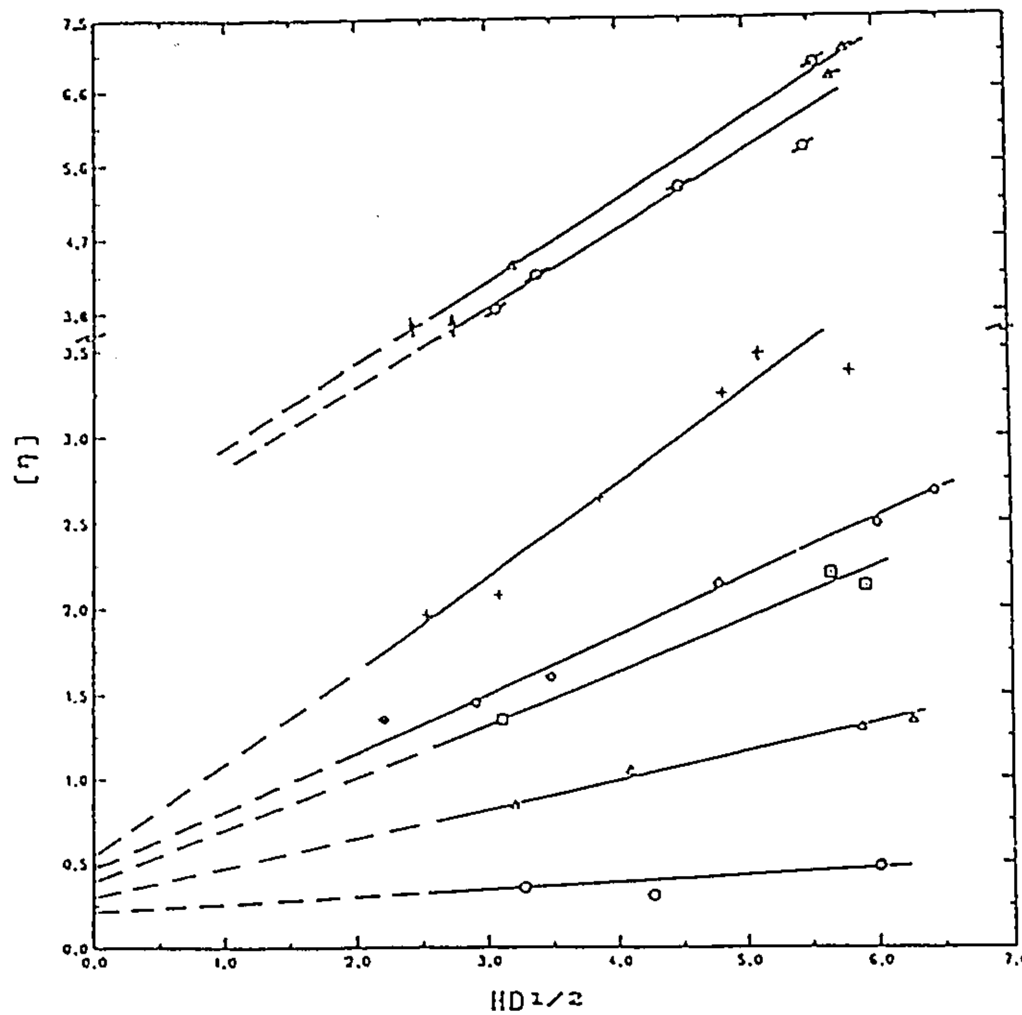

Figure 2.5 Dependence intrinsic viscosity of HPAM on the square root of hydrolysis degree

(⊙): F7HY, (△): F5HY, (⊡): F4HY, (◇): HY2, (+): F3HY, (ø): HY5, (△̸): F2HY

Table 2.2 Parameters A and B in equation (2.2) for HPAM from the PAM with various molecular weights

Sample*	Parent $[\eta]_0$ (dL/g)	A (dL/g)	B (dL/g)
F7HY	0.2741	0.0462±0.011	0.201±0.056
F5HY	0.6502	0.159±0.027	0.363±0.137
F4HY	1.096	0.300±0.098	0.428±0.495
HY2**	1.257	0.348±0.026	0.428±0.128
F3HY	1.733	0.507±0.085	0.634±0.375
F2HY	3.555	1.010±0.173	1.109±0.872

* In the names of samples, F2 - F7 represent the parent PAM's are the fractions listed in Table 2.1; HY represents hydrolysed PAM.

** M_{w0} = 246900; PDI = 1.8

Obviously, both A and B are functions of the molecular weight of the parent PAM (M_{w0}) and therefore functions of intrinsic viscosity of the parent PAM ($[\eta]_0$). The plots in Figures 2.6 and 2.7 reveal fairly good linear relationships between A, B and $[\eta]_0$. The data calculated from Kulkarni's results are also plotted in the figures. The same trends were observed. The difference between the curves from Kulkarni's data and this work may arise from the salt type and concentrations. Kulkarni's intrinsic viscosity data were measured in 0.12 M NaCl, while those of this work were measured in 0.2 M Na_2SO_4.

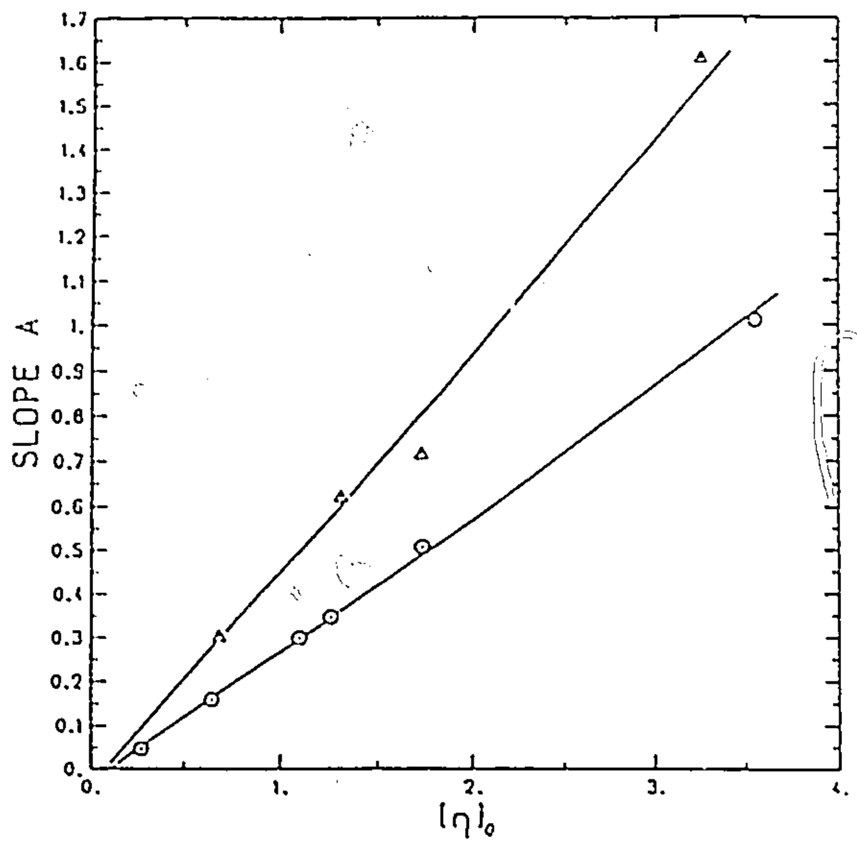

Figure 2.6 Slope of ($[\eta]$-$HD^{1/2}$ plot) for HPAM vs $[\eta]$ of the parent PAM

(⊙): this work, (△): Kulkarni's work

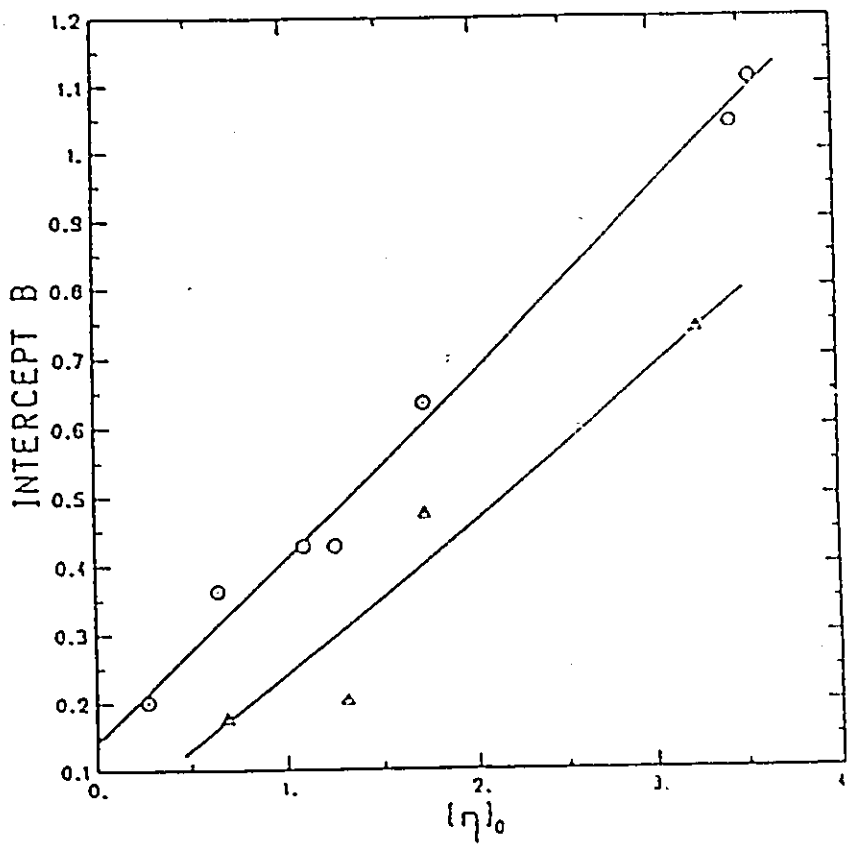

Figure 2.7 Intercept of ($[\eta]$-$HD^{1/2}$ plot) for HPAM vs $[\eta]$ of the parent PAM

(⊙): this work, (△): Kulkarni's work

Using linear regression, equations for A and B have been found to be:

$$A = f([\eta]_0) = 0.294\,[\eta]_0 - 0.0246 \tag{2.3}$$

$$B = f([\eta]_0) = 0.266\,[\eta]_0 + 0.144 \tag{2.4}$$

Hence, an empirical equation of $[\eta]$ as a function of $[\eta]_0$ and HD can be obtained for HPAM in 0.2 M Na_2SO_4 at 25.0±0.05 ^{0}C:

$$[\eta] = (0.266 + 0.294\,HD^{1/2})[\eta]_0 + 0.144 - 0.0246\,HD^{1/2} \tag{2.5}$$

From this equation one can readily estimate the intrinsic viscosity of HPAM of any composition in the range of 6 ~ 40% if the $[\eta]_0$ and HD are known.

(3) MARK-HOUWINK EQUATIONS FOR HPAM

In Mark-Houwink equation

$$[\eta] = k\,\overline{M_w}^{\alpha} \tag{2.6}$$

the parameters k and α are constant only if the polymer composition, solvent and temperature are unchanged. For HPAM under the given conditions, k and α are functions of hydrolysis degree. Klein et al[8] observed a maximum value of exponent α at about 40% HD and a minimum value of k at about 20% HD. McCarthy et al[7] showed some changes in the values of k and α with HD but did not show definite trends.

Since the intrinsic viscosities of HPAM, especially those for high molecular weight samples, strongly depend on HD, it is necessary to choose the HPAM samples with exactly the same HD to determine the parameters k and α. Because of the difficulties in preparing

HPAM samples with exactly desired HD, interpolation was done with the square root law, Equation (2.2), this, the intrinsic viscosities of HPAM at HD = 6, 10, 15, 20, 25, 30, 35, 40% were obtained. Assuming that all the hydrolysed acrylamide groups are in Na form, the molecular weights of HPAM were calculated from the stoichiometric equation

$$\overline{M}_{wT} = \frac{\overline{M}_{wPAM}}{71.08}(94.04x + 71.08(1-x)) \tag{2.7}$$

where x is the mole fraction of hydrolysed groups, and x=HD/100%. A set of Mark-Houwink constants were determined by correlating the intrinsic viscosities with the molecular weights, and are listed in Table 2.3. Some examples of log-log plots of $[\eta]$ and M_w are given in Figure 2.8 for HPAM with various compositions.

Table 2.3 Mark-Houwink constants k and α for HPAM with various HD

HD (mol%)	α	$k(10^{-4})$ $(dL.mol^{\alpha}/g^{1+\alpha})$	regression coefficient
6	0.669	3.31	0.9982
10	0.694	2.85	0.9991
15	0.712	2.57	0.9995
20	0.725	2.41	0.9997
25	0.734	2.30	0.9997
30	0.742	2.22	0.9998
35	0.748	2.16	0.9997
40	0.753	2.12	0.9997

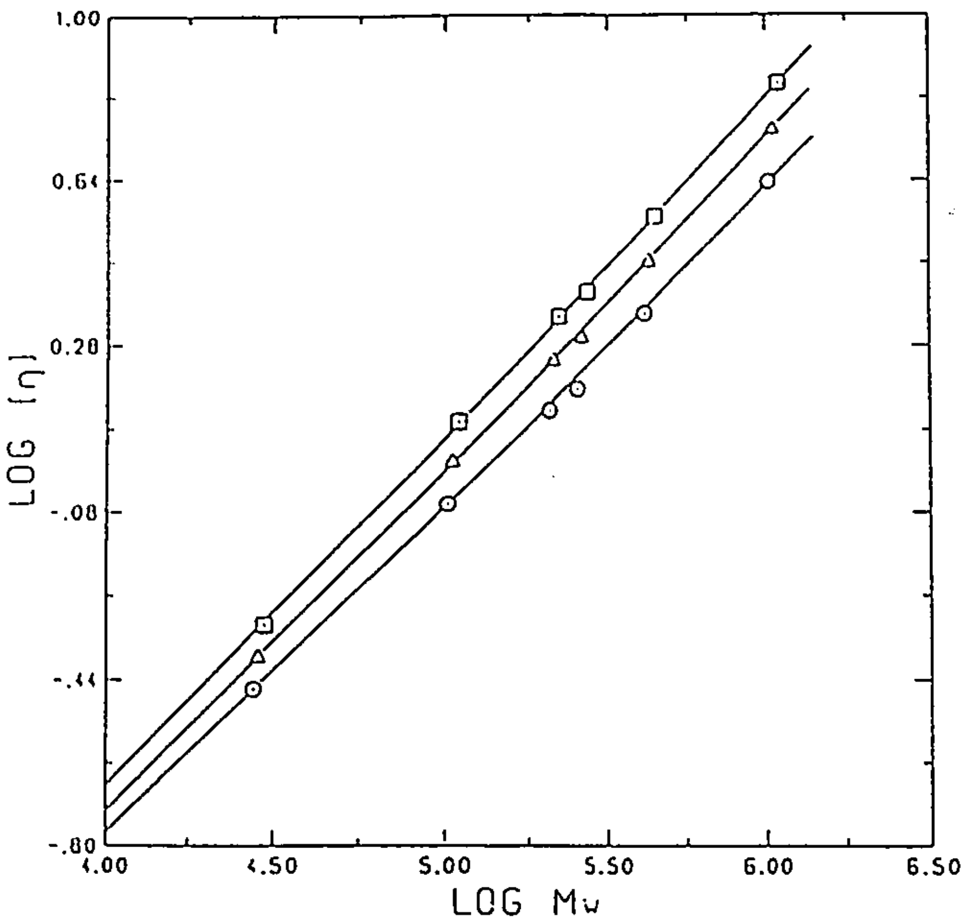

Figure 2.8 Plot of log[η] vs logMw for HPAM of various hydrolysis degree

(⊙): HD = 10%, (Δ): HD = 20%, (⊡): HD = 35%

Using polynomials to regress the above data, two empirical equations were obtained for HPAM. The equations, parameters and 95% confidence intervals are summarized below:

$$\alpha = C_0 + C_1 HD + C_2(HD^2) + C_3(HD^3)$$

where $C_0 = 0.625 \pm 0.007$

$C_1 = 8.86\times10^{-3} \pm 1.27\times10^{-3}$ $(\text{mol\%})^{-1}$

$C_2 = -2.405\times10^{-4} \pm 0.617\times10^{-4}$ $(\text{mol\%})^{-2}$

$C_3 = 2.48\times10^{-6} \pm 0.89\times10^{-6}$ $(\text{mol\%})^{-3}$

$$\log k = d_0 + d_1 HD + d_2(HD^2) + d_3(HD^3)$$

where $d_0 = -3.36 \pm 0.024$

$d_1 = -2.39\times10^{-2} \pm 0.42\times10^{-2}$

$d_2 = 6.96\times10^{-4} \pm 2.05\times10^{-4}$

$d_3 = -7.37\times10^{-6} \pm 2.95\times10^{-6}$

The regressed curves are plotted together with the k, α data in Figure 2.9; these show a good fit with the polynomials and thus confirm the applicability of the interpolation via the square root law. One can calculate the values of k and α precisely at any polymer composition of interest over the range, 6 ~ 40% acrylate from these polynomials.

(4) MOLECULAR WEIGHTS OF HYDROLYSED POLYACRYLAMIDE

The molecular weights of HPAM samples were calculated using the Mark-Houwink equations (as M_{wv}) established in this work as well as from the stoichiometric equation (as M_{ws}). In the former, the values of k and α applied were obtained from the polynomials and the [η]'s and HD's were from the experiments. The two kinds of molecular weights together with those measured by light scattering are listed in Table 2.4.

Table 2.4. Molecular weights of HPAM from Mark-Houwink equations, stoichiometric equation(eq.2.7) and from light scattering

Sample	HD(mol%)	[η](dl/L)	M_{wLS}	M_{wv}	M_{ws}	Err(%)[a]
F7HY	10.77	0.3524	35800	28300	27800	1.53
	36.00	0.4692	31700	28800	30000	-4.19
	36.08	0.4872	/	30200	30000	0.64
F5HY	10.30	0.8468	119600	101500	102300	-0.80
	16.70	1.049	/	112300	104300	7.61
	34.42	1.303	/	114700	110000	4.30
	39.20	1.342	135500	112900	111500	1.22
F4HY	9.68	1.353	247000	205000	207300	-1.08
	31.90	2.200	/	238600	221700	7.62
	34.90	2.127	268000	219900	223700	-1.67
HY2	4.86	1.355	/	267400	250800	6.62
	8.42	1.451	/	241100	253600	-4.92
	12.10	1.601	/	235800	256600	-8.10
	22.80	2.137	/	262200	265100	-1.11
	36.00	2.486	/	267300	275600	-3.01
	41.50	2.677	/	273100	280000	-2.46
F3HY	6.40	1.961	/	421400	409300	2.97
	9.53	2.075	468000	383800	413300	-7.15
	14.90	2.640	/	431200	420300	2.59
	23.20	3.242	/	459800	431100	6.68
	26.00	3.470	/	479700	434700	10.35
	33.10	3.372	467000	417200	443900	-6.00
HY5[b]	9.46	3.979	/	925500	1061500	-12.81
	11.50	4.228	/	969500	1068300	-9.25
	20.15	5.329	/	974700	1097000	-11.16
	36.60	6.893	/	1126800	1132500	-0.51
F2HY	10.30	4.354	1014000	1076500	1022900	5.24
	32.20	6.709	/	1064500	1093000	-2.60
	33.40	7.067	822000	1122000	1096800	2.30
			average	absolute	error (%)	4.70

a Err (%) = $(M_{wv} - M_{ws})/M_{ws} \times 100\%$
b HY5 is from unfractionated PAM with PDI 2.5

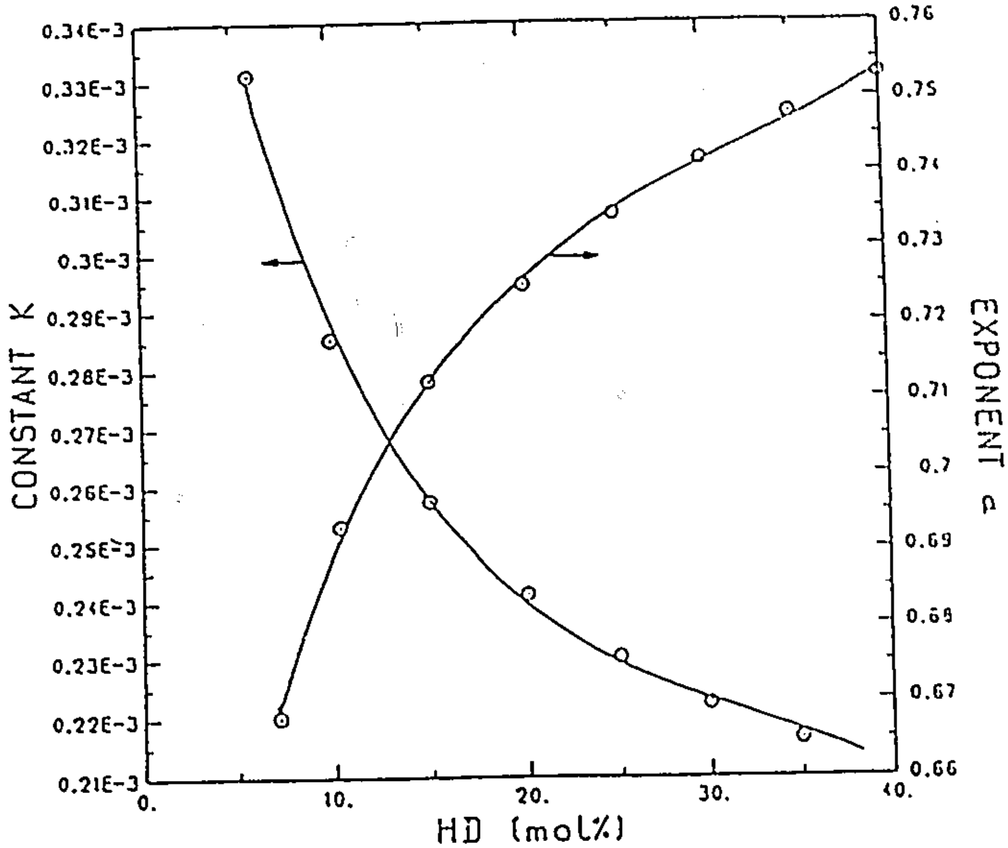

Figure 2.9 Mark-Houwink constants k and α for HPAM at various hydrolysis degree

(____): from correlated polynomials, (⊙): data point

An average error in molecular weight determination of 4.7% is relatively low as compared with values obtained by light scattering, osmometry and GPC. These values have errors of 10 - 20%. The agreement between viscometric method through $[\eta]$-Mw correlation and stoichiometric method is good even for the samples of high polydispersities (eg. HY5). For even broader samples ($\overline{M_w}/\overline{M_n}$ > 2.5), a polymolecularity correction might be necessary to reduce the error.[7,26,27,28]

2.4 DISCUSSION

(I) MARK-HOUWINK CONSTANTS

As shown in Table 2.3 and Figure 2.9, the value of k decreases exponentially with increase in hydrolysis degree. Klein[8] found a similar dependency. Parameter k is a measure of flexibility of ploymer chains. It is proportional to the viscosity constant Φ and related to linear expansion ε[28,29]

$$k \propto \Phi$$

where $$\Phi = \Phi_0 (1 - 2.63\varepsilon + 2.86\varepsilon^2)$$

for nondraining polymer coils. Since Φ becomes smaller when the polymer chains become more rigid, it is reasonable for k to reduce when the concentration of the charged groups increases.

The values of the exponent a obtained in this work is in the range, 0.67 to 0.76. This is in agreement with the theoretical predictions[28] for unbranched, non-solvent-draining coils with excluded volumes and implies that 0.2 M Na_2SO_4 is not a good solvent for polyacrylamide or poly(acrylamide-co-sodium acrylate). Therefore the conformation of the polymer chain is probably a random coil in this solvent.

Constants k and exponent α are not independent parameters, since from the theoretical derivation, α is also a function of "ε":

$$\alpha = 0.5(1 + 3\varepsilon) \tag{2.8}$$

Hence, k and α are related as summarized by Elias[28] for various coil-like polymers:

$$\log_{10}k = B_1 - B_2\alpha \tag{2.9}$$

where B_1 and B_2 are positive constants. Our data show a similar relationship between k and α for the copolymer with various compositions as follows and in Figure 2.10:

$$\log_{10} k = -1.946 - 2.302\alpha \tag{2.10}$$

(In this work, the constant B_1 is negative.) The agreement again suggests the coil-like conformation of poly(acrylamide-co-sodium acrylate) in the salt solution of 0.2 M Na_2SO_4.

(2) LIMITATION OF SQUARE ROOT LAW

A theoretical interpretation of the square root law will be attempted in future work, so the discussion here only concerns the limitations of the square root law.

A fact should be noted that in Table 2.2 and Figure 2.5 involving the square root law

$$[\eta] = A * HD^{1/2} + B \tag{2.2}$$

the intercept B is always smaller than the intrinsic viscosity of the parent PAM ($[\eta]_0$). Therefore equation (2.1) will overpredict the intrinsic viscosity when HD approaches zero. The deviation of B from $[\eta]_0$ increases with increase in the molecular weight of the parent PAM

(Figure 2.11 shows the dependence of the deviation ($[\eta]_0$ - B) on $[\eta]_0$). This suggests that there is a minimum value of HD, or say, a minimum distance between charged groups at which the intrinsic viscosity of HPAM equals that of the parent PAM. Above this charge density, electrostatic forces cause an expansion of the polymer chain and therefore the increase of the intrinsic viscosity. Below the minimum HD the square root law is invalid.

To determine the applicable range of HD, the general square root equation (Equation (2.5)) is divided by $[\eta]_0$ to obtain the form:

$$\frac{[\eta]}{[\eta]_0} = 0.266 + 0.294\,HD^{1/2} + \frac{(0.144 - 0.0246\,HD^{1/2})}{[\eta]_0} \qquad (2.11)$$

Values of HD_{min}, calculated using this equation at $[\eta]/[\eta]_0 = 1$ for various values of $[\eta]_0$, are listed in Table 2.5.

Table 2.5 Minimum values of HD at various $[\eta]_0$

$[\eta]_0$ (dL/g)	0.2741	0.500	1.00	1.50	2.00	3.00	4.00	5.00
HD_{min} (%)	1.66	3.65	4.69	5.01	5.16	5.31	5.39	5.43

It is clear that the HD_{min} values vary with the molecular weight of the parent PAM. This might infer that it is more reasonable for one to consider the charge density of coil-like polyelectrolytes based on the coil volume than on the chain length.

When HD is higher than 40 ~ 50%, the slope A changes sign and the values of A and B may be different. This range of hydrolysis degree is beyond the scope of this work.

One can conclude, however, that the square root law is valid for the molecular weight range of 10^4 ~ 10^6 when HD is larger than 6% and smaller than 40%.

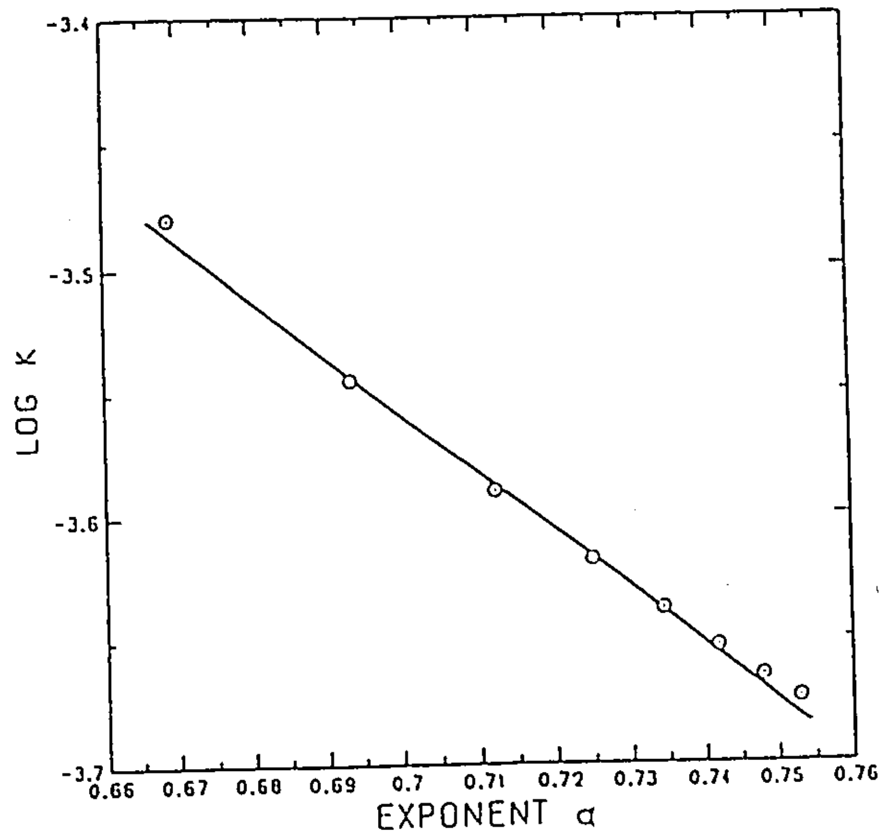

Figure 2.10 log$k$ versus exponent a of HPAM at various hydrolysis degree

from top left to bottom right, the data points are at HD = 6, 10, 15, 20, 25, 30, 35, 40%

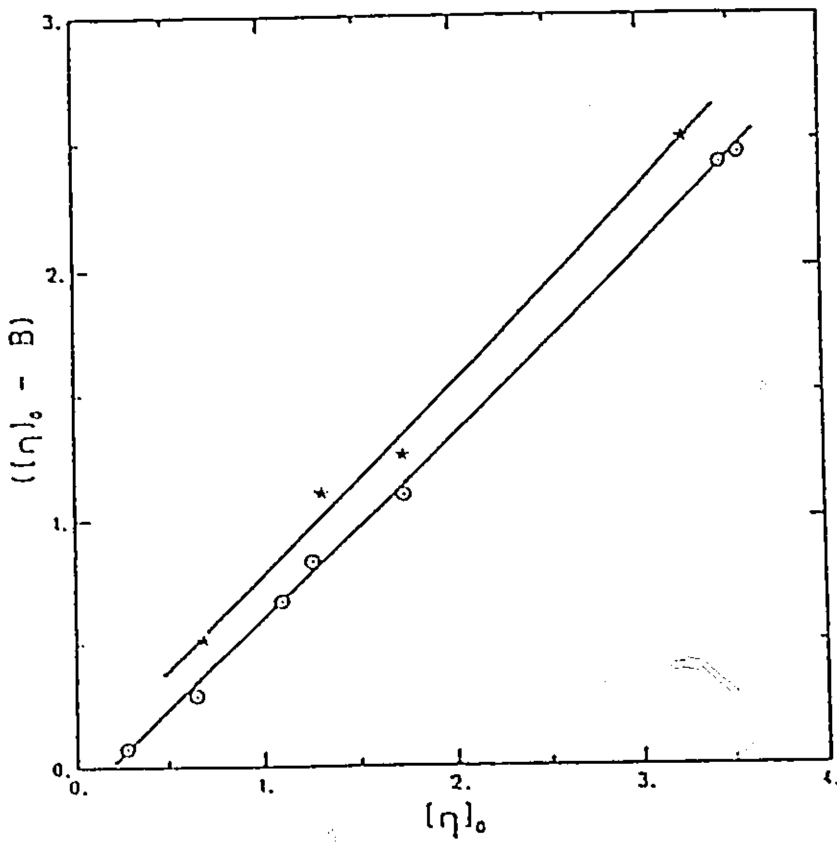

Figure 2.11 Dependence of ($[\eta]_0$ - B) of HPAM on [n] of parent PAM

(⊙): this work, (★): Kulkarni's work

(2) POTENTIAL APPLICATION FOR GPC MEASUREMENTS

This determination of a set of Mark-Houwink parameters k and α for HPAM with various hydrolysis degrees, makes it possible to evaluate universal calibration for GPC of HPAM or poly(acrylamide-co-sodium acrylate) if the latter is of narrow composition distribution. This study is now in progress in our laboratory.

2.5 CONCLUSION

The measurement of intrinsic viscosity of hydrolysed polyacrylamide in 0.2 M Na_2SO_4 can be used to estimate the weight average molecular weights given the appropriate Mark-Houwink constants for the ionic polymers. The relationship between the intrinsic viscosity and the composition of the copolymer can be expressed by a square root law from which the intrinsic viscosity at any level of hydrolysis in the range, 6 to 40% can be readily calculated. Mark-Houwink constants in this range can be found as functions of copolymer composition. Applying these constants, weight average molecular weights determined by viscometry for hydrolysed PAM samples were accurate to within 5% for degrees of hydrolysis in the range, 6 to 40% and molecular weights in the range, 10^4 to 1.24×10^6.

References

1. F. Halverson, J.E. Lancaster and M.N. O'Connor, Macromolecules, 18, 1139-1144 (1985)
2. N.D. Truong, J.C. Galin and J. Francois, Polymer, 27, 459-466 (1986)
3. N.D. Truong, J.C. Galin and J. Francois, Polymer, 27, 467-475 (1986)
4. W.-M. Kulicke and H.-H. Horl, Colloid and Polymer Science, 263, 530-540 (1985)
5. R.A. Kulkarni and S. Gundiah, Makromol.Chem. 185, 957-967 (1984)
6. K.J. McCarthy, C.W. Burkhardt and D.P. Parazak, J.Appl.Poly.Sci. 33, 1683-1698 (1987)

7. K.J. McCarthy, C.W. Burkhardt and D.P. Parazak, J.Appl.Poly.Sci. 33, 1699-1714 (1987)

8. J. Klein and K.-D. Conrad, Makromol.Chem. 179, 1635-1638 (1978)

9. J. Klein and R. Heitzmann, Makromol.Chem. 179, 1895-1904 (1978)

10. H. Rios, L. Gargallo, D. Radic, Makromol.Chem. 182, 665-668 (1981)

11. G. Muller, J.P. Laine and J.C. Fenyo, J.Poly.Sci., Poly.Chem.Ed. 17, 659-672 (1979)

12. M.S. Jacovic and Z. Rajic, J.Poly.Sci.Symp., No.42, 1147-1155 (1973)

13. J.C. Fenyo, J.P. Laine and G. Muller, J.Poly.Sci.,Poly.Chem.Ed. 17, 193-202 (1979)

14. T. Schwartz and J. Francois, Makromol.Chem. 182, 2757 (1981)

15. A.E. Hamielec and W.H. Ray, J.Appl.Polym.Sci. 13, 1317 (1969)

16. S.T. Balke and A.E. Hamielec, J.Appl.Polym.Sci. 13, 1381 (1969)

17. K.K. Chee, J.Appl.Polym.Sci. 30, 2607-2614 (1985)

18. M.H.R. Fanood and M.H. George, Polymer, 28, 2241-2243 (1987)

19. D. Hunkeler, X.Y. Wu, A.E. Hamielec, J.Appl.Polym.Sci. in press

20. T.L. Sutton and J.F. MacGreger, Canadian J.Chem.Eng. 55, 609-613 (1977)

21. P.M. Reilly and H. Patino-Leal, Technometrics, 23(3), 221-231 (1981)

22. D. Hunkeler and A.E. Hamielec, J.Appl.Polym.Sci. 35, 1603-1620 (1988)

23. W.-M. Kulicke and N. Bose, Polymer Bulletin, 7, 205 (1982)

24. X.Y. Wu, Ph.D. thesis, Appendix A-2

25. M. Kowblansky and P. Zema, Macromolecules, 14, 1451 (1981)

26. J. Brandrup and E.H. Immergut, Polymer Handbook, 2nd Ed, Chap.IV (1975)

27. W.-M. Kulicke, R. Kniewske and J. Klein, Prog.Polym.Sci. 403 (1982)

28. H.-G. Elias, "Macromolecules", vol.1, 2nd Ed, Plenum Press, New York, pp358-365 (1984)

29. B.Vollmert, "Polymer Chemistry", Springer-Verlag, New York Inc., pp513 (1973)

CHAPTER 3

MOLECULAR WEIGHT CHARACTERIZATION OF POLY(ACRYLAMIDE-CO-SODIUM ACRYLATE) BY GEL PERMEATION CHROMATOGRAPHY

3.1 INTRODUCTION

3.1.1 REVIEW OF PROBLEMS IN AQUEOUS GEL PERMEATION CHROMATOGRAPHY OF POLYELECTROLYTES

The determination of molecular weight distribution of polyelectrolytes by aqueous gel permeation chromatography (GPC) is much more difficult than that for organic-soluble polymers due to non-size-exclusion effects. These effects include ion exchange, ion exclusion, ion inclusion, adsorption, and polyelectrolyte swelling. For more details see reviews by Stenlund,[1] Cooper and Derveer,[2] and Barth.[3,4,5]

The effects of ion exchange, ion exclusion and ion inclusion are caused by electrostatic interactions between the packing and polyelectrolytes. The ion exchange usually occurs between cationic polymers and silanol groups on silica-based packing, or carboxyl groups on other type of gels, at higher pH and lower ionic strength.

The ion exclusion is a result of electrostatic repulsion of anionic polymers from the surface of packing containing anionic groups. When this effect exists, the polyelectrolytes are excluded from the pores of the packing, and hence smaller elution volumes are observed resulting in an overestimation of the molecular weight. To eliminate the ion exclusion and ion exchange effects, low pH (< 4) and high ionic strength, e.g. 0.01 ~ 0.2 M should be applied.

The ion inclusion effect was first defined by Stenlund[1] as the phenomenon in which Donnan equilibrium is established between packing and solutions. The packing acts as a semipermeable membrane, and the ions of the same charge as the polyelectrolyte are concentrated into the pores thus causing a peak due to ion inclusion. When the mobile phase has zero or low ionic strength, the low molecular weight component of the polyelectrolyte (with a molecular weight distribution MWD) may be included, so their molecular weight is underestimated if account for ion inclusion is not made. When enough salt is added to the mobile phase, the salt becomes included instead of the low molecular weight components and ion inclusion of polymer is negligible. Unlike other electrostatic effects, the ion inclusion effect of added salt is not eliminated, and thus a column with small pore size packing should be used together with a set of columns containing packing with larger pores to ensure complete separation of the permeated salt peak from the polymer peak.

Adsorption effects can be caused by hydrogen bonding, hydrophobic interaction and ionic interaction. The hydrogen bonding can be eliminated by the addition of a hydrogen-bonding-breaker, e.g. urea. Hydrophobic interactions can be reduced by the addition of an ionic surfactant, or by decreasing the ionic strength or polarity of the aqueous mobile phase. Ionic interaction between polyelectrolyte and packing may be minimized by elevating ionic strengths of mobile phase or pretreating packing. But high ionic strength may also enhance the hydrophobic interaction.

Polyelectrolyte swelling is the term defined by Stenlund[1] to describe the phenomena of polyelectrolyte chain expansion variation during the course of fractionation in a GPC column. If the ionic strength of the mobile phase is not high enough, the polyelectrolyte coil or chain expands upon dilution during the fractionation. This causes the elution volume to decrease; and the polyelectrolyte shrinks when the polymer concentration increases. The later phenomenon was also described by Barth[4] as macromolecular crowding. Nefedov et al.[6] illustrated this for a GPC chromatogram: the polymer at the peak has a smaller hydrodynamic volume than those at the leading and trailing edges of the chromatogram even though all of the chains have the same molecular weight. The polyelectrolyte swelling can be minimized by addition of enough salt in mobile phase.

In summary, high ionic strength (or together with low pH) can suppress most of non-size-exclusion effects including ion exchange, ion exclusion, ion inclusion (of polyelectrolyte), and polyelectrolyte swelling. However, one should be aware that high ionic strength can not eliminate the ion inclusion of added salt, and may enhance the hydrophobic interaction. Besides the composition of mobile phase, the material of the column packing is important. For the analysis of polyelectrolytes, it is best to use a hydrophillic, polymeric packing or a surface-modified silica packing in which most of silanols are derived.[5] In this work, columns with hydrophillic polyether packing, and a 0.2 M Na_2SO_4 aqueous solution were used. These were expected to minimize the non-size-exclusion effects. In 0.2 M Na_2SO_4, as shown by previous work,[7] the viscosity dependence of poly(AM/NaAA) on polymer concentration exhibited a behaviour almost identical to that observed for non-ionic polymers.

3.1.2 CALIBRATION METHOD

The calibration methods for molecular weight by GPC measurement include the method of monodisperse standards, secondary standards, polydisperse standards, universal calibration and absolute molecular weight detector (For a comprehensive discussion see reference 3). The first method is to use monodisperse standards that have the same composition and conformation as the sample and thus provides the most accurate result. But the application of this method is limited for lack of variety of monodisperse standards. The second method is more widely applied than the first one since it uses the standard that have the chemical composition of the standard fairly close to that of sample. The second method, however, can only determine relative difference among molecular weights of samples. Universal calibration method is a particular secondary calibration and has found wide applicability.[2,3,8,9,10,11,12,13,14,15] In this method, the hydrodynamic volume, measured by the product of molecular weight and intrinsic viscosity, is plotted against peak elution volume. If a size exclusion mechanism is operative, all kinds of polymers, whether homo- or copolymer, linear or branched polymer, should fall on the same calibration curve. Therefore, for determination of molecular weights of samples with quite different molecular structures from that of standard, universal calibration is often an effective method. It is especially useful for copolymers, since a set of well-characterized copolymer standards of varying molecular weight and composition are rarely available.[16] If Mark-Houwink constants of the sample is known, or a viscometry detector is employed, from the universal calibration average molecular weights may be calculated.

Universal calibration was first proven valid experimentally for polymers soluble in organic solvents by Benoit and coworkers,[8,17] who tested nine polymers covering homo- and copolymers, linear and graft (star, comb and ladder) polymers. It has gained wide acceptance in the field of "organic" GPC (organic solvent as eluent) since then.[16,18] For aqueous GPC, however, much of the work published has been to establish the validity of the calibration method.[11,13,16,19,20] Duval et al.[11] plotted the log of hydrodynamic volume against elution volume for both polyethylene oxide and polyacrylamide and obtained a single calibration curve. Spatorico and Beyer[13] analyzed dextran, copolymers of acrylic acid and ethyl acrylate, and sodium polystyrene sulfonate (NaPSS) in a mobile phase containing 0.2 and 0.8 M Na_2SO_4, with controlled pore glass (CPG) columns. They also obtained a single curve of $\log_{10}[\eta]\overline{M_w}$ as a function of V_e for all the studied polymers (where $[\eta]$ is the intrinsic viscosity and $\overline{M_w}$ is the weight average molecular weight of polymers). Cooper and Matzinger[19] studied the reference polymer NaPSS in a buffer of 0.01, 0.1 and 1.0 M phosphate and found universal calibration to be valid at high ionic strength (>0.1 M) for both non-ionic and anionic polymers. The universal calibration method was also reported successful by Rochas et al.[20] for the reference polymer NaPSS in 0.1 M $NaNO_3$, and by Klein and Westerkamp for NaPSS in 0.1 M Na_2SO_4.[21]

The first test for universal calibration was conducted by generating calibration curves consisting of a plot of the product of $[\eta]$ and $\overline{M_w}$ versus elution volume V_e.[8,17] Since then, the product of $[\eta]$ and $\overline{M_w}$ is often used in applications of universal calibration,[8,11,12,13,17,22] because $\overline{M_w}$ can be determined by light scattering accurately, while the accurate number average molecular weight ($\overline{M_n}$) is not available in many cases. For linear polymers, Hamielec and Ouano[23] pointed out that, the product $[\eta]\overline{M_w}$ is valid because the polymer in the detector cell is monodisperse, thus for a given V_e, $\overline{M_n}(V_e) = \overline{M_w}(V_e) = \overline{M_z}(V_e)$, (or approximately, when the polymer has a narrow molecular weight distribution[15]); For branched polymers, the hydrodynamic volume should be the product of $[\eta]$ and $\overline{M_n}$ instead of $\overline{M_w}$, that is, if a viscometry detector is connected with GPC, the molecular weight calculated from [η] should be $\overline{M_n}$.

In this work, the weight average molecular weights of PAM and some poly(AM/NaAA) were measured by light scattering. The polydispersity (PDI) of the polymers was estimated from the GPC data using poly(ethylene oxide) (PEO) as standards. Although the $\overline{M_n}$ of them can be calculated from the PDI and the $\overline{M_w}$, some overestimation of $\overline{M_n}$ would be expected since the calibration curve, $\log_{10}\overline{M_w}$ vs. V_e, was used. Therefore, in this work, a conventional way was adopted: $\overline{M_w}$ was used to test the validity of the universal calibration and to investigate the dependence of V_e on the $\overline{M_w}$ and the hydrolysis degree.

3.1.3 OBJECTIVE OF THIS WORK

The objective of this work was to investigate the validity of universal calibration for poly(AM/NaAA) and nonionic polyacrylamide (PAM), and therefore establish a methodology for molecular weight characterization of poly(AM/NaAA) by aqueous GPC. Poly(AM/NaAA) is a copolymer in addition to being a polyelectrolyte. Its hydrodynamic volume varies with NaAA content as well as salt concentration, which makes it more difficult for one to determine its molecular weight by aqueous GPC. In this study, a series of poly(AM/NaAA) samples were prepared by mild alkaline hydrolysis of fractionated PAM samples thus they had relatively homogeneous composition distribution,[24,25] and a narrow molecular weight distribution.[7] The heterogeneity in composition and molecular weight were therefore not considered important in assessing the validity of universal calibration.

3.2 THEORETICAL CONSIDERATIONS

Universal calibration method is based on Einstein viscosity theory and for spherical particles

$$[\eta] = 2.5 N_A (V_h / M) \tag{3.1}$$

where $[\eta]$ is the intrinsic viscosity, V_h the hydrodynamic volume of the particles, M their molecular weight, and N_A Avogadro's number. Rearranging Equation (3.1) one can get

$$[\eta] M = 2.5 N_A V_h \tag{3.2}$$

that is, $[\eta]M$ is proportional to hydrodynamic volume. Since GPC separates polymer molecules in the mobile phase on the basis of hydrodynamic volume, one would expect that $[\eta]M$ to be a function of elution volume V_e, $[\eta]M = f(V_e)$. In this correlation, the molecular weight M could be a simple molecular weight (for monodispersed polymers), or an average (for polydispersed polymers) as reviewed before.

According to this theory, all polymer molecules which have the same hydrodynamic volume elute at the same time. If this is true for the non-ionic polymer PAM and the ionic polymer poly(AM/NaAA), then at a given V_e the following equality holds:

$$[\eta]_o \overline{M_{w_o}} = [\eta]_x \overline{M_{w_x}} \tag{3.3}$$

where the subscript 'o' represents PAM, and 'x' represents poly(AM/NaAA) with various NaAA content (x could be said to represent the degree of hydrolysis of the PAM samples). If Equation 3.3 holds, the plot of logarithm of $[\eta]\overline{M_w}$ versus V_e for both polymers would drop on the same curve. This criterion was used in this work to test the validity of the universal calibration for poly(AM/NaAA) and PAM.

To investigate the dependence of V_e on the hydrolysis degree and $\overline{M_w}$, the correlation between $\overline{M_w}$ and V_e for PAM and poly(AM/NaAA) of various hydrolysis degree was analyzed. Theoretically, the peak elution volume corresponds to the geometric mean molecular weight $<M>_G$ ($<M>_G = \sqrt{\overline{M_w} \times \overline{M_n}}$). For monodispersed polymer, $<M>_G = \overline{M_w} = \overline{M_n}$; For narrowly distributed polymer, $<M>_G$ can be approximated by $\overline{M_w}$. Again, in many cases, $\overline{M_w}$ has been used due to the lack of accurate $\overline{M_n}$. In these cases, the $\overline{M_w}$ determined from the correlation of $\overline{M_w}$ and V_e is correct, but the $\overline{M_n}$ is overestimated.

The correlation of molecular weight with elution volume, for a single polymer over a considerable range of V_e, can often be written by:[26]

$$\overline{M_w}(V_e) = D_1 \exp(-D_2 V_e) \qquad D_1,\ D_2 > 0 \tag{3.4}$$

The plot of $\log_{10}\overline{M_w}$ against V_e gives a straight line

$$\log_{10}\overline{M_w} = D_1' - D_2' V_e \tag{3.5}$$

where $D_1' = \log_{10}D_1$, and $D_2' = 0.4343\,D_2$. Unlike the universal calibration curve, the coefficients D_1, D_2, D_1', D_2' vary with the type of polymer. One would expect different values for them as the hydrolysis degree changes in poly(AM/NaAA).

In this work, the effect of hydrolysis degree on the peak elution volume and on the coefficients was investigated.

3.3 EXPERIMENTAL

GPC measurement

Varian 5000 Liquid Chromatograph was used to determine the molecular weight and molecular weight distribution of the polymers in this work. Three TSK Type PW columns (Varian), G3000PW, G5000PW and G6000PW, each of which had diameter of 7.5 mm and length of 30 cm, were connected in series. These columns contained polyether gel packing with hydrophillic -OH groups on the surface.[27] One of the advantages of this gel was that the surface groups were neither charged, nor highly polar, therefore the adsorption and electrostatic interactions were greatly reduced.[16] The average pore sizes of the gels were 20 nm, 100 nm and > 100 nm for each column respectively. The concentration of eluting polymer fractions was determined by a differential refractometer (Varian, Series RI-3). An aqueous solution of 0.2 M Na_2SO_4 (ionic strength 0.6 M) was used as the mobile phase; the flow rate of which was 1 mL/min. The polymer solutions of 0.1% (w/v) were prepared from the dry polymer and the mobile phase. The reason for using the mobile phase as the solvent was to eliminate the salt peak. The polymer solution of 100 μL was injected for the analysis.

3.4 RESULTS AND DISCUSSION

This section presents and analyzes the investigation results of the universal calibration curve, the effect of charge density on the elution volume and on the correlation between molecular weight and elution volume.

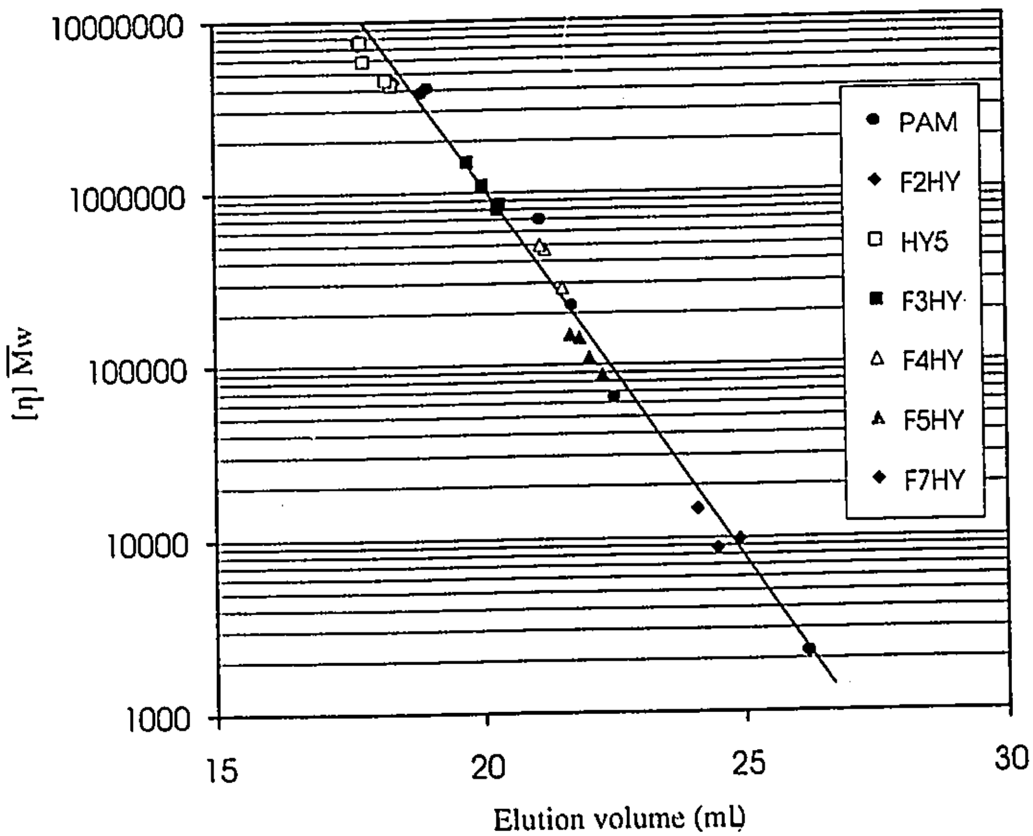

Figure 3.1 Logarithm of hydrodynamic volume versus elution volume for PAM and poly(AM/NaAA) of various hydrolysis degree

3.4.1 HYDRODYNAMIC VOLUME AND ELUTION VOLUME OF PAM AND POLY(AM/NaAA)

The $[\eta]\overline{M_w}$ of PAM and poly(AM/NaAA) is plotted against the peak elution volume on semi-log scale in Figure 3.1, where the values of $[\eta]$ were measured by viscometer, and those of the $\overline{M_w}$ were measured by light scattering for PAM, and calculated from Equation 2.7 for poly(AM/NaAA) (see Part A chapter 2). The data for both ionic and nonionic polymers show the same correlation between $\log_{10}[\eta]\overline{M_w}$ and elution volume. The universal calibration curve based on nonionic PAM seems to be a reasonable way to determine the molecular weights of poly(AM/NaAA). $\log_{10}[\eta]\overline{M_w}$ was correlated with V_e linearly in this work

$$\log_{10}[\eta]\overline{M_w} = C_1 - C_2 V_e \qquad C_1,\ C_2 > 0 \tag{3.6}$$

The values of the parameters C_1 and C_2 were found to be 14.59 and 0.4247 respectively with regression coefficient of 0.995:

$$\log_{10}[\eta]\overline{M_w} = 14.59 - 0.4247\,V_e \tag{3.7}$$

If the GPC column, as well as the column conditions are the same, one could expect that the data points would drop on the curve expressed by the above equation, no matter what kind of polymer is analyzed.

3.4.2 EFFECT OF CHARGE DENSITY ON ELUTION VOLUME

Figure 3.2a and Figure 3.2b present the GPC chromatograms for PAM and poly(AM/NaAA) with various hydrolysis degree for two molecular weight fractions (F5HY,

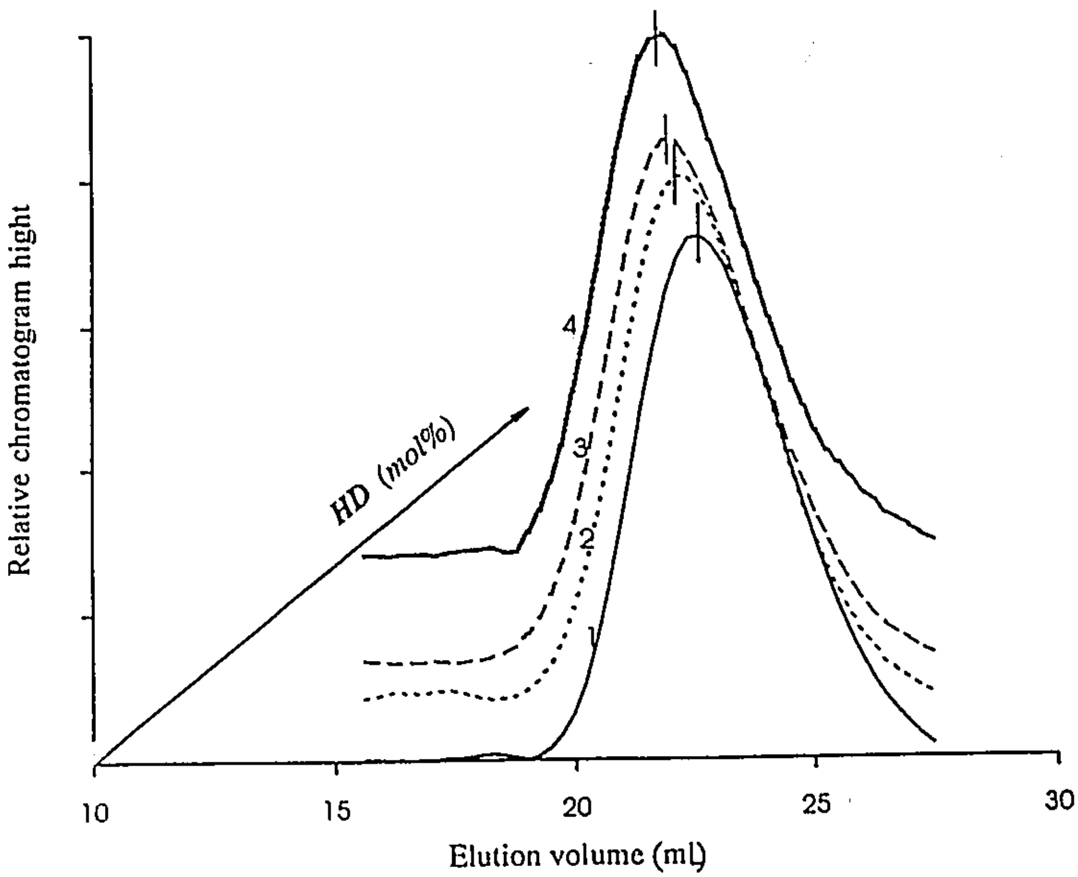

Figure 3.2a Effect of hydrolysis degree on elution volume for F5HY
(Curve 1: HD = 0; 2: 10.3%; 3: 16.6%; 4: 34.4%)

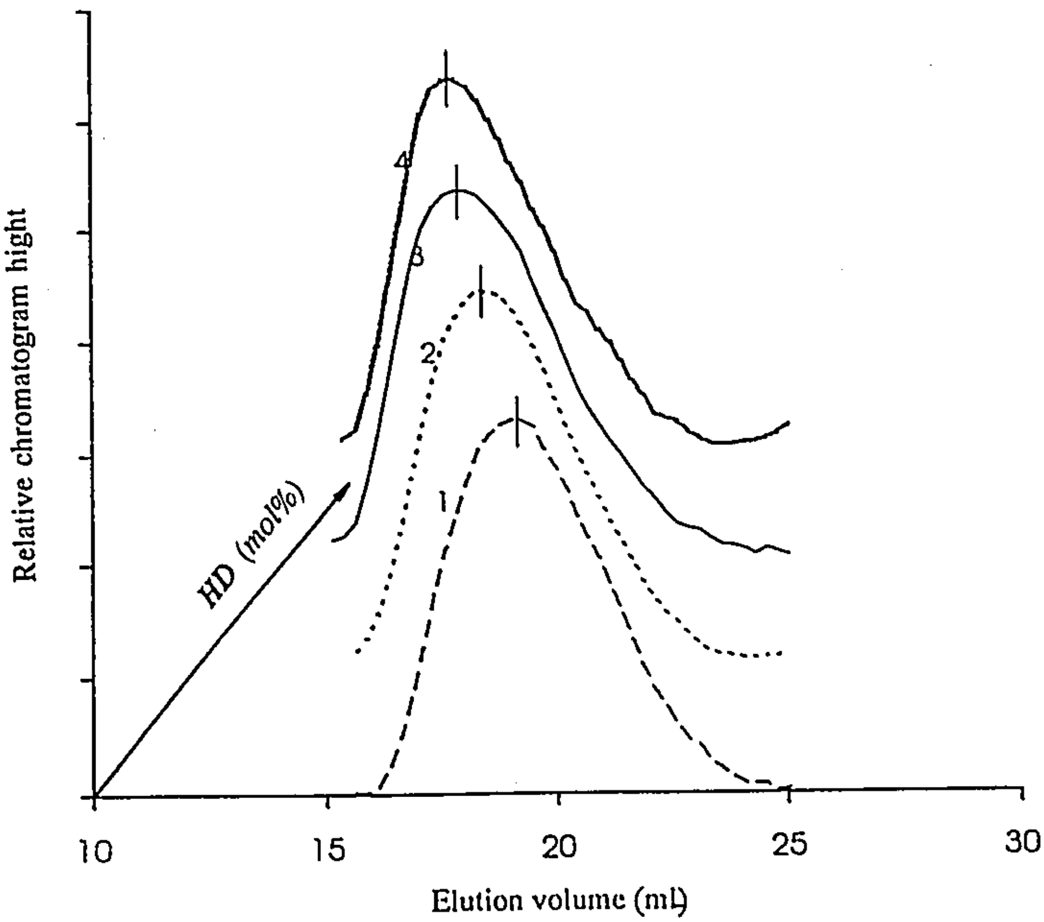

Figure 3.2b Effect of hydrolysis degree on elution volume for HY5
(Curve 1: *HD* = 0; 2: 11.5%; 3: 19.8%; 4: 30.8%)

chain length r: F5HY r = 1393; HY5, r = 13928). It can be seen that when the hydrolysis degree (or charge density) was increased, the GPC curve was shifted to lower elution volumes indicating a higher hydrodynamic volume. This is expected when expansion of the polymer coil occurs due to electrostatic repulsion which is consistent with the observation that intrinsic viscosity increases with charge density (see Part A Chapter 2 and Ref.17 for details). A clearer picture of how V_e changing with composition is given in Figure 3.3a. The V_e decreased with increasing contents of NaAA for all the fractions of different chain lengths. To compare all the fractions, the normalized elution volume $\hat{V}_e$ was defined as the V_e at various HD divided by the V_e at HD = 0 (i.e., PAM), $\hat{V}_e = V_{ex}/V_{eo}$. Figure 3.3b illustrates the dependence of $\hat{V}_e$ on the NaAA content. This figure shows that the $\hat{V}_e$ of fractions of higher chain length (curves 4, 5, 6) tended to decrease with NaAA content more rapidly than the fractions of smaller chain length (curves 1, 2, 3).

3.4.3 RELATIONSHIP BETWEEN $\overline{M_w}$ AND V_e FOR PAM AND POLY(AM/NaAA)

Figure 3.4 is a plot of logarithm $\overline{M_w}$ of nine nonionic PAM samples versus elution volume. A linear relationship was obtained with regression coefficient 0.998:

$$\log_{10}\overline{M_{w_o}} = 10.78 - 0.2505\,V_e \tag{3.8}$$

i.e., $D_1' = 10.78$, $D_2' = 0.2505$ for PAM in the studied region.

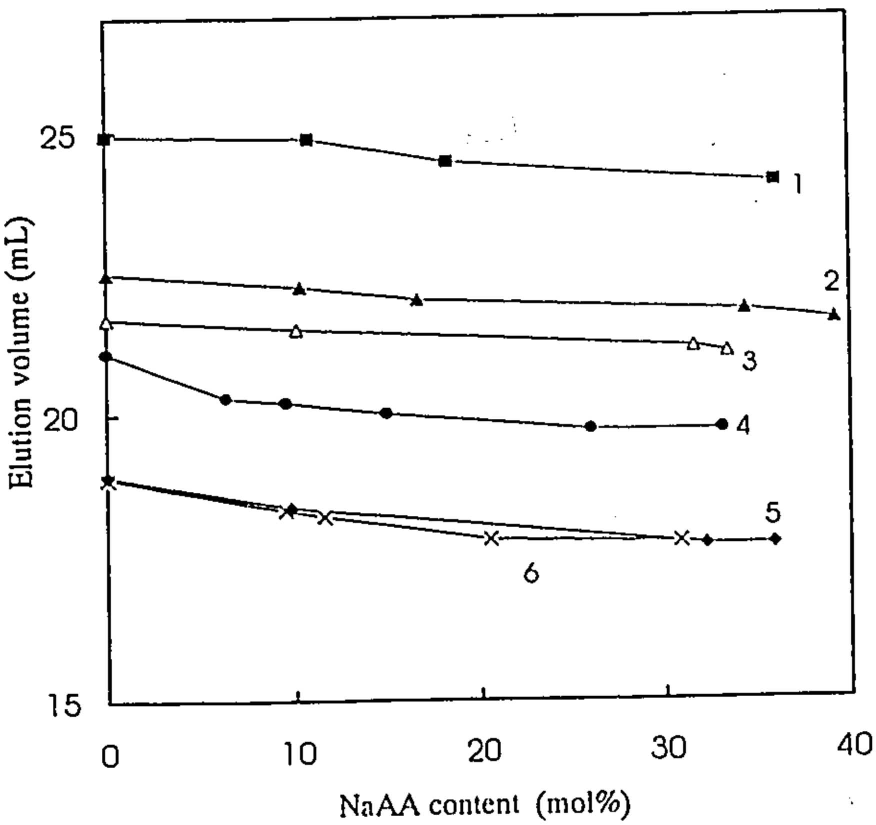

Figure 3.3a : Dependence of peak elution volume on copolymer composition for various molecular weight fraction. chain length r: curve 1, r=378; 2, r=1393; 3, r=2828; 4, r=5642; 5, r=13928; 6, r=14209

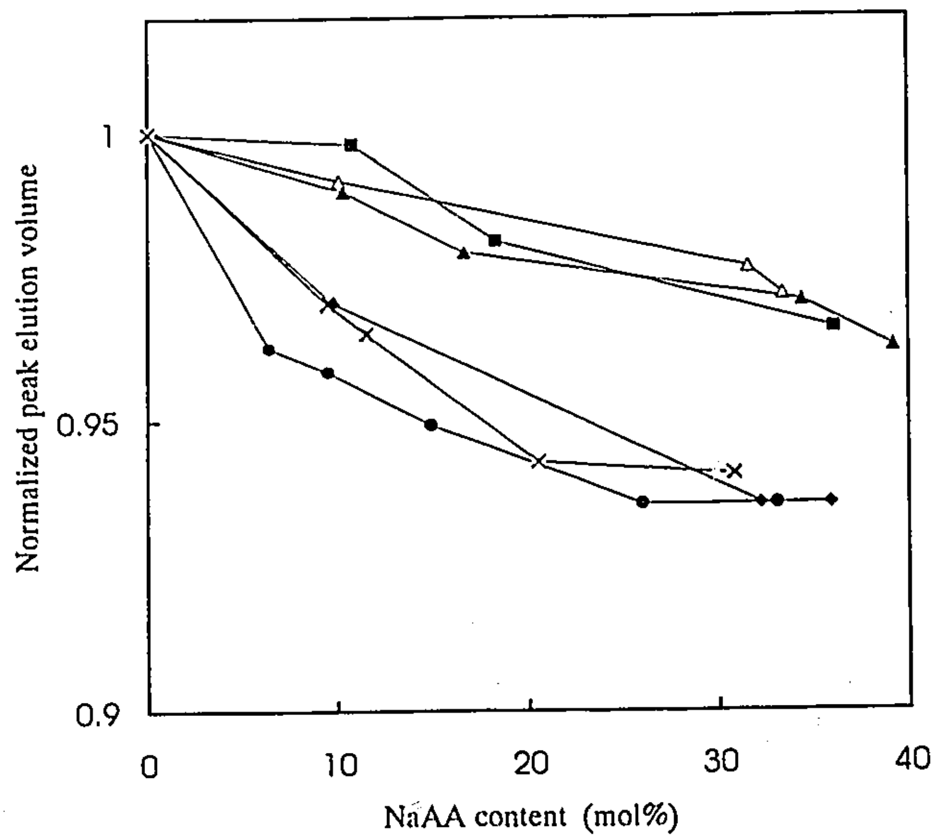

Figure 3.3b Normalized peak elution volume versus NaAA content of poly(AM/NaAA). The chain length of each curve is given in Figure 3.3a.

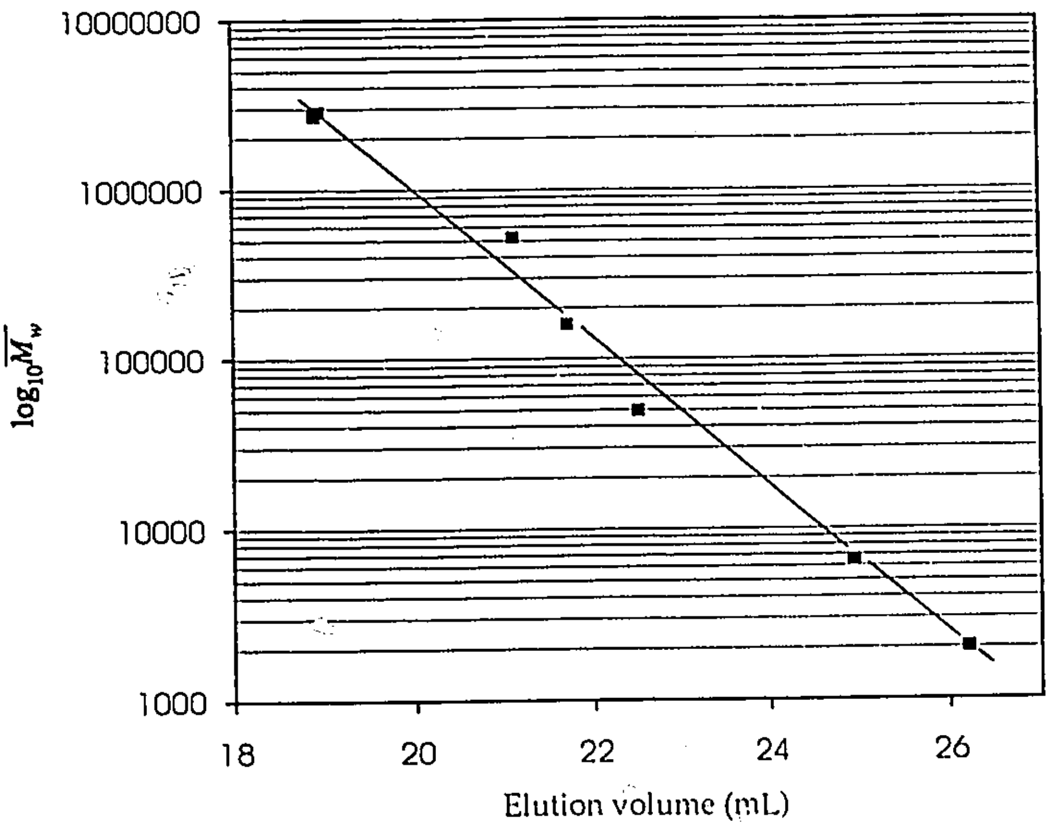

Figure 3.4 Logarithm of weight average molecular weight of PAM versus peak elution volume

To find the relationship between $\overline{M_w}$ and V_e for poly(AM/NaAA) of various NaAA content, some derivation and calculations were conducted. The reason for this was that it was difficult to prepare the poly(AM/NaAA) samples which had different $\overline{M_w}$ but had the same hydrolysis degree or vice versa. The equation for calculating V_{e_x} was derived as the follows:

(1) Applying Equation 3.6 for both PAM and poly(AM/NaAA):

$$\log_{10}[\eta]_o\overline{M_{w_o}} = C_1 - C_2 V_{e_o} \tag{3.9}$$

$$\log_{10}[\eta]_x\overline{M_{w_x}} = C_1 - C_2 V_{e_x} \tag{3.10}$$

(2) Subtracting Equation 3.9 from 3.10

$$\log_{10}[\eta]_x\overline{M_{w_x}} - \log_{10}[\eta]_o\overline{M_{w_o}} = C_2(V_{e_x} - V_{e_o}) \tag{3.11}$$

(3) Rearranging Equation 3.11

$$V_{e_x} = V_{e_o} + \frac{1}{C_2}(\log_{10}[\eta]_x\overline{M_{w_x}} - \log_{10}[\eta]_o\overline{M_{w_o}}) \tag{3.12}$$

(4) Substituting Mark-Houwink equation to Equation 3.12

$$V_{e_x} = V_{e_o} + \frac{1}{C_2}(\log_{10}k_x\overline{M_{w_x}}^{a_x+1} - \log_{10}k_o\overline{M_{w_o}}^{a_o+1}) \tag{3.13}$$

where the subscript 'o' represents PAM, and 'x' represents poly(AM/NaAA). The values of a_x, k_x for poly(AM/NaAA) with various copolymer composition can be calculated from the following empirical correlations (see Part A Chapter 2):

$$a_x = 0.625 + 8.86\times10^{-3}HD - 2.405\times10^{-4}HD^2 + 2.48\times10^{-6}HD^3 \qquad (3.14)$$

$$\log_{10}k_x = -3.36 - 2.39\times10^{-2}HD + 6.96\times10^{-4}HD^2 - 7.37\times10^{-6}HD^3 \qquad (3.15)$$

where HD is the hydrolysis degree or NaAA content in mole percent, and x is the NaAA content in mole fraction ($x = HD/100\%$).

The stoichiometric weight average molecular weight of poly(AM/NaAA) can be calculated by the following equation assuming that the poly(AM/NaAA) samples have the same chain length as the parent polymer, PAM samples (the fractionated PAM before hydrolysis)

$$\overline{M_{w_x}} = \frac{\overline{M_{w_o}}}{71.08}(94.04x + 71.08(1 - x)) \qquad (2.7)$$

where $\overline{M_{w_o}}$ is the molecular weight of the parent PAM sample.

The elution volume of poly(AM/NaAA) for various values of HD was computed using Equations 3.13 - 3.15. And the molecular weights were calculated from Equation 2.7. These values of V_e and $\overline{M_{w_x}}$ were then used to obtain the correlation between $\overline{M_{w_x}}$ and V_e. Figure 3.5 is the plot of $\log_{10}\overline{M_{w_x}}$ versus V_e for poly(AM/NaAA) of various HD. The parameters D_1', D_2' were estimated by regression of the curves in this figure.

The dependence of parameters D_1', D_2' on the HD is shown in Figures 3.6. The values of D_1' were higher than those for PAM when the HD was less than approximately 8 mol%. The

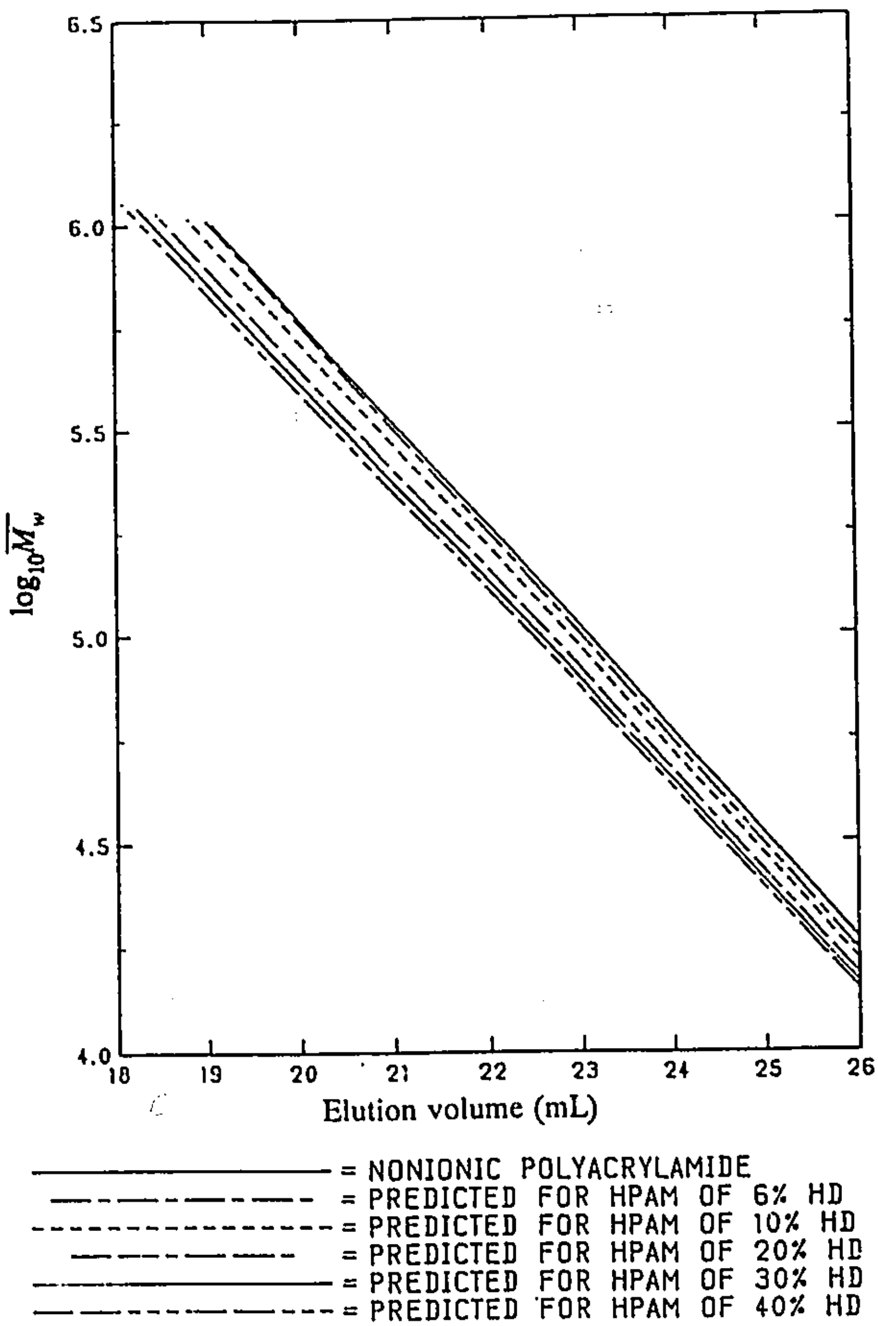

Figure 3.5 Calculated logarithm of weight average molecular weight versus peak elution volume for PAM and poly(AM/NaAA) of various hydrolysis degree

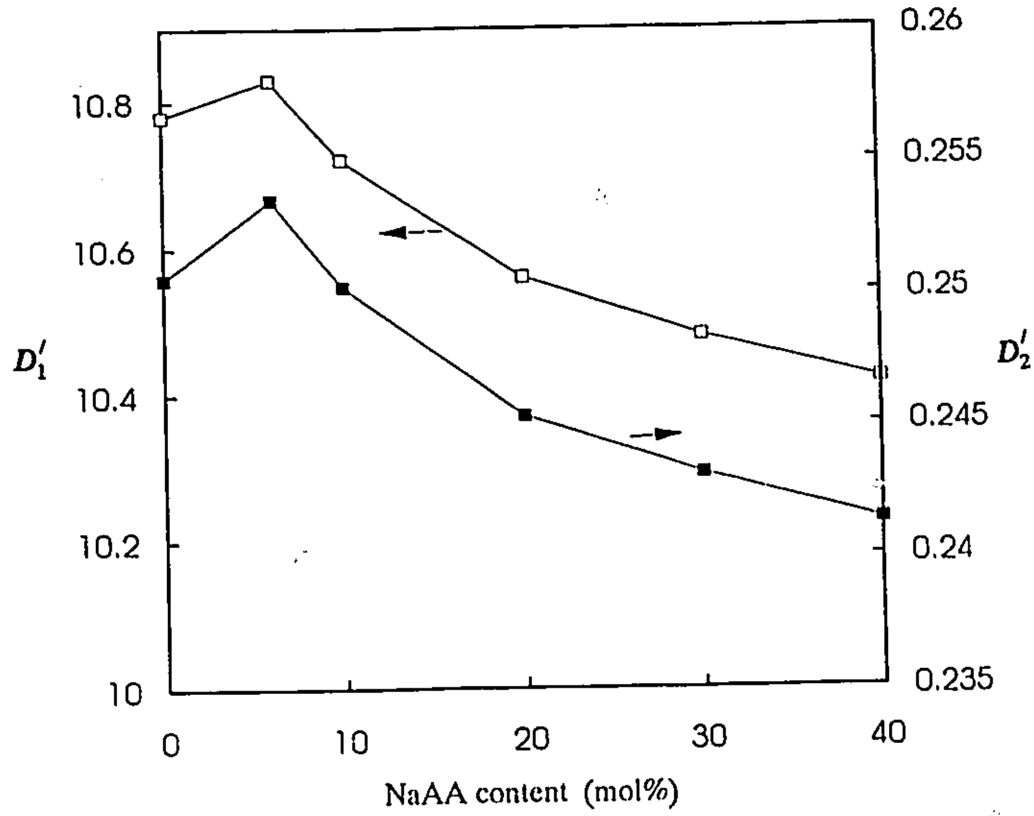

Figure 3.6 Dependence of parameters D_1' and D_2' on the NaAA content of poly(AM/NaAA)

parameter D_2' showed trends similar to D_1'. When the HD was higher than 8 to 9 %, however, both D_1' and D_2' decreased with HD. This decrease can be described by the following empirical equations (HD > 9%):

$$D_1' = 11.22 - 0.5005\log_{10}HD \qquad (\gamma = 0.9985) \qquad (3.16)$$

$$D_2' = 0.2650 - 0.0148\log_{10}HD \qquad (\gamma = 0.9994) \qquad (3.17)$$

where γ is the regression coefficient.

If the NaAA content in poly(AM/NaAA) is known and the elution volume is measured, one can apply Equations 3.16 and 3.17 to find coefficients D_1', D_2', and then calculate $\overline{M_{w_x}}$ by using Equation 3.5.

It is worthy to notice that the Mark-Houwink constant a had similar trend as D_1', D_2' did according to the previous work.[17] The value of a was also higher for PAM than poly(AM/NaAA) of NaAA < ~ 9 %. These observations may be explained as follows: Without NaAA, PAM molecules have extended segments of oriented structure from intramolecular hydrogen bonds between C=O and NH_2 groups, according to Kulicke et al.[28]. With low NaAA content the oriented structure of PAM was partly reduced due to the lack of NH_2 groups; in the meantime the number of ionic COO^- group was not great enough to generate an electrostatic expansion. Therefore the hydrodynamic size of poly(AM/NaAA) was smaller than that of PAM. When the NaAA content was higher than 8 to 9 mol%, the COO^- groups start to "feel" one another. Thus the polymer chains expanded more when the NaAA content increased.

3.4.4 COMPARISON OF PREDICTIONS WITH EXPERIMENTAL DATA

The calculated elution volume for poly(AM/NaAA) of various NaAA content was compared with the values by experiments. Also, the molecular weights determined by light scattering and by stoichiometric calculation were compared with the prediction by the correlation of $\log_{10}\overline{M_{w_x}}$ with V_e.

(i) Prediction of Elution Volume Shift due to Hydrolysis Degree

The predicted elution volume for poly(AM/NaAA) of various NaAA content was calculated using Equation 3.13. The predicted V_{x_e} and the experimental data of F5HY and F3HY are listed in Table 3.1. It is seen that the agreement was good.

(ii) The Calculated Molecular Weights

The logarithm weight average molecular weights of poly(AM/NaAA) with HD = 10% and 30% were computed by using Equations 3.16, 3.17 and 3.5. The elution volume of the polymers was obtained from Equation 3.13. The calculated $\log_{10}\overline{M_{w_x}}$ and V_e are plotted in Figure 3.7, together with the experimental data. Because of the difficulty in preparing the poly(AM/NaAA) with exact values of HD, 10% and 30%, only 3 samples were examined although many samples were analyzed. Figure 3.7 shows a fairy good agreement between the prediction and the experiments.

Table 3.1 Comparison of predicted and measured elution volume

sample	chain length r	HD (mol%)	$V_{e\ meas}$	$V_{e\ cal}$	deviation %
F5HY	1393	0	22.797	22.79699	
		10.3	22.539	22.49307	- 0.20378
		16.7	22.313	22.25455	- 0.26197
		34.4	22.068	21.97841	- 0.40599
		39.2	21.908	21.93440	+ 0.12049
F3HY	5642	0	20.781	20.781	
		6.4	20.545	20.63441	+ 0.43518
		9.53	20.530	20.56593	+ 0.17501
		14.9	20.198	20.3025	+ 0.51736
		23.2	19.831	20.0665	+ 1.18754
		26.0	19.864	19.9885	+ 0.62675
		33.1	19.793	19.99638	+ 1.02752
				Average	0.50 ± 0.36

3.4.5 DISCUSSION

In the application of equations derived in this work, other polymers other than PAM may be used as standards. For example, an ionic poly(AM/NaAA) sample with known molecular weight and NaAA content can be employed as the reference. In this case, the subscript 'o' in Equations 3.9, 3.11 - 3.13 will represent the reference poly(AM/NaAA). The procedures to estimate the elution volume of unknown sample is the same as described before. The molecular weight of the sample can also be calculated from the universal calibration curve.

For samples with both broad distributions of molecular weight and charge density, additional corrections may be needed because $V_e \propto [\eta], [\eta]M - f(x), \partial[\eta]/\partial x - f(M)$. For poly(AM/NaAA) prepared by copolymerization in a batch reactor, heterogeneity in chemical

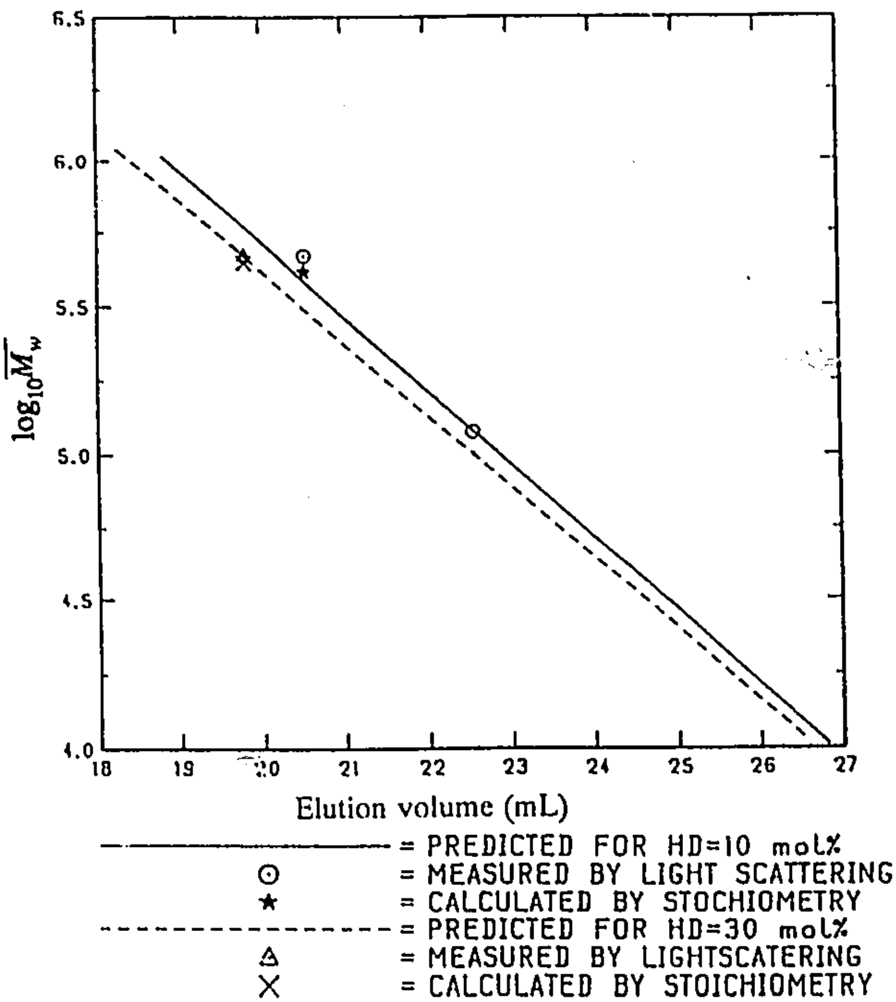

Figure 3.7 Comparison of predicted $\log_{10}\overline{M_{w_x}}$ - V_e correlation with the experimental data for poly(AM/NaAA)

composition, such as, NaAA content, can vary in different polymer molecules. In these cases, multiple detectors and/or orthogonal chromatography may be needed to give valid molecular weight measurement.[18]

3.5 CONCLUSION

Universal calibration method is valid for the estimation of molecular weight of ionic poly(AM/NaAA) using nonionic PAM as secondary standards. The molecular weight of poly(AM/NaAA) can be determined either by direct application of the universal calibration method, i.e., using equation $\overline{M_{w_x}} = \alpha \overline{M_{w_o}}^{\beta}$, or by use of the correlation found in this work,

$$\overline{M_{w_x}} = D_1(x)\exp[-D_2(x)V_e].$$

References

1. B. Stenlund, "Polyelectrolytes Effects in Gel Chromatography", in Advances in Chromatogr. 14, 37-74 (1976)

2. A.R. Cooper and D.S.Van Derveer, J. Liq. Chromatogr. 1, 693-726 (1978)

3. H.G. Barth, J. Chromatogr. Sci. 18, 409-429 (1980)

4. H.G. Barth, "Characterization of Water-Soluble Polymers Using Size-Exclusion Chromatography", in Adv. Chem. Ser. (Am. Chem. Soc.), **213**, 31-55 (1986)

5. H.G. Barth, "Nonsize Exclusion Effects in High-Performance Size Exclusion Chromatography", in ACS Symp. Ser. (Am. Chem. Soc.), **352**, 29-46 (1987)

6. P.P. Nefedov, M.A. Lazareva, B.G. Belenskii, S.Ya. Frenkel, and M.M. Morton, J. Chromatogr. 11, 170 (1979)

7. X.Y. Wu, D. Hunkeler, A.E. Hamielec, R.H. Pelton and D.R. Woods, "Molecular Weight Characterization of Poly(acrylamide-co-sodium acrylate) I. Viscometry, J. Appl. Polym. Sci., 42, 2081-2093 (1991)

8. Z. Grubisic, P. Rempp and H. Benoit, Polymer Letters, 5, 753-759 (1967)

9. J.E. Rollings, A. Bose, J.M. Caruthers, G.T. Tsao, and M.R. Okos, "Aqueous Size Exclusion Chromatography", in Adv. Chem. Ser. (Am. Chem. Soc.), **203**, 345-360 (1983)

10. L.H.G. Rubio, J.F. MacGregor and A.E. Hamielec, "Size Exclusion Chromatography of Copolymers", in Adv. Chem. Ser. (Am. Chem. Soc.), **203**, 311-344 (1983)

11. M. Duval, J. Francois and D. Sarazin, Polymer, **26**, 397-405 (1985)

12. C. Rochas, A. Domard and M. Rinaudo, Eur. Polym. J. **16**, 135-140 (1980)

13. A.L. Spatorico and G.L. Beyer, J. Appl. Polym. Sci. **19**, 2933-45 (1975)

14. S. Mori, Anal. Chem. **53**, 1813-18 (1981)

15. G.N. Foster, T.B. MacRury and A.E. Hamielec, *in Liquid Chromatography of Polymers and Related Materials II*, ed. by J. Cazes and X. Delamare, Marcel Dekker (1980)

16. A. Hamielec and M. Styring, Pure & Appl. Chem. **57**(7), 955-970 (1985)

17. H. Benoit, Z. Grubisic and P. Rempp, J. Polym. Sci. Part B, **5**, 573 (1967)

18. W.M. Yau, J.J. Kirkland and D.D. Bly, *Modern Size Exclusion Liquid Chromatography*, Wiley-Interscience, New York (1979)

19. A.R. Cooper and D.P. Matzinger, J. Appl. Polym Sci. **23**, 419-427 (1979)

20. C. Rochas and M. Rinaudo, Eur. Polym. J. **16**, 135-140 (1980)

21. J. Klein and A. Westerkamp, J. Polym. Sci. Polym. Chem. **19**, 707-718 (1981)

22. M.G. Styring, J.E. Armonas and A.E. Hamielec, Polym. Mater. Sci. Eng. **54**, 88 (1986)

23. A.E. Hamielec and A.C. Ouano, J. Liq. Chromatogr. **1**, 111 (1978)

24. F. Halverson, J.E. Lancaster and M.N. O'Conner, Macromolecules, **18**, 1139-1144 (1985)

25. N.D. Truong, J.C. Galin and J. Francois, Polymer, **27**, 459-466; 467-475 (1986)

26. A.E. Hamielec and W.H. Ray, J. Appl. Polymer. Sci. **12**, 1319-1321 (1969)

27. T. Hashimoto, H. Sasaki, M. Aiura and Y. Kato, J. Polym. Sci. Polym. Phys. Ed. **16**, 1789-1800 (1978)

28. W.M. Kulicke, R. Kniewske and J. Klein, Prog. Polym. Sci., **8**, 373-468 (1982)

APPENDIX A-1

Preparation of Polyacrylamide on Pilot Scale

The polyacrylamide (PAM) used in this research was prepared on pilot scale. A typical recipe is listed in Table A.1.

Table A.1 Recipe for acrylamide polymerization

Acrylamide (50% solution)	DDI water*	Versenex 100 (40% solution)	$K_2S_2O_8$	Ethanol mercapton
3000 g	4300 g	5.1 g in 50 mL DDI water	0.6 g in 100 mL DDI water	10.8 g in 50 mL DDI water

* DDI water means distilled and deionized water.

The acylamide solution, Versenex 100, ethanol mercapton, and DDI water were added to an 8 L stainless steel reactor. The solution was then heated to 55 °C and purged with N_2 for half an hour. The polymerization was started by the addition of $K_2S_2O_8$ solution. The mixture was stirred for 3 hours with the temperature control at 55 - 60 °C.

APPENDIX A-2

Evaluation of the Methods for Analysis of Hydrolysis Degree

A. Atomic Absorption Spectroscopy

The hydrolysis degree (HD) of hydrolysed polyacrylamide (HPAM) was determined by atomic absorption spectroscopy from the Na content. The results were about 20% lower than that determined by titration. This might infer a loss of Na^+ from HPAM during washing with methanol. A test of the Na content in one sample before immersing and after immersing supported this hypothesis.

However, a comparison of internal and external standard methods revealed that the viscosity of the polymer solution may influence the flow rate of the solution, and thus affect the analysis result. In the external standard method, the calibration curve was obtained from a series of NaCl solutions of known concentration, while in the internal method, various amounts of NaCl were added to HPAM solution (containing 10 - 50 ppm HPAM) and the Na content in HPAM was determined from the intercept of the calibration curve. The relative viscosity (viscosity of HPAM solution divided by that of DDI water) of the HPAM solution was measured with a Cannon-Ubbelohde viscometer. The deviation of hydrolysis degree from two methods, G, was defined as:

$$G = \frac{HD - HD^*}{HD^*}$$

where HD is the hydrolysis degree by the internal method, and HD^* is by the external method. The dependence of G on the relative viscosity of HPAM solution is plotted in Figure A-2.1. It is seen that the higher the viscosity, the larger the deviation.

B. Effect of Salt and Salt Concentration on Conductometric titration

A test for the effect of salt and salt concentration was done with a HPAM sample (HY7-3) in DDI water, 1.3×10^{-3} M, 2.6×10^{-3} M, and 7.8×10^{-3} M KCl. The titration curves are compared in Figure A-2.2. The results show that the titration in 2.6×10^{-3} M KCl gives sharpest plateau region, but lower (1.3×10^{-3} M) and higher (7.8×10^{-3} M) KCl concentration give worse result, and DDI water is in the order of middle. Therefore, 2.6×10^{-3} M KCl was used for the titration.

C. Comparison of Conductometric Titration with Potentiometric Titration

An evaluation of conductometric titration and potential titration was conducted using four HPAM samples. The hydrolysis degree of these samples determined by both methods and the standard deviation are listed in Table A-2.1.

Table A-2.1 Comparison of reproducibility of conductometric titration with potential titration

Sample	HD (mol%) from		Standard deviation from	
	Conduct.	Potent.	Conduct.	Potent.
HY6-3	14.2 15.5	13.3 16.7	0.92	2.40
HY6-6	34.4 32.9	31.5 34.8	1.06	2.33
HY7-1	10.08 9.27	9.36 7.47	0.57	1.34
HY7-3	31.6 31.7 32.3	21.5 26.7 20.4	0.38	3.37
	Average		0.73	2.36

Conductometric titration had better reproducibility than that of potentiometric titration.

Figure A-2.1 Deviation of hydrolysis degree from two methods versus the relative viscosity of HPAM solution

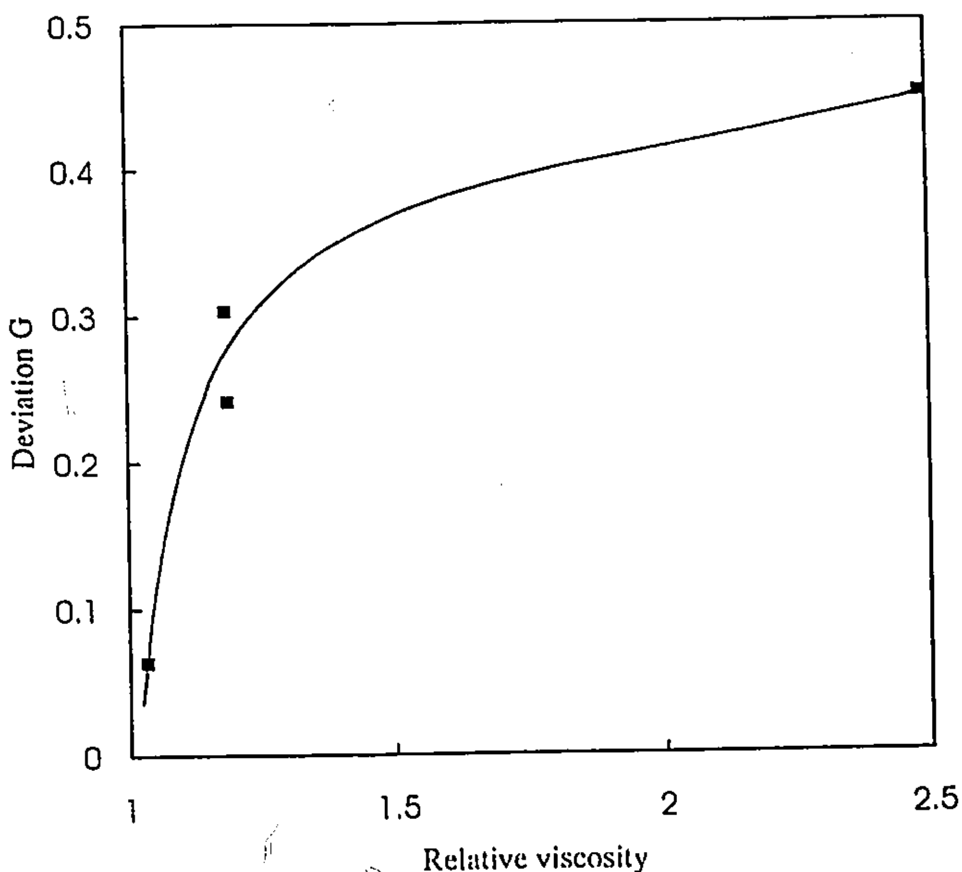

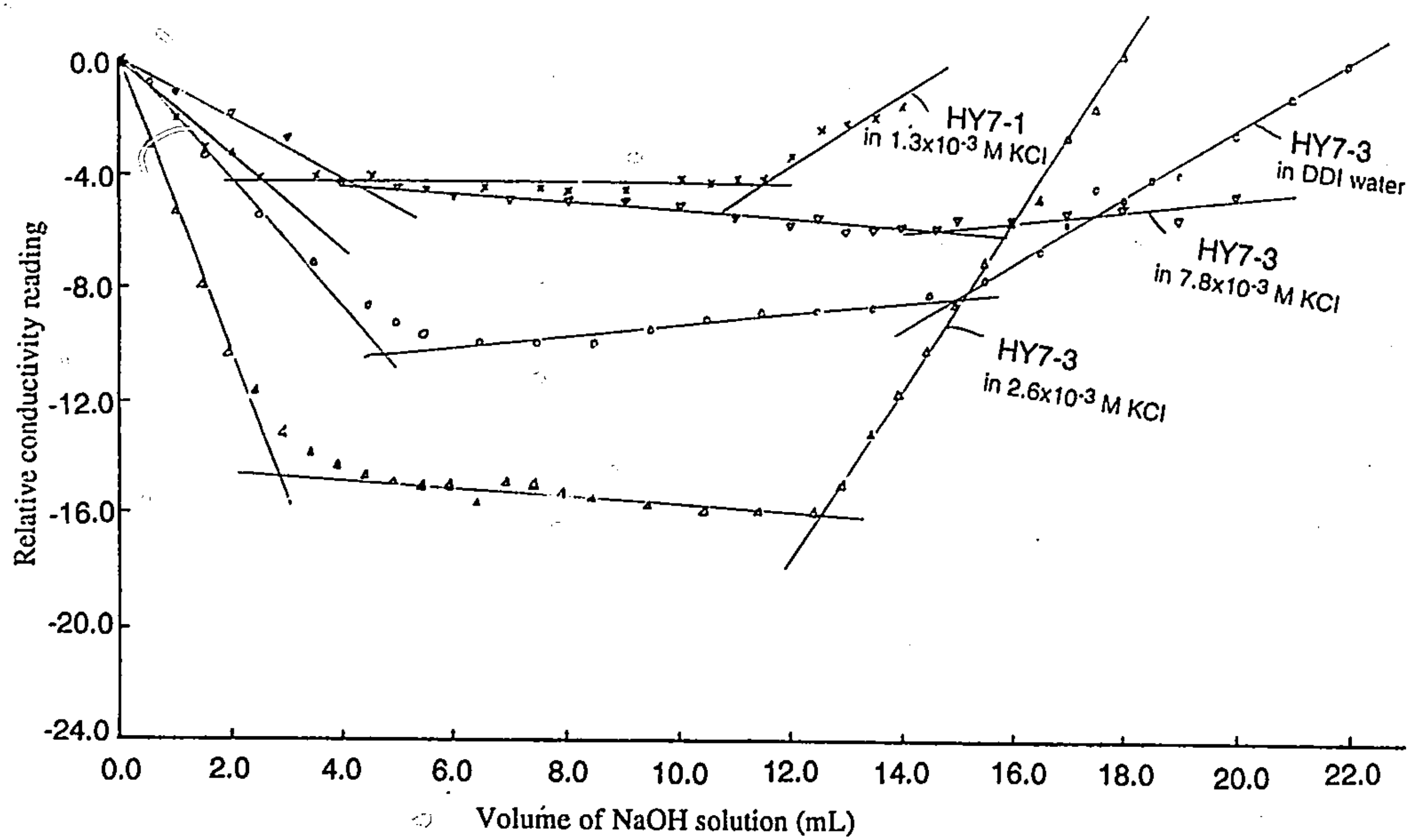

Figure A-2.2 Effect of KCl concentration on the conductivity titration curve of HPAM solution

APPENDIX A-3

Determination of Type and Amount of Non-solvent Needed for Large Scale Fractionation of Polyacrylamide

In order to find a better non-solvent for large scale (50 L) fractionation of PAM, and to determine the amount of non-solvent needed to "just precipitate" the first fraction, two sets of experiments were conducted on small scale (10 ~ 20 mL). In these experiments, non-solvents, methanol, acetone, or propanol were added dropwise to 5 - 10 mL PAM aqueous solutions (0.2 ~ 5 %) with a burette (reading up to 0.005 mL). The minimum volume fraction of non-solvent needed to cause polymer precipitation, γ value, was determined by measuring the turbidity with a UV-Vis spectrophotometer (Spectronic 20).

The change of turbidity with the volume fraction of non-solvents in the whole mixture is plotted in Figures A-3.1. The γ value for three non-solvents were read from the curves as volume fractions where the turbidity just started to increase dramatically: $\gamma_{isopropanol}$ = 0.32, $\gamma_{acetone}$ = 0.34, and $\gamma_{methanol}$ = 0.42. Therefore, the order of the non-solvents for precipitating PAM from aqueous solution was: isopropanol > acetone > methanol. However, it seemed that acetone was superior to the other two non-solvents since the polymer precipitated by addition of acetone was readily settled to give a clearer supernatant. Although methanol was the weakest of three, there are some advantages when methanol is used to fractionate the polymer: (1) The amount of precipitated polymer was smaller, which gave more scope for subsequent fractionation; (2) It was easier to control the volume added beyond the γ value. Therefore, a combination of acetone and methanol was tested. Acetone was added to 4% PAM water solution to reach a volume fraction of acetone = 0.3 (just below turbid point 0.34), followed by addition of methanol. Figure A-3.2 compares the change of turbidity with volume fraction of non-solvent for 1. methanol added to PAM water/acetone solution, 2. acetone added to PAM water solution. Case 1 shows less abrupt change before and after turbid point.

The first fraction obtained from the three non-solvents was purified and then dried for GPC measurement. GPC chromatograms showed that the fraction obtained with acetone was relatively narrower.

Based on the above results, acetone and methanol were selected as non-solvents to fractionate PAM samples on large scale. To obtain the first fraction, a slow stage of addition of methanol was applied after a fast addition of acetone to PAM water solution. For the subsequent fractions, however, acetone was used to reduce the consumption of non-solvent.

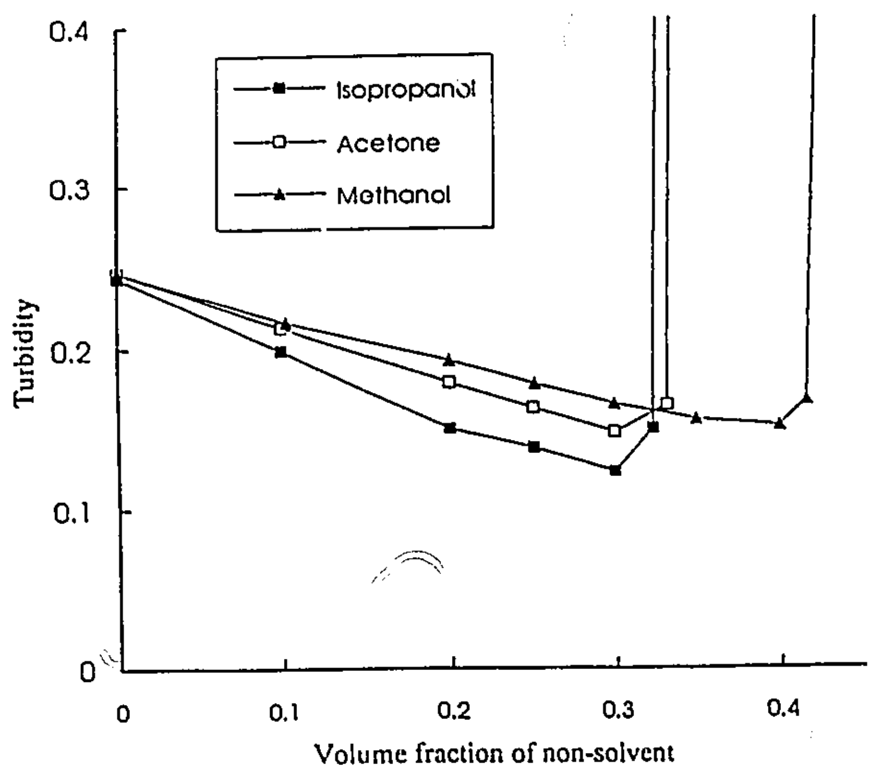

Figure A-3.1: Turbidity of PAM solution varies with volume fraction of non-solvent. 2% PAM (Mw = 1.1×10^6) water solution titrated with various non-solvents at room temperature

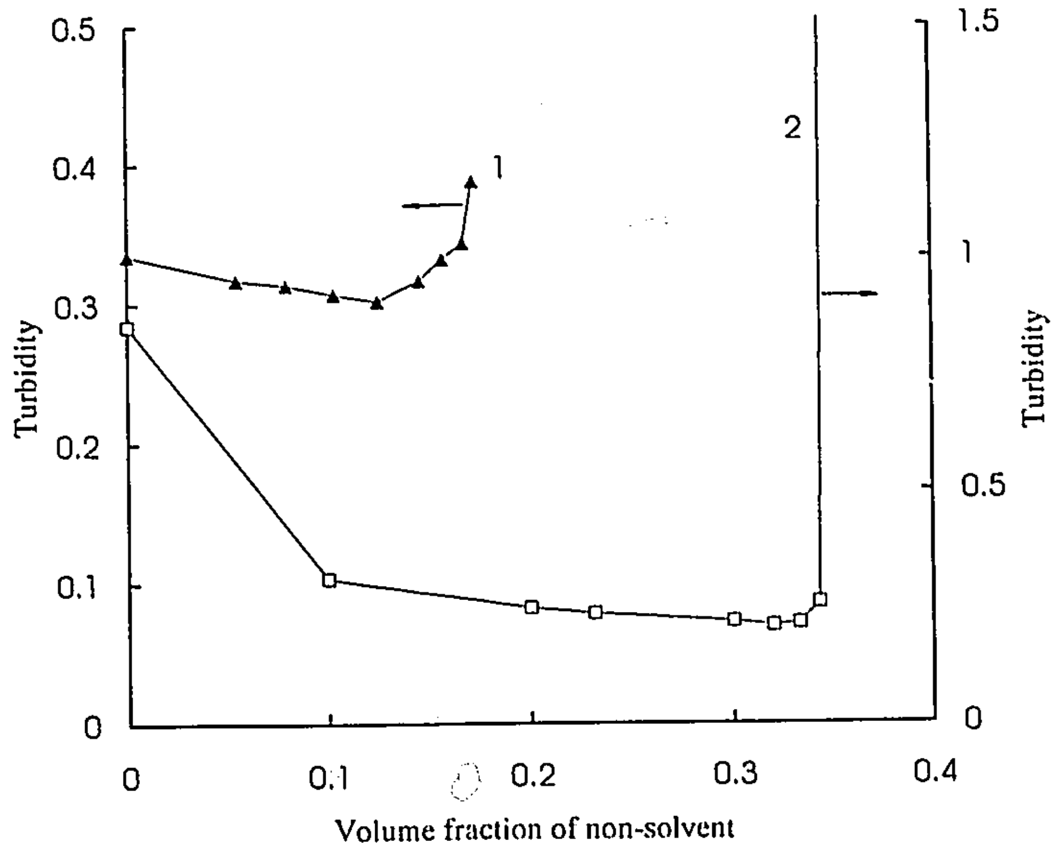

Figure A-3.2 Turbidity of PAM solution versus non-solvent volume fraction. Curve 1: 4% PAM water/acetone solution (acetone volume fraction=0.3) + methanol; Curve 2: 3% PAM water solution + acetone

APENDIX A-4

Huggins' Constant and Hydrolysis Degree

To describe the relationship between the viscosity of a polymer solution and the polymer concentration, Huggins (1942)[1] derived a viscosity equation from a modified Stokes' law, to account for the interaction of solvent with solute:

$$\frac{\eta_{sp}}{C} - \left(\frac{\eta_{sp}}{C}\right)_{C\to 0} + k'\left(\frac{\eta_{sp}}{C}\right)^2_{C\to 0} C$$

where k' is called Huggins' constant which depends on the sizes, shapes and cohesional properties of both solvent molecules and solute submolecules, but does not depend on the length of the solute molecuie chain. Therefore, k' is a characteristic of a given solute-solvent system. It should be the same for solutions of different members of a homologous-polymer series in a given solvent. This was supported by Schulz and Blaschke's (1941)[2] experimental results who found the same value of k' (0.30) to be satisfactory for unfractionated and fractionated poly(Methyl Methacrylate) of various sizes in chloroform.

Later, however, many authors reported the dependence of k' on many factors, such as, molecular weight[3,4,5] and molecular weight distribution,[6] chain branching,[4,6] comformation

---

[1] M.L. Huggins, J. Am. Chem. Soc. 64, 2716 (1942)

[2] G.W. Schulz and F. Blaschke, J. Prakt. Chem. 158, 130 (1941)

[3] W.-M. Kulicke, R. Kniewske and J. Klein, Prog. Polym. Sci. 8, 373-468 (1982)

[4] W.-M. Kulicke and H.-H. Höri, Coll. Polym. Sci. 258, 817 (1980)

of polymer (hydrogen bonding, stiffness),[6] shear rate,[6] solvent,[5,6] and the content of ionic groups.[7]

In the present work, a clear trend of k' decreasing with an increase in hydrolysis degree was observed for PAM fractions of different molecular weights. Figure A-4.1 is the plot of Huggins' constant vs. hydrolysis degree. This trend is in agreement with Klein and Heitzmann's results,[7] but is opposite to the theoretical prediction of Itskovich and Kabo's.[8]

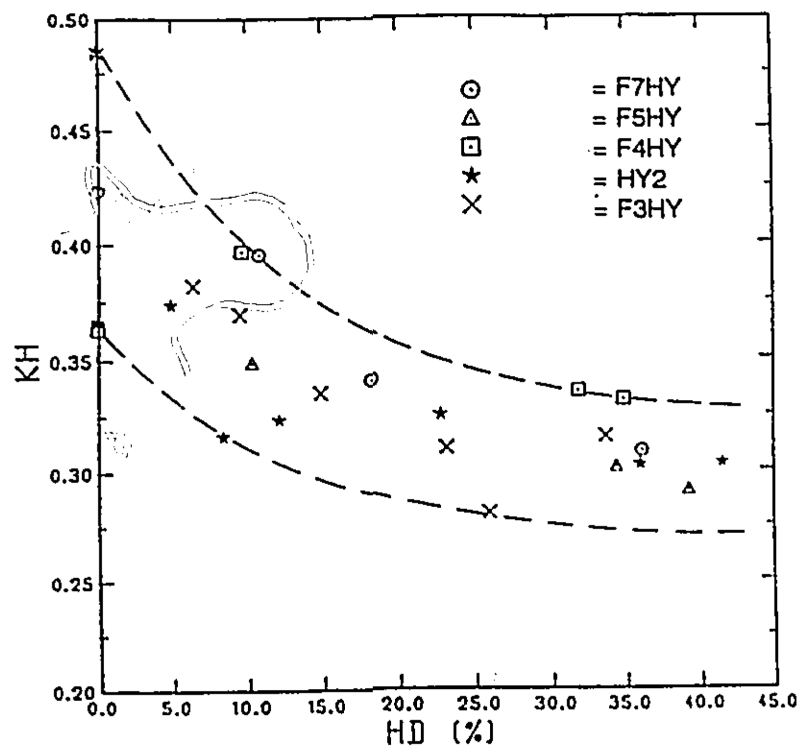

Figure A-4.1: Huggins constant versus hydrolysis degree of hydrolysed PAM

---

[5] P. Munk, T.M. Aminabhavi, P. Williams, D.E. Hoffmann and M. Chmelir, Macromolecules, 13, 871 (1980)

[6] M.H. Rafi'ee Fanood and M.H. George, Polymer, 28, 2241 (1987)

[7] J. Klein and R. Heitzmann, Makromol. Chem. 179, 1895 (1978)

[8] L.A. Itskovich and V.Y. Kabo, Polym. Sci. U.S.S.R. 29(9), 2202-05 (1987)

PART B

SYNTHESIS AND CHARACTERIZATION OF N-ISOPROPYLACRYLAMIDE POLYMER LATICES

CHAPTER 1

INTRODUCTION TO PART B -- SYNTHESIS AND CHARACTERIZATION OF N-ISOPROPYLACRYLAMIDE POLYMERS

1.1 OBJECTIVE OF PART B

The objective of this part is to describe the investigation of the kinetics and mechanism of heterogeneous polymerization of N-isopropylacrylamide (NIPAM) and NIPAM with N,N'-methylene bisacrylamide (BAM) in aqueous medium with sodium dodecylsulfate (SDS) as the dispersant. To reach the goal, several technical problems had to be solved: 1. the determination of the particle concentration; 2. the analysis of the microstructure of latex particle; and 3. the identification of the role of SDS in the polymerization.

1.2 LITERATURE REVIEW

This section summarizes the work has been done on studies of NIPAM and related polymers. After this chapter had been finished, a comprehensive review by Schild[1] about poly(NIPAM) was published. This review covers all the aspects of the experiment, theory and application of poly(NIPAM) and thus is a good reference for people studying poly(NIPAM) related systems.

1.2.1 History of N-isopropylacrylamide and Related Polymers

In 1951, Plaut and Ritter[2] first reported the preparation of N-isopropylacrylamide (NIPAM) monomer which has the following structure

$CH_2 = CH$
|
$C = O$
|
$HN - CH(CH_3)_2$

Six years later, Wooten et al. (Eastman Kodak Co.)[3] published the first paper about the homopolymerization of NIPAM. In the 1960's, most publications were about the preparation of NIPAM monomer; many of them were patents.[4] Later, there were a few papers describing the hydrophillic and thermally reversible properties of NIPAM related polymers. However, the NIPAM polymers did not attract much attention until the late 1970's. In the last decade, many applications and investigations were published about the thermal properties of NIPAM polymers. The number of publications about NIPAM and related polymers is summarized in Figure 1.1 based on a search of the Chemical Abstracts.[5]

1.2.2 Polymerization of N-isopropylacrylamide

This section reviews polymerization methods, especially free radical polymerization, applied to prepare NIPAM polymers, and the kinetic study about polymerization of NIPAM or NIPAM with other monomer.

(i) Polymerization conditions

Most NIPAM polymers were prepared by free radical polymerization in solution or in suspension. Some of them were prepared by solid state polymerization induced by gamma rays[6,7,8], ionic solution polymerization[9,10,11], and bulk polymerization initiated by heat and catalyst.[12] Table 1.1 summarizes the conditions used in free radical polymerization of NIPAM and comonomers.

(ii) Investigation of kinetics and mechanism of polymerization

Studies of the kinetics and mechanism of polymerization of NIPAM is far behind the studies of the solution properties of poly(NIPAM). Three articles have been published: one is about homopolymerization of NIPAM,[3] two are about copolymerization of NIPAM with

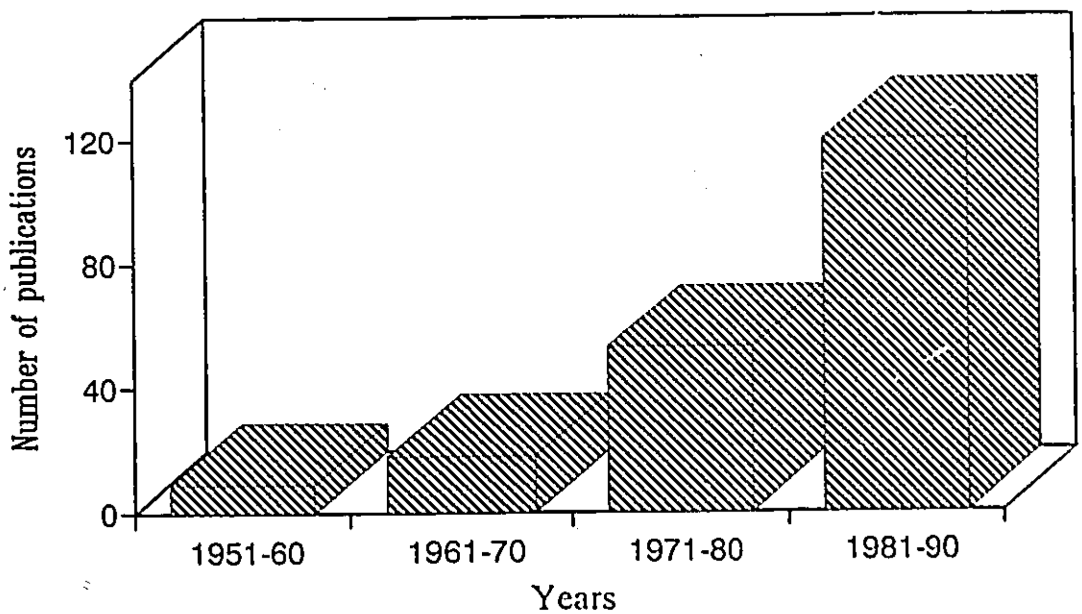

Figure 1.1: History of publications about NIPAM and related polymers

Table 1.1 Reported conditions for free radical polymerization of NIPAM and comonomers

Medium	Initiator(s)*	Temp (°C)	Reference
water	$(NH_4)_2S_2O_8/Na_2S_2O_5$	25 - 32	Wooten(1957)[2]
"	$NaBrO_3/Na_2S_2O_5$	10 - 50	Scarpa(1967)[11]
"	$(NH_4)_2S_2O_8/NaHSO_3$	25 - 32	Heskins(1968)[17]
"	$(NH_4)_2S_2O_8/NaHSO_3$	R.T.	Chiklis(1970)[12]
"	$K_2S_2O_8/Na_2S_2O_5$	NA	Khune(1981)[18]
"	$K_2S_2O_8$	70	Pelton(1986)[19]
"	$(NH_4)_2S_2O_8$/TEMED	R.T.	Cole(1987)[20]
"	$(NH_4)_2S_2O_8$/TEMED	R.T.	Priest(1987)[14]
"	$K_2S_2O_8/NaHSO_3$, $FeCl_3$ above+$FeNH_4(SO_4)_2 \cdot 12H_2O$	25, R.T. 23	Pelton(1988)[21]
"	H_2O_2	27	Meewes(1991)[22]
chloroform	lauroyl peroxide	60	Smidsrφd(1969)[23]
benzene	benzoyl peroxide	reflux	Snyder(1975)[24]
"	"	50	Eliassaf(1978)[25]
methanol	AIBN	50 - 70	Chiantore(1979)[26]
parafin oil	$(NH_4)_2S_2O_8$/TEMED	20	Hirokawa(1985)[27] Tanaka(1985)[28]
benzene/acetone	AIBN	60	Fujishige(1987)[29]
	$(NH_4)_2S_2O_8$/TEMED	NA	Dong(1987)[30]
benzene or THF or both	AIBN	50	Cole(1987)[19]
benzene	"	49	Schild(1989)[31]
tert-butyl alcohol	AIBN	70	Winnik(1990)[32,33]
dioxane	AIBN	60	Ringsdorf(1991)[34]

* In this table, AIBN is 2,2-Azodiisobutyronitrile, TEMED is tetramethylethylendiamine. NA - not available. R.T. means Room Temperature.

acrylamide (AM).[13,15] All of these studies involved the solution polymerization below 32 °C.

In 1957, Wooten et al.[2] described the aqueous solution polymerization of NIPAM initiated by persulfate/bisulfite redox system. They investigated the effects of pH and initiator concentration on the polymerization rate and the intrinsic viscosity of the polymer.

Chiklis and Grasshoff[13] prepared the copolymer of NIPAM/AM in aqueous solution using ammonium persulfate and sodium bisulfite at pH 6.5. They estimated the monomer reactivity ratios, $r_1 = 0.50$ and $r_2 = 1.00$ (M_1 = NIPAM, M_2 = AM), by the method of Fineman and Ross[14]. They determined the copolymer composition by carbon analysis at the monomer conversion between 8 - 13%.

Priest et al.[15], however, found that the copolymerization of NIPAM and AM was almost perfectly random (since they found $r_1 = r_2 = 1.0$ which implies that the two monomers are equally reactive with each radical) when they carried out the polymerization in buffer solution of pH 7.4 using ammonium persulfate and tetramethylethylendiamine (TMEDM) as initiators. In their work the copolymer composition was determined by measuring the residual monomer concentration with a HPLC equipped with a C_{18} column. Their analytical method was more sensitive and more accurate than carbon analysis. However, the composition data used to compute the reactivity ratios were obtained at high monomer conversion (at least 87%); this is not a valid procedure because when monomer conversion is high ($x \rightarrow 100\%$) the copolymer composition approaches to the monomer composition in recipe no matter what values of r_1 and r_2 are.

1.2.3 Molecular Weight Characterization of N-isopropylacrylamide Polymers

Heskins and Guillet[16] measured the number average molecular weight ($\overline{M}_n$) of poly(NIPAM) by osmometry and the weight average molecular weight ($\overline{M}_w$) by light scattering. They found the polydispersity index (PDI = $\overline{M}_w/\overline{M}_n$) to be 3.45 which was quite broad. Smidsrφd and Guillet[22] also claimed that the molecular weight distribution (MWD) of poly(NIPAM) was somewhat broader than normal based on their results of gel permeation chromatography. Snyder and Klotz[23] fractionated poly(NIPAM) by dialysis and chromatography, and measured $\overline{M}_n$ by analyzing the sulphur-containing endgroups and the weight average molecular weight ($\overline{M}_w$) by sedimentation. From the fractionation, they obtained the polymers of low MWD over a molecular weight range from 100 to 200,000. Priest et al.[14] determined the relative molecular weights of poly(NIPAM) and poly(NIPAM/AM) by size exclusion chromatography (SEC) equipped with Sephacryl S-400 column.

Three groups investigated the relationship between intrinsic viscosity, dynamic size and the molecular weight of poly(NIPAM). Chiantore et al.[25] established the Mark-Houwink equations in water and in methanol using unfractionated poly(NIPAM), while Fujishige[28] and Kubota et al.[16] used fractionated poly(NIPAM). The equations and the conditions are summarized in Table 1.2. Under the same conditions (20 °C, in aqueous solution), quite different values for exponent α were obtained: $\alpha = 0.93$ for $\overline{M}_w$ by Chiantore et al., $\alpha = 0.50$ for $\overline{M}_n$ by Fujishige, and $\alpha = 0.51$ for $\overline{M}_w$ by Kubota et al. The first α value corresponds to very expanded polymer chains, and the other two, however, to the ideal random coils under theta conditions (see Part A section 2.4). The reason for the disagreement of the data might be that the polymer samples used by Chiantore would have had a broader molecular weight distribution.

Table 1.2 Viscosity - Molecular Weight relationship*

Correlation	Method for Mw	Temp.°C	Solvent	$\frac{\partial n}{\partial C}$
Chiantore et al.(1979)[25]				
$[\eta] = 4.58\times10^{-4}\ \overline{M}_w^{0.5}$[illegible]	unfractionated,	20	H_2O	
$[\eta] = 2.26\times10^{-4}\ \overline{M}_w^{0.97}$	PDI = ?	25	H_2O	0.169
$[\eta] = 2.99\times10^{-2}\ \overline{M}_w^{0.64}$	light scattering	25	CH_3OH	0.201
Fujishige(1987)[28]				
$[\eta] = 14.5\times10^{-2}\ \overline{M}_n^{0.50}$	fractionated,	20	H_2O	
$[\eta] = 9.59\times10^{-3}\ \overline{M}_n^{0.65}$	PDI = ?	27	THF	
	osmometry			
Kubota et al.(1990)[15]				
$[\eta] = 11.2\times10^{-2}\ \overline{M}_w^{0.51}$	fractionated,	20	H_2O	0.162
$R_G = 2.24\times10^{-2}\ \overline{M}_w^{0.54}$	PDI= 1.2 - 1.4			
	light scattering			
$R_h = 1.60\times10^{-2}\ \overline{M}_w^{0.54}$				

* In this table $[\eta]$ is in cm^3/g, and $\frac{\partial n}{\partial C}$ is in cm^3/g; R_G and R_h are gyration radius and hydrodynamic radius of polymer chain respectively (nm).

1.2.4 Property Studies of N-isopropylacrylamide Polymers

This section covers the studies about the properties of gel, solution, and latex of NIPAM polymers.

(i) Gel properties

See the Introduction in Part B Chapter 4.

(ii) Solution properties

Most studies on the solution properties of NIPAM polymers are about their lower critical solution temperature (LCST) and their interaction with surfactant. A few are about their molecular shape and size in dilute solutions which are related with the molecular weight characterization, and thus classified into section 1.2.3. In this section only the studies on the LCST and the interaction with surfactant are reviewed.

(1) Lower critical solution temperature

The most interesting property of NIPAM polymers is the existence of LCST in aqueous solution. The first article about the LCST of poly(NIPAM) was published by Heskins and Guillet[16] in 1968. They observed that the aqueous solution of poly(NIPAM) underwent phase separation at about 31 °C. The phase separation was endothermic and the enthalpy change per unit poly(NIPAM) decreased with increased polymer concentration. They considered entropy to be the driving force for the phase separation.

Subsequently, Chiklis and Grasshoff[12] studied the phase separation of copolymers of NIPAM with AM, and found that the cloud point temperature (T_c) of 5% polymer solution increased with the AM content in polymers and disappeared when AM content was beyond a value between 34 and 57 mol%.

Priest et al.[14] observed that the addition of more hydrophillic monomer units to the polymer elevated the T_c while more hydrophobic monomers decreased it. Similarly, Kungwatchakun and Irie (1988)[35] studied the effect of hydrophobic units on the T_c. They introduced a photoresponsive monomer to the NIPAM polymer. The monomer changed to more hydrophobic conformation upon UV irradiation and elevated the T_c. The change was reversible when the polymer was exposed to visible light.

Taylor and Cerankowski (1975)[36] prepared several hundred polymers exhibiting T_c. On the basis of theoretical and experimental results, they concluded that the more hydrophobic the polymer, the lower the T_c in water. They found that the phase separations were endothermic, and the curves of cloud point temperature versus polymer concentration were essentially flat.

Chiantore et al.[37] studied the effect of lateral substituents on polymer chain conformation. In their work the steric factors and the characteristic ratios, which are the measures of flexibility of polymers, were calculated for acrylamide polymer series including poly(NIPAM).

Winnik and coworkers[38] studied the T_c dependence on the methanol content of a water-methanol mixture. They found that the T_c decreased with increase of methanol content up to a mole fraction 0.35, and then increased with further addition of methanol. There was no T_c observed when the methanol mole fraction was higher than 0.45. They interpreted this to be that the interaction between water and polymer was more important when the methanol content was low, while the interaction between methanol and polymer was more important when methanol content was high.

Fluorescence studies of poly(NIPAM) solution have been published by several groups. Schild and Tirrell (1989)[30] investigated the effect of the hydrophobic monomer N-hexadecylacrylamide (HDAM) content on the T_c of poly(NIPAM) by fluorescence probe techniques. They observed that the T_c decreased and the transition region broadened as the HDAM content increased. Winnik (1990)[32,39] measured quenching of fluorescence labelled polymer to the study of the phase separation of poly(NIPAM) aqueous solutions. In her work the energy transfer efficiency was observed,to increase with the elevation of temperature, and it reached a constant value above the T_c. Winnik and co-workers[33,40] also studied hydrophobically modified poly(NIPAM) by fluorescence labelling and probe techniques. They detected the presence of hydrophobic clusters below T_c and the disruption of them at T_c. Binkert et al. (1991)[41] applied fluorescence depolarization to study the coil-globule transition of poly(NIPAM) upon heating through T_c. Their findings confirm the conformational transition from extended coils to a compact globular state of the polymer.

(2) Interaction of Poly(NIPAM) with Surfactants

The first report of the surfactant effects on the solution properties of poly(NIPAM) was published by Eliassaf (1978).[24] More recent studies of interaction of poly(NIPAM) with surfactants have been reported by Schild and Tirrell (1989),[42] Rička et al. (1990, 1991),[43,44] Winnik and co-workers (1991).[45,46] More details are given section 3.1 in Chapter 3.

(iii) Latex properties

The pioneering work on the preparation of poly(NIPAM) latex along with the studies of the latex stability and electrophoretic mobility was conducted by Pelton and coworkers (1986, 1989)[18,47]. The influence of polymerization conditions and recipes on the latex stability was studied, and the optimal conditions for preparing quite uniform, stable latex were found.[18] The effects of temperature and added salts on the electrophoretic mobility of the particles and the particle size were also studied.[46] It was observed that both the diameter and the mobility of the particles displayed the transition with the temperature; The sharpness of the transition decreased with the salt concentration as well as the valence of the salts.

(iv) Other Properties of poly(NIPAM)

Several authors[48,49,50,51,52] calculated the physical constants, such as the solubility parameter (δ), partial molar volume ($\overline{V}$), density and dielectric constant, of the acrylamide polymer family by group contribution methods. They calculated the $\overline{V}$ values for poly(NIPAM) to be in the range 101 - 108 cm^3/mol monomer units, and $\delta = 11$ $(cal/cm^3)^{1/2}$ which is close to that of isopropanol ($\delta = 11.4$). Ahmad et al.[54] found that the values of dielectric constant decreased with increasing molar volume for the polyacrylamide family.

The glass temperature (T_g) of poly(NIPAM) was determined by gas chromatography[20], inverse gas chromatography[53], and differential thermal analysis.[54] Similar T_g values (130 and 134 °C) were obtained.

1.3 RHEOLOGICAL PROPERTIES

The rheological properties of poly(NIPAM) solution varying with temperature were investigated by Tam et al.[55] They observed that the viscosity of poly(NIPAM) aqueous solution decreased as temperature was raised to about 28 °C; And then underwent a sharp increase as temperature approached the cloud point; The viscosity reached the peak value at the cloud point (ca.31 °C) and then decreased dramatically with the further increase in temperature. The viscosity peak was interpreted as the intermolecular aggregation by hydrophobic bonding.

1.4 SAFETY OF HANDLING MONOMERS

Monomers NIPAM and BAM are toxic chemicals. They can be inhaled or adsorbed by skin. They can cause disorder of nervous system. NIPAM is also a suspect of carcinogen. Hence extra caution is needed when handling these monomers, especially NIPAM since it sublimates easily and adsorbs to skin firmly. All the experiments involving the monomers were carried out in a fume hood. Two pairs of vinyl gloves and a lab coat were used. In case of contacting skin with the monomers, continuous rinse with water for more than 15 minutes was used. All the solutions containing the monomers, and the solids, e.g., gloves and paper towels contaminated by the monomers, should be collected as waste and sent to waste centre.

1.5 SUMMARY

Up to date, large amounts of work has been done about the thermal responsibility of poly(NIPAM) solution, but the studies on the kinetics of the polymerization is insufficient and no work has been reported about the kinetics and mechanism of the formation of poly(NIPAM) latex particles.

The objective of Part B of this thesis was to study the kinetics and mechanism of the formation of poly(NIPAM) latex particles. To realise this goal, the investigation on the interaction between SDS and poly(NIPAM), the investigation on the microstructure of the particles, and the development of the methodology to determine the particle concentration were conducted.

References

1. H.G. Schild, Prog. Polym. Sci., **17**, 163-249 (1992)

2. H. Plaut and J.J. Ritter, J. Am. Chem. Soc. **73**, 4076-77 (1951)

3. W.C. Wooten, R.B. Blanton, and H.W. Coover,Jr., J. Polym. Sci. **25**, 403-12 (1957)

4. Chemical Abstracts Index, Vol.46-54

5. Chemical Abstracts Index, Vol.46-113

6. J. Zurakowska-Orszagh, J. Poly. Sci. Pt.C **16**(6), 3291-3300 (1965)

7. A. Orszagh and J. Zurakowska-Orszagh, Proc.Tihany Symp. Radiat. Chem., 2nd, Meeting Date, 583-589 (1966)

8. J. Zurakowska-Orszagh, J. Bartnik, A. Chajewski and K. Mirowski, Polymer, **24**, 1484-90 (1983)

9. D.J. Shields and H.W. Coover,Jr., J. Polym. Sci., **39**, 135 (1959)

10. A. Leoni, M. Guaita and G. Saini, Chim. Ind. (Milan), **47**(4), 373-377 (1965); Chemical Abstracts Index **63**: 4397f

11. K.D. Kiss and J.W.L. Fordham, Diamond Alkali Co., Belg. 660,413 (1965); Chemical Abstracts Index **64**: PC3719d (1966)

12. J.S. Scarpa, D.D. Mueller and I.M. Klotz, J. Am. Chem. Soc. **89**(24), 6024-30 (1967)

13. C.K. Chiklis and J.M. Grasshoff, J.Polym. Sci.: Pt **A-2**, **8**, 1617-26 (1970)

14. M. Fineman and S.D. Ross, J. Polym. Sci. **5**, 259 (1950)

15. J.H. Priest, S.L. Murray, R.J. Nelson, and A.S. Hoffman, in *Reversible Polymeric Gels and Related Systems* (ACS Symposium Series **350**, 255-64, 1987)

16. K. Kubota, S. Fujishige and I. Ando, Polymer J., **22**(1), 15-20 (1990)

17. M. Heskins and J.E. Gullet, J. Macromol. Sci.-Chem., A2(8), 1441-55 (1968)

18. G.D. Khune, L.G. Donaruma, M.J. Hatch, N.H. Kilmer, J.S. Shepitka, and F.D. Martin, Polym. Prep. (ACS Div. Polym. Chem.) **22**(2), 76 (1981)

19. R.H. Pelton and P. Chibante, Colloid and Surfaces, **20**, 247-56 (1986)

20. C.-A. Cole, S.M. Schreiner, J.H. Priest, N. Monji, and A.S. Hoffman, in *Reversible Polymeric Gels and Related Systems* (ACS Symposium Series **350**, 236-44, 1987)

21. R.H. Pelton, J. Polym. Sci.: Pt A: Polym. Chem., **26**, 9-18 (1988)

22. M. Meewes, J. Rička, M. de Silva, R. Nyffenegger, and Th. Binkert, Macromolecules, **24**, 5811-16 (1991)

23. O. Smidsrφd and J.E. Guillet, Macromolecules, **2**(3), 272-77(1969)

24. W.D. Snyder and I.M. Klotz, J. Am. Chem. Soc., **97**(17) 4999-5003, (1975)

25. J. Eliassaf, J. Appl. Polym. Sci., **22**, 873-74 (1978)

26. O. Chiantore, M. Guaita and L. Trossarelli, Makromol. Chem. **180**, 969-73 (1979)

27. Y. Hirokawa and T. Tanaka, J. Chem. Phys., **81**(12), Pt.II, 6379 (1984)

28. T. Tanaka, E. Sato, Y. Hirokawa, S. Hirotsu, and J. Peetermans, Physical Review Letters, **55**(22), 2455-58 (1985)

29. S. Fujishige, Polymer J., **19**(3), 297-300 (1987)

30. L.C. Dong and A.S. Hoffman, in *Reversible Polymeric Gels and Related Systems*(ACS Symposium Series **350**, 236-44, 1987)

31. H.G. Schild and D.A. Tirrell, Polymer Preprints (ACS Div.Poly.Chem.), **30**(2),342-343 (1989)

32. F.M. Winnik, Macromolecules, **23**, 233 (1990)

33. F.M. Winnik, Polymer, **31**, 2125-34 (1990)

34. H. Ringsdorf, J. Venzmer and F.M. Winnik, Macromolecules, **24**, 1678-86 (1991)

35. D. Kungwatchakun and M. Irie, Makromol. Chem., Rapid Commun. **9**, 243-46 (1988)

36. L. Taylor and L. Cerankowski, J. Polym. Sci. Polym. Chem., **13**, 2551-70 (1975)

37. O. Chiantore, L. Trossarelli, M. Guaita, Makromol. Chem., **183**, 2257-63 (1982)

38. F.M. Winnik, H. Ringsdorf and J. Venzmer, Macromolecules, **23**, 2415-16 (1990)

39. F.M. Winnik, Macromolecules, **23**, 1647-49 (1990)

40. F.M. Winnik, M.A. Winnik, H. Ringsdorf, and J. Venzmer, J. Phys. Chem., **95**, 2583-87 (1991)

41. Th. Binkert, J. Oberreich, M. Meewes, R. Nyffenegger, and J. Rička, Macromolecules 24, 5806-10 (1991)

42. H.G. Schild and A. Tirrell, Polymer Preprints (ACS Div. Poly. Chem.), **30**(2), 350-51 (1989)

43. J. Rička, M. Meewes, R. Nyffenegger, and Th. Binkert, Physical Review Letters, **65**(5), 657-60 (1990)

44. M. Meewes, J. Rička, M. De Silva, R. Nyffenegger, and Th. Binkert, Macromolecules, **24**, 5811-16 (1991)

45. F.M. Winnik, H.Ringsdorf and J.Venzmer, Langmuir 7, 905-911, (1991)

46. F.M. Winnik, H.Ringsdorf and J.Venzmer, Langmuir 7, 912-917, (1991)

47. R.H. Pelton, H.M. Pelton, A. Morphesis, and R.L.Rowell, Langmuir, 5(3), 816-818 (1989)

48. J.H. Sewell, J. Appl. Polym. Sci. **17**, 1741-47 (1973)

49. H. Ahmad and M. Yaseen, J. Oil Colour Chem. Assoc. **60**(12), 488-94 (1977)

50. R. Zana, J. Polym. Sci. Polym. Phys. **18**, 121-126 (1980)

51. H. Ahmad, K. Chand, R.K. Singh, and S. Krishnamoorthy, J. Colour Soc. (India), **19**(4), 227-31 (1980)

52. H. Ahmad, J. Macromol. Sci.-Chem. A17(4), 585-600 (1982)

53. J.-M. Braun and J.E. Guillet, Macromolecules, **9**(2), 340-344 (1976)

54. O. Chiantore, L. Costa, and M. Guaita, Makromol. Chem., Rapid Commun. **3**, 303-309 (1982)

55. K. C. Tam, X. Y. Wu and R. H. Pelton, "Viscometry - A Useful Tool for Studying Conformational Change of Poly(N-isopropylacrylamide) in Solutions", Polymer Communications, **33**(2), 436-438 (1992)

CHAPTER 2

THE INTERACTION BETWEEN N-ISOPROPYLACRYLAMIDE POLYMERS AND SODIUM DODECYL SULFATE

2.1 INTRODUCTION

As the application of water-soluble polymers increases, the interest in the properties of mixtures of polymers and surfactants is increasing since, in many of the applications, e.g., enhanced oil recovery, anti-deposition of detergent, deinking of paper, polymers co-exist with surfactants. In the past decades, much has been published on the interactions of surfactants with well-known nonionic polymers[1,2], such as polyethylene oxide (PEO)[3,4,5,6,7,8,9,10,11], polyvinyl alcohol (PVA)[5], polyvinylpyrrolidone (PVP)[5,12,13], polyalkyl glycol (PAG)[13], polyvinyl acetate (PVAc)[14], and polyalkyl cellulose (PAC)[15,16,17,18]. In recent years some work has been reported about the interactions between surfactants and N-isopropylacrylamide (NIPAM) homopolymer and copolymers[19,20,21,22,23,24].

Eliassaf[19] first reported the interaction between poly(N-isopropylacrylamide) (poly(NIPAM)) and surfactants. He observed that the addition of 1% sodium dodecyl sulfate (SDS) caused about a four-fold increase in the intrinsic viscosity of poly(NIPAM) and eliminated the phase separation of poly(NIPAM) solution up to 100 °C. He attributed these effects to the hydrophobic bonding. Schild and Tirrell[20,21] systematically studied the effect of surfactant type on the lower critical solution temperature (LCST) of poly(NIPAM). In their studies on the influence of alkyl chain length of sodium alkyl sulfates, they found that when the chain length $n \leq 4$, the LCST decreased linearly with increase in surfactant concentration; when $n = 5 \sim 8$, the LCST was depressed at low surfactant concentrations and increased at concentrations exceeding the critical aggregation concentration (CAC or C_1). However, when

n = 10 and 12, the LCST was elevated, and aggregates formed at concentrations five- to ten-fold lower than the critical micelle concentration (CMC) of pure SDS. They did not observe a second critical concentration C_2. Therefore, they explained this by assuming free micelle formation at all surfactant concentrations above C_1. Winnik and coworkers[23,24] studied the interactions of surfactants with poly(NIPAM) and hydrophobically modified poly(NIPAM) by means of fluorescence probe and fluorescence labelling techniques. They did not observe the C_2 for poly(NIPAM)/SDS either. They found that for hydrophobically modified poly(NIPAM) the mixed clusters consisted of fatty alkyl groups of the polymer surrounded by surfactant molecules, and that the aggregation number of surfactant molecules per alkyl group on poly(NIPAM) was about 30 for C_8 and C_{12} surfactants and about 15 for C_{16} surfactants.

Rička et al[22] investigated the solubilization and conformational transition of poly(NIPAM) in dilute surfactant solution by dynamic light scattering. They observed that small amounts of SDS could prevent the aggregation of poly(NIPAM) which occurs in the absence of SDS at temperatures higher than the LCST. Also, the cloud point increased to about 38 °C when SDS concentration was 550 mg/L (1.91 mmol/L). They measured the apparent hydrodynamic size of poly(NIPAM) at 36 °C in the presence of various SDS levels. They found that the size decreased, and then increased with SDS concentration, and reached the same value as that measured at 25 °C when SDS concentrations were beyond ca. 500 mg/L (1.73 mmol/L). They attributed these to intra- and inter-molecular solubilization. However, they ignored the fact that the cloud points at higher SDS concentrations (> ca. 500 mg/L) were higher than 36 °C, according to Schild and Tirrell's[20,21] and their own findings. Therefore it is improper to compare the hydrodynamic size at 36 °C when SDS concentration is equal to or greater than 500 mg/L.

Our interest in the interaction of SDS with NIPAM polymers stems from the role of SDS in the heterogeneous polymerization of NIPAM and the effect of SDS on the properties of the latex particles and polymers. The results should provide information about whether free SDS micelles exist in the polymerization system and whether polymer chains precipitate under the polymerization conditions, i.e., whether the formation of polymer particles is by micellar or by homogeneous nucleation.

To study the interactions between polymers and surfactants, various classical techniques can be applied[1,25]. Conductometric titration has the advantage of simplicity of operation, and no disturbance to the polymer structure. It produces accurate results which have unambiguous physical meaning and agree well with those from other methods, such as surface tension, gel filtration measurements[1,25]. Conductometric titration is based on the principle that there are different ionization degrees for ionic surfactants in different states[4,26,27,28,29]: free surfactants, bound micelles and free micelles. At low surfactant concentrations, the surfactants fully dissociate and display the highest differential conductivity. When the surfactant concentration reaches the first critical concentration C_1 (or sometimes called critical aggregation concentration), polymer-bound micelles start to form. This is indicated by a lower rate of increase in conductivity due to smaller ionization degree of surfactants in the micelles. When the surfactant concentration achieves the second critical concentration C_2, free micelles begin to form and the smallest rate of increase in conductivity appears and this is attributed to the the fact that free micelles have the lowest degree of ionization. The graphical

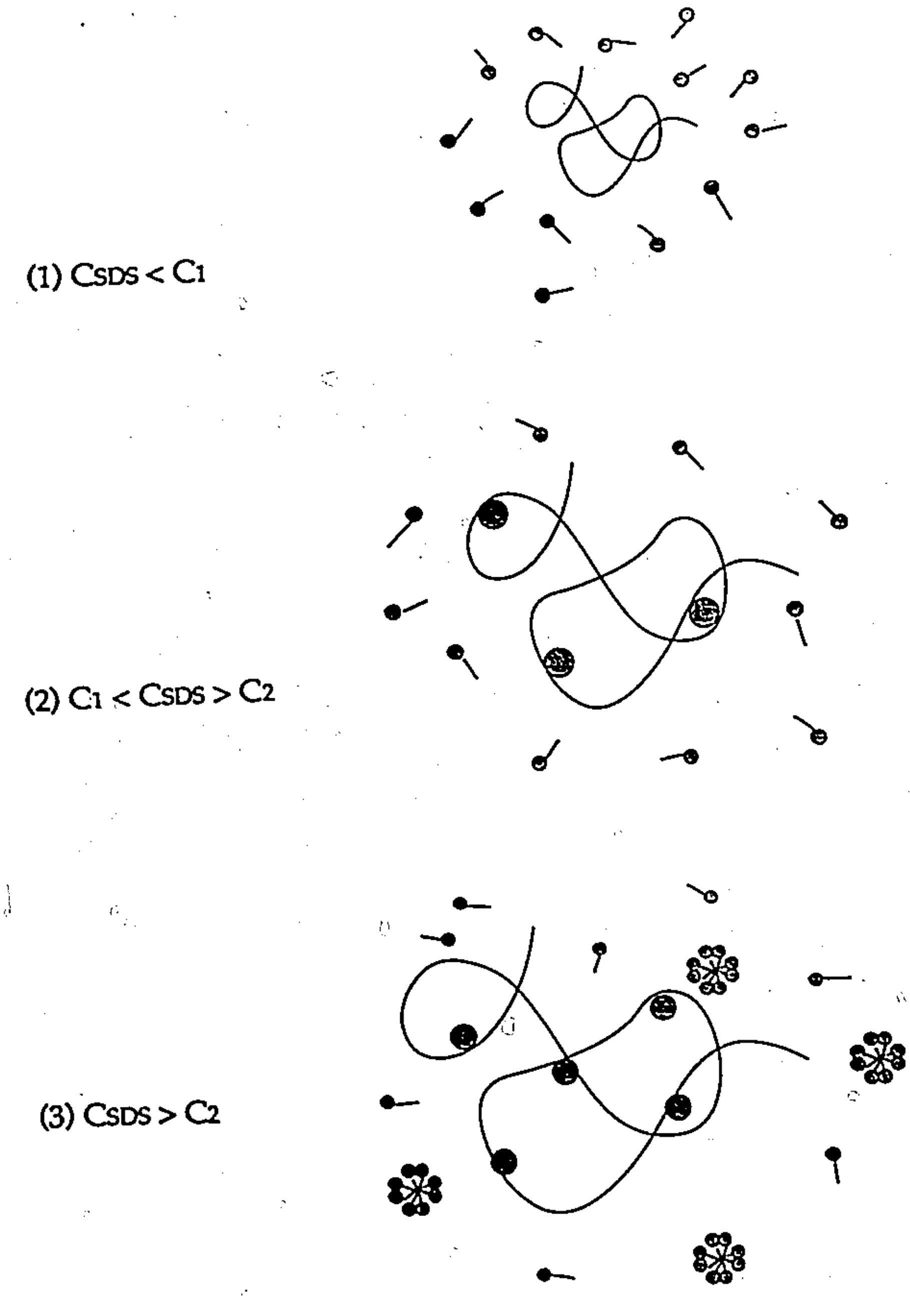

Figure 2.1 Schematic representation of three states of SDS molecules.

Polymer-bouded micelles   Free SDS micelles

Free SDS molecules

illustration of the above mechanism is given in Figure 2.1.

In this work, the influence of NIPAM polymers on the CMC of SDS and the effect of SDS on the polyelectrolyte features of the polymer were investigated mainly by means of conductometry. This is the first work which applies conductometry to a systematic study of the effect of poly(NIPAM) concentration on the CMC of SDS, and the interaction between SDS and the copolymeric latex of NIPAM and N,N'-methylene bisacrylamide (BAM).

2.2 EXPERIMENTAL

Materials NIPAM monomer (Eastman Kodak) was recrystallized from a mixture of toluene and hexane. N,N'-methylene bisacrylamide (electrophoresis grade, Aldrich), SDS (biochemical reagent, BDH), and potassium persulfate (analytical reagent, BDH) were used as purchased. Deionized and distilled water was obtained by passing distilled water through Milli-Q water system (Millipore).

Polymer preparation The homopolymer of NIPAM was prepared in two ways: (a) Polymer LS12 - heterogeneous polymerization above the LCST - 37.6 g NIPAM dissolved in 490 mL deionized water, followed by addition of 2.94 g 2% (w/v) SDS solution; the solution was heated to 50 °C and degassed by purging with nitrogen for half an hour, and then 0.28 g potassium persulfate in 7 mL water was added to the above solution. (b) Polymer SS1 - solution polymerization below the LCST - 20 g 10% (w/w) NIPAM solution was mixed with 43.2 g deionized water and 24.6 g 0.1% (w/w) $NaHSO_3$ solution, and then 12.3 g 0.22% (w/w) potassium persulfate solution was introduced; the polymerization was carried out at room temperature (18.4 - 21 °C). The polymers were precipitated from the diluent by salt addition to the warm suspension followed by filtration. The polymer was then redissolved in cold water, precipitated again, and then washed with hot water. The purified polymer was dried in a vacuum oven at 60 °C until constant weight.

The latex of NIPAM/BAM copolymer LS6 was prepared using the above method (a) which is similar to that developed by Pelton and coworkers[30,31]: 7 g NIPAM and 0.7 g BAM dissolved in 490 mL deionized water, followed by the addition of 0.059 g SDS in 2 mL water, and then 0.28 g KPS in 8 mL water after purging with N_2; the polymerization was carried out at 50 °C. The polymer particles were isolated from the medium by ultracentrifugation at a speed of 50,000 rpm for 0.5 ~ 1.0 hour. The particles were re-dispersed in cold water and refrigerated over night. The procedures were repeated three times to obtain clean latexes.

Conductometric Titration Aliquots of 100 mL solution with and without polymers were transferred to a jacketed flask connected with a water bath. A 2% (w/v) SDS solution was automatically added to the above solution (increment of 0.5 - 1.0 mL) with a high-precision burette station (ABU93 Triburette, Radiometer Copenhagen). The conductivity of the solution was measured by CDM83 conductivity meter (Radiometer Copenhagen). Titrations were controlled by ALIQUAT[32] software running on a IBM personal computer. In order to keep constant ionic strength and to simulate the polymerization conditions, titrations were conducted in 10^{-4} and 10^{-3} M KCl, and 2.07×10^{-3} M potassium persulfate (KPS) solutions. For KPS solution, a period (165 minutes) at the titration temperature was spent before titration to avoid the fast decomposition of KPS during titration. After this period, the pH and conductivity of the solutions were 2.86 and 2820 μS/cm respectively at 70 °C.

Determination of Cloud Point The cloud point of the aqueous solutions of poly(NIPAM) was mainly determined from the turbidity measured with a HP 8452 Diode Array UV/Vis spectrophotometer (Hewlett Packard) equipped with a temperature controller. For lower polymer concentrations, dynamic light scattering (NICOMP 370, NICOMP Particle Sizing Systems) was used to measure the cloud point from the intensity change since the turbidity measurement was not sensitive enough. At high levels of SDS, the cloud point was above the temperature limitation of the instruments. In these cases the cloud points were determined visually.

2.3 RESULTS AND DISCUSSION

The intrinsic viscosity of the polyNIPAM SS1 in water at 25 °C was 207.5 cm^3/g, and LS12 in water at 20 °C was 376.8 cm^3/g. The weight average molecular weights of two polymers were estimated by $[\eta]$ - Mw correlations: $\overline{M_w} = 1.40\times10^6$ for SS1 from Chiantore's equation;[33] $\overline{M_w} = 8.23\times10^6$ for LS12 from Kubota's equation.[34] Attempts to measure the molecular weight distribution of SS1 and LS12 by GPC failed due to clogging of the cellulose filters (pore size 0.22 ~ 0.8 μm), which may be caused by the long chain branching on the polymers.

The intensity average diameter of poly(NIPAM/BAM) latex (LS6) particles at 25 °C was 466 nm with a standard deviation of 26% by the measurement of dynamic light scattering (DLS). The interaction of SDS with poly(NIPAM) was studied at polymer concentrations of 0.05 -0.30 % (w/v) at 25, 50 and 70 °C.

2.3.1 NIPAM POLYMERS AND CRITICAL CONCENTRATIONS OF SDS

Figure 2.2a shows the change of conductivity with SDS concentration at the absence and presence of polyNIPAM. The shape of the curves were similar to those of PEO/SDS[1] obtained

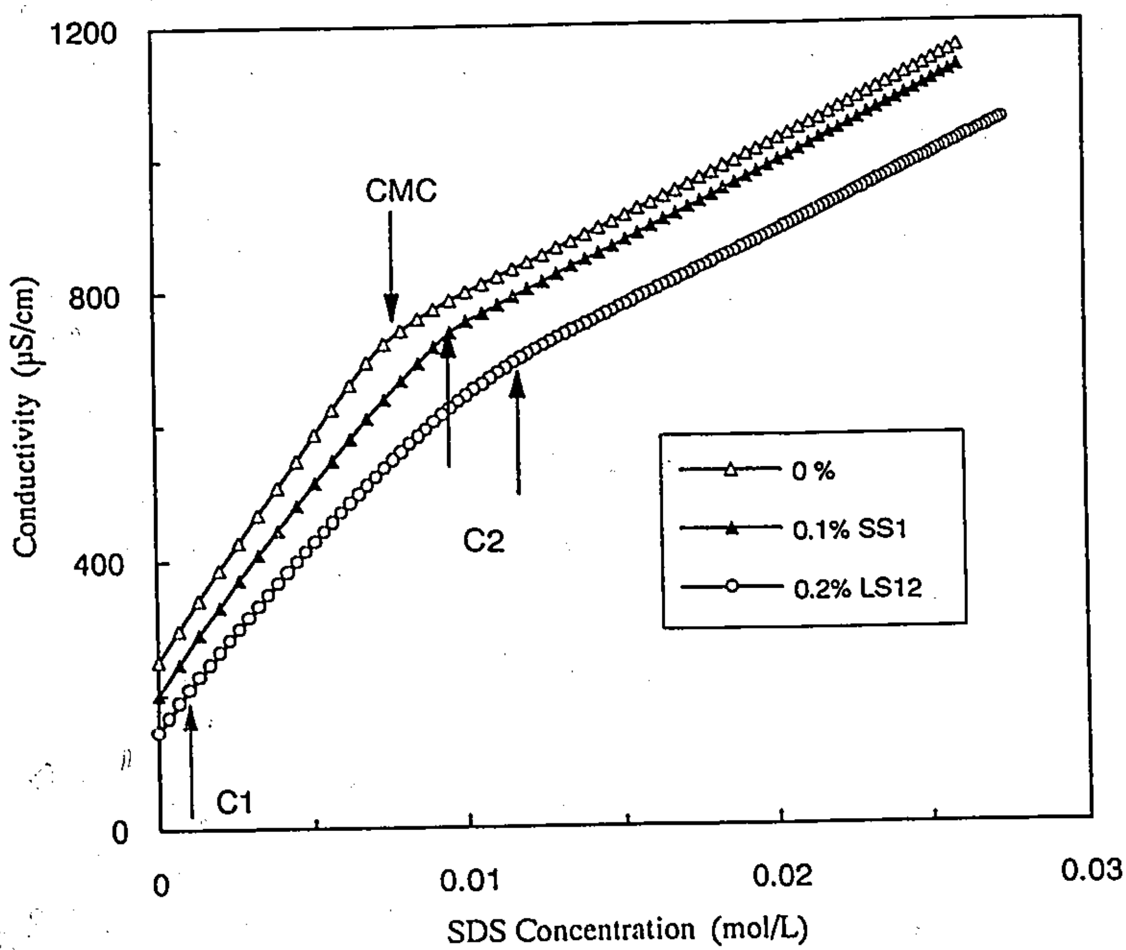

Figure 2.2a: Conductivity of 10^{-3} M KCl with and without poly(NIPAM) versus SDS concentration at 25 °C

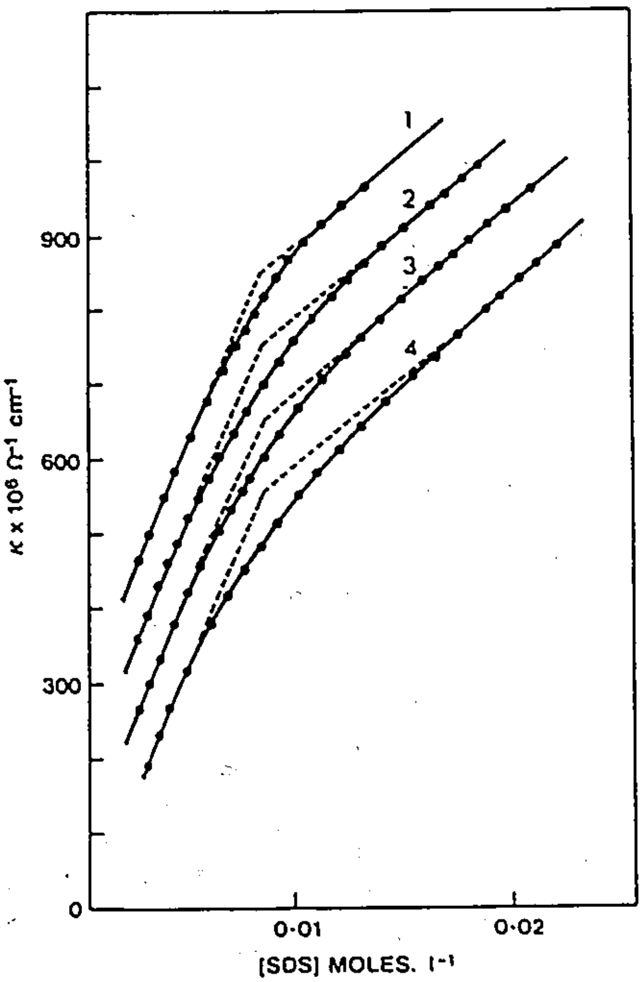

Figure 2.2b Specific conductance/ concentration plot of SDS in the presence of PEO: (1) 0.025% PEO; (2) 0.05% PEO; (3) 0.065% PEO; (4) 0.09% PEO. Scale is for curve 4; curve 3, 2 and 1 raised by 100, 200, and 300 units, respectively. Dotted line: pure SDS solution. Reproduced from Ref.(1).

from the literature and shown in Figure 2.2b. The curves for polymer solutions depart from the straight line of SDS alone at a very low concentration and then are linear again at concentrations higher than the CMC of SDS. They show a less sharp transition than that for the case of SDS alone (no polymer present). The results show a strong effect of polyNIPAM on the micellization concentration of SDS.

A clearer picture of the critical concentrations can be seen from the rate of change of conductivities with SDS concentration (differential conductivity) plotted in Figures 2.3 and 2.4. Two distinct transitions exist in all the curves for polymer solutions while only one transition was observed for polymer-free solutions. The first transition corresponded to C_1, and was nearly independent of polymer concentration in the range studied, which agrees with other polymer systems reported[1]. The second transition corresponds to C_2 at which the polymer is saturated by surfactant. This is the first reported observation of a C_2 transition for the poly(NIPAM)/SDS system. C_2 was not observed by other authors using fluorescence methods.[20,21,24] Beyond C_2, all of the curves become straight and merge with the lines for polymer-free solutions. This suggests that:

(1) only free micelles formed when additional surfactant is added above C_2;

(2) the dissociation degree of free micelles is the same both in the presence and absence of poly(NIPAM) (polymer and particles).

As the polymer concentration increased, the C_2 value increased, but the steepness at the transition became less and eventually disappeared at a concentration of 0.25 - 0.3% polymer, although the C_2 was still distinguishable. At the same SDS concentration the differential conductivity had a trend showing an increase with polymer concentration. A discussion of the

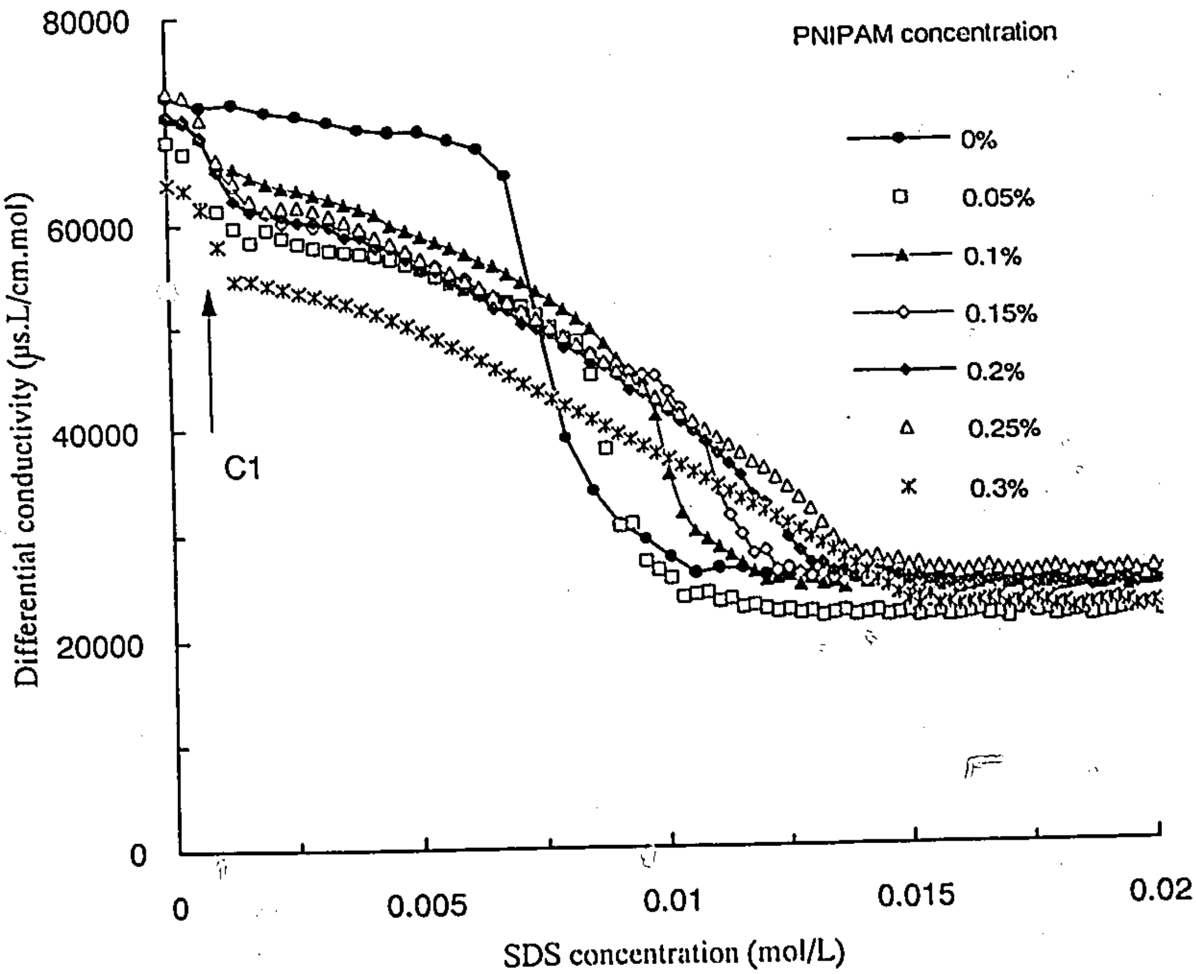

Figure 2.3 Differential conductivity of poly(NIPAM) in 10^{-4} M KCl versus SDS concentration at 25 °C

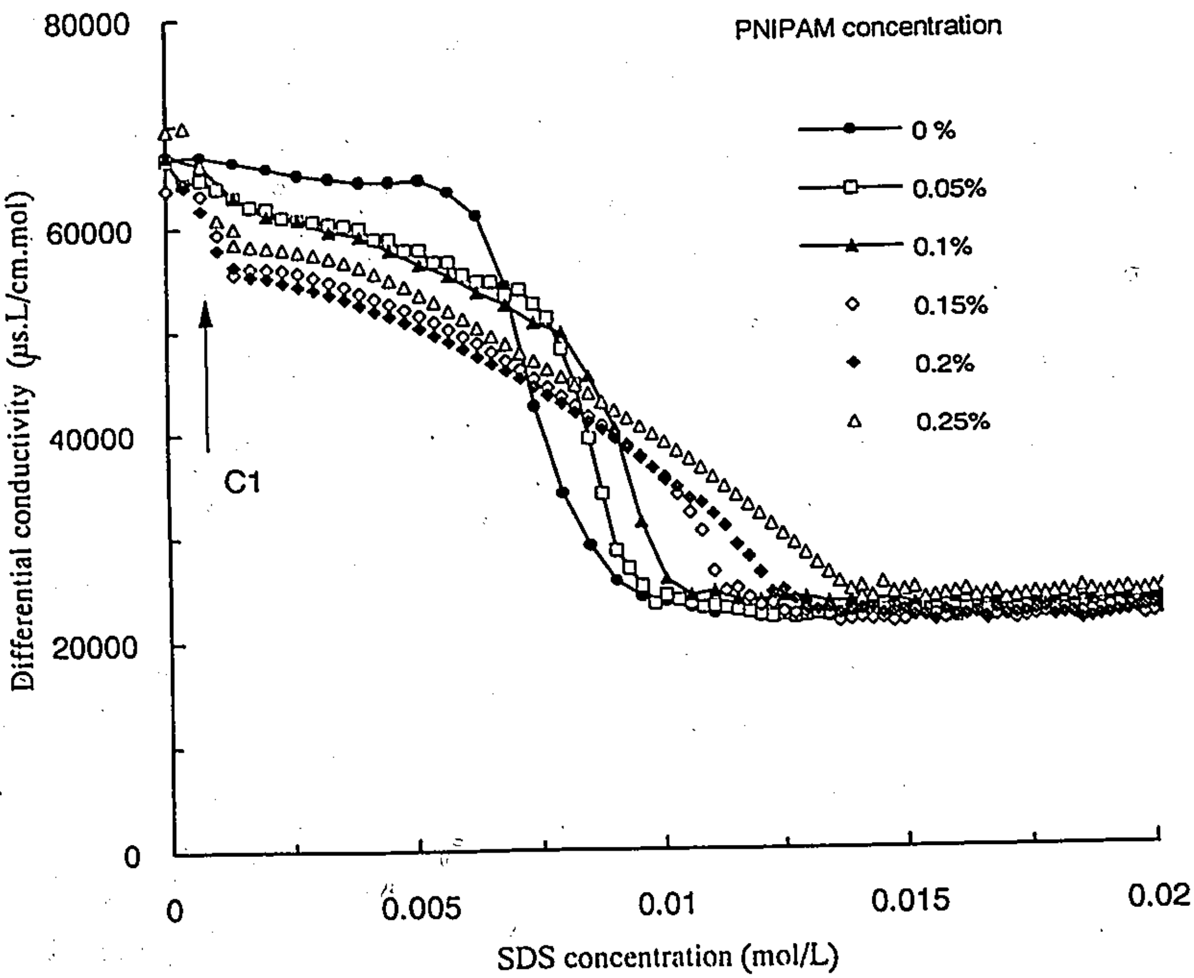

Figure 2.4 Differfntial conductivity of poly(NIPAM) in 10^{-3} M KCl versus SDS concentration at 25 °C

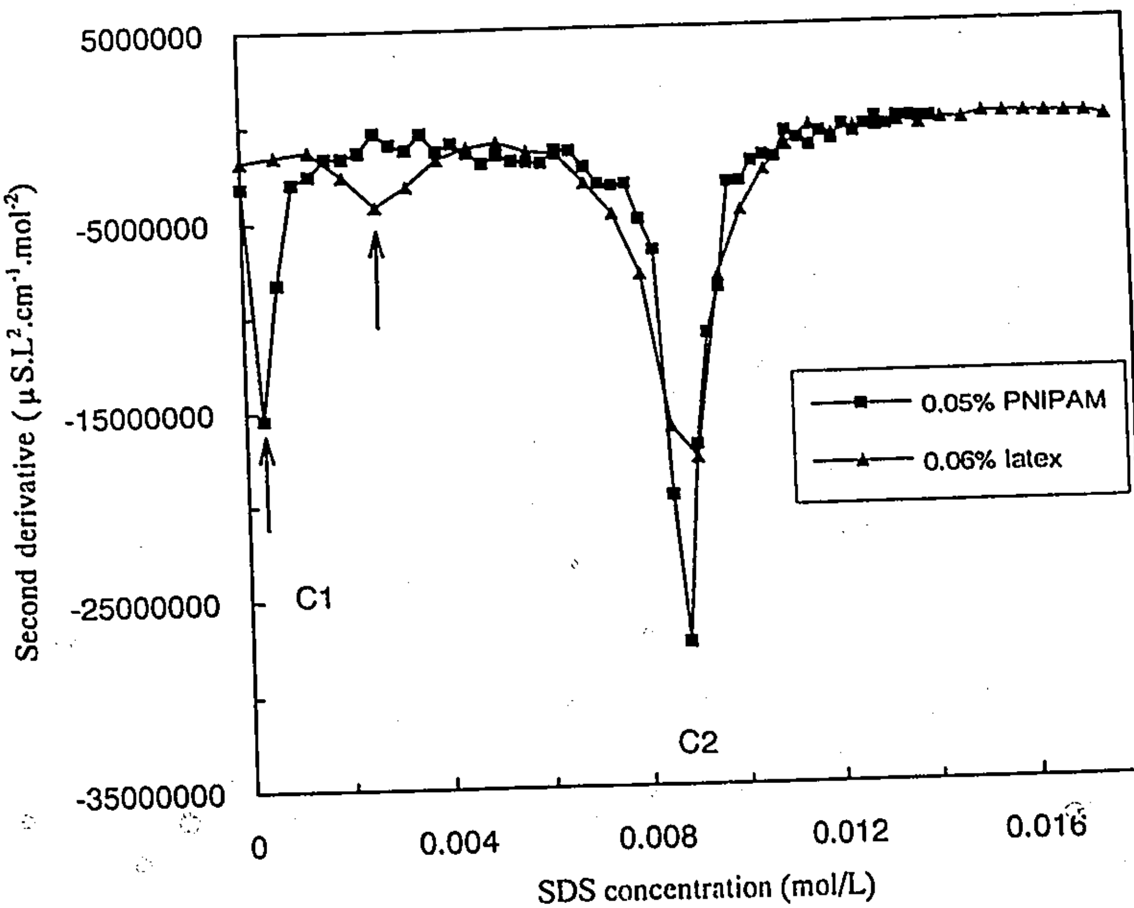

Figure 2.5 Second derivative of conductivity-[SDS] curve for poly(NIPAM) in 10^{-4} M KCl at 25 °C

above observations will be given later.

The C_1 and C_2 values were obtained from the mid-points of the transitions in first derivatives which corresponded to the peaks of second derivatives of the conductivity-SDS concentration curves (see the examples in Figure 2.5). At higher polymer concentrations (0.25 and 0.3 %), the C_2 values were determined directly from the interception of the curve and straight line instead of using the mid-point due to the absence of a steep descent. The C_1 values for poly(NIPAM) in 10^{-4} and 10^{-3} M KCl at 25 °C were ca. 0.69 mmol/L, about the same for the two levels of KCl concentration, and are close to the values in distilled water (free of salt) obtained by fluorescence measurements (0.79 and 0.8 mmol/L).[20,21,24] For copolymeric latex of poly(NIPAM)/BAM in 10^{-4} M KCl at 25 °C, C_1 was 2.7 mmol/L, about three times higher than that for poly(NIPAM). For comparison, the values of C_1 and C_2 determined in this work and available in the literature are summarized in Table 2.1.

Table 2.1 Summary of critical aggregation concentrations and critical saturation concentrations

Critical concentrations	[a]PNIPAM in 10^{-3},10^{-4} M KCl 25 °C	[b]PNIPAM in pure water 24.5 °C	[c]PNIPAM in pure water 20 °C	[d]Poly(NIPAM/BAM) latex 25 °C
$C_1\times10^3$(mol/L)	0.69	0.79	0.8	2.7
$C_2\times10^3$(mol/L)	7.8 - 15	none observed	none observed	9.6

a - PNIPAM represents poly(NIPAM); this work, polymer (SS1 and LS12) concentration $C_p = 0.79\times10^{-3} - 21\times10^{-3}$ mol/L monomer units
b - ref.20,21, by fluorescence probe, C_p = 0.4 g/L = 3.5×10^{-3} mol/L
c - ref.24, by fluorescence lable, C_p = 0.04 g/L = 0.35×10^{-3} mol/L
d - this work, LS6 $C_p = 4.4\times10^{-3}$ mol/L in 10^{-4} M KCl

The C_1 values found in this work were much lower than the CMC of SDS in salt-free water (8.0 mmol/L)[35] indicating a lower free energy for the formation of polymer-bound micelles than that for free micelles. This was proven by Cabane and Duplessix[6] who found that the chemical potential of SDS molecules in PEO/SDS aggregates was 0.3 kT lower than that in free micelles.

In the polymer concentration range studied, the C_2 values are higher than the CMC of SDS and increase with polymer concentration nearly linearly as shown in Figure 2.6. This is in agreement with the observations for the PEO/SDS system.[1,4,6,9] The C_2 values at the higher KCl concentration (10^{-3} M) are slightly smaller than those at the lower concentration (10^{-4} M), e.g., for polymer-free solutions, the CMCs are 8.0 and 7.4 mM respectively, which agrees with the values and trends in the literature[1,28,29,35]. It seems that curves for different salt levels merge at high polymer concentrations. This may imply a depression of the salt effect on the aggregation of surfactant in the presence of poly(NIPAM).

Figure 2.6 can be used as a phase diagram to determine which species exist in poly(NIPAM)/SDS system at given polymer and SDS concentrations. It is postulated that in region I, there are only free SDS molecules and unassociated poly(NIPAM); in region II, poly(NIPAM)/SDS aggregates are in equilibrium with excess poly(NIPAM) and free SDS molecules; in region III, poly(NIPAM)/SDS aggregates are in equilibrium with free micelles and free SDS molecules.

2.3.2 THE AMOUNT OF SDS BOUND TO POLY(NIPAM)

The amount of bound SDS, C_b was obtained by subtracting C_{DS^-} from C_2. However, estimating a value for C_{DS^-} is not easy. If it is assumed that the amount of SDS in excess of the CMC of pure SDS is consumed by binding to polymer, then C_{DS^-} equals CMC. Francois et al.[4] performed their calculation for the ionization degree of bound micelles by taking the

Figure 2.6 Critical concentrations C1 and C2 versus poly(NIPAM) concentration at 25 °C

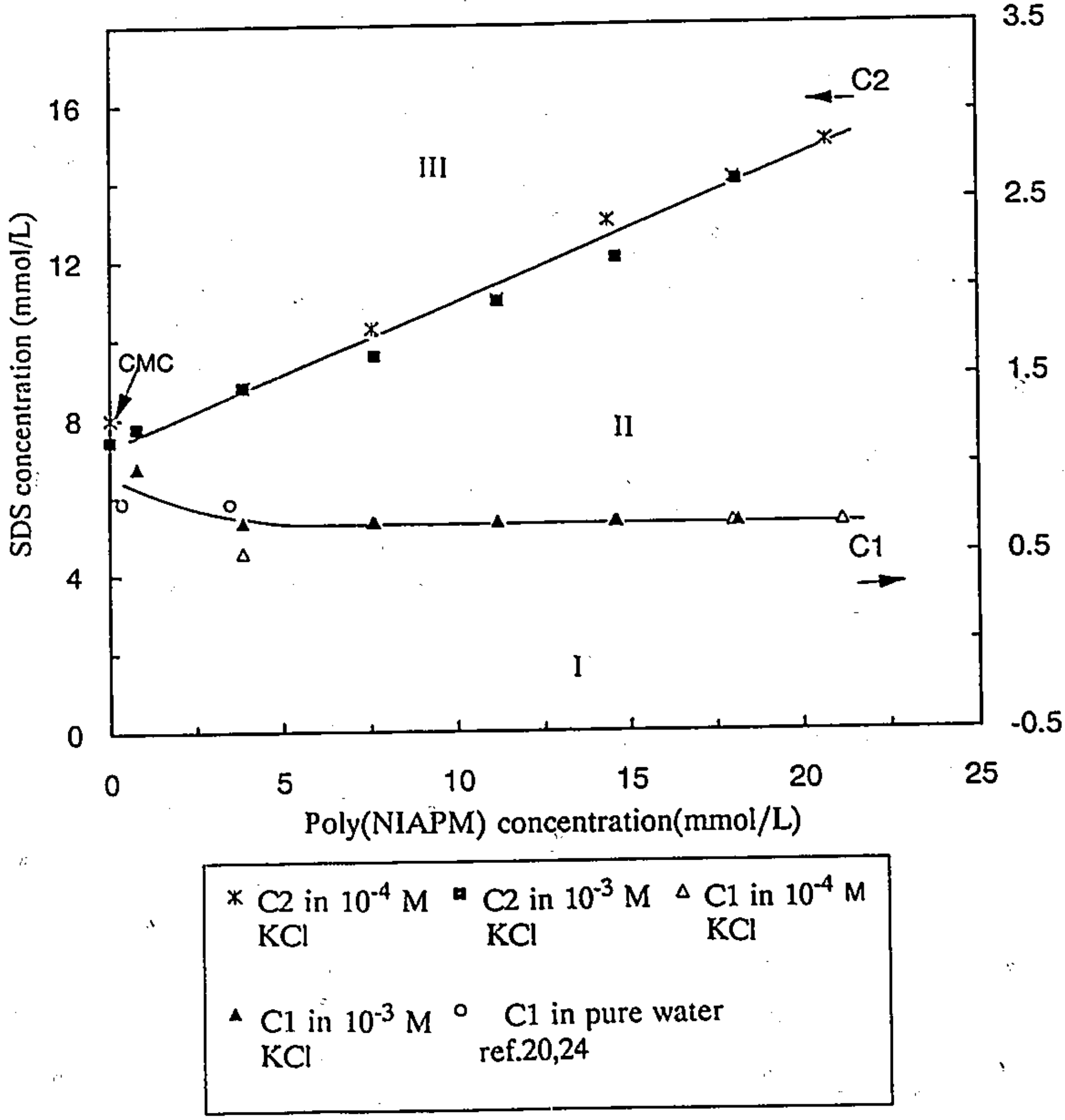

CMC of SDS (8×10^{-3} mol/L) as initial C_{DS}, and obtained the C_{DS} value of 6.5×10^{-3} after iteration. Many authors[5,6,9,18,23,24] considered C_1 as equal C_{DS} based on the assumption that above C_1, all the added SDS binds to polymer until saturation.

In this work, we adopted Cabane[9], Arai and coworkers'[36] concept - using (C_2 - C_1) as the measure of the amount of SDS bound to polymer, C_b. The C_b increased linearly with the polymer concentration as shown in Figure 2.7, which was similar to that observed by Cabane[9] for the PEO/SDS system. No dependence of C_b values on KCl concentration (10^{-3} and 10^{-4} M) was observed.

2.3.3 DISSOCIATION DEGREE OF BOUND MICELLES

(i) Theoretical Considerations

The general and well-accepted model for surfactant binding to polymers[3,4,5,6,9,10,16,18,22,24] assumes a stepwise sequence of several chemical equilibria governed by the law of mass action. Thus, the binding process is: at surfactant concentration $C_{surf} < C_1$, polymer and surfactant molecules are free and there is no binding; at $C_1 < C_{surf} < C_2$, most surfactant molecules are bound to the polymer and in equilibrium with the free molecules; at $C_{surf} > C_2$, the free surfactant molecules are in equilibrium with free micelles and with bound molecules.

According to the manner of surfactant binding to polymer, the general model can include three mechanisms as illustrated in Figure 2.8[5]: the surfactant binds (1) in monomeric form, or (2) in the form of micelles, or (3) a combination of (1) and (2). The first mechanism can explain the saturation of polymer by surfactant at C_2, but cannot explain the critical aggregation concentration which is similar to CMC. However, the mechanism is reasonable for non-cooperative binding system as observed by Winnik[24] for copolymers of NIPAM and

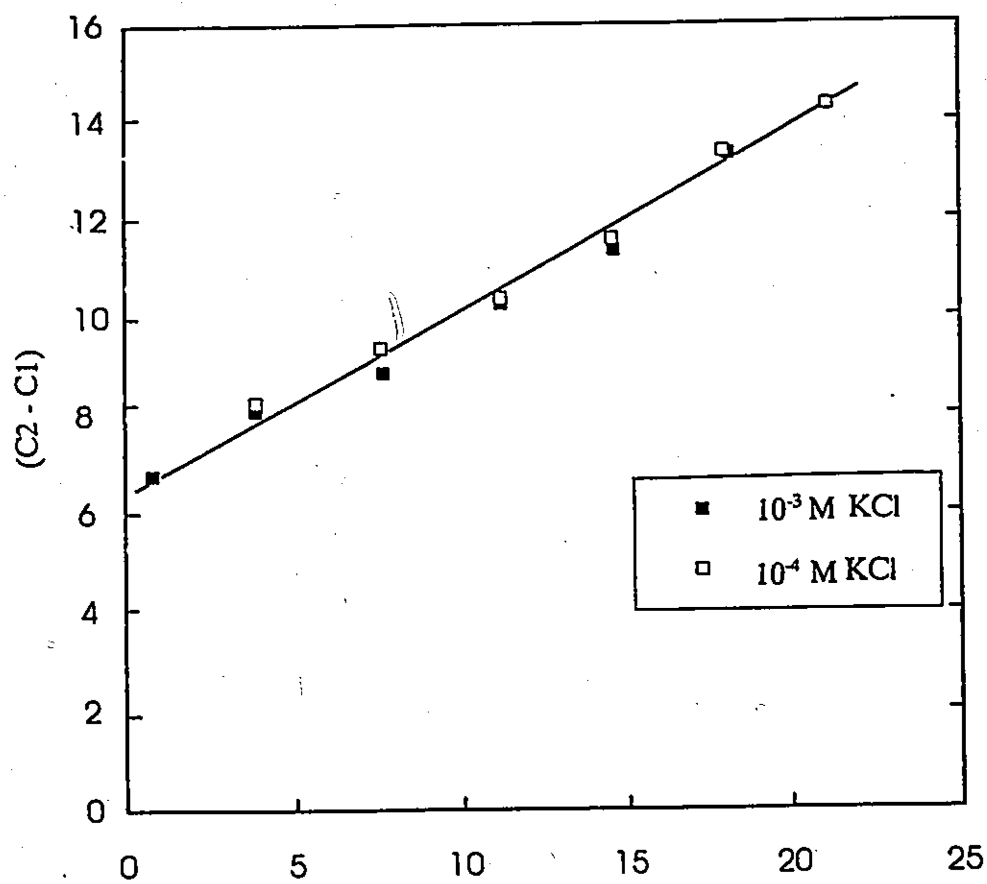

Figure 2.7 Amount of SDS bound to poly(NIPAM) at saturation concentration C2 at 25 °C

Mechanism 1
surfactant in
monomer form

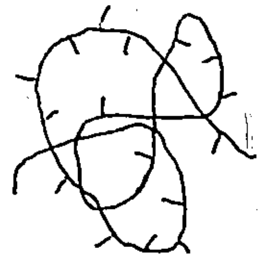

Mechanism 2
surfactant in the
form of micelles

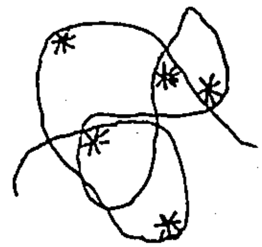

Mechanism 3
surfactant in both
monomer form and
micelle form

Figure 2.8 Proposed mechanisms in literature for surfactant binding to polymer

C_{18} substituted acrylamide. The second mechanism can explain most of the binding processes in which the binding is in cooperative mechanism that yields two critical concentrations. This mechanism is supported by a large volume of results using fluorescence methods[4,10,12,18,20,23,24], NMR[9], especially using neutron scattering[6] which directly measures the size of polymer-bound micelles and the distance between the micelles. The last mechanism is for the case where two binding mechanisms co-exist. Which mechanism is dominant may depend on the nature of the polymer, and the nature and concentration of surfactant.

The present conductometry results, as described previously, show a sharp transition in all the polymer solutions at a concentration far lower than the CMC of SDS in pure water. This suggests the formation of a micelle-like structure between poly(NIPAM) and SDS as proven by the fluorescence studies[20,23,24]. The micelle-like structure may be composed of the hydrophobic group of poly(NIPAM) and the hydrocarbon tails of SDS[23] because very little interaction has been found between surfactant and polyacrylamide[1], a less hydrophobic analogue of poly(NIPAM). Therefore, it is reasonable to use the second mechanism for cooperative binding to describe the structure. Using this mechanism, the total conductivity L_t of the solution measured at C_2 is the sum of the contributions from all the species including bound micelles:

$$1000 L_t = C_{KCl}\Lambda_{KCl} + C_{DS^-}\Lambda_{DS^-} + C_{Na^+}\Lambda_{Na^+} + C_{bm}\Lambda_{bm} \qquad (2.1)$$

where C_{DS^-} and C_{Na^+}, Λ_{DS^-} and Λ_{Na^+} are concentrations and equivalent conductivities of free DS^- and Na^+ respectively, C_{bm} and Λ_{bm} are concentration and equivalent conductivity of bound micelles. The quantity C_{bm} can be determined from the bound SDS concentration C_b

and the aggregation number of SDS in bound micelle, n. Thus,

$$C_{bm} = \frac{C_b}{n} = \frac{C_2 - C_{DS^-}}{n} \tag{2.2}$$

The total free Na^+ should be more than the free DS^- since some of them form by the dissociation of SDS in the bound micelles

$$C_{Na^+} = C_{DS^-} + \frac{C_2 - C_{DS^-}}{n} . m \tag{2.3}$$

where m is the dissociation number of bound micelles, and the ratio m/n is defined as the dissociation degree, β.

The equivalent conductivity of bound micelles is lower than that of free micelles by a factor R_m/R_{Gx} due to the lower mobility of polymer segments[4]

$$\Lambda_{bm} = \Lambda_m \frac{R_m}{R_{Gx}} \tag{2.4}$$

where R_m is the average radius of a bound micelle and R_{Gx} is the average radius of gyration of polymer segments between two bound micelles, as illustrated in Figure 2.9.

With the assumption of a spherical form for the bound micelle, R_m can be solved for using the following equation

$$\frac{V_{mic}}{v} = \frac{4/3\pi R_m^3}{10^{24} M_s/Nd_s} = n \tag{2.5}$$

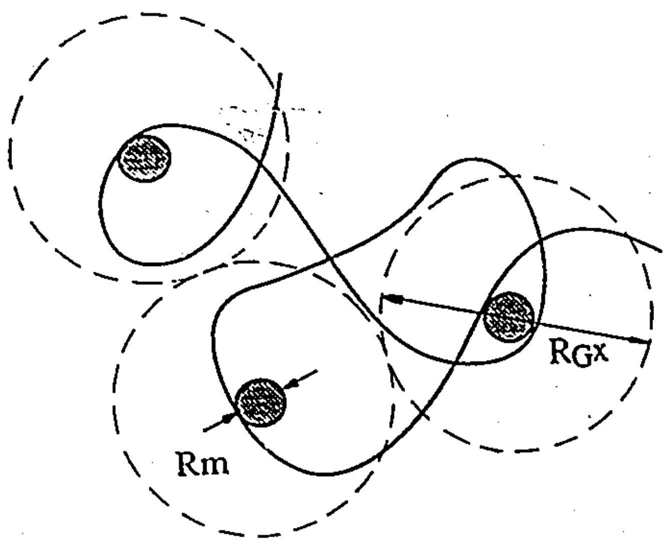

Figure 2.9 Bead-necklace model of SDS micelles bound to poly(NIAPM) chain

where V_{mic} and v are the volumes of a micelle and a single surfactant chain; M_s and d_s are the molar mass and the density of SDS, and N is Avogadro's number. By applying n = 40 to 47[4] and d_s = 1.16[37] the R_m value was estimated to be about 16 to 19 Å which is close to the value (20 Å) measured by neutron scattering for the PEO/SDS system[6]. Assuming that the polymer has the same radius of gyration-molar mass relationship in the presence and absence of SDS (which is true for PEO/SDS system in 0.4 M NaBr[6]), the R_{Gx} value of poly(NIPAM) can be estimated from the equation established by Kubota et al[34]

$$R_{Gx} = 0.22_4 \overline{M}_{wx}^{0.54} \qquad (\text{Å}) \tag{2.6}$$

where $\overline{M}_{wx}$ is the weight average molar mass of poly(NIPAM) segments between two bound micelles and is derived as follows

$$\frac{(C_2 - C_{DS^-})/n}{C_p} = \text{number of bound micelles per NIPAM unit}$$

$$\frac{n\, C_p}{C_2 - C_{DS^-}} = \text{number of NIPAM units per bond micelle}$$

$$\overline{M}_{wx} = \frac{n\, C_p\, M_m}{C_2 - C_{DS^-}} \tag{2.7}$$

where C_p is the polymer concentration (mol/L monomer units), M_m is the molar mass of a monomer unit.

Considering the expansion of polymer chains caused by electrical repulsion between the bound micelles, one can make corrections for the radius of gyration using a factor φ, where φ is a function of the charge density on the polymer chains. It equals unity for SDS-free solution. For various SDS concentrations, its value can be estimated from viscosity data as will be discussed later.

The equivalent conductivity of free micelles Λ_m can be calculated after Van Rysselberghe[38] using

$$\Lambda_m = \frac{m^2}{n^{1/3}}\Lambda_{DS^-} \tag{2.8}$$

To determine the aggregation number of SDS in a bound micelle and the dissociation degree of the micelles, a combination of Equations (2.1) ~ (2.5) and (2.8) can be used

$$1000L = C_{DS^-}\Lambda_{DS^-} + \Lambda_{Na^+}(C_{DS^-} + \frac{C_2 - C_{DS^-}}{n}m) + \frac{m^2}{n^{4/3}}\frac{R_m}{R_{Gx}}\Lambda_{DS^-}(C_2 - C_{DS^-}) \tag{2.9}$$

where L is the net conductivity obtained by deducting the initial conductivity of the solution from the total conductivity L_t. The R_{Gx} is first calculated using Equations (2.6) and (2.7) and then corrected for the temperature and charge effect by a factor of 1.49 which was estimated from the viscosity measurements[39,40]. The Λ_{DS^-} is computed using equation[41]

$$\Lambda_{Na^+} = \Lambda_0(1 - a\sqrt{c} + bc) \tag{2.10}$$

where Λ_0 is the equivalent conductivity of Na^+ ($\Omega^{-1}cm^{-1}equiv.^{-1}$) in infinite dilute solution, a and b are parameters, the respective values of which are 0.70 and 0.74 for NaCl solution at 25 °C, and c is the molar concentration of the ion. Taking all the extra salt effect into account, the c includes not only free Na^+ at CAC, but also the added K^+, the dissociated Na^+ and the polyelectrolyte. The value of Λ_{DS^-} and its concentration dependence are estimated from the conductivity of polymer-free solution below the CMC:

$$\Lambda_{DS^-} = (1000L - \Lambda_{Na^+} C_{Na^+}) / C_{DS^-} \tag{2.11}$$

(ii) Calculation of Dissociation Degree

Based on the results that the bound number of SDS per NIPAM unit decreases with polymer concentration, it is assumed that at various polymer concentrations, the size of the bound micelles is the same, but the number of bound micelles varies. Doing this, the R_{Gx} was found to increase with poly(NIPAM) concentration. To solve for the dissociation number, m, using Equation (2.9), $R_m = 16$, and the calculated values of R_{Gx}, Λ_{Na^+} and Λ_{DS^-} were used, and the aggregation number of SDS in a bound micelle, n, was chosen to be 40. The n value was chosen as suggested by results in the literature[1,4,5,10,23]. The reported n values were: for PEO/SDS system, 35 ~ 50 in distilled water[1,4,5,10], and about 45 in 0.1 M KCl[1]; for PVP/SDS system, 30 ~ 45[1,5]; for hydrophobically modified poly(NIPAM)/SDS, 30 in distilled water[23]. Therefore, a value of 40 for poly(NIPAM)/SDS system is reasonable. Moreover, the results from the estimation of values of m and n by trial-and-error methods support the observation that the aggregation number is about 40. In this estimation, a series of values of n were used in the range 30 ~ 50, and the optimum m values were calculated by setting the a minimum difference between the calculated conductivity by Equation (2.9) and the measured value. A set of values of n and m were then obtained at these minima. These calculations yielded n

= 42 ± 3 in 10^{-4} M KCl, and 41 ± 1 in 10^{-3} M KCl; β = 0.30 ± 0.02 in 10^{-4} M KCl, and 0.31 ± 0.01 in 10^{-3} M KCl.

Considering the effect of ionic strength on the equivalent conductivities, an initial value of 0.4 for β was used to calculate Λ_{Na^+} and Λ_{DS^-}, and then the new value calculated by solving Equation (2.9) was used to make a correction for the ion concentration until β became constant. The calculated dissociation number m is in the range 17 ~ 20, and the dissociation degree β is in the range 0.42 ~ 0.51. The values of m and β for 10^{-3} M KCl are somewhat lower than those for 10^{-4} M KCl as shown in Table 2.2. The m and β seem to increase slightly with polymer concentration for 10^{-4} M KCl but there is no obvious trend for 10^{-3} M KCl. For comparison, the m and β for polymer-free solution, calculated from Equation (3.12) by using n = 65, are also listed in the Table 2.2.

Table 2.2 Dissociation number and dissociation degree of the micelles

Original poly(NIPAM) concentration % (w/v)	In 1.0x10^{-4} M KCl		In 1.0x10^{-3} M KCl	
	m	β	m	β
0.	13.5	0.20_9	13.5	0.20_8
0.05	16.5_9	0.41_5	16.9_7	0.42_4
0.10	19.0_9	0.47_7	18.9_7	0.47_4
0.15	19.4_8	0.48_7	18.1_7	0.45_4
0.20	19.5_3	0.48_8	18.2_1	0.45_5
0.25	20.2_5	0.50_6	18.6	0.46_5
0.30	18.1_0	0.45_3	/	/

2.3.4 TEMPERATURE EFFECT ON C_2 AND β

Figure 2.10 gives conductivity titration curves for 10^{-4} M KCl and poly(NIPAM/BAM) latex (0.06 wt.% LS6) in 10^{-4} M KCl at temperatures 25, 50, and 70 °C. The CMC of SDS in 1.0×10^{-4} M KCl are 8.0, 8.5, 11 mM at 25, 50 and 70 °C respectively, that is, when the temperature increases the CMC of surfactant increases.[1] In the presence of 0.06 % cross-linked poly(NIPAM) latex, the critical micelle concentration rose to 9.0 mM at 25 °C, however its values were the same as those of polymer-free solution at 50 and 70 °C. This implies that at a temperature above the LCST of poly(NIPAM), the interaction between SDS and poly(NIPAM) occurs in another manner due to the precipitation of polymer chains, or the association between polymer and surfactant decreases. Compared with the procedures for polymer solution, the method to determine the dissociation degree of polymer-free solution is much simpler. A widely applied equation[4,26,27,36] was used for this purpose:

$$1000S_2 = \frac{m'^2}{n'^{4/3}}(1000S_1 - \Lambda_{Na^+}) + \frac{m'}{n'}\Lambda_{Na^+} \tag{2.12}$$

where m' and n' are respectively dissociation number and aggregation number of free micelles, S_1 and S_2 the slopes of conductivity-concentration curve before and after the CMC. The Λ_{Na^+} values at 50 and 70 °C in this calculation were interpolated from the data given in the literature[42] and then corrected for ion concentration by Equation (2.10). The aggregation number of free micelles $n' = 65$, a value for free micelles in water[4,43,44] was used to calculate the dissociation number in dilute KCl solution, because, according to Lianos and Zana's study[43,44], the aggregation number does not increase much with salt concentration

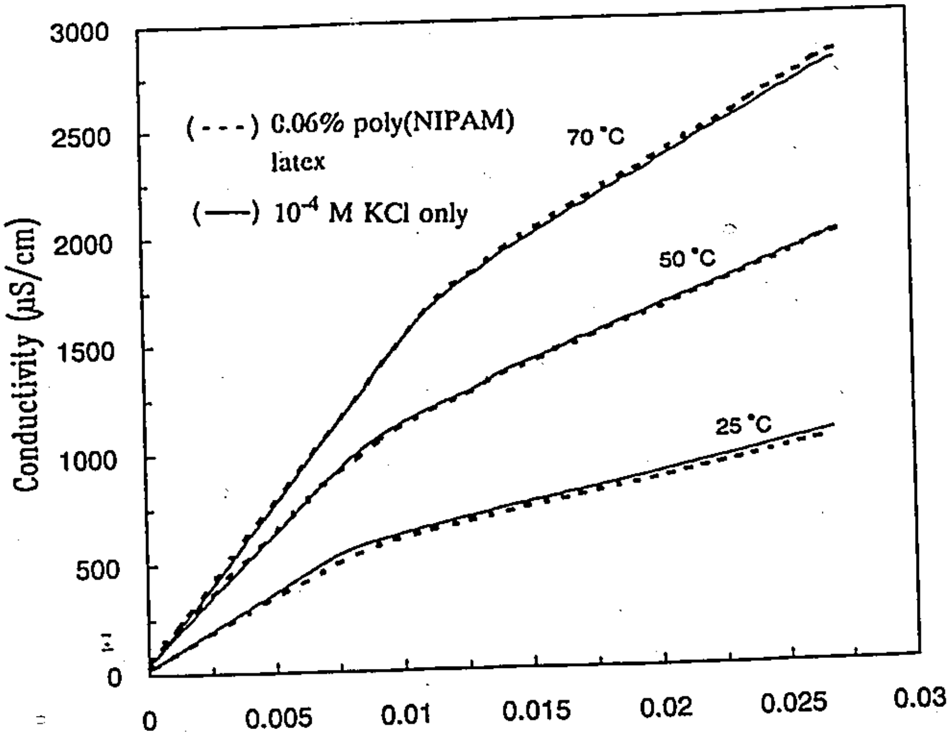

Figure 2.10 Temperature effect on CMC of SDS in 10^{-4} M KCl with and without poly(NIAPM)

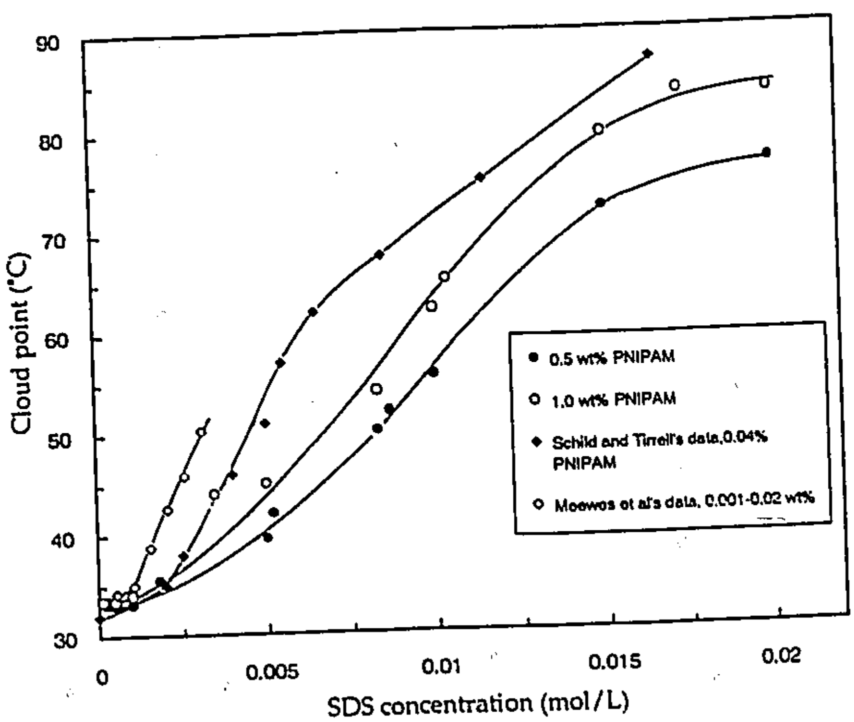

Figure 2.11 Effect of SDS concentration on cloud point of poly(NIAPM)

unless it is above 0.4 mol/L, and thus in 10^{-4} ~ 10^{-3} M KCl it should be almost the same as that in water. Assuming that same aggregation number is valid over the studied temperature range, the dissociation degree was found to increase with temperature, from 0.21 at 25 °C to 0.25 at 70 °C. The calculated dissociation number and dissociation degree for KCl solutions and poly(NIPAM) latex in KCl solution are listed in Table 2.3. In order to investigate whether potassium persulfate (KPS, free-radical initiator used for polymerization of NIPAM) affects the CMC of SDS, a conductivity titration in 2.07×10^{-3} has been performed at 70 °C. The result in Tables 2.3 shows that the effect of KPS is similar to 10^{-3} M KCl.

Table 2.3 Temperature effect on the CMC of SDS, C_2, dissociation number and dissociation degree of SDS micelles

Solution	Temperature (°C)	CMC×10³ (mol/L)	C_2×10³ (mol/L)	m	β
10^{-4} M KCl	25	8.0_5*	/	13.5	0.21
	50	8.5_2	/	14.4	0.22
	70	$11._1$	/	15.4	0.24
10^{-4} M KCl +0.06% latex	25	/	9.0	/	/
	50	/	8.5	/	/
	70	/	11	/	/
10^{-3} M KCl	25	7.4_3*	/	13.5	0.21
	50	9.0_5	/	15.2	0.23
	70	$10._1$*	/	16.3	0.25
2.07×10^{-3} M KPS	70	9.0_5	/	16.3	0.25

* Two to four repetitions gave same values.

2.3.5 INFLUENCE OF SDS ON THE CLOUD POINT OF POLY(NIPAM) SOLUTION

Usually, when a polymer is in solution with an ionic surfactant, the solubility of the polymer is enhanced due to the "polyelectrolyte effect", which results in an elevation of the cloud point[1]. This phenomenon was observed by many authors for hydrolysed PVAc, methyl cellulose and other polymers[1], and for poly(NIPAM)[20,21,22,45]. In this work, the cloud points of poly(NIPAM) in aqueous solution containing 0 ~ 20 mM SDS were determined for two levels of the polymer concentration. The results are plotted in Figure 2.11 compared with the data from Ref.(20) and Ref.(45). The cloud point increased at SDS concentrations above ca.1 mM, which represents the onset of the association. This agrees well with the data of references(20, 24). The increment of cloud point with SDS concentration began to reduce at about C_2. This phenomenon can be explained as cease of the expansion of poly(NIPAM) due to the saturation of polymer by bound SDS micelles.

It is worth mentioning that the poly(NIPAM) solution of higher concentration (1%) displayed greater elevation of cloud point than that of lower concentration (0.5%) at the SDS concentration beyond ca.2 mM. This contrasts to the observations for surfactant-free poly(NIPAM) solution[22,46], although the two curves are both lower than that obtained by Schild and Tirrell[20]. In their work, Rička et al.[22] found that the cloud point decreases with polymer concentration in the range of 10^{-6} to 10^{-1} % (w/v). Similarly, Heskins and Guillet[46] found that the cloud point decreases and then increases, and the LCST is at a polymer concentration ca.15 %. According to the above observations, the cloud point of 1.0 % polymer solution must be somewhat lower than that of a 0.5 % solution. This may suggest that the existence of SDS not only elevated the cloud point, but also shifted the LCST to the lower polymer concentration.

2.3.6 DISCUSSION

(i) Effect of Polymer Concentration on the Sharpness of Transition and the Differential Conductivity

In section 2.3.1 it was shown that the transition at C_2 became less sharp and the differential conductivity tended to lower values at higher polymer concentration. Winnik et al.[23] also reported a broad transition range rather than a sharp one for a solution of 1.87 g/L poly(NIPAM/N-C_{10} substituted acrylamide) (poly(NIPAM)/C_{10}). They pointed out that this is different from observations with other polymers such as PEO, PVP, HPC or poly(NIPAM). However, the concentration of poly(NIPAM)/C_{10} was significantly higher than the poly(NIPAM) concentrations 0.4 g/L[20] and 0.04 g/L[24], and the HPC concentrations 0.3 and 1.0 g/L[17]. These agree with our observation that the sharpness of transition decreased with polymer concentration.

The decrease of the sharpness and the differential conductivity with polymer concentration may be caused by the viscosity effect. According to Falkenhagen et al (1952), Wilshaw and Stokes (1954)[47], at a given electrolyte concentration the equivalent conductance of ions is proportional to the viscosity ratio η_{H_2O}/η_{soln}: $\Lambda_e \propto \eta_{H_2O}/\eta_{soln}$, where "soln" represents solution. Thus the higher the solution viscosity, the lower the equivalent conductance. This is reflected by the decrease in the differential conductivity with polymer concentration. At a given polymer concentration, the viscosity of the solution increases with increase in SDS concentration due to the polyelectrolyte feature of the SDS-bound polymer. Tam et al[40] found that the viscosity of 1 wt.% poly(NIPAM) at C_{SDS} = 1.0 wt.% was about 3.4 times of that at C_{SDS} = 0.012 wt.%, i.e., η_{H_2O}/η_{soln} decreased 3.4 times. The extent of the decrease will be higher for higher polymer concentration. This may explain why the curve of differential conductivity was less sharp for solutions containing more polymer.

(ii) Dependence of Specific Binding Number on Polymer Concentration

Based on the analysis and assumption presented in section 2.3.2 the specific binding number of SDS per NIPAM unit N_s decreases with poly(NIPAM) concentration. When assuming no dependence of the size of bound micelles on polymer concentration, then two explanations are possible for this phenomenon: (1) at relatively high polymer concentrations, the number of hydrophobic sites available for binding SDS is diminished due to the dynamic entanglement among polymer chains, and thus the number of bound micelles is reduced; (2) the binding mechanism changes from that of the micelles sticking on the polymer chains to polymer chains wrapping the micelles. Alternatively, if assuming independence of number of bound micelles, then the decrease of N_s with polymer concentration can be attributed to the reduction of micelle size (as observed by Winnik[18] in the HPC/SDS system). This reduction may be caused by the "salt effect", that is, the polymer in association with SDS acting as an added salt, or by the wrapping mechanism. To clarify the real reason, direct methods, such as neutron scattering, are needed to measure the size of the micelles.

2.4 CONCLUSION

This work has provided new information on the effect of poly(NIPAM) concentration on the interaction between poly(NIPAM) and SDS: (1) the C_2 increases linearly with increase in poly(NIPAM) concentration, which is in agreement with other polymer-surfactant systems[1,4,6]; (2) the amount of SDS bound per NIPAM monomer unit at the saturation is in the range 2.1 to 0.7, decreasing as the polymer concentration increases; (3) Based on an aggregation number of 40 SDS molecules in a bound micelle, the dissociation degree of the bound micelles is in the range 0.42 to 0.51, relatively independent of poly(NIPAM) concentration, while slightly higher for lower KCl concentration; (4) the cloud point of 0.5, 1.0 % (w/w) poly(NIPAM) aqueous solution increases with SDS concentration. The increasing extent of cloud point is larger for more concentrated polymer solution. This results in a higher cloud point for 1.0 % poly(NIPAM) at SDS concentration above ca.2 mM in disagreement with the results for surfactant-free poly(NIPAM) solutions[22,44].

The results of this work support the homogeneous nucleation mechanism of polymer particles in the studied heterogeneous polymerization of NIPAM or NIPAM and BAM, since the SDS levels employed in the polymerization are much lower than C_2, and the polymerization temperature is higher than the cloud point of poly(NIPAM) in the presence of SDS.

References

1. E.D.Goddard, Colloids and Surfaces 19, 255-299 (1986), and the references therein
2. *Surfactant Science and Technology*, Ed. by Drew Myers, Chap. 3 (VCH Publisher, 1988)
3. R. Nagarajan and B. Kalpakci, Polymer Preprints (ACS Div.Poly.Chem.) 23, 41 (1982)
4. J. Francois, J. Dayantis and J. Sabbadian, Eur. Polym. J. 21(2), 165-174 (1985)
5. T. Gilányi and E. Wolfram, Colloids and Surfaces 3, 181-198 (1981)
6. B. Cabane and R. Duplessix, J. Physique 43, 1529-1542 (1982)
7. K. W. Evanson and M. W. Urban, J. Appl. Polym. Sci. 42, 2287-2296 (1991)
8. K. W. Evanson, T. A. Thorstenson and M. W. Urban, J. appl. Polym. Sci. 42, 2297-2307 (1991)

9. B. Cabane, J. Phys. Chem. 81(17), 1639-1645 (1977)

10. R. Zana, P. Lianos and J. Lang, J. Phys. Chem. 89, 41-44 (1985)

11. N. J. Turro, B. H. Baretz and P.-L. Kuo, Macromolecules 17, 1321 (1984)

12. R. Zana, J. Lang, and P. Lianos, Polymer Preprints (ACS Div.Poly.Chem.) 23, 39 (1982)

13. G. C. Kresheck and W. A. Hargraves, J. Coll. Interface Sci. 83(1), 1-10 (1981)

14. N. Sata and S. Saito, Kolloid. Z. 128, 154 (1952)

15. A. Carlsson, G. Karlström, and B. Lindman, Langmuir 2, 536(1986)

16. A. Carlsson, G. Karlström, B. Lindman, and O. Stenberg, Coll. Polym. Sci. 266,1031-36 (1988)

17. B. Lindman, A. Carlsson, G. Karlström, and M. Malmsten, Advances in Colloid and Interface Science 32, 183-203 (1990)

18. F. M. Winnik and M. A. Winnik, Polymer Journal 22(6), 482-488 (1990)

19. J. Eliassaf, Journal Appl. Polym. Sci. 22, 873-4 (1978)

20. H. G. Schild and A. Tirrell, Polymer Preprints (ACS Div. Poly. Chem.) 30(2), 350-51 (1989)

21. H. G. Schild, Ph. D. Thesis, University of Massachusets (1990)

22. J. Rička, M. Meewes, R. Nyffenegger, and T. Binkert, Physical Review Letters 65(5), 657-60 (1990)

23. F. M. Winnik, H. Ringsdorf and J. Venzmer, Langmuir 7, 905-911, (1991)

24. F. M. Winnik, H. Ringsdorf and J. Venzmer, Langmuir 7, 912-917, (1991)

25. B. Lindman, in *Surfactants*, Chap.4, Ed. by Th. F. Tadros, Academic Press Inc. (Florida, 1984)

26. H. C. Evans, J. Chem. Soc. 579-586 (1956)

27. E. Hutchinson, J. Coll. Sci. 9, 191-196 (1954)

28. M. Abu-Hamdiyyah and L. Al-Mansour, J. Phys. Chem. 83(17), 2236-2243 (1979)

29. H. Hoffmann and B. Tagesson, Z. Phys. Chem. N. F. 110, 113-134 (1978)

30. R.H. Pelton and P. Chibante, Colloids and Surfaces, **20**, 247-256 (1986)

31. R.H. Pelton, H.M. Pelton, A. Morphesis and R.L. Rowell, Langmuir, 5, 816-818 (1989)

32. ALQUAT, R. H. Pelton, personal communication (1990)

33. O. Chiantore, M. Guaita and L. Trossarelli, Makromol. Chem. **180**, 969-973 (1979)

34. K. Kubota, S. Fujishige and I. Ando, Polymer Journal 22(1), 15-20 (1990)

35. P.Mukerjee and K.J.Mysels, "Critical Micelle Concentrations of Aqueous Surfactant Systems", NSRDS-NBS 36 (1971)

36. H. Arai, M. Murata, and K. Shinoda, J. Colloid Interface Sci. 37, 223 (1971)

37. G. M. Musbally, G. Perron and J. E. Desnoyers, J. Coll. Interface Sci. **48**, 494 (1974)

38. P. Van Rysselberghe, J. Phys. Chem. 48, 62-65 (1944)

39. K. C. Tam, X. Y. Wu and R. H. Pelton, "Viscometry - A Useful Tool for Studying Conformational Change of Poly(N-isopropylacrylamide) in Solutions", Polymer Communications, 33(2), ?? (1992)

40. K. C. Tam, X. Y. Wu and R. H. Pelton, "Effect of polymer concentrations, temperature and surfactant on the viscosity of poly(N-isopropylacrylamide) solutions", submitted for publication

41. *Handbook of Electrochemical Constants*, Ed. by R. Parsons, pg. 81-82 Butterworths Scientific Publications (London 1959)

42. *The Determination of Ionization Constants*, 3rd Ed., by A. Albert and E. P. Serjeant (Chapman and Hall, 1984)

43. P. Lianos and R. Zana, J. Phys. Chem., **84**, 3339-41 (1980), and the references herein

44. P. Lianos and R. Zana, J. Coll. and Interface Sci., **84**, 100-107 (1981)

45. M. Meewes, J. Rička, M.De Silva, R. Nyffenegger, and Th. Binkert, Macromolecules, **24**, 5811-16 (1991)

46. M. Heskins and J. E. Guillet, J. Macromol. Sci., A2(8), 1441-55 (1968)

47. *Handbook of Aqueous Electrolytes Solutions*, Chapter 2.11, p280-281, Ed. by A.L. Horvath, Ellis Horwood, New York (1985)

CHAPTER 3

MICROSTRUCTURE OF POLY(NIPAM) AND POLY(NIPAM/BAM) LATEX PARTICLES

3.1 INTRODUCTION

The study on cross-linked poly(NIPAM) gels started in mid-1980's because of their thermally reversible swelling with water offered many possible applications. These included controlled release of immobilized enzymes,[1] drug delivery,[2,3] and selective absorption.[4,5] Some investigations about the volume phase transition of poly(NIPAM) gels were carried out by Tanaka's group,[6,7,8,9,10] and some by other groups.[11,12,13,14,15] The preparation of poly(NIPAM) gels with various structure and compositions was described in recent publications.[16,17,18,19,20]

The objective of this work was to determine the microstructure of poly(NIPAM) particles prepared by the polymerization above the lower critical solution temperature, LCST. The microstructure information will be used to analyze the mechanism of particle formation. The microstructure, such as cross-linking density and density distribution, is related to the swelling behaviour of the polymer. Therefore, the swelling behaviour of poly(NIPAM) particles at various temperatures and various polymerization time (or monomer conversions), and the particle size distribution at different temperatures and in different solvents, were studied to obtain the information about the microstructure of poly(NIPAM) particles.

3.2 THEORETICAL CONSIDERATIONS

This section describes the theoretical basis of the swelling behaviour of cross-linked polymeric particles, the formula of various particle size distribution, and the principles of two techniques, dynamic light scattering and centrifugal sedimentation, which are employed to determine the particle size and size distribution.

3.2.1 Dependence of Swelling Ratio on Particle Size and Composition

Flory[21] considered that the free energy change of mixing pure solvent with a polymer network in a bulk form consisted of two parts: the free energy of mixing ΔF_m, and the elastic free energy ΔF_{el}:

$$\Delta F = \Delta F_m + \Delta F_{el} \tag{3.1}$$

For the polymer without network but in a form of micro-spheres, the elastic contribution is absent; Morton et al.[22] considered that the free energy included the contribution from the interfacial energy and from mixing:

$$\Delta F = \Delta F_m + \Delta F_t \tag{3.2}$$

For the micro-spheres of cross-linked polymer, all the contributions by mixing, stretching of the network and expansion of surface should be included

$$\Delta F = \Delta F_m + \Delta F_{el} + \Delta F_t \tag{3.3}$$

where ΔF_m = free energy of mixing is given by

$$\Delta F_m = kT(n_1 ln v_1 + \chi n_1 v_2) \tag{3.4}$$

ΔF_{el} = elastic free energy caused by the expansion of network structure is:

$$\Delta F_{el} = (3kTv_e/2)(\alpha^2 - 1 - \ln\alpha) \tag{3.5}$$

ΔF_t = interfacial free energy between the latex particle and the medium which opposes the swelling force.

The latter term can be expressed as follows. Considering the increase in radius dr is caused by imbibing of dn_1 moles of solvent, the increase in interfacial free energy is:[22]

$$\Delta F_t = 8\pi r dr\gamma + 4\pi r^2 d\gamma = \frac{2dn_1\overline{V_1}\gamma}{rN_A} + 4\pi r^2 d\gamma \tag{3.6}$$

where k is Boltzmann's constant, T the Kelvin temperature, χ the polymer-solvent interaction parameter, v_1 and v_2 the volume fraction of solvent and polymer respectively, n_1 the number of solvent molecules, v_e effective number of polymer chains in gel, r radius of particle, γ interfacial energy, $\overline{V_1}$ molar volume of solvent, and α the linear swelling ratio defined as

$$\alpha = (V/V_o)^{1/3} = (\phi_o/\phi)^{1/3} \tag{3.7}$$

where V and V_o are respectively the volume of the gel at present state and reference state, ϕ and ϕ_o the volume fraction of polymer in the gel at the two states.

The chemical potential of solvent in the swollen gel is given by

$$\mu_1 - \mu_1^{\circ} = N_A\left(\frac{\partial \Delta F_m}{\partial n_1}\right)_{T,P} + N_A\left(\frac{\partial \Delta F_{el}}{\partial \alpha}\right)_{T,P}\left(\frac{\partial \alpha}{\partial n_1}\right)_{T,P} + N_A\left(\frac{\partial \Delta F_t}{\partial n_1}\right)_{T,P} \tag{3.8}$$

where N_A is Avogadro's number. The partial derivative of α to n_1 was derived by Flory[21]

$$(\partial\alpha/\partial n_1)_{T,P} = \overline{V}_1/3\alpha^2 V_o N_A \tag{3.9}$$

Substituting Equations (3.4) - (3.6) and (3.9) to Equation (3.8), and at swelling equilibrium the left hand side of Equation (3.8) $\mu - \mu_o = 0$, one can obtain the following equation:

$$\frac{2\overline{V}_1\gamma}{rRT} + \left(\frac{4\pi r^2 N_A}{RT}\right)\left(\frac{d\gamma}{dn_1}\right) = -[\ln(1-\phi)+\phi+\chi\phi^2] - \frac{\overline{V}_1\nu_e}{V_o N_A}[(\phi/\phi_o)^{1/3} - \frac{1}{2}(\phi/\phi_o)] \tag{3.10}$$

The above equation describes the dependence of the volume fraction of polymer on the particle size and the interfacial energy.

If the interfacial energy is nearly independent of the amount of solvent, i.e., $d\gamma/dn_1 \approx 0$, as Morton et al.[22] assumed in their derivation, Equation (3.10) can be rearranged as:

$$\frac{2\overline{V}_1\gamma}{r\phi^2 RT} + \chi = -\frac{\ln(1-\phi)+\phi+\overline{V}_1\nu_e/V_o N_A[(\phi/\phi_o)^{1/3}-(\phi/\phi_o)/2]}{\phi^2} \tag{3.11}$$

For a given solvent and a fixed temperature, χ is assumed to be a function of only the polymer composition or cross-linking density. Therefore, if the swelling ratio is measured for a series of latex particles of the same cross-linking density, but of various particle size, the values of χ and γ may be determined from the intercept and the slope of the plot of right hand side of Equation (3.11) versus $(\gamma\phi^2)^{-1}$.

3.2.2 Particle size distribution

The particle size distribution of polymeric particles can be described by two distributions: normal distribution and log-normal distribution. Since most polymer colloid populations are skewed, log-normal distribution is more often used.

Normal distribution In this distribution, the particle size distribution function is given by:

$$f(D) = \frac{1}{\sqrt{2\pi}\,\sigma}\exp\left[-\frac{(D-\overline{D})^2}{2\sigma^2}\right] \tag{3.12}$$

Log-normal distribution In this distribution, the distribution function is:

$$f(D) = \frac{1}{\sqrt{2\pi}\,\sigma_g}\exp\left[-(lnD-lnD_g)^2/2\sigma_g^2\right] \tag{3.13}$$

where D and $\overline{D}$ are respectively particle diameter and mean diameter, D_g is geometric mean diameter defined as the diameter at the cumulative probability of 50%, $D_{50\%}$; σ and σ_g are standard deviations of normal distribution and log-normal distribution. They are defined as the difference and the ratio of diameters at 84% and 50% cumulative probability after Woods:[23]

$$\sigma = D_{84\%} - D_{50\%} \tag{3.14}$$

$$\sigma_g = \frac{D_{84\%}}{D_{50\%}} \tag{3.15}$$

From Equations (3.12) and (3.13), it is seen that the normal distribution is different from the log-normal distribution. In this work, both dynamic light scattering (DLS) and centrifugal sedimentation (CSD) were used. The software of DLS equipped with the instrument offered normal distribution analysis; while that of the CSD only gave the raw data of particle diameter and the fraction. Therefore, in the comparison of the particle size distribution determined by the two methods, the same distribution type, log-normal distribution, was obtained by converting the original data. Details will be given later.

3.2.3 Principles of Dynamic Light Scattering and Centrifugal Sedimentation

Dynamic Light Scattering

The Brownian movement of particles causes fluctuations in the intensity of scattered light. The decay of the fluctuations are described by the decay constant τ which is inversely proportional to the particle diffusivity $\bar{D}$

$$1/\tau = 2\ \bar{D}\ K^2$$

where K is the scattering wave vector. This is a function of refractive index of the medium n, the wave length λ, and the scattering angle θ

$$K = (4\ \pi\ n\ /\ \lambda)\ \sin\ (\theta/2)$$

The particle diffusivity is related to the particle radius R by Stokes-Einstein equation

$$\bar{D} = k\ T\ /\ 6\ \pi\ \eta\ R$$

where k is the Boltzman's constant (erg/°K), T Kelvin temperature (°K), η viscosity of the medium. From this analysis, one can obtain an intensity average, and then a volume average for the size of the particle.

Centrifugal Sedimentation

The sedimentation time t (sec) for a single particle of diameter D (cm) is determined by Stokes' equation

$$D = \left[\frac{18\eta_o \ln(x_2/x_1)}{(\rho - \rho_o)\,\omega^2(t)\,t}\right]^{1/2} \tag{3.16}$$

where η_o is the viscosity of the dispersion medium, ρ and ρ_o are densities of particles and dispersion medium (g/cm^3), x_1 is the distance between the centre of rotation and the sedimentation plane (cm), x_2 is the distance between the centre of rotation and the measuring plane (cm), and ω(t) is the rotational angular velocity (rad/sec).

In a given medium and a fixed instrument, the time required for a particle passing by the measuring plane varies with the particle size and particle density. Therefore, if the particle density is constant as usually assumed, the particle size is determined by the time t. The number of the particles at a time t is calculated from the amount of transmitted light by the following equation:

$$\log_{10} I_o - \log_{10} I_t = C \sum_{i=1}^{n} k(D_i) N_i D_i^2 \tag{3.17}$$

where I_o is the intensity of light beam at the sample, I_t is the intensity of light transmitted through sample, C is the optical coefficient of the cell and the particle form, k(D_i) is the absorption coefficient of particles of D_i, and N_i is the number of particles of diameter D_i. The value of D_i is computed using Equation (3.16).

The data obtained by the above equation are an area based distribution. The volume based distribution F_i is calculated by the following equation:[24]

$$F_i = \frac{(\log_{10} I_o - \log_{10} I_i) \times D_i}{\sum_{i=1}^{n} [(\log_{10} I_o - \log_{10} I_i) \times D_i]} \tag{3.18}$$

From the above equations, the particle size and size distribution can be obtained.

3.3 EXPERIMENTAL

Particle diameters were determined by dynamic light scattering (DLS). The DLS measurements were conducted with a Nicomp 370 Autodilute Submicro Sizer (Nicomp Particle Sizing System, U.S.A.), which was equipped with a HeNe laser light source (wavelength 632.8 nm) and a computing software (version 10.3). The intensity of scattered light was detected at an angle of 90 °. The particle diameters were determined at various temperatures. The swelling ratios of the particles were calculated from the diameters or volumes determined by DLS at 25 °C divided by those at 50 °C.

Particle diameters were also measured by centrifugal sedimentation. The CSD measurements were carried out with Particle Size Distribution Analyzer (CAPA-700, Horiba, Ltd., Japan). A gradient mode of acceleration rate 960 rpm/min with a maximum final speed of 10,000 rpm was used to achieve a good fractionation. The light source for particle concentration was Green LED of wavelength about 560 nm. The transmitted light was measured by a Silicon photo-diode detector. Acetonitrile was used as the dispersion medium because of its low viscosity, low density and poor swelling capability for poly(NIPAM/BAM) particles.

3.4 RESULTS

The ratios of the particle size measured at 25 °C to that at 50 °C were measured as a function of monomer conversion, particle size and temperature. The results were used to investigate the microstructure of the poly(NIPAM/BAM) particles. The effects of temperature and solvent on the particle size and size distribution were analyzed. The particle density and density distribution were then investigated by comparing the particle size distribution determined by two different methods, DLS and CSD.

3.4.1 Swelling Ratio and Monomer Conversion and Preparation Temperature

The swelling ratio of the particles from three latex samples (LS1, LS6 and LS10) is plotted against reaction time in Figure 3.1. In all the cases, the swelling ratios were the lowest at the beginning and then increased rapidly to an almost constant value.

The swelling ratio as a function of total monomer conversion is given in Figure 3.2. interestingly, the swelling ratio did not increase with the conversion all the time but decreased beyond certain conversions. This phenomenon can be explained by examining the relationship between swelling ratio and BAM content in polymers as shown in Figure 3.3. The BAM content was the highest in the earliest stage of the particles and the lowest in the latest stage of the particles due to the higher reactivity of BAM relative to NIPAM (see Part B Chapter 5). As a result, the swelling ratio became higher with the increase in reaction time. However, this was not the case at BAM content beyond certain value for LS1 and LS10. This may suggest the existence of unreacted pendant double bonds of BAM. Some of double bonds of reacted BAM monomers might not cross-link at early stages of polymerization. They might react later, and produce additional cross-links, which could cause the swelling ratio to decrease at the later stages of the polymerization.

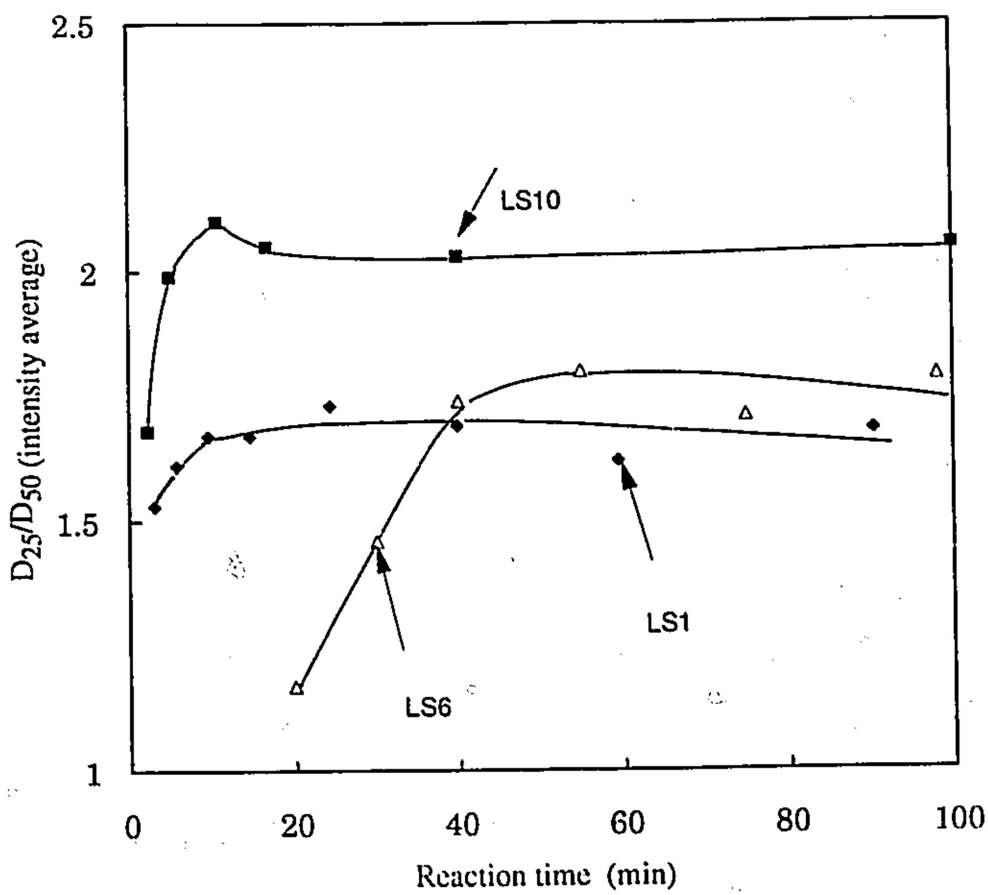

Figure 3.1: Swelling ratio of poly(NIPAM/BAM) varies with reaction time. BAM content 0.068 mole, polymerized at 70 °C with SDS (LS1) 0.409 mmol/L, (LS10) 2.45 mmol/L; polymerized at 50 °C (LS6) with 0.409 mmol/L SDS

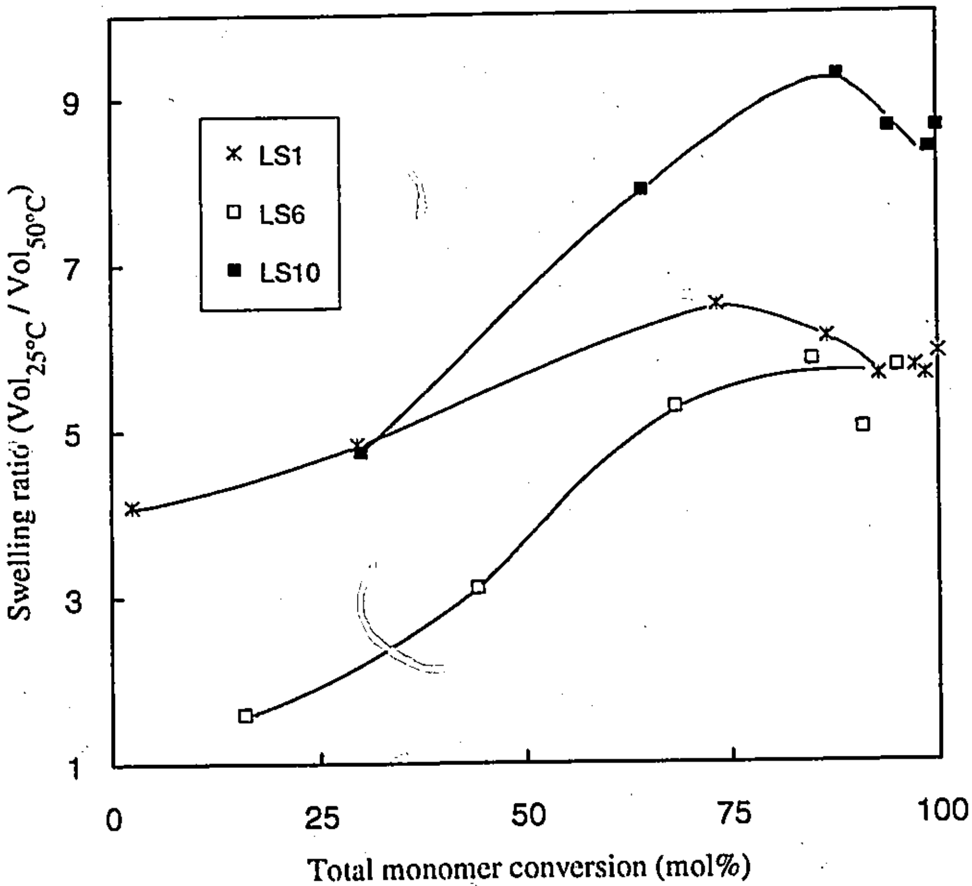

Figure 3.2: Dependence of swelling ratio on total monomer conversion. The conditions for preparing LS1, LS6 and LS10 are presented in Figure 3.1.

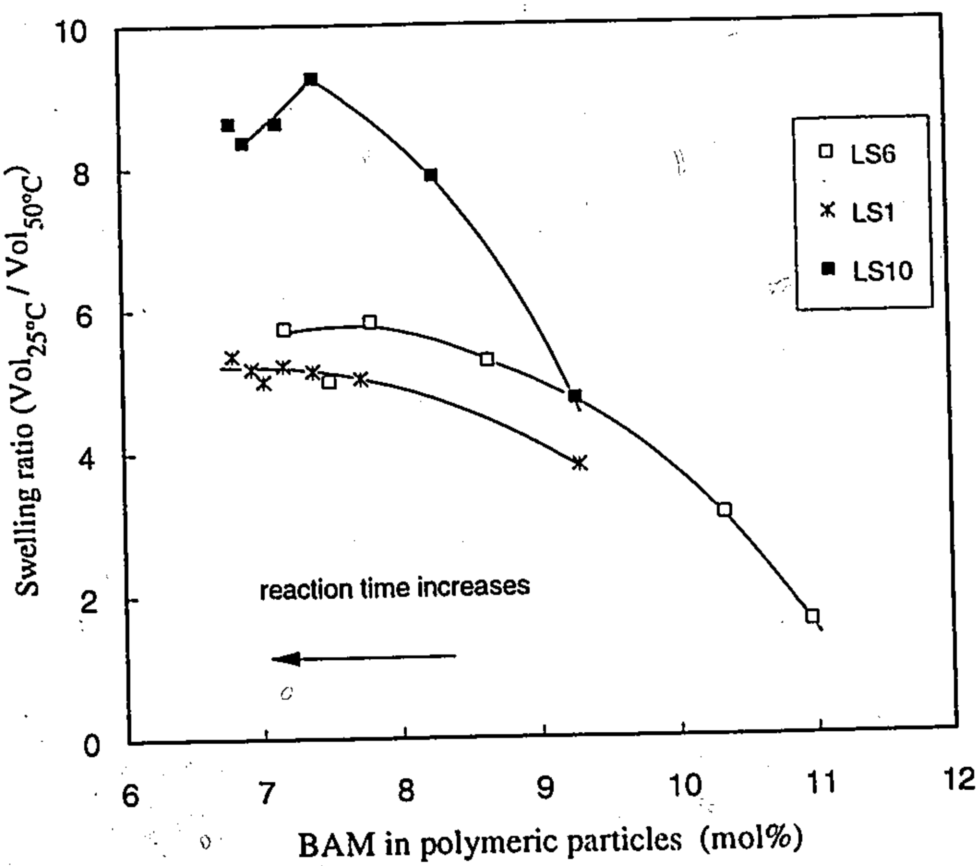

Figure 3.3: Dependence of swelling ratio on BAM content in polymeric particles

3.4.2 Swelling ratio and SDS Level in Polymerization Media

Figures 3.1 - 3.3 show that the particles prepared with a high SDS level (2.45 mmol/L) had higher swelling ratios than those with a low SDS level (0.409 mmol/L), even though the particles contained the same amount of BAM (see Figure 3.3). This implies that the particle size may influence the swelling extent because the diameter of LS10 was the smallest (the diameters at 25 °C: LS10, 140 nm; LS1, 430 nm; LS6, 500 nm).

3.4.3 Swelling Ratio and Particle Size

Four latex samples (LS1, LS2, LS5, and LS10) with the same BAM content but different average particle sizes were prepared using the same recipe except for the SDS concentration (see Part B Chapter 5 Table 5.1). Their swelling ratios (diameter at 25 °C over that at 50 °C) are plotted against the inverse of particle radius (by DLS at 50 °C) in Figure 3.4. It is seen that the swelling ratio increased linearly with the reciprocal of the particle radius, i.e., the smaller the particles, the greater the swelling extent. Morton et al.[22] also observed the similar phenomenon for polystyrene latex particles in various solvents including styrene, toluene and chlorocyclohexane. They interpreted their results as the balance between the interfacial energy and the solvency effect. They also reported that their results could be predicted by theory which was represented by a equation similar to Equation 3.11 but without the elastic term.

3.4.4 Particle Size and Measuring Temperature

In this section all the particle diameters were measured by DLS in various solvents.

(i) Particles of different cross-linking density

A comparison of diameter-temperature curve for two latex samples (LS1 and LS13) with BAM mole fraction 0.068 and 0.128 respectively is given in Figure 3.5. The same *volume*

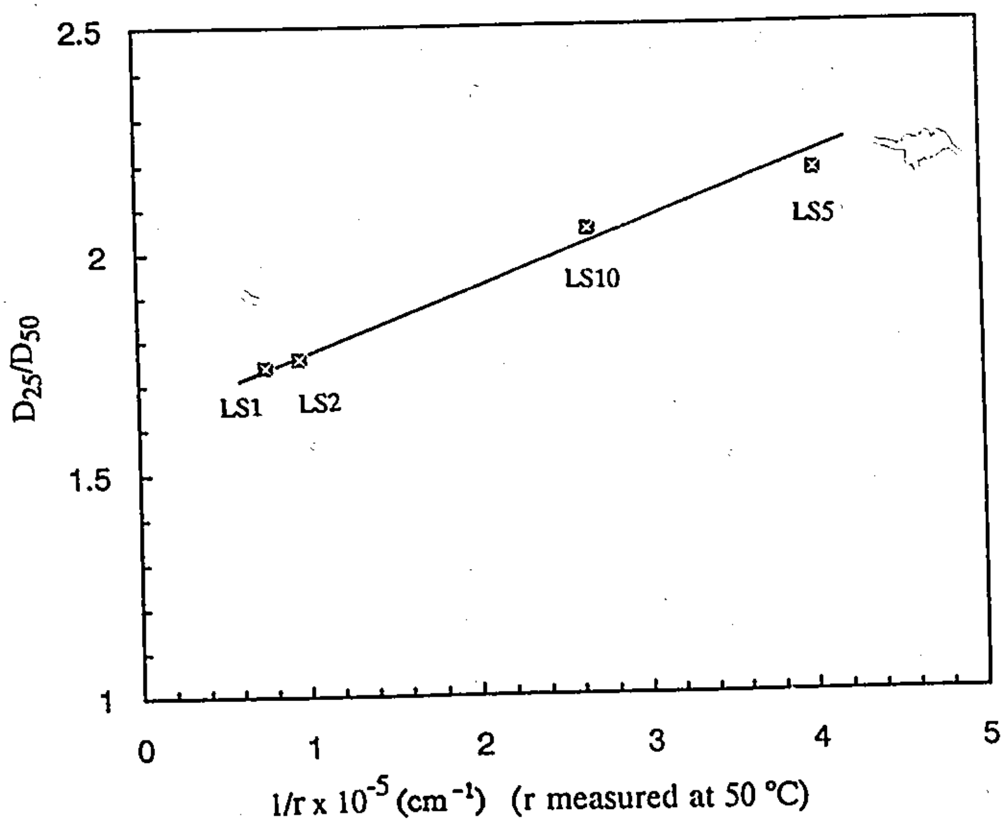

Figure 3.4: Dependence of swelling ratio on the inverse of particle radius poly(NIPAM/BAM). BAM content was 0.068 mole fraction, polymerized at 70 °C using various SDS concentration

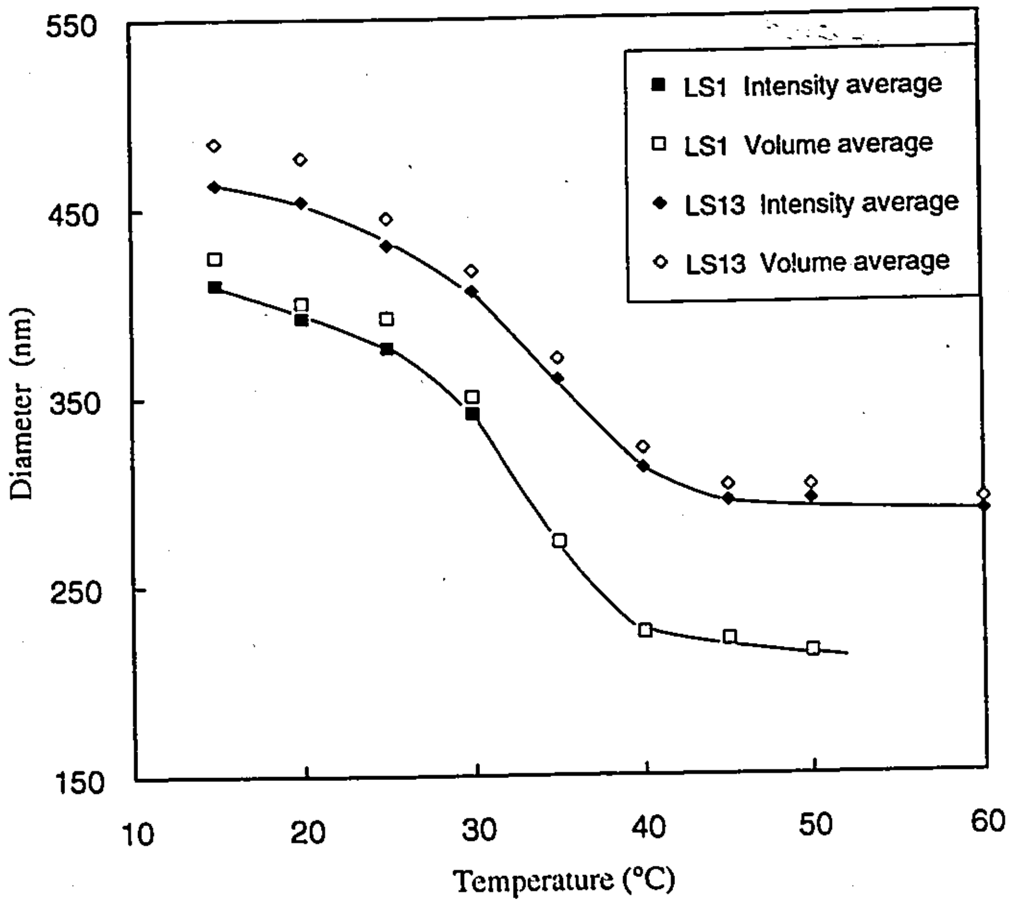

Figure 3.5: Dependence of particle size of poly(NIPAM/BAM) on temperature. BAM mole fraction: LS1 0.068; LS13 0.128

phase transition temperature, T_{tr}, (ca. 34 °C) was found from two curves, although the bottom one (lower BAM content) had sharper diameter change around T_{tr}.

(ii) Particles at different conversion

Figure 3.6 displays the temperature effect on the diameter of homopolymer of NIPAM at conversion 8.9% and 100%. The same *cloud point temperature*, T_c, (ca. 32 °C) was observed for the two samples. The LS8-8 (100% conversion) sample had a much larger size at temperatures above T_c, but was less swollen below the T_c, than was the LS8-2 (8.9% conversion) sample. An explanation for this is given later.

3.4.5 Particle Size and Size Distribution

(i) Particle size distribution and temperature

In Figures 3.5 and 3.6, the open squares and diamonds represent the intensity average diameters, the solid ones represent the volume average diameters. The differences between two averages were greater at temperatures below T_{tr} for poly(NIPAM/BAM) (Figure 3.5), or below T_c for poly(NIPAM) (Figure 3.6). This implies a broader particle size distribution (PSD) at lower temperature since the difference between the two averages is a measure of the width of the PSD. The lager the difference, the bigger the standard deviation. For monodispersed particles $\overline{D}_{vol} = \overline{D}_I$. Figure 3.7 is a plot of standard deviation of Gaussian distribution by DLS against temperature. The standard deviation showed a dramatic increase when temperature was lower than T_c.

(ii) Particle size distribution and conversion

Figure 3.6 gives the temperature dependence of diameter for two poly(NIPAM) samples taken at different monomer conversions: LS8-2, x = 8.9%; LS8-8, x = 100%. Interestingly,

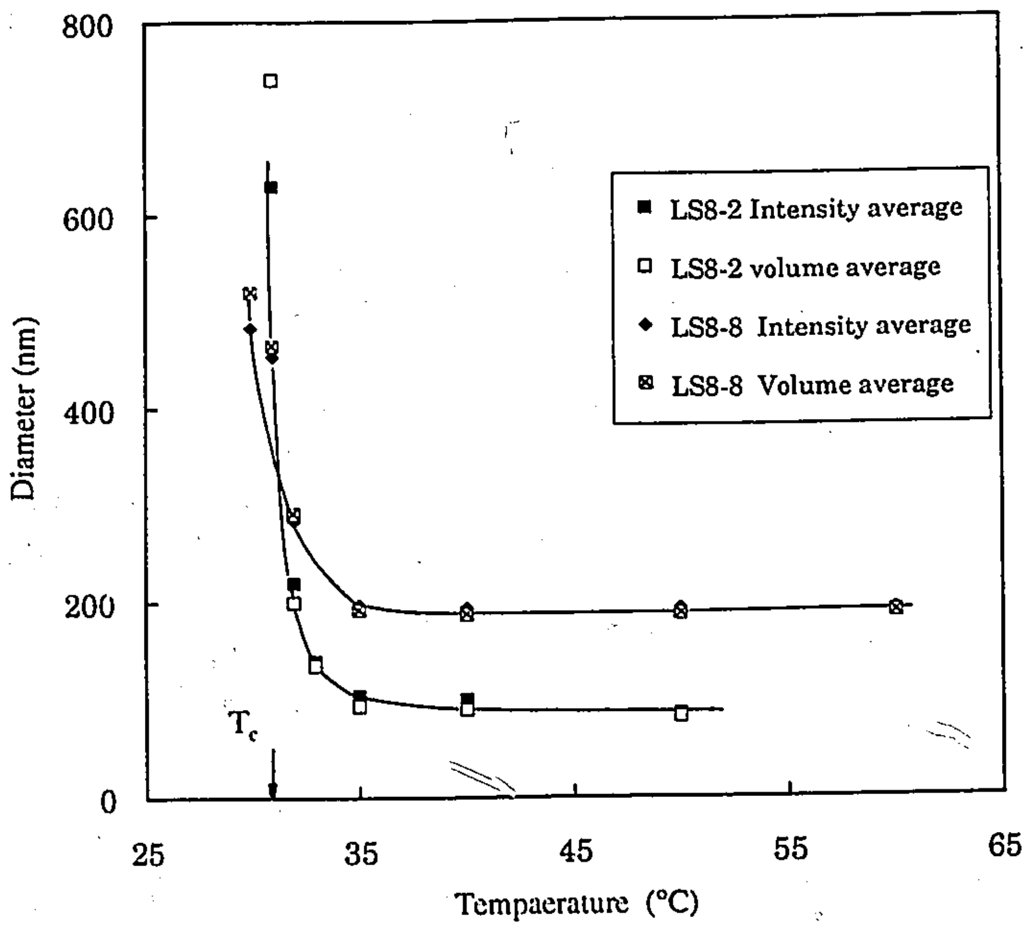

Figure 3.6: Hydrodynamic size of poly(NIPAM) (LS8) in water versus temperature. Monomer conversions: LS8-2 8.9%; LS8-8 100%

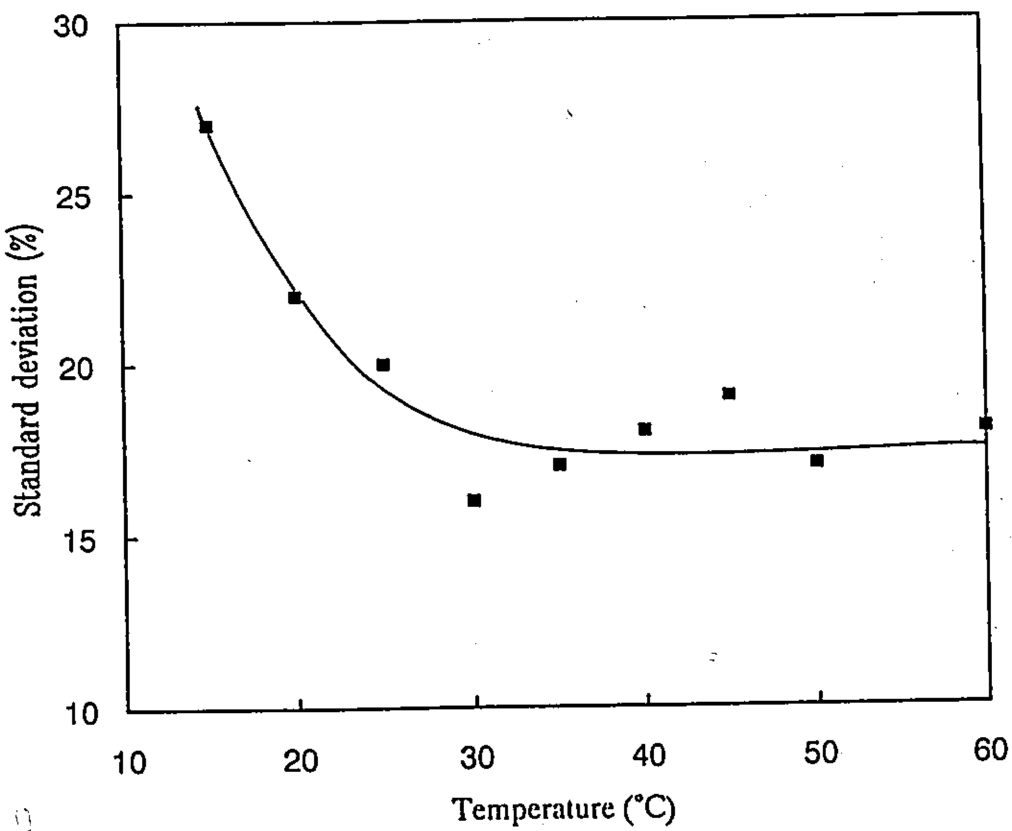

Figure 3.7: Standard deviation of particle size distribution versus temperature. poly(NIPAM/BAM) LS13 with BAM 0.128 mole fraction

at temperatures above T_c, the diameter of LS8-8 was larger than that of LS8-2; At temperatures lower than T_c, the diameter, as well as the difference between intensity average and volume average of LS8-8 were smaller than those of LS8-2. This suggests that the poly(NIPAM) chains at different conversion had different structure - more compact structure at higher conversion.

(iii) Particle size, PSD and solvent

Table 3.1 is a summary of LS1 particle diameter measured in various solvents. It is found that among the studied solvents, isopropanol is the best, acetonitrile is the poorest, although they have similar values of solubility parameters. Probably, this is because isopropanol has hydrophobic isopropyl group as well as polar hydroxyl group, which provide best association with NIPAM repeat units.

Table 3.1 Particle diameters of LS1 in various solvents at 25 °C

Solvent	n_D	δ	η	Diameter (nm)	
				Volume average	Intensity average
Isopropanol	1.375	11.5	2.13	480	427
Methanol	1.329	14.5	0.547	475	456
Water	1.333	23.4	0.894	450	428
Butanol-1	1.397	11.4	2.50	430	400
Acetonitrile	1.342	11.8	0.345	290	284

Figure 3.8 shows the diameter of NIPAM polymeric particles in organic solvents at various temperature. The thermal behaviour was different from that in water. In acetonitrile the particles expanded when temperature increased. In methanol the particle size decreased a bit when temperature elevated from 20 °C to 40 °C. Within the studied temperature range, no

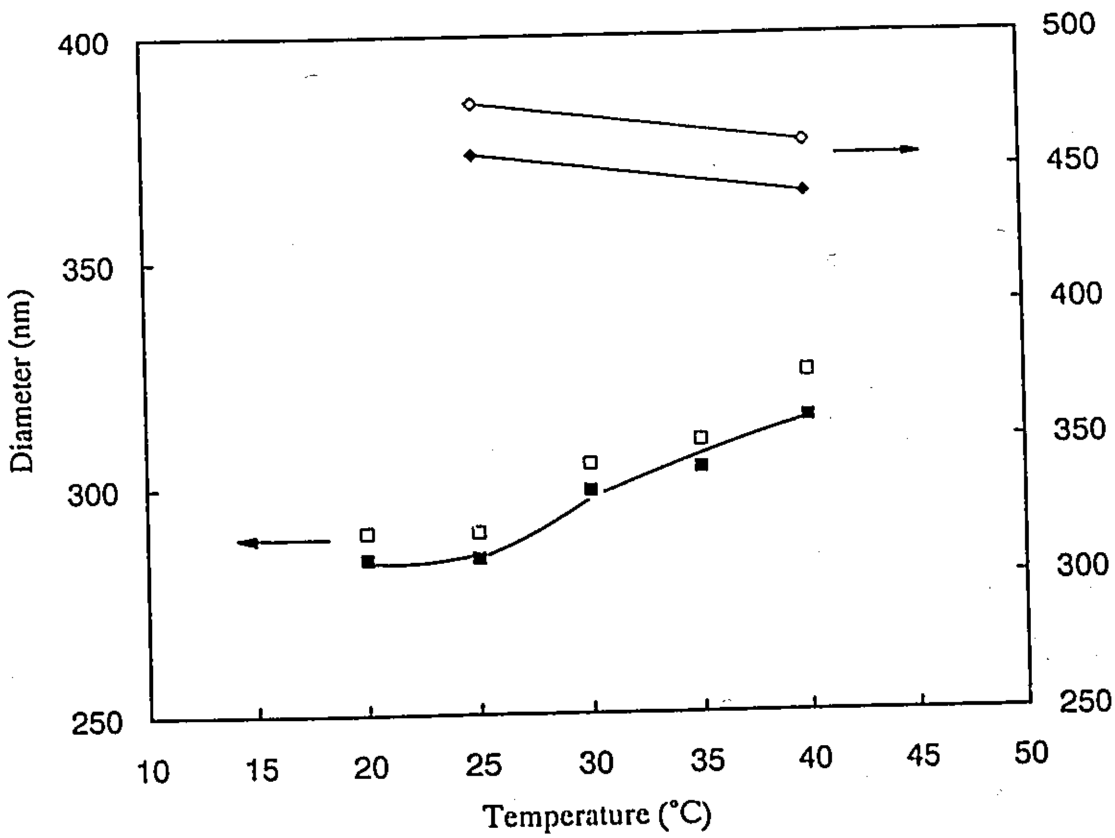

Figure 3.8: Diameter of LS5 in organic solvent at various temperature. Square represents diameter in acetonitrile, diamond in methanol; solid symbols are intensity average, blank are volume average.

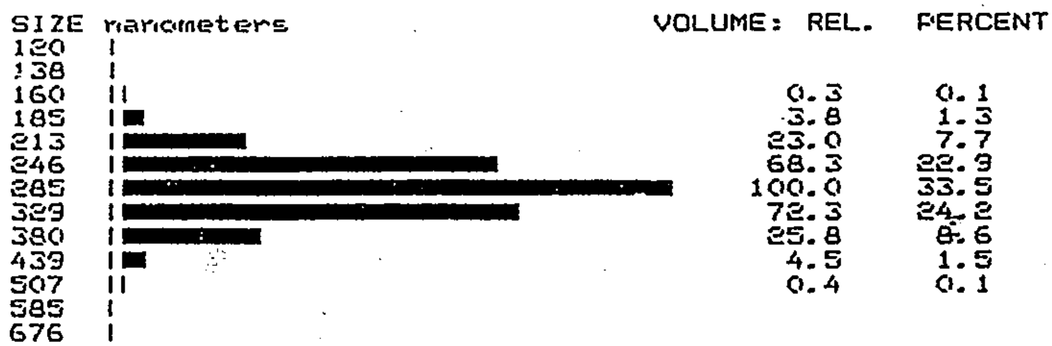

(a)

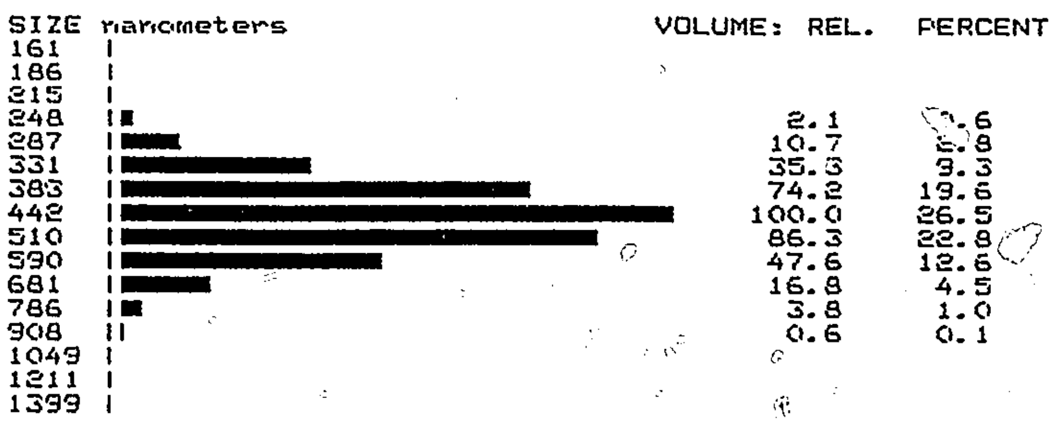

(b)

Figure 3.9: Particle size distribution of LS1 by DLS from Gaussian analysis. (a) in acetonitrile at 25 °C; (b) in methanol at 40 °C

volume transition temperature was observed in both cases.

Figures 3.9 (a) and (b) are the original particle size distribution of LS1 in methanol and in acetonitrile determined by DLS from Gaussian analysis based on volume. The probability (P %) of each particle fraction, which is defined as the percentage of the particles larger than certain size, has been calculated from the original data (diameter D and fraction F). The computation results are listed in Table 3.2 and plotted in Figure 10.

It is seen that in both cases the particle population can be described well by log-normal distribution since good straight lines were obtained. The standard deviations were calculated

Table 3.2 Probability of particle fractions of LS1 by DLS
(F is the percentage of each fraction)

(a) in acetonitrile at 20 °C			(b) in methanol at 40 °C		
D (μm)	F (%)	P (%)	D (μm)	F (%)	P (%)
0.541 <	0.0	100.0	0.969 <	0.1	99.8
0.541 - 0.468	0.1	99.9	0.969 - 0.838	1.0	99.7
0.468 - 0.406	1.5	99.8	0.838 - 0.726	4.5	98.7
0.406 - 0.351	8.6	98.3	0.726 - 0.630	12.6	94.2
0.351 - 0.304	24.2	89.7	0.630 - 0.544	22.8	81.6
0.304 - 0.262	33.5	65.5	0.544 - 0.472	26.5	58.8
0.262 - 0.227	22.9	32.0	0.472 - 0.409	19.6	32.3
0.227 - 0.198	7.7	9.1	0.409 - 0.356	9.3	12.7
0.198 - 0.171	1.3	1.4	0.356 - 0.307	2.8	3.4
0.171 - 0.149	0.1	0.1	0.307 - 0.264	0.6	0.6

using Equation (3.15) according to Woods' notation,[23] and found σ_g = 1.21 and 1.24 units for the particles in acetonitrile and in methanol respectively, i.e., slightly broader distribution for the latter.

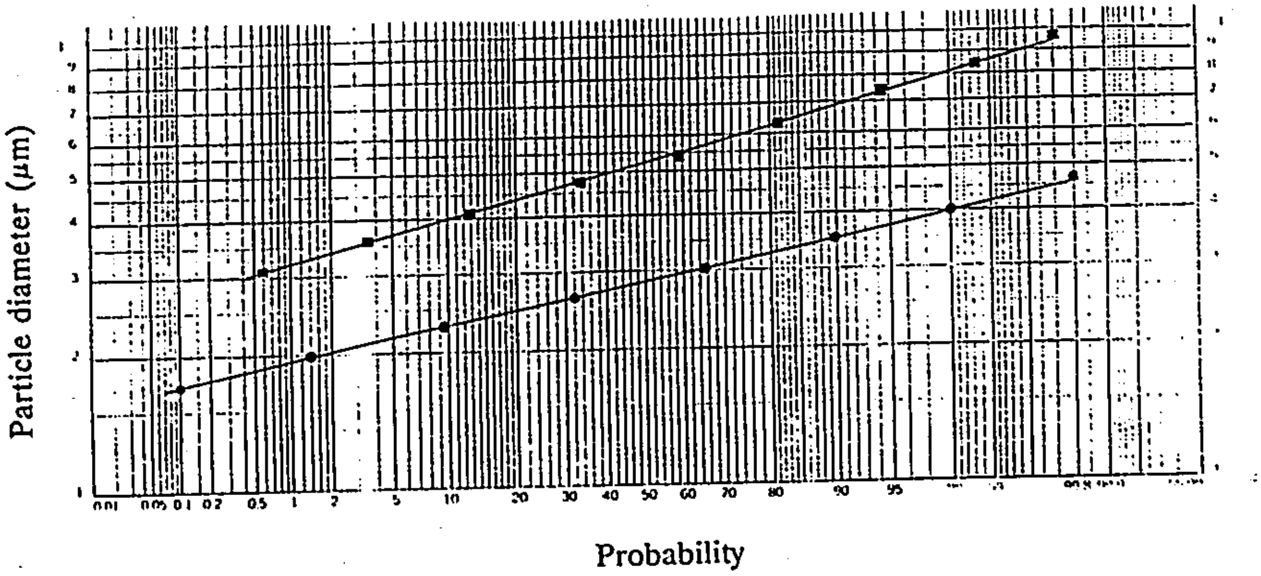

Figure 3.10 Probability of particle fractions of LS1 by DLS. (■) in methanol at 40 °C; (●) in acetonitrile at 25 °C

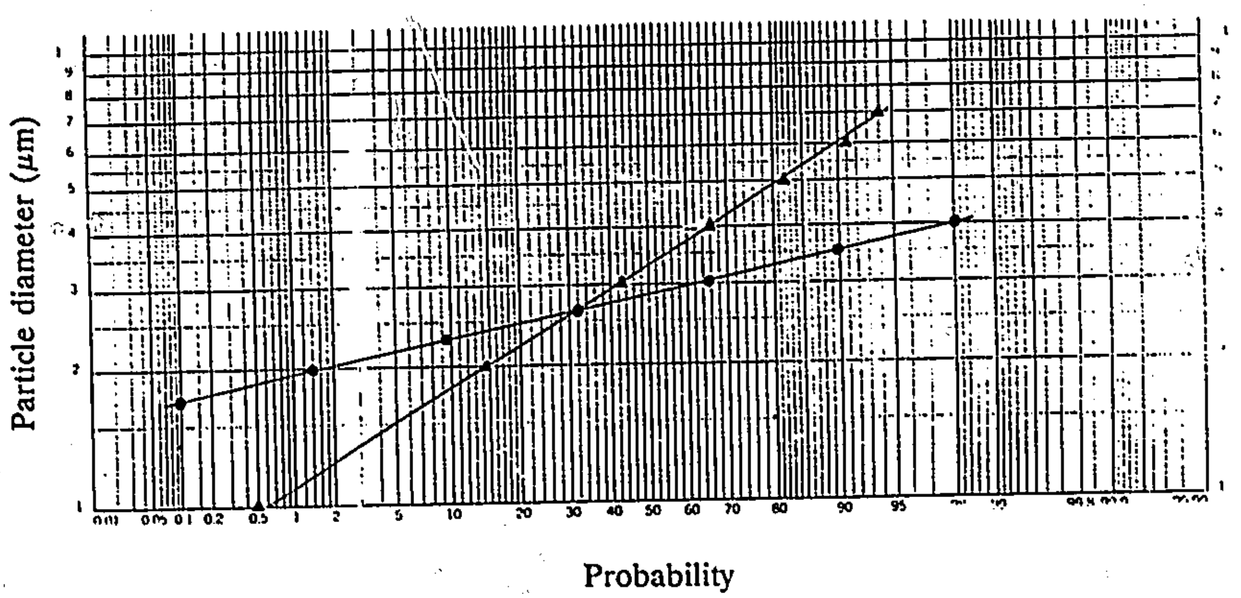

Figure 3.11 Probability of particle fractions of LS1 in acetonitrile at 25 °C (▲) by CSD; (●) by DLS

(iv) PSD by DLS and CSD

The particle size and particle size distribution of LS1 in acetonitrile were determined by both dynamic light scattering and centrifugal sedimentation. The data by DLS are in Figure 3.9 (a) and Table 3.2, and those by CSD is given in Table 3.3.

Table 3.3 Particle size distribution by CSD (volume average)

D (μm)	[a]F (%)	[b]P (%)
1.00 <	0.0	100.0
1.00 - 0.90	0.0	100.0
0.90 - 0.80	0.0	100.0
0.80 - 0.70	6.0	100.0
0.70 - 0.60	3.0	94.0
0.60 - 0.50	9.0	91.0
0.50 - 0.40	16.3	82.0
0.40 - 0.30	23.1	65.7
0.30 - 0.20	28.1	42.6
0.20 - 0.10	14.0	14.5
0.10 - 0.09	0.4	0.5
0.09 - 0.00	0.1	0.1

a - F is the fraction of the particles with the diameter D.
b - P is the cumulative fraction of the particles with diameters smaller than the top limit D. For example, P = 42.6% is the cumulative fraction of particles with diameters smaller than 0.30 μm.

The data by two methods were described by log-normal distribution and plotted in Figure 3.11. The geometric mean diameter of particles measured by CSD D_g was 320 nm which was larger than that by DLS (280 nm). The particle size distribution from CSD was broader than that from DLS. The standard deviation σ_g of the former was 1.66, and the latter was 1.21.

3.5 DISCUSSION

3.5.1 Heterogeneity within Particles

(i) Radial distribution of cross-linking density in poly(NIPAM/BAM) particles

The particles formed at very beginning had the highest BAM content which was evidenced by the higher reaction rate of BAM than NIPAM, and evidenced by the smallest swelling ratio. As the polymerization proceeded, more and more NIPAM was combined to particles, and hence higher and higher swelling ratios were observed. Therefore, it is believed that most compact structure exists in the core, and gradually increased loose structure in the shell of poly(NIPAM/BAM) particles.

A more quantitative picture to describe the structure of poly(NIPAM/BAM) particles is presented by the plot of average across-linking density against particle radius (Figure 3.12). The figure shows that the cross-linking density decreases with the increase in particle radius. In the figure, the cross-linking density ρ was calculated after Flory[21]

$$\rho = \nu / xN_{o} = 2N_{BAM_x} / xN_{o} \tag{3.19}$$

where ν is the number of cross-linked units; N_o is the total number of monomer units, x is the total monomer conversion, and thus xN_o is the total monomer units contained in the polymer; N_{BAM_x} is the number of BAM combined to polymer, assuming no cyclization and complete conversion of double bonds.

(ii) Long chain branching in homopolymer of NIPAM

The homopolymer of NIPAM prepared in this work, as described in Section 3.4.5 (ii), had less swelling capability at higher conversion. This suggests that the long chain branching may

Figure 3.12 Average cross-linking density varies with particle radius

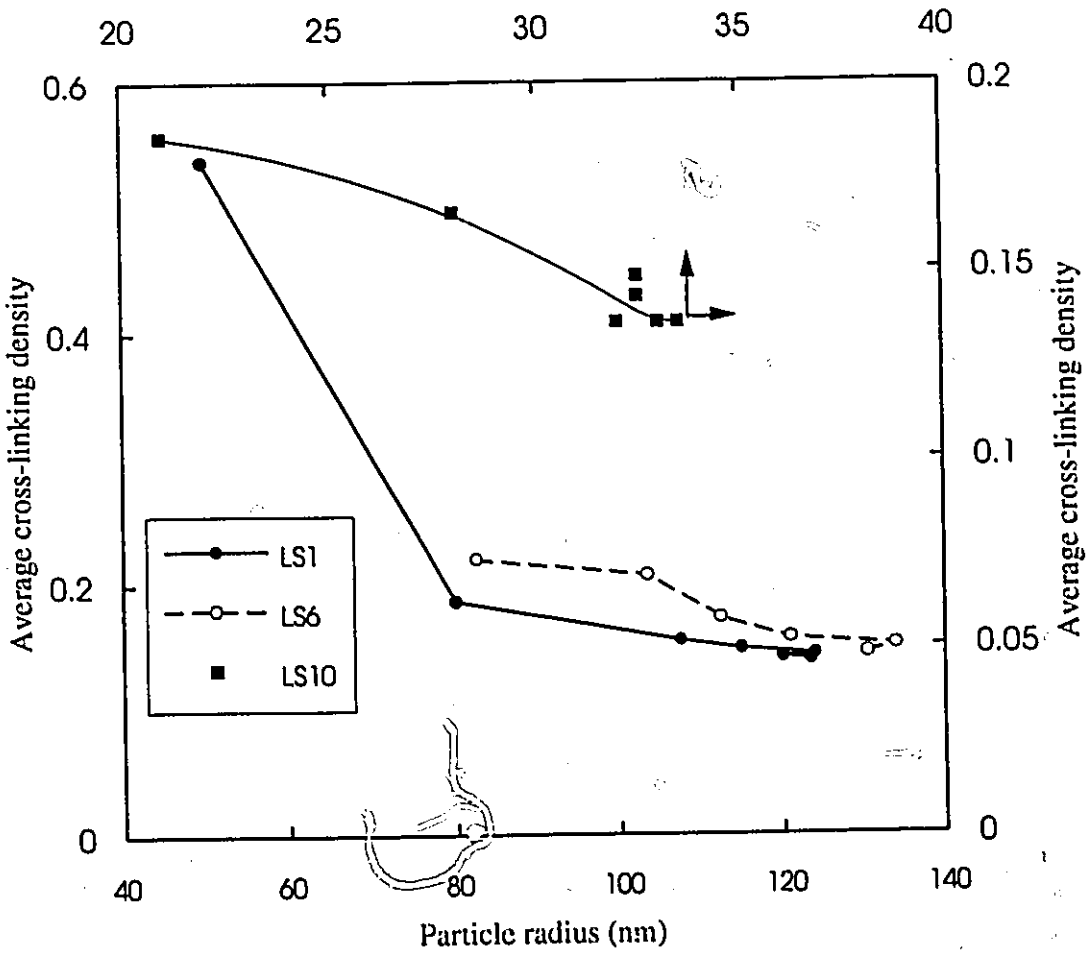

be formed at high conversion. A polymer with long chain branching has fewer free chain-ends but higher molecular weight per unit volume, therefore it shows less swelling capability. The failure of filtrating poly(NIPAM) through cellulose membrane up to pore size 0.8 μm may support the hypothesis of long chain branching structure.

It is worthy to mention that the particles of poly(NIPAM) can be detected by DLS even at the temperature below the cloud point T_c. Also the diameters were ca. 500 - 700 nm. These imply that the poly(NIPAM) chains have super-high molecular weights, since the molecular weight of a particle with hydrodynamic radius of 250 - 350 nm is in the range of 0.6 - 1×10^8 g/mol, according to Kubota et al.'s correlation (see Part B Table 1.2). The super-high molecular weight again supports the long chain branching.

3.5.2 Heterogeneity among Particles

(i) Broader distribution at lower temperature

In Figure 3.7 the standard deviation of the particle size distribution increased with temperature at temperature lower than 30 °C. This may be the case if the particles swell to different extent as temperature decreases and hence may suggest heterogeneity, such as cross-linking density difference, among particles.

(ii) Density distribution from comparison of DLS and CSD results

The particle size distributions of LS1 in acetonitrile by CSD and by DLS were quite different as shown in Figure 3.11. If assuming that the distribution by DLS is correct, the differences by two methods may be caused by a density distribution of particles, because CSD is sensitive to particle density whereas DLS is not. The particle density distributions were obtained using the following procedure: forcing the particle size determined by CSD equal to that by DLS and recalculating the particle density for each slice.

The calculation was based on Stokes' sedimentation equation (Equation 3.16). Rearranging Equation 3.16, one can obtains:

$$D_{CSD}^2\,(\rho - \rho_o) = \frac{18\eta_o \ln(x_2/x_1)}{\omega^2(t)\,t} \qquad (3.20)$$

where D_{CSD}^2 is the diameter determined by CSD. For a given system and at a fixed time, Equation 3.20 equals constant. If let

$$D_{correct} = D_{DLS} \qquad (3.21)$$

then

$$D_{DLS}^2(\rho_{cal} - \rho_o) = \text{constant} = D_{CSD}^2(\rho_{set} - \rho_o) \qquad (3.22)$$

$$\rho_{cal} = (D_{CSD}/D_{DLS})^2(\rho_{set} - \rho_o) + \rho_o \qquad (3.23)$$

where ρ_{set} is the value of particle density input to CSD instrument for particle size calculation; ρ_{cal} is the value of particle density calculated from Equation 3.23. In the calculation, ρ_{set} = 0.86 and ρ_o = 0.78 (density of acetonitrile) were used.

The particle densities were then calculated for the particle fractions of various diameters. The results are plotted in Figure 3.13. The average particle density and the standard deviation were 0.90 and 1.08 respectively based on log-normal analysis. Since the density of acetonitrile is ~ 0.78, and the density of dry polymer is ~ 1.3 (see Part B Chapter 5), the average density of swollen particles 0.90 implies about 77 % solvent in the swollen particles which is quite

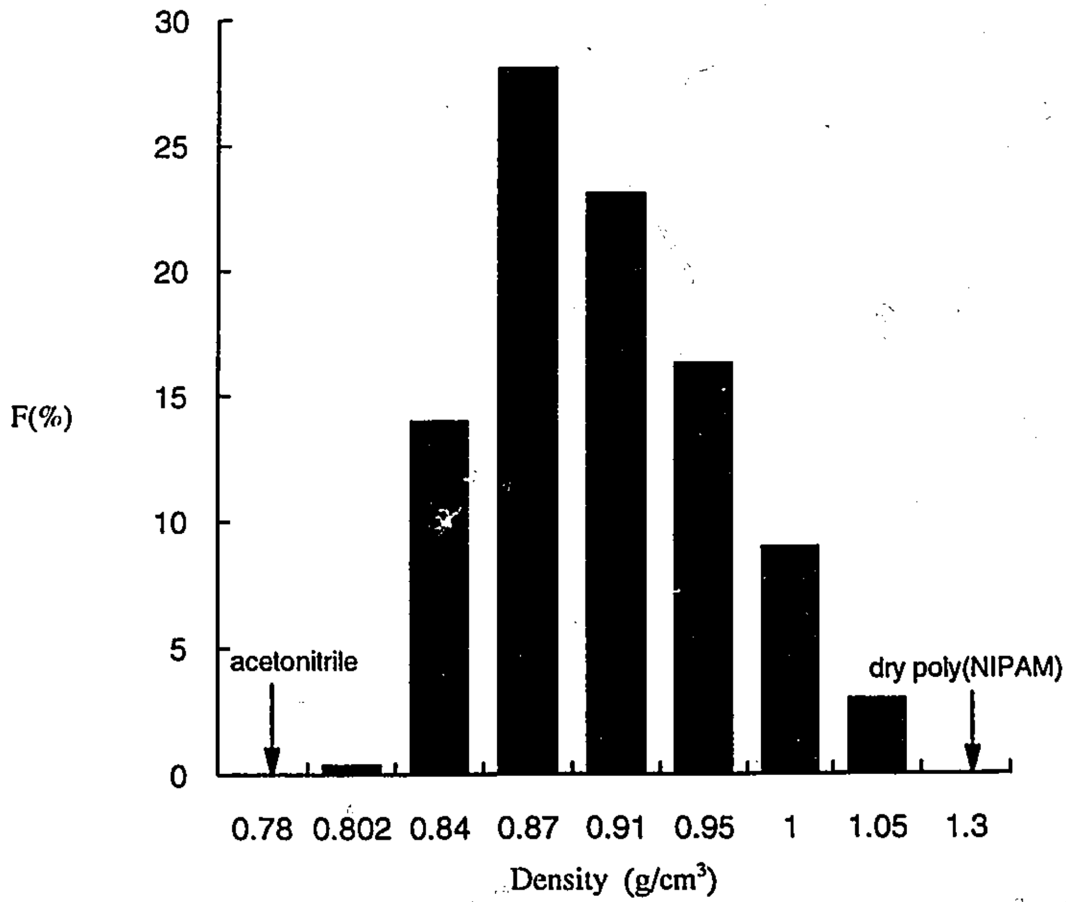

Figure 3.13 Density distribution of poly(NIPAM) latex (LS1) in acetonitrile at 25 °C

reasonable compared with the water content ~ 90 % in water-swollen particles at room temperature.

3.6 SUMMARY

The average cross-linking density of poly(NIPAM/BAM) particles decreased as the polymerization proceeded, which was evidenced by the increasing swelling ratios with the reaction time or monomer conversion, and by the decreasing swelling ratios with the BAM content in the polymers. If assuming that almost all the particles were formed at the early stage of polymerization, then the average cross-linking density of the particles was believed to be decreasing along the particle radius. The swelling extent of the particles was observed to be a function of not only BAM content but also particle size.

References

1. L.C. Dong and A.S. Hoffman, in *Reversible Polymer Gels and Related Systems*(ACS Symposium Series **350**, 236-244, 1987)
2. K.Mukae, Y.H.Bae, T.Okano, and S.W.Kim, Polymer Journal, **22**(3), 250-65 (1990)
3. R. Yoshida, K. Sakai, T. Okano, and Y. Sakurai, Polymer Journal, **23**, 1111-21 (1991)
4. C.-A.Cole, S.M.Schreiner, J.H.Priest, N.Monji, and A.S.Hoffman, in *Reversible Polymeric Gels and Related Systems*(ACS Symposium Series **350**, 245-54, 1987)
5. R.F.S. Freitas and E.L. Cussler, Separation Science and Technology, **22**(2&3), 911-19 (1987)
6. Y. Hirokawa and T. Tanaka, J. Chem. Phys., **81**(12), Pt.II, 6379 (1984)
7. Y. Hirokawa, E. Sato, S. Hirotsu, and T. Tanaka, Proceedings (ACS Div. Poly. Mater. Sci. Eng.), **52**, 520-22 (1985)
8. T. Tanaka, E. Sato, Y. Hirokawa, S. Hirotsu, and J. Peetermans, Physical Review Letters, 55(22), 2455-58 (1985)

9. T. Amiya, Y. Hirokawa, Y. Hirose, Y. Li, and T.Tanaka, J. Chem. Phys., **86**(4), 2375-79 (1987)

10. S. Hirotsu, Y. Hirokawa, and T. Tanaka, J. Chem.Phys.,**87**(2), 1392-95,(1987)

11. S. Hirotsu, Journal of Physical Society of Japan, **56**(1), 233-42 (1987)

12. S. Hirotsu, J. Chem. Phys. **88**(1), 427-31 (1988)

13. S. Hirotsu, Proceedings of the Sixth International Meeting on Ferroelectricity, Kobe 1985, Japanese Journal of Applied Physics, **24**, Supplement **24-2**, 396-398 (1985)

14. M. Marchetti, S. Prager, and E.L. Cussler, Macromolecules, **23**, 3445-50 (1990)

15. M. Marchetti, S. Prager, and E.L.Cussler, Macromolecules, **23**, 3445-50 (1990)

16. H. Inomata, S. Goto, and S. Saito, Macromolecules, **23**, 4887-88 (1990)

17. K. Otake, H. Inomata, M. Konno, and S. Saito, Macromolecules, **23**(1), 283-89 (1990)

18. B.G. Kabra and S.H. Gehrke, Polymer Communications, **32**, 322(1991)

19. X.S. Wu, A.S. Hoffman and P. Yager, Polym. Preprints (Am. Chem. Soc., Div. Polym. Chem.), **32**(3), 463-464 (1991)

20. K. Mukae, Y.H. Bae, T. Okano, and S.W. Kim, Polymer Journal, **22**(3), 206-17 (1990)

21. P.J. Flory, *Principle of Polymer Chemistry* and the references herein, Cornel University, Ithaca, 1953

22. M. Morton, S. Kaizerman and M.W. Altier, J. Coll. Sci. **9**, 300-312 (1954)

23. D.R. Woods, Surface Phenomena and Unit Operations, McMaster University, Hamilton, Canada (1989)

24. *Instruction Manual for Particle Size distribution Analyzer*, Horiba, Ltd., Kyoto, Japan

CHAPTER 4

DETERMINATION OF PARTICLE CONCFNTRATION OF POLY(N-ISOPROPYLACRYLAMIDE) LATICES BY MULTIPLE TECHNIQUES

4.1 Introduction

The number concentration of particles was a key variable in studying the mechanism and the kinetics of emulsion polymerization and dispersion polymerization. Usually, for non-swollen or slightly swollen particles, the densities and the refractive indices are easily found in literature or measured in laboratory. In this case, the number concentration of particles is easily determined from the particle size and the solid content[1,2]. For highly swollen particles, however, determining the density or refractive index of the particles becomes difficult due to the slight difference between the particles and the medium and the uncertainty of solvent content in the particles. Poly(NIPAM) hydrogel particles are highly swollen in water at room temperature so particle concentration is a difficult parameter to estimate.

In this work, three approaches were used to estimate the particle concentration of this system. The first was based on the density measurements. The second was based on light scattering measurements combined with theoretical calculation. The third was based on viscosity measurements.

4.2 THEORETICAL CONSIDERATIONS

The theoretical background of three techniques, densitometry, turbidimetry and viscometry is given in this section.

4.2.1 Densitometry Approach

In this approach the particle concentration was estimated based on experimental measurements of density and particle size. The theory and assumptions are now presented.

The weight concentration of particles (unspecified, e.g., swollen or non-swollen particles) C (g/cm^3) was defined as

$$C = N_p \frac{\pi}{6} \bar{D}^3 \rho_p \tag{4.1}$$

Therefore, the number of particles in one cubic centimetre can be found:

$$N_p = \frac{6\ C}{\pi \bar{D}^3 \rho_p} \tag{4.2}$$

where $\bar{D}$ is the volume average particle diameter in cm, ρ_p is the density of unspecified particles in g/cm^3. ρ_p may be estimated from the density of diluted suspension by assuming no volume change of particles with dilution of suspension, i.e., the densities of wet particles and the medium are linearly additive,

$$\rho_s = \phi_m \rho_m + \phi_p \rho_p \tag{4.3}$$

where ρ_s and ρ_m are respectively the densities of the suspension and the medium, ϕ_m and ϕ_p are the volume fractions of the medium and the wet particles.

It is difficult to determine the volume fraction of highly-swollen particles because the maximum packing fraction of particles is shear-dependent.[3] In order to eliminate ϕ_p some rearrangement of Equation 4.3 is needed.

Since the particle concentration $\quad C\ (\mathrm{g/cm^3}) = \rho_p \phi_p$

and the volume fraction of particles $\quad \phi_p = C/\rho_p$

the Equation 4.3 can be rearranged as the follows

$$\rho_s = \rho_m + C\left(1 - \frac{\rho_m}{\rho_p}\right) \tag{4.4}$$

$$\rho_p = \frac{C\,\rho_m}{C - \rho_s + \rho_m} \tag{4.5}$$

If the dilute suspension for the density measurement is prepared from the concentrated latex (the packed bed on the bottom of ultracentrifuge tube after ultracentrifugation, from now on it will be defined as "wet latex"), the concentration of swollen particles can be estimated from the weight of latex bed based on the assumption of the interstitial fraction.

Moreover, using a suspension prepared from dry polymer, the density of dry polymer ρ_{pdry} can be obtained by Equation 4.7 following the computation of the apparent molal volume of dry polymer $\tilde{V}$ by Equation 4.6:[4]

$$\tilde{V} = \frac{M}{\rho_m} - \frac{1000}{C_p\,\rho_m}(\rho_s - \rho_m) \tag{4.6}$$

$$\rho_{pdry} = \frac{M}{\tilde{V}} \tag{4.7}$$

where M is the molecular weight of solute (g/mol), and C_p is the molarity of solute (mol/L). Actually Equation 4.7 is equivalent to Equation 4.5 but is derived by a different approach.

Both the densities of the swollen particles and the dry polymer are useful in determination of particle concentration as will be described later.

4.2.2 Turbidimetry approach

In this approach the scattering coefficient K is calculated by Mie theory, and then substituted into the turbidity equation to solve for the particle concentration.

The scattering coefficient K is a function of wavelength λ, particle diameter D (cm), and the ratio of refractive index of particles to that of medium m ($m = n_p/n_m$), and given by Mie theory[5]

$$K = \frac{2}{\alpha^2}\sum_{n=1}^{\infty}(2n+1)\left(|a_n|^2+|b_n|^2\right) \tag{4.8}$$

where α is the size parameter defined as $\alpha = \pi D/\lambda_m$, and $\lambda_m = \lambda_0/n_m$ is the ratio of the wavelength of the incident light in vacuo to the refractive index of medium. a_n and b_n are Mie coefficients. $|a_n|$ and $|b_n|$ are modules of a_n and b_n.

If the absorption of light by particles is negligible, the turbidity τ of a suspension is only caused by the scattering of the particles, and thus can be determined from the following equation:

$$\tau = \frac{1}{\iota}\ln\left(\frac{I_0}{I_s}\right) = \frac{1}{\iota}\ln\left(\frac{1}{T_r}\right) \tag{4.9}$$

where ι is the length of optical path in cm, I_0 and I_s are respectively the intensity of incident light and transmitted light, and T_r is transmittance given by the following equation:

$$T_r = \exp\left[-N_p\frac{\pi\iota}{4}D^2K(\lambda, D, m)\right] \tag{4.10}$$

For monodispersed, isotropic spherical particles, the turbidity can be correlated with other parameters as follows

$$\tau = N_p R_{scat} = N_p\frac{\pi}{4}D^2K(\lambda, D, m) \tag{4.11}$$

where R_{scat} is the cross section area of scattering, N_p is number of particles in one cubic centimetre suspension, and m is as defined previously.

Since the refractive index of swollen particles is unknown, the K value can not be directly determined from the above equations. Thus, there are two unknown parameters N_p and K in the turbidity and transmittance equations, even if the values of D and τ are measured by experiments. One more equation is needed to solve for N_p.

Because the N_p and D are identical at different wavelengths for a given sample, the unknown parameter N_p can be eliminated by taking the ratio of two turbidities at different wavelengths:

$$\frac{\tau_i}{\tau_j} = \frac{N_p \frac{\pi}{4} D^2 K_i}{N_p \frac{\pi}{4} D^2 K_j} = \frac{K_i}{K_j} \tag{4.12}$$

where subscripts i and j represent different wavelengths. If the optimal ratio of refractive indices m_{opt} can be found, the calculated scattering coefficients should satisfy the following relation:

$$\left(\frac{K_i}{K_j}\right)_{calculated} (m \rightarrow m_{opt}) = \left(\frac{\tau_i}{\tau_j}\right)_{measured} \tag{4.13}$$

Therefore, the minimum deviation between calculated (K_i/K_j) and the measured (τ_i/τ_j) gives the optimal ratio of refractive indices m_{opt}. The following objective function can be used to find the minimum deviation:

$$\min S = \min \sqrt{\sum_{i,j}\left(\frac{K_i}{K_j} - \frac{\tau_i}{\tau_j}\right)^2} \tag{4.14}$$

where the summation is for the quantities at various wavelengths.

The computing procedure is outlined in Figure 4.1.

Figure 4.1 Flow chart of computation

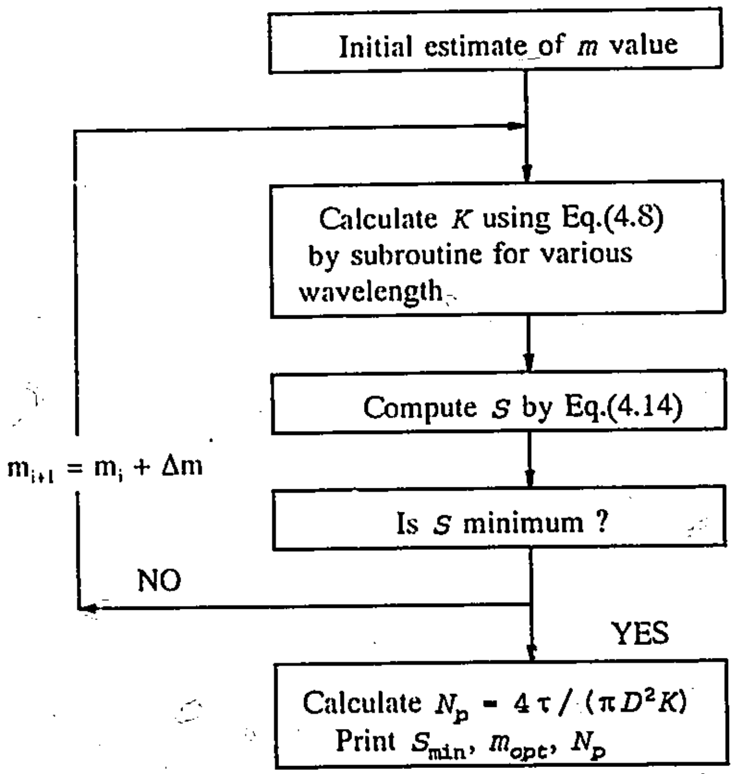

Thus, the particle concentration N_p can be estimated.

4.2.3 Viscometry Approach

The theoretical basis for this approach is that the relative viscosity of the suspension η_r (η_r is the ratio of viscosity of suspension η_{susp} to the viscosity of medium η_m, $\eta_r = \eta_{susp}/\eta_m$) is a function of the volume fraction of particles ϕ.[6,7,8,9,10,11] Numerous equations have been developed theoretically or empirically to correlate the relative viscosity with the volume fraction.

Einstein (1905)[11] first derived the theoretical equation of viscosity for dilute suspensions

$$\eta_r = 1 + 2.5\phi \tag{4.15}$$

Later on, many authors[6,7,8,9] evaluated this equation and found that it is only valid for extremely dilute suspensions, say $\phi < 0.01$.[4,7]

Frankel and Acrivos[12] derived a theoretical equation to describe the viscosity-concentration behaviour for high concentrations:

$$\eta_r = \frac{9}{8}\left(\frac{(\phi/\phi_{max})^{1/3}}{1-(\phi/\phi_{max})^{1/3}}\right) \tag{4.16}$$

where ϕ_{max} is the maximum attainable concentration about 0.534 to 0.74 depending on shear stress, particle shape and particle size distribution, according to Wildemuth and Williams[13].

Mooney[6] suggested a semi-theoretical equation in which the self-crowding factor k was determined empirically in the range 1.35 to 1.91 for a monodisperse system

$$\eta_r = \exp\left(\frac{2.5\phi}{1-k\phi}\right) \tag{4.17}$$

Many equations were proposed as a form of power series including Ford's,[14] Simha's[15] and Thomas'.[7] These equations can be applied to a wide range of concentration but require the estimation of one or two parameters from experimental data. Among them, Thomas' equation has same prediction of η_r as Simha's equation, but consists an exponential term accounting for the probability of transferring a particle from one shear plane to another:

$$\eta_r = 1+2.5\phi+10.05\phi^2+A\exp(B\phi) \tag{4.18}$$

where the coefficients of first three terms were determined from previous theoretical analysis, while A = 0.00273 and B = 16.6 were obtained by fitting the data in six reference sources. This equation can fit the data as well as a seventh order power series.[4]

The simplest empirical equation was originated by Maron and Pierce[16], and evaluated by Kitano, Kataoka and their coworkers[17,18] for particles in polymer melt:

$$\eta_r = [1 - (\phi/a)]^{-2} \tag{4.19}$$

where the only empirical constant, a, was determined to be 0.68 for suspensions of smooth spheres and a = 0.44 for rough crystals in a liquid.[8]

Since the particle size, or the fluid viscosity, has no effect on the relative viscosity of suspensions,[8] and the particle size distribution has little effect on the viscosity up to volume fraction $\phi \leq 0.20$,[4,8] all the above equations, except the equation for extremely dilute suspensions (Equation 4.15), can be used to find the volume fraction of poly(NIPAM/BAM) latex particles when the relative viscosity is measured.

4.3 EXPERIMENTAL

Particle size

The particle size and particle size distribution of the latices were measured with NICOMP 370 Autodilute Submicron Particle Sizer (NICOMP Particle Sizing System) comprised of a laser light source of 514 nm and a thermal-controlled holder for sample cell. The scattered light was collected at a 90° angle.

The particle diameter and the distribution were obtained using NICOMP Autocorrelator Interface Program (version 10.3) which, by assuming a Gaussian distribution, estimated a mean diameter and standard deviation. Both intensity average and volume average diameter were recorded.

Preparation of wet latex and dry polymer

After the ultracentrifugation of dilute latex, packed beds of swollen particles concentrated at the bottom of centrifugal bottles. These packed beds were collected as "wet latex". Part of the wet latex was dried in vacuum oven at 60 °C until constant weight to give the dry polymer. The weight fraction of dry polymer in wet latex, w_{dry}, was determined by weighing the wet latex and the dry polymer.

Transmittance

The transmittance of diluted wet latex was measured by Spectronic 20 and UV/Vis spectrophotometer (HP89531A).

Density

The density of suspension was determined at room temperature with the vibrating U tube densitometer DMA 401 (Anton Paar) using four dilute samples with wet latex sample of LS1:

Suspension I: prepared from wet latex of LS1. Weight fractions of wet latex in the suspension were w_{woc} = 0.09950, and 0.14751;

Suspension II: prepared from dry polymer of LS1. Weight fraction of dry polymer in the suspension was 0.004256.

The density is correlated with the period of oscillation of tube, T, by the following equation

$$\rho_s = \zeta T^2 - \beta \tag{4.20}$$

where ζ and β are constants, containing mass of oscillating tube, volume of the sample in the tube, the elasticity constant and other constants. Their values are estimated from the sample of known density, e.g. water. After calibration, for an aqueous medium Equation 4.20 becomes[19]

$$(\rho - 1.002966) = \mathrm{E}(T^2 \times 10^{-9} - 4.297977) \tag{4.21}$$

where E is constant and equals 0.518199 here.

Viscometry

The viscosity of latices was measured with #75 Cannon-Ubbelohde viscometer at 25 °C. The viscosity of the solvent was determined using deionized water as well as the supernatant of the latex.

4.4 RESULTS

The particle concentration of poly(NIPAM) latex determined by densitometry, turbidimetry and viscometry is given in this section.

4.4.1 Densitometry Approach

In this section, the densities of wet latex, dry polymer and swollen particles will be first presented. And then the particle concentration estimated from these densities will be reported.

(i) Densities of wet latex, dry polymer and swollen particles

The densities of wet latex ρ_{pwot}, dry polymer ρ_{pdry}, and swollen particles ρ_{sp} were determined by applying Equations 4.5 - 4.7 using four suspensions of different concentrations. In all the cases, the densities were assumed to be linearly additive (see Equation 4.3). The equations used for the calculation of the densities are summarized in Table 4.1 and the calculation procedures are illustrated in Figure 4.2.

Table 4.1 Equations for density calculation

Eq.#	Density	Equation	Definitions
(a)	General	$\rho_p = \dfrac{C\rho_m}{C-\rho_s+\rho_m}$	C - concentration of any particles (g/cm^3)
(b)	Wet latex	$\rho_{pwot} = \dfrac{C_{wot}\rho_m}{C_{wot}-\rho_s+\rho_m}$	C_{wot} - concentration of wet latex in suspension. $C_{wot} = W_{wot}\times\rho_s$
(c)	Dry polymer from Suspension I	$\rho_{pdry} = \dfrac{C_{dry}\rho_m}{C_{dry}-\rho_{pwot}+\rho_m}$	$C_{dry} = C_{wot}\times w_{dry}$ w_{dry} - weight fraction of dry polymer in the wet latex. w_{dry} = 0.12 here.
(d)	Dry polymer from Suspension II	$\rho_{pdry} = \dfrac{M}{\tilde{V}}$ $\tilde{V}$ from Eq.(4.6)	M - molecular weight of monomer unit. For poly(NIPAM/BAM) $M = M_{NIPAM}F_{NIPAM} + M_{BAM}F_{BAM}$ F - mole fraction of monomer
(e)	swollen particles	$\rho_{sp} = \dfrac{\rho_{pwot}-\phi_t\rho_m}{\phi_{sp}}$	ϕ_t - interstitial volume fraction ϕ_{sp} - volume fraction of swollen particles. Both values were assumed.

Figure 4.2 Flow chart of determination of densities

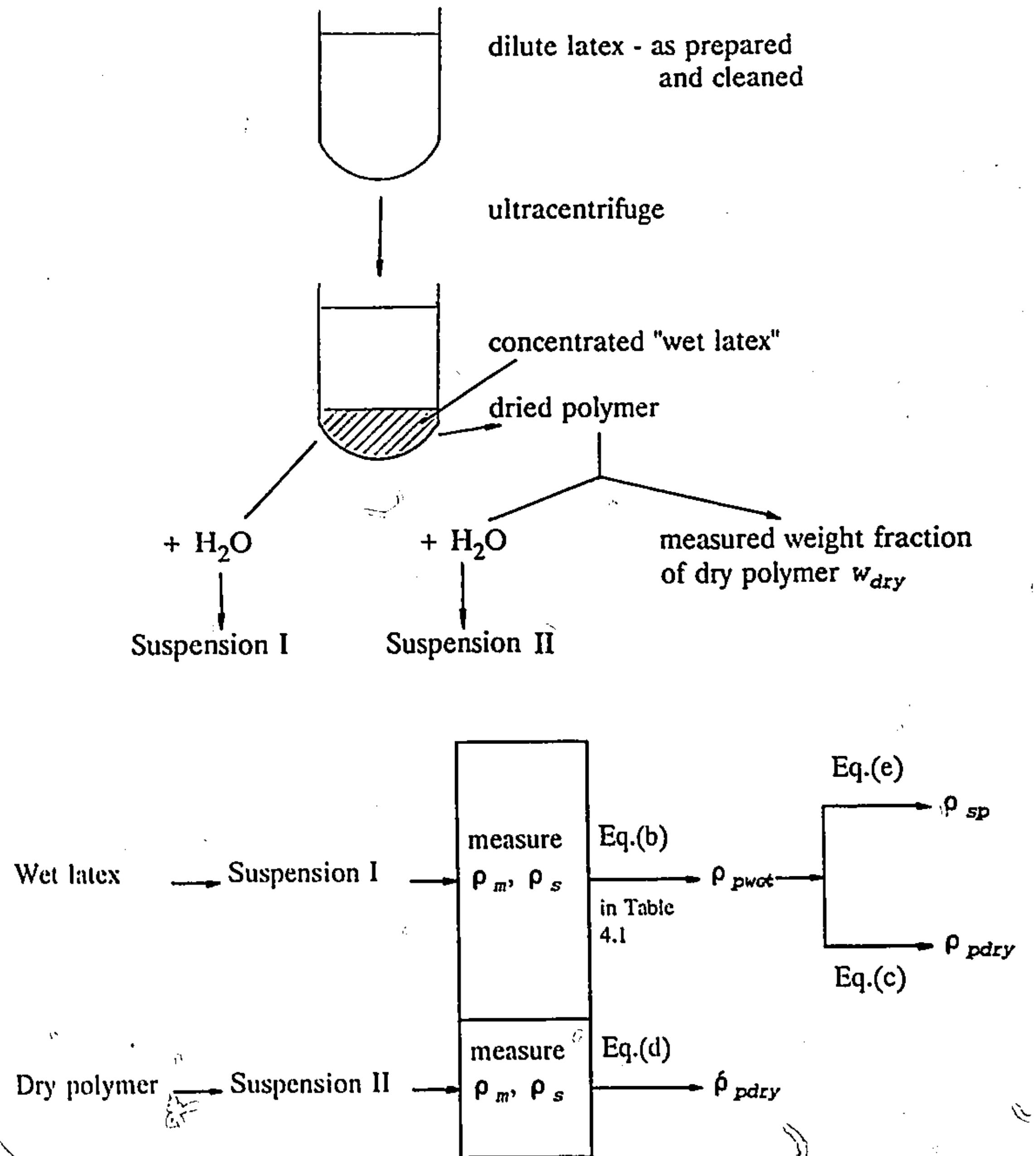

According to the above procedures, the densities of wet latex and dry polymer of LS1 were calculated using the measured densities of water and suspensions. The molecular weight of monomer unit in LS1 used to compute the density of dry polymer was estimated as follows: $M = 113.16 \times 0.932 + 154.2 \times 0.068 = 115.95$, since LS1 contained 0.068 mole fraction of BAM. The results are summarized in Table 4.2. It is seen from the table that the density of wet latex from two concentrations of Suspension I were very close, while the density of dry polymer had larger deviation. The densities of dry polymer determined from Suspension II were exactly same by using two equations, Equation 4.5 and Equation 4.7. This suggests that the two equations are equivalent.

Table 4.2 Densities of suspension, wet latex and dry polymer of LS1

weight fraction	concentration (g/cm^3)	ρ_s*	ρ_m*	ρ_{pwet}	ρ_{pdry}	$\hat{\rho}_{pdry}$
Suspension I	C_{wet}					
0.099950	0.100027	1.000768	0.998170	1.0249	1.2754	/
0.14751	0.14776	1.001700	0.999040	1.0226	1.2463	/
Suspension II	C_{dry}					
0.004256	0.0042556	0.999968	0.998968	/	/	1.3058$_1^{a}$
	C_p (mol/L)					
	0.036702					
	$\tilde{V}$ (cm^3/mol)					
	88.795					1.3058$_1^{b}$
Average				1.0238 ±0.0012	1.2609 ±0.0146	1.3058 ±0.0000

* The error in the measurements of densities ρ_s and ρ_m was estimated to be $\pm 6 \times 10^{-5}$ from the repetitions.
a using Equation 4.5
b using Equation 4.6 and 4.7

Since the wet latex was obtained by ultracentrifugation, extra water among swollen particles might present. To determine the density of swollen particles ρ_{sp}, the volume fraction of the extra water in wet latex, defined as volume fraction of interstitial water ϕ_ε, was assumed. For comparison, two assumptions about ϕ_ε value were made: (1) $\phi_\varepsilon = 0$, i.e., there is no interstitial water in wet latex and thus the volume fraction of the swollen particles in wet latex $\phi_{sp} = 1.0$; and (2) $\phi_\varepsilon = 0.3$, i.e., $\phi_{sp} = 0.7$. In the first case, the density of swollen particles ρ_{sp} is equal to that of wet latex, $\rho_{sp} = \rho_{pwet}$. In the second case, substituting the values of ϕ_ε, ϕ_{sp}, and ρ_{pwot} into Eq.(e) in Table 4.1, one can estimate ρ_{sp}. As an example, $\phi_\varepsilon = 0.3$, $\phi_{sp} = 0.7$, and $\rho_{pwot} = 1.0249$ (calculated from Eq.(b), see Table 4.2) were used to obtain ρ_{sp},

$$\rho_{sp} = \frac{\rho_{pwot} - \phi_\varepsilon \rho_m}{\phi_{sp}} = 1.0364 \qquad (4.22)$$

The concentration of swollen particles in wet latex C_{sp}

$$C_{sp} = \rho_{sp} \times \phi_{sp} = 0.7254 \qquad (g/cm^3) \qquad (4.23)$$

Thus the calibrated concentration of swollen particles in dilute suspension is

$$\acute{C}_{sp} = \frac{C_{sp}}{\rho_{pwot}} \times C_{wot} = 0.7048 \qquad (g/cm^3) \qquad (4.24)$$

In summary, the density of swollen particles with the consideration of $\phi_\varepsilon = 0.3$ is about 1% higher than that with $\phi_\varepsilon = 0$; and the densities in the both cases are close to unity, which implies a large amount of water in the swollen particles.

(ii) Determination of number concentration of particles

Applying the values of density and concentration described previously, the particle concentration was computed by Equation 4.2. The results for a latex of particle diameter

4.30×10^{-5} cm with and without consideration of interstitial volume are compared in Table 4.3.

Table 4.3 Particle concentrations of LS1 obtained by densitometry

w_{wot} (g/g)	$\acute{C}_{sp}$ (g/cm^3)	ρ_{sp}	N_{pSusp} (#/L) 10^{15}	*N_{pOrig} (#/L) 10^{15}
$\phi_\varepsilon = 0$	$\acute{C}_{sp} = w_{wot}\rho_s$	1.0238		
0.14751	0.14776		3.47	2.43
0.099504	0.099580		2.34	2.43
$\phi_\varepsilon = 0.3$	$\acute{C}_{sp} = C_{sp}\times C_{wot}/\rho_{pwot}$	1.0364		
0.14751	0.10450		2.43	1.70
0.09950	0.07048		1.64	1.70

* N_{pSusp} - particle concentration in dilute suspension. N_{pOrig} - particle concentration in original latex. Since the yield of wet latex by ultracentrifuge was 0.10339 of the weight of original latex, the N_p in original latex was calculated by $N_{pOrig} = N_{pSusp}\times\frac{0.10339}{w_{wot}}$.

It is seen from Table 4.3 that the same values of N_{pOrig} were obtained from suspensions with various particle concentrations (N_{pSusp}). However, when $\phi_\varepsilon = 0.3$ was assumed the N_{pOrig} values were about 40% lower than those for $\phi_\varepsilon = 0$.

Assuming the swelling extent is the same for all the particles in studied samples, the densities of swollen particles found for LS1 can be applied to other latexes, and therefore the number concentration of other samples may be calculated by the following procedures.

If hundred percent of the monomer is converted to the particles, then the dry particle concentration in the suspension C_{dry} (g/cm^3) equals the monomer concentration (0.0154 g/cm^3

in this work), and the concentration of swollen particles in the suspension will be found by Equation 4.25.

$$C_{sp} = \frac{C_{dry}}{f_{dry}} \qquad (g/cm^3) \qquad (4.25)$$

where f_{dry} is the weight fraction of dry polymer in swollen particles, which can be derived as follows:

$$f_{dry} = \frac{C_{dry}}{\rho_{sp}} = \frac{\phi_{dry}\rho_{pdry}}{\rho_{sp}} \qquad (4.26)$$

where ϕ_{dry} is the volume fraction of dry polymer in the swollen particles, calculated from the following equation based on assumption of linear additive of densities:

$$\phi_{dry} = \frac{\rho_{sp} - \rho_m}{\rho_{pdry} - \rho_m} \qquad (4.27)$$

Substituting Equation 4.28 into 4.27, f_{dry} becomes

$$f_{dry} = \frac{1 - \rho_m/\rho_{sp}}{1 - \rho_m/\rho_{pdry}} \qquad (4.28)$$

By applying the data set $\rho_m = 0.99817$, $\rho_{pdry} = 1.3058$ (average of ρ_{pdry} in Table 4.2), $\rho_{sp} = 1.0238$ for $\phi_\varepsilon = 0$ and 1.0364 for $\phi_\varepsilon = 0.3$ (see Table 4.2), the concentrations of swollen particles C_{sp} of LS2, LS3, LS5 and LS10 were estimated using Equations 4.25 and 4.28. Substituting the values of C_{sp} into Equation 4.2 ($C = C_{sp}$, $\rho_p = \rho_{sp}$ in this case), the particle concentrations of these latexes were calculated and listed in Table 4.4.

Table 4.4 Particle concentrations of LS2, LS3, LS5 and LS10 by densitometry

Samples	$\overline{D} \times 10^5$ (cm)	N_{pOrig} (#/L) (ϕ_ϵ = 0) 10^{15}	N_{pOrig} (#/L) (ϕ_ϵ = 0.3) 10^{15}
LS2	4.00	4.12	2.90
LS3	1.48	81.5	57.3
LS10	1.40	96.1	67.7
LS5	0.88	387	272

4.4.2 Turbidimetry Approach

The change of the summation S (see Equation 4.14) with the refractive index ratio is illustrated in Figure 4.3, in which the top and the bottom curves were obtained using K_j, τ_j values at λ = 700 and 400 nm respectively, while the middle curve corresponds to K_j, τ_j values determined at the wavelength of previous step, i.e., j = i-1. In these data, the top curve showed the largest change rate of S with m.

For the latices of particle size around 400 nm, a minimum value of S was found to give optimal m, while for those of particle size in the range 90 ~ 150, and 750 nm, no minimum S was observed. Therefore the number of particles was obtained only for the samples of particle diameter 430 (LS1) and 400 nm (LS2). The particle concentration in dilute suspension N_{pSusp} was obtained by Equation 4.11 using the K value at m_{opt}. The particle concentration in the original suspension N_{pOrig} was calculated from N_{pSusp}/C(wt.%). The results are listed in Table 4.5.

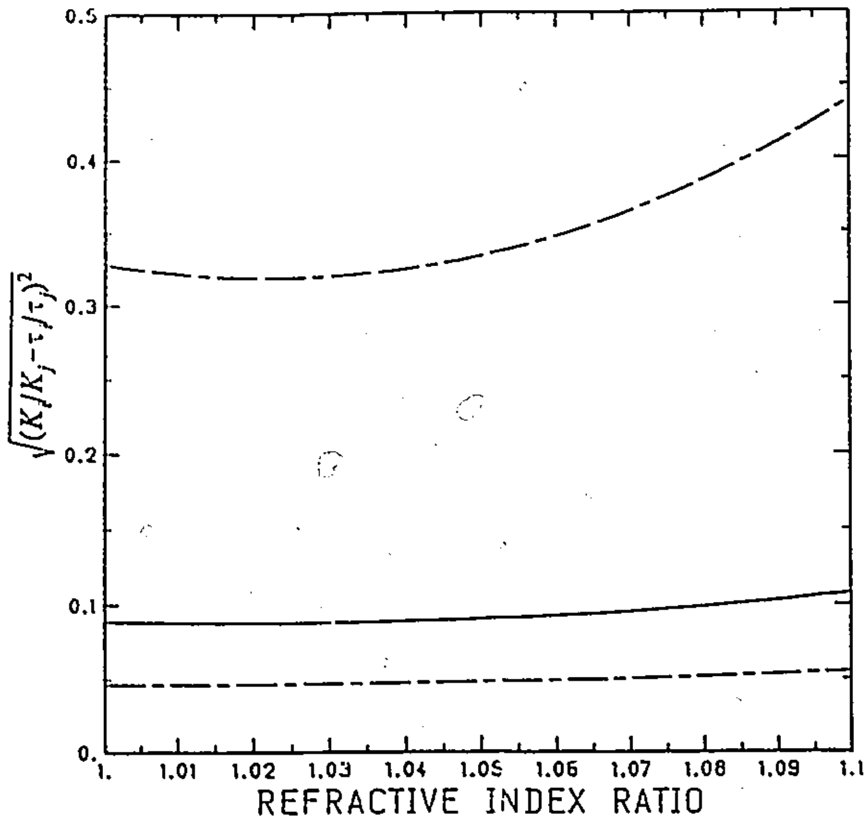

Figure 4.3: $\sqrt{(K_i/K_j-\tau_i/\tau_j)^2}$ versus refractive index ratio

Table 4.5 The refractive index ratio and particle number concentration from turbidimetry

Sample	[a]C (wt%)	m_{opt}	N_{pSusp} (#/L) 10^{13}	N_{pOrig} (#/L) 10^{15}	Denominator at λ = (nm)	[c]$<N_{pOrig}>$ (#/L) 10^{15}
LS1	0.2035	1.0225	2.85	1.45	700	
	(wet latex)	1.0200	3.83	1.95	400	1.70
	2.731	1.0185	4.17	1.53	400	
		1.0230	6.47	2.37	700	1.95
LS1-B[b]	3.320	1.0228	5.30	1.60	400	1.60
LS2	5.403	1.0215	6.75	1.25	400	1.25
	10.80	1.0210	1.45	1.35	400	1.35
Average		1.0213 ±0.0015				

a Except for the suspension of 0.2035 wt.% LS1 which was prepared from wet latex, the other suspensions were prepared from unpurified original latexes, and thus the concentrations refer to the amount of original latices in suspension.
b McPhee's sample, prepared under the same conditions as LS1.
c $<N_{pOrig}>$ - For LS1 it is arithmetic mean of N_{pOrig} at λ = 700 nm and 400 nm; For LS1-B and LS2, it is the same as N_{pOrig}.

From Table 4.5, the ratios of refractive index of the swollen particles to that of medium, m_{opt}, were similar for different samples (95% confidence interval was 0.0015). The near unity values of m_{opt} support the results by densitometry that the particles contain large amounts of water (see Discussion for the details). The particle concentration of LS1 and LS1-B obtained are 1.60 - 1.95×10[15] close to that by densitometry (1.70×10[15]) based on the assumption of 0.3 interstitial volume (see Table 4.3). However, no assumption about the interstitial volume in wet latex was required by this approach.

4.4.3 Viscometry Approach

The volume fraction of swollen latex particles was determined from the relative viscosity of the latex by Equations 4.15 - 4.19. And then the number concentration of the particles was solved from the volume fraction: $\phi = N_p \overline{D}^3 \pi / 6$. Results for five latices calculated with five viscosity models are compared in Table 4.6.

Table 4.6 Number concentration of particles in latices determined by various viscosity models*

[a]Sample			N_{pOrig} (#/L)	10^{15}	
	Eq. 4.15	[b]Eq. 4.16	[c]Eq. 4.17	Eq. 4.18	Eq. 4.19
LS1	2.97	2.34	2.23	2.11	2.06
LS2	4.38	3.08	3.14	3.00	2.94
LS3	133	72.5	8[illegible]	81.5	80.4
LS10	175	89.9	105	104	102
LS5	987	429	513	524	516

* The error in viscosity measurements was estimated to be $\pm 4 \times 10^{-6}$ from the repetitions.

a Samples LS2, LS3 and LS5 were supplied by Mr. W.C. McPhee.

b $\phi_{max} = 0.625$ was used in the calculation of volume fraction.

c In this computation $k = 1.5$.

Apparently, the Equations 4.16 - 4.19 provide close estimations of the particle concentration, while the Equation 4.15 always gives higher values. Equation 4.16 gives values similar to those obtained from Equations 4.17 - 4.19 for the samples of larger particle size but smaller values for those of smaller particle size. This may suggest that different ϕ_{max} values may be required for the particles of different size.

Since Equation 4.15 is only valid for extremely dilute suspension,[4,7] Equations 4.16 and 4.17 contain parameters of broad range of values (ϕ_{max} = 0.534 to 0.74, k = 1.35 to 1.91. The selection of parameter values is arbitrary), only Equations 4.18 and 4.19 were considered more suitable for the estimation of particle concentration in this work. Equation 4.18 will be used in later calculations although Equation 4.19 gave close N_{pOrig} values, because the parameters in Equation 4.18 were estimated from a large amounts of data.

4.4.4 Comparison of Three Approaches

The particle concentration of five latex samples obtained by three approaches are compared in Table 4.7. The values in brackets were approximated by using the refractive index ratio from latexes LS1 and LS2 (m = 1.0213), and the values by viscometry were calculated from Equation 4.18.

It seems that the results by viscometry are close to those by densitometry using ρ_{sp} = 1.0238, i.e., viscometry results support the assumption that the water volume in between swollen particles is nearly zero (ϕ_{ε} = 0). The results by turbidimetry, however, are closer to the results by assuming ϕ_{ε} = 0.3.

4.5 Discussion

This section will discuss the validity of the assumptions used in the determination of the densities, the error in N_{pOrig} caused by density evaluation, the problems in turbidimetry, and the error in viscometry.

Table 4.7 Number concentration of particles by various methods

Sample	By viscometry (Eq. 4.18)	NpOrig (#/L) 10^{15}		
		By densitometry		By turbidimetry
		$\phi_\varepsilon = 0$	$\phi_\varepsilon = 0.3$	
LS1	2.11	2.43	1.70	1.82*
LS2	3.00	4.12	2.90	1.30*
LS3	81.5	81.5	57.3	(13.1)
LS10	104	96.1	67.7	(25.1)
LS5	524	387	272	(30.6)

* These are arithmetic average of the values in Table 4.5.

4.5.1 Validity of the assumption of density and the effect of the density determination

In the densitometry approach, an assumption was made in the determination of the density of swollen particles: the density of a mixture is the linear addition of the contribution from each component (see Equation 4.3). For a suspension consisting of swollen particles and water, this assumption is supported by the plot of suspension density against weight fraction of wet latex. A reasonably good linear relationship between the two variables is shown by Figure 4.4. Moreover, the density of dry polymer obtained from molal volume of polymer (Equation 4.6 and 4.7) was the same as that from Equation 4.3. This also supports the validity of Equation 4.3 since Equation 4.6 was not based on the assumption of linear additive of individual densities.

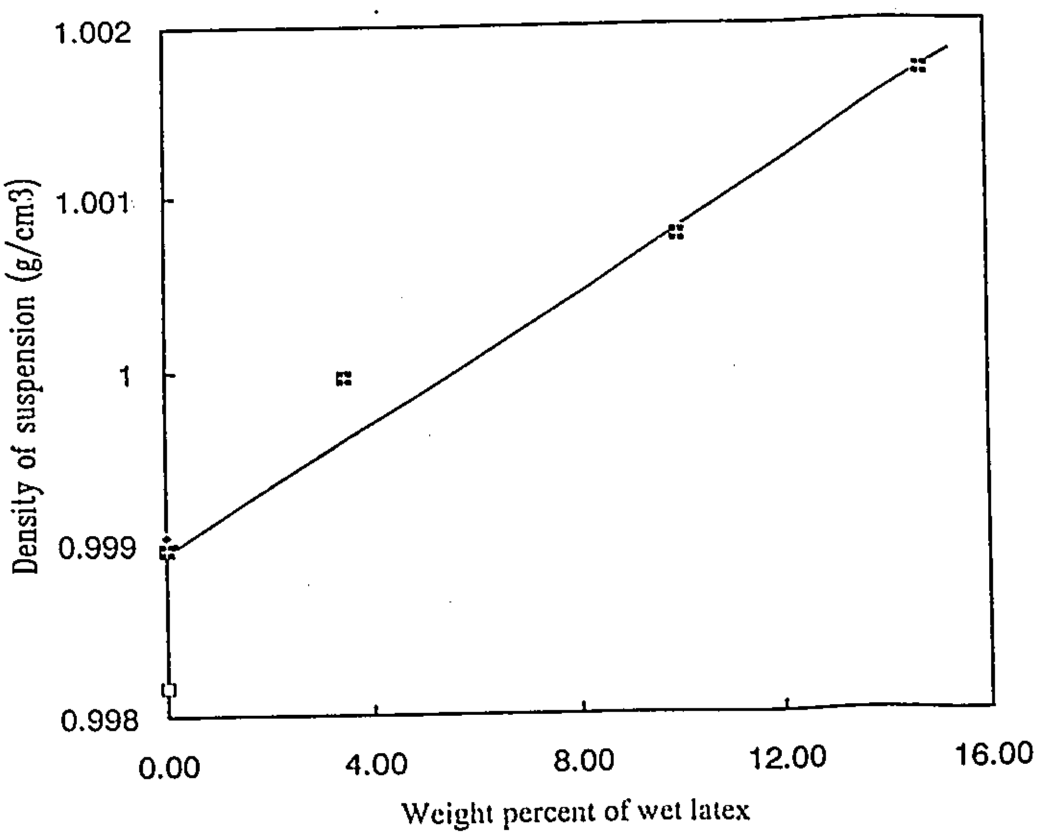

Figure 4.4: Dependence of density on the latex concentration.

However, in this approach, the change in N_{pOrig} caused by ρ_{sp} determined by assuming ϕ_{ϵ} = 0 or ϕ_{ϵ} = 0.3 was large. As illustrated by Table 4.3 and 4.4, the N_{pOrig} for ϕ_{ϵ} = 0 was about 40% higher than that for ϕ_{ϵ} = 0.3. This large difference arises from the evaluation of concentration of swollen particles $\acute{C}_{sp}$. When ϕ_{ϵ} changes from 0 to 0.3, ρ_{sp} only increases 1%, but $\acute{C}_{sp}$ reduces by a factor 0.7 (Equations 4.23 and 4.24). Since N_p is proportional to ρ_p^{-1}, and proportional to C as shown by Equation 4.2, the value of N_{pOrig} decreases by 40% if ϕ_{ϵ} changes from 0 to 0.3. Therefore, ϕ_{ϵ} is a crucial factor in the determination of N_{pOrig} by densitometry. A technique is needed to measure ϕ_{ϵ} independently.

4.5.2 Problems in Turbidimetry

From the Table 4.7 and the description in 4.4.2, there were difficulties in determining the particle concentration of LS3 - LS5 with the turbidimetry approach: (1) no minimum was found for the objective function (Equation 4.14); (2) The N_{pOrig} values, calculated using m = 1.0213 (which was determined for LS1 and LS2), were far smaller than those by viscometry or densitometry approach. One of the reasons for this might be that the particle sizes of samples LS3, LS5 and LS10 are small; hence the scattering coefficient K is insensitive to the refractive index ratio m. Figure 4.5 illustrates the dependence of K on size parameter α ($\alpha = \pi D/\lambda_m$) at two levels of m. When α becomes smaller (equivalent to smaller D value), the slope of the curves decreases. Also the K shows much less dependence on α as m reduces only 3% (from 1.05 to 1.02). Therefore, another reason causing the failure in the determination of N_p by turbidimetry for most poly(NIPAM) samples might be the small value of m (very close to unity).

The N_p values were obtained from the calculated K and the measured turbidity, and

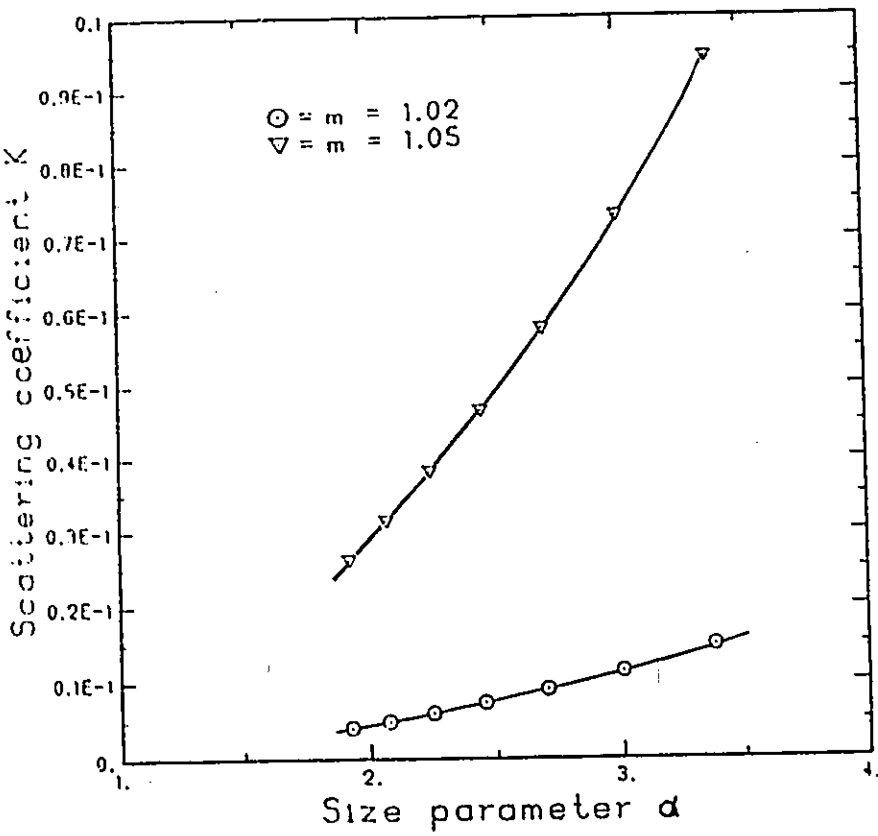

Figure 4.5: Dependence of K on α for poly(NIPAM) latex particles

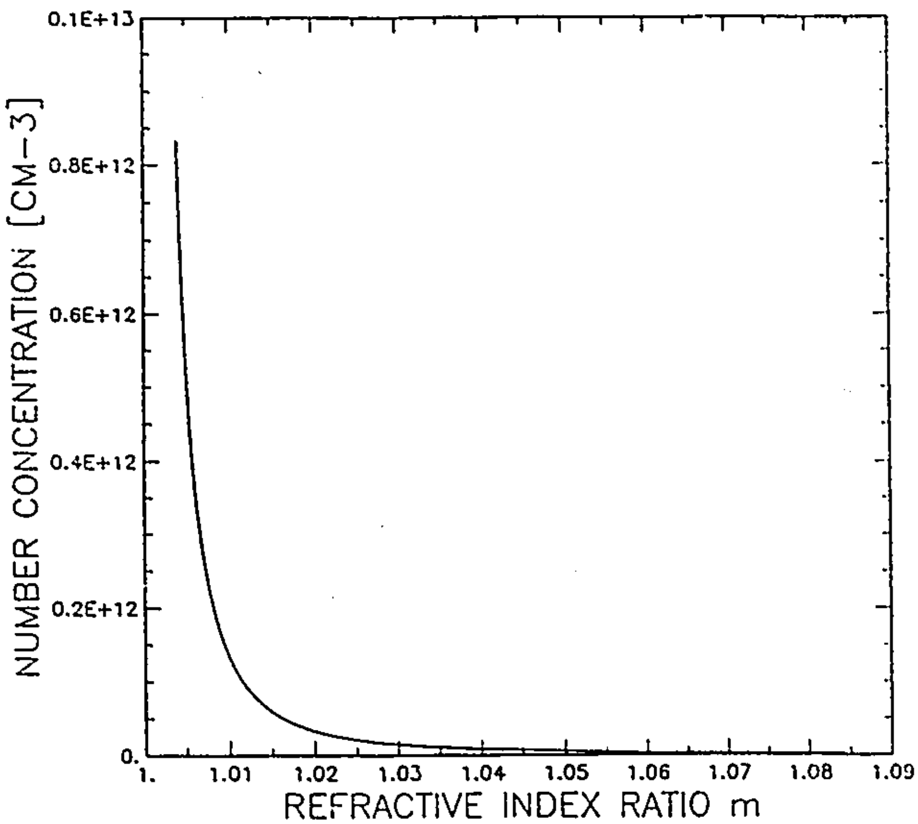

Figure 4.6: Number concentration of particles versus refractive index ratio.

plotted in Figure 4.6 against the corresponding m at which K was evaluated. This figure shows that a slight change in m value causes a dramatic change of N_p in the region of m < 1.01. This may infer that a trivial error in experiments or in computation cut-off will introduce a large error to N_p or even cause a divergent solution for the objective function.

4.5.3 Error in Viscometry

With the first order approximation, the particle concentration is proportional to the specific viscosity η_{sp} ($\eta_{sp} = \eta_r - 1$) and reciprocal cubic hydrodynamic diameter of particles (see Equation 4.15). Therefore the error in the determination of particle diameter D is the main source of the error in N_{pOrig}. Besides the possible error in the measurement of the diameter by dynamic light scattering (ca.2 % estimated from repetitions), the solvent associated with the particle surface may contribute some error in hydrodynamic diameter. The thickness of the solvent layer depends on the ionic strength, and its influence on viscosity will vary with the particle size - the smaller the particles, the larger the influence of the solvent layer. If the thickness of solvent layer is 3 nm, the overestimation of N_{pOrig} will be 4% for the particles of diameter 430 nm, and 22% for those of diameter 88 nm.

4.5.4 Water Content in Swollen Particles

The water content in swollen particles was determined from the density measurement and Equations 4.27 and 4.28. The volume fraction and the weight fraction of water are respectively given by

$$\phi_w = 1 - \phi_{dry} = 1 - \frac{\rho_{sp} - \rho_m}{\rho_{pdry} - \rho_m} \tag{4.29}$$

$$f_w = 1 - f_{dry} = 1 - \frac{1 - \rho_m/\rho_{sp}}{1 - \rho_m/\rho_{pdry}} \qquad (4.30)$$

Using the same data set as for Table 4.2, the water content at 25 °C was obtained as given in Table 4.8. For comparison, the water content at 50 °C has been calculated from the volume ratio at two temperatures (25 and 50 °C) by assuming that the volume change of the particles with temperature is merely due to the difference in water content and thus: the volume fraction of the polymer in the swollen particles at 50 °C, $(\phi_{dry})_{50°C} = (\phi_{dry})_{25°C} \times (Vol_{25°C} / Vol_{50°C})$, where Vol represents the volume of swollen particles; the subscripts "25 °C" and "50 °C" represent the temperatures at which the values were determined.

Table 4.8 Water content and volume fraction of polymer in swollen particles at 25 and 50 °C

	ρ_{sp} (g/cm^3)	Water content		Volume fraction of polymer	
		ϕ_w	f_w	25°C	50°C
$\phi_\varepsilon = 0$	1.0238	0.91	0.89	0.09	0.60
$\phi_\varepsilon = 0.3$	1.0346	0.88	0.85	0.12	0.80

That is, there was about 90% water in the swollen particles at 25 °C, which is very close to the water content of poly(NIPAM) determined by Dong and Hoffman[20] with FTIR (0.914).

4.6 SUMMARY

The particle concentration of poly(NIPAM/BAM) latexes was determined by densitometry, turbidimetry and viscometry. The values of N_{pOrig} were in the range of 2×10^{15} to $3 \sim 5\times10^{17}$ (#/L) which were comparable to latices prepared by emulsion polymerization in other systems.

The results by viscometry and densitometry agreed each other, while the turbidimetry method did not.

Acknowledgement

The author would like to thank Drs. Th. Kourti, P. Gossen and H. Mousa for the valuable discussions and the technical assistance.

Symbols

a —— Empirical constant in Eq. 4.19

a_n, b_n —— Mie coefficients in Eq. 4.8

A, B —— Coefficients in Eq. 4.18

C —— Concentration of particles which are not specified (g/cm^3)

C_{wet} —— Concentration of wet latex in suspension (g/cm^3)

C_{dry} —— Concentration of dry polymer in suspension (g/cm^3)

C_p —— Molarity of solute (mol/L)

C_{sp} —— Concentration of swollen particles in wet latex (g/cm^3)

$\acute{C}_{sp}$ —— Concentration of swollen particles in dilute suspension (g/cm^3)

$\bar{D}$ —— Average diameter of particles (cm)

E —— Constant in Eq. 4.21

F —— Mole fraction of monomer

f_{dry} —— Weight fraction of dry polymer in swollen particles

f_w —— Weight fraction of water in swollen particles

K —— Scattering coefficient

l —— Length of optical path (cm)

m —— Refractive index ratio $m = n_p / n_m$

M —— Molecular weight of solute (g/mol)

N_p —— Number of particles in a unit volume (#/L)

N_{pSusp} —— Number of particles in a diluted suspension (#/L)

N_{pOrig} —— Number of particles in original latices (#/L)

R_{scat} —— Cross section area of scattering (cm^2)

T —— Period of oscillation of tube

T_r —— Transmittance of suspension

$Vol_{25\,°C}$, $Vol_{50\,°C}$ —— Volume of the swollen particles at 25 and 50 °C

$\tilde{V}$ —— Apparent molal volume of dry polymer

w_{wet} —— Weight fraction of wet latex in suspension

α —— Size parameter $\alpha = \pi D / \lambda_m$

ζ, β —— Constants in Eq. 4.20

η_r —— Relative viscosity

η_{sp} —— Specific viscosity

λ —— Wavelength of light (nm)

ρ_m —— Density of medium (g/cm^3)

ρ_p —— General term for density of particles (g/cm^3)

ρ_{pdry} —— Density of dry polymer (g/cm^3)

$\hat{\rho}_{pdry}$ —— Density of dry polymer determined from suspension II (g/cm^3)

ρ_{pwet} —— Density of wet latex (g/cm^3)

ρ_s ——— Density of suspension (g/cm^3)

ρ_{sp} ——— Density of swollen particles (g/cm^3)

τ ——— Turbidity of suspension

ϕ ——— Volume fraction of particles used in viscosity equations

ϕ_{dry} ——— Volume fraction of dry polymer in swollen particles

ϕ_m ——— Volume fraction of medium

ϕ_{max} ——— Maximum attainable particle fraction

ϕ_p ——— Volume fraction of particles

ϕ_{sp} ——— Volume fraction of swollen particles in wet latex

ϕ_w ——— Volume fraction of water in swollen particles

ϕ_ε ——— Volume fraction of interstitial water in wet latex

References

1. Th. Kourti, Latex Particle Size Determination by Dynamic Light Scattering, Ph.D. Thesis, McMaster University, Hamilton, Canada, 1989

2. J.B. Bateman, E.J. Weneck and D.C. Eshler, J. Coll. Sci. **14**, 308-329 (1959)

3. C.R. Wildemuth and M.C. Williams, Rheol Acta, **23**, 627-635 (1984)

4. G.M. Musbally, G. Perron and J.E. Desnoyers, J. Colloid and Interface Sci. **48**(3), 494 (1974)

5. H.C. Van de Hulst, "Light Scattering by Small Particles", J. Wiley and Sons, Inc., New York, 1957

6. M. Mooney, J. Coll. Sci. **6**, 162 (1951)

7. D.G. Thomas, J. Coll. Sci. **20**, 267-277 (1965)

8. J.W. Goodwin, The Microstructure and the Rheology of Surfactant and Related Systems, in "Surfactants" (Ed. by Th.F. Tadros), Academic Press, New York, 1984

9. A.B. Metzner, Journal of Rheology, **29**(6), 739-775 (1985)

10. J. Mewis, W.J. Frith, T.A. Strivens and W.B. Russel, AIChE Journal **35**(3), 415-422 (1989)

11. A. Einstein, Ann. Physik, **17**, 459 (1905); *ibid.* **19**, 271, 289 (1906); *ibid.* **34**, 591 (1911)

12. N.A. Frankel and A. Acrivos, Chem. Eng. Sci. **22**, 847-853 (1967)

13. C.R. Wildemuth and M.C. Williams, Rheol Acta, **23**, 627-635 (1984)

14. T.F. Ford, J. Phys. Chem. **64**, 1168 (1960)

15. R. Simha, J. Appl. Phys. **23**, 1020 (1952)

16. S.H. Maron and P.E. Pierce, J. Colloid Sci. **11**, 80 (1956)

17. T. Kataoka, T. Kitano, M. Sasahara and K. Nishijima, Rheol. Acta, **17**, 149-155 (1978)

18. T. Kitano, T. Kataoka and T. Shirota, Rheol. Acta, **20**, 207-209 (1981)

19. P. Gossen, personal communication, Hamilton, Canada, 1990

20. L.-C. Dong and A.S. Hoffman, Proceed. Intern. Symp. Control. Rel. Bioact. Mater., **17**, 116-117 (1990)

CHAPTER 5

DISPERSION POLYMERIZATION OF N-ISOPROPYLACRYLAMIDE IN THE PRESENCE OF LOW LEVEL SODIUM DODECYL SULFATE

5.1 INTRODUCTION

Since the first synthesis of poly(N-isopropylacrylamide) (poly(NIPAM)) was reported in 1957[1], hundreds of papers have been published on the subject. Most of them concern linear poly(NIPAM) solutions, and a few consider poly(NIPAM) gels. Pelton and coworkers[2,3] were the first to report the synthesis of poly(NIPAM) micro gel colloids. These preparations were done in aqueous media without emulsifier. But no studies on the kinetics and mechanisms of the micro gel formation have been reported to date.

The objectives of this work were to investigate the mechanisms and kinetics of the polymerization of NIPAM. Polymerizations were carried out in aqueous media using sodium dodecyl sulphate (SDS) as anionic emulsifier to produce water-based poly(NIPAM) latices.

5.2 EXPERIMENTAL

Materials

N-isopropylacrylamide monomer was obtained from Eastman Kodak Co. and was recrystallized once from a mixture of toluene and hexane. N,N-methylenebisacrylamide (BAM) and methoxyphenol (Aldrich Chemical Company, Inc.), potassium persulfate (KPS) (analytical reagent grade) and sodium dodecyl sulfate (SDS)(specially pure grade from BDH Chemicals) were used as received. Distilled water was further purified with a Milli-Q Water System (Millipore Corporation). The water had a conductivity of less than 1 μS/cm.

Polymerization Conditions

Polymerizations were carried out in an 1 L four-necked glass reactor equipped with a condenser, a nitrogen inlet, a thermometer and a motor-driven straight paddle stirrer. Mixing was provided by the stirrer at a rate of 200 rpm since the stirring rate was believed not to be important for the kinetics of emulsion polymerization. The reactor was immersed in a water bath kept at constant temperature. The total moles of monomers added to the reactor was constant for all the runs and 500 mL deionized water was added to obtain the desired total monomer concentration 0.1328 mol/L. SDS dissolved in deionized water was then added to the reactor. Oxygen was removed by bubbling nitrogen through the solution at reaction temperature (50, 70 °C) for 30 minutes. The reaction was started by adding KPS solution (KPS dissolved in ~ 10 mL water). At specified time intervals 10 mL samples of reaction mixture was taken with a syringe and transferred to 1 g 1% methoxyphenol solution which stopped the polymerization.

A buffer solution with pH 6.7 (prepared from K_2HPO_4 and KH_2PO_4; 0.0025 mol/L each in deionized water) was used for the study of the influence of pH and ionic strength on the kinetics of latex synthesis (particle size, polymerization rate).

The recipes and the polymerization conditions used are summarized in Table 5.1.

Measurement of Monomer Conversion and Characterization of Polymer Particles

Particle size and size distribution of the latexes were measured using a NICOMP 370 Autodilute Submicron Particle Sizer (NICOMP Particle Sizing System) which had a laser light source of wave length 514 nm and a temperature-controlled sample cell. The temperature control was accurate to ± 0.02 °C. The scattered light intensity was measured at a 90° angle.

The particle size and size distribution were computed by the NICOMP Autocorrelator Interface Program version 10.3 based on a Gaussian analysis.

Table 5.1 Recipes and polymerization conditions

Runs	[a][NIPAM]$_0$ mmol/L	[BAM]$_0$ mmol/L	[KPS]$_0$ mmol/L	[SDS]$_0$ mmol/L	T(°C)	pH
LS1	123.7	9.08	2.07	0.409	70	4.7 - 2.7
LS6	123.7	9.08	2.07	0.409	50	4.7 - 4.0
LS7	123.7	9.08	2.07	0.409	70	buffer 6.7 - 6.3
LS8	123.7	0	2.07	0.409	70	
LS9	123.7	9.08	2.07	0.409	70	
LS10	123.7	9.08	2.07	2.46	70	
LS11	132.8	0	4.14[b]	0.409	50	
LS12	663.9	0	4.14[b]	0.409	50	
LS2[c]	123.7	9.08	2.07	0.728	70	
LS3	123.7	9.08	2.07	2.00	70	
LS4	123.7	9.08	2.07	0.208	70	
LS5	123.7	9.08	2.07	4.00	70	
LS13	123.7	18.2	2.07	0.409	70	

a [ ] represents the concentrations in mmol/L. Subscripts '0' represent initial values. T is polymerization temperature in °C.

b Half of the initiator was added at the beginning, the other half was added after 35 and 45 minutes.

c LS2 - LS5, LS13 are the samples (5-76, 5-72, 5-77, 5-70, 5-78) prepared by McPhee[4].

The latexes were cleaned with three to four successive ultracentrifugations, decanations, and dispersions in deionized water.

The monomer conversion was determined by HPLC using distilled deionized water as mobile phase. The apparatus included a LC-CN column (Supelco, Inc.), a Beckman 160 UV-Vis absorbance detector (Beckman Instruments, Inc.) and a SP4200 integrator (Spectra-Physics). Residual monomer(s) in every sample was measured three times. The standard deviation of mean value from the HPLC measurements was 0.5 %, estimated from the repetitions.

5.3 EXPERIMENT RESULTS

5.3.1 Influence of Temperature

The effect of temperature on polymerization rate, particle growth rate and particle size, were studied. The activation energy of polymerization was estimated.

(i) Polymerization rate

The total monomer conversion at 70 and 50 °C is plotted against reaction time in Figure 5.1. The polymerization at 70 °C was much faster than at 50 °C: with a polymerization rate at the end of induction period R_p = 1.88 mol/L.min (where R_p was calculated from the initial monomer concentration $[M]_0$ and the derivative of monomer conversion **x** to the reaction time t: $R_p = [M]_0 (dx/dt)_0$), and the monomer conversion reached 80 % in about 12 minutes. In contrast with this, the polymerization at 50 °C was slower; the induction period ended after about 10 minutes, R_p = 0.363 mol/L.min, and required about 50 minutes to reach 80 % conversion. The polymerization rate increased about five times when the temperature was increased by 20 °C. This is a typical free-radical dispersion polymerization.[5,6] The induction periods are likely due to the presence of low levels oxygen in the reactor.

The individual monomer conversions at 70 and 50 °C are given in Figure 5.2. As expected BAM which has two double bonds polymerizes faster than NIPAM. The difference between the polymerization rates of the two monomers is smaller at the higher temperature. This implies that the reactivity ratios depend on the polymerization temperature and that the reactivity ratio for NIPAM has a higher activation energy.

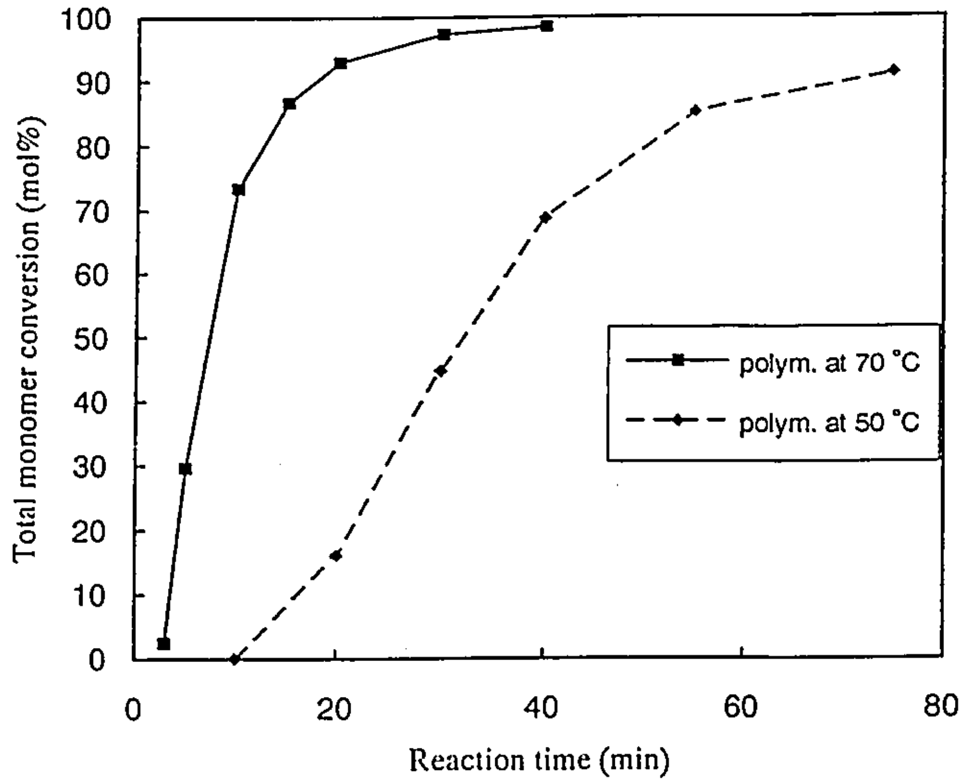

Figure 5.1: Influence of temperature on the reaction rate of copolymerization of NIPAM/BAM (runs LS1, LS6, mole fraction of BAM f_{10} = 0.068, [SDS] = 0.409 mmol/L). The description of runs LS1 and LS6 is given in Table 5.1

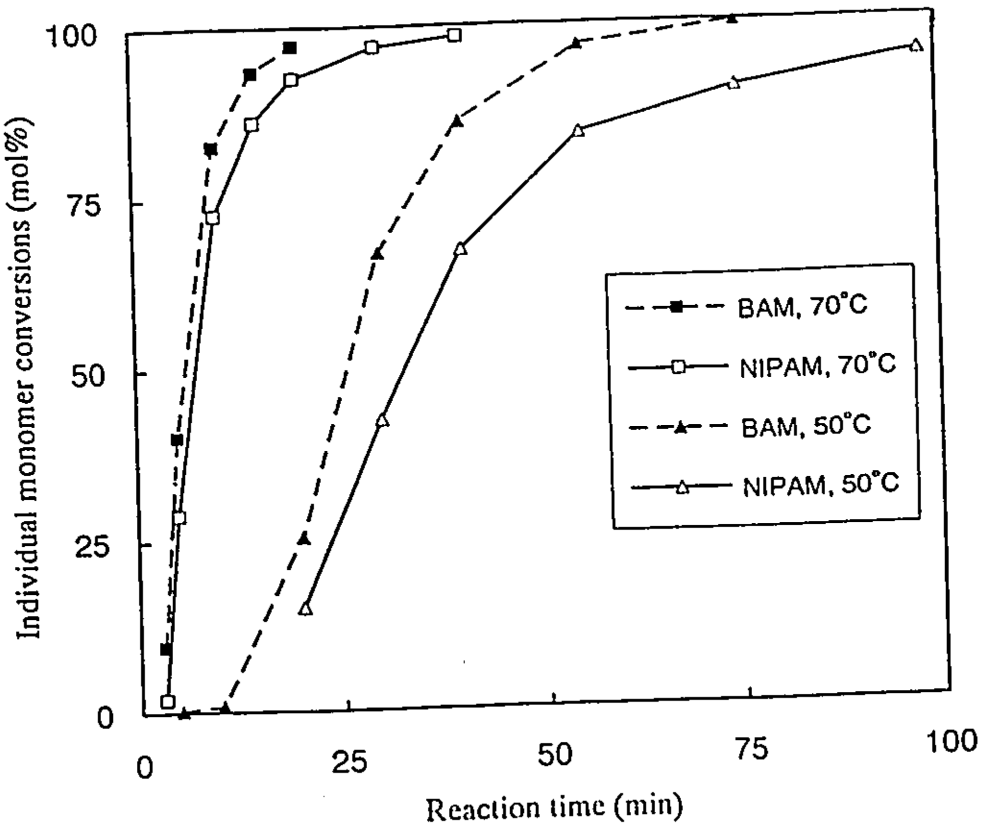

Figure 5.2: Individual monomer conversion versus reaction time for different polymerization temperatures (runs LS1, LS6)

(ii) Particle growth rate and particle size

The latex particle size was measured at 50 °C by dynamic light scattering, DLS. The change in particle size with polymerization time is plotted in Figure 5.3. At 70 °C the polymeric particles formed and a bluish tinge appeared at about three minutes of polymerization. This was the end of induction period. The particle size then increased rapidly reaching a constant value after about 20 minutes. At 50 °C particles formation occurred later, and the size increased more slowly. The particles in the final latex synthesized at 50 °C were about 10 % larger than those synthesized at 70 °C.

Goodwin et al.[7] summarized the effect of temperature on the particle size of polystyrene latices prepared using persulfate initiator. The logarithm of particle diameter was inversely proportional to the polymerization temperature T (°K) if the ionic strength Z, monomer concentration $[M]_0$ and initial initiator concentration $[I]_0$ (in mol/L) are fixed. Goodwin et al. found the following relationship for surfactant-free polystyrene latices:

$$\log D = 0.238\left(\log\frac{Z[M]_0^{1.723}}{[I]_0} + \frac{4929}{T}\right) - 0.827 \tag{5.1}$$

where D is the particle diameter in nm.

Using this expression, the predicted diameter increment for a temperature increase of 20 °C (from 50 °C to 70 °C) is only 0.04%. For the particles of poly(NIPAM/BAM) synthesized in this study, the volume average diameter ($\overline{D}_{vol}$) increment was about 10%. The dependence of $\overline{D}_{vol}$ on temperature can be better expressed as: $\overline{D}_{vol} \propto T^{\alpha}$, where $\alpha < 0$. Because

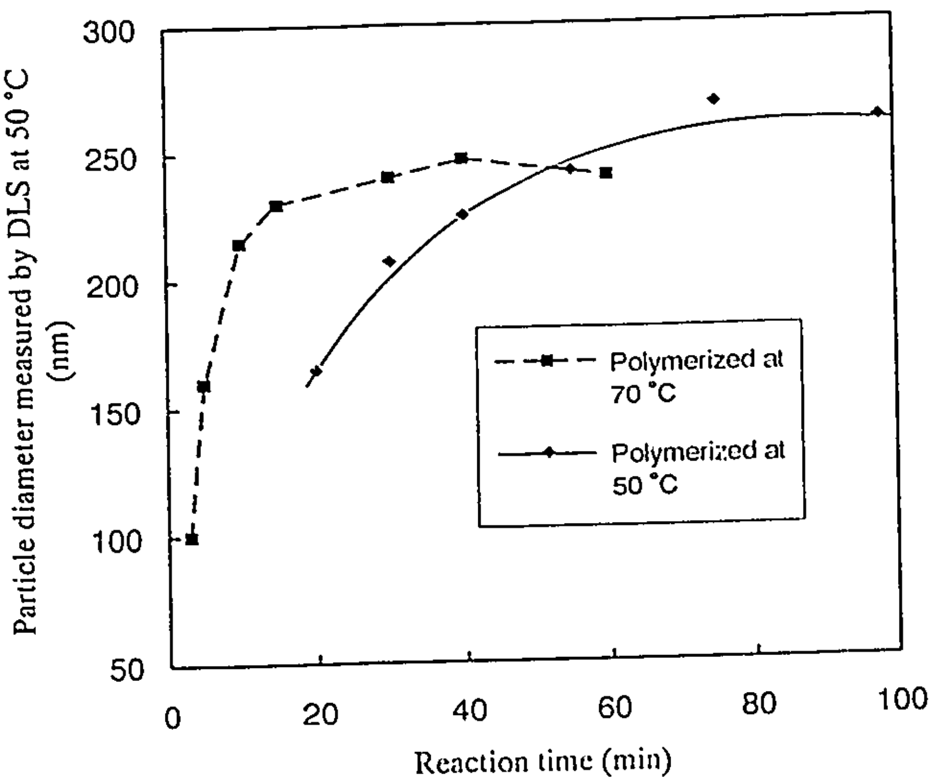

Figure 5.3: Effect of synthesis temperature on the particle growth rate of poly(NIPAM/BAM) latex particles(runs LS1, LS6)

only two data points ($\overline{D}_{vol}$ at 50 and 70 °C) were obtained, Equation (5.1) cannot be tested for NIPAM/BAM system.

The particle volume as a function of total monomer conversion is illustrated in Figure 5.4. At both temperatures the particle volumes increased linearly with total monomer conversion up to ~ 85 %. Above ~ 85 % conversion, the volume increased more rapidly, and the curves departed from straight lines. The linear portions of two curves have almost the same slope. This implies that the volumetric growth mechanism of the particles was the same. This important point will be discussed later.

(iii) Activation energy for polymerization

The activation energy for copolymerization of NIPAM with BAM (NIPAM/BAM = 0.932/0.068 mole/mole) can be estimated if the overall polymerization rate is expressed by the following equation:

$$R_p = \hat{k}_p \left(\frac{f\,k_d}{\hat{k}_t}\right)^{1/2} [M]^a\ [I]^b\ [S]^c \tag{5.2}$$

where $\hat{k}_p$ and $\hat{k}_t$ are pseudo propagation rate constant and pseudo termination rate constant. For copolymerization, $\hat{k}_p$ is defined by the following equation after Hamielec:[8]

$$\hat{k}_p = k_{p11}\varphi_1 f_1 + k_{p12}\varphi_1 f_2 + k_{p21}\varphi_2 f_1 + k_{p22}\varphi_2 f_2 \tag{5.3}$$

where k_{pij} $(i, j = 1, 2)$ is the propagation rate constant for the reaction of radical i with monomer j. Also φ_i, φ_j are the mole fraction of radicals with terminal monomer units i, j.

Finally f_i, f_j are the mole fractions of monomer i and j.

For a termination by both disproportionation and combination, the pseudo rate constant of termination is:

$$\hat{k}_t = \varphi_{td}\hat{k}_{td} + (1 - \varphi_{td})\hat{k}_{tc} \tag{5.4}$$

where φ_{td} is the fraction of the termination manners, $\hat{k}_{td}$ and $\hat{k}_{tc}$ are pseudo constants for termination by disproportionation and by combination respectively, and are given by

$$\hat{k}_{td} = k_{td11}\varphi_1^2 + k_{td22}\varphi_2^2 + 2k_{td12}\varphi_1\varphi_2 \tag{5.5}$$

$$\hat{k}_{tc} = k_{tc11}\varphi_1^2 + k_{tc22}\varphi_2^2 + 2k_{tc12}\varphi_1\varphi_2 \tag{5.6}$$

If we assume that all the k_{pij}'s have the same activation energy, then Equation (5.3) can be written as:

$$\hat{k}_p = (k_{p11_0}\varphi_1 f_1 + k_{p12_0}\varphi_1 f_2 + k_{p21_0}\varphi_2 f_1 + k_{p22_0}\varphi_2 f_2)\exp(-E_p/RT) \tag{5.7}$$

that is

$$\hat{k}_p = \hat{k}_{p_0}\exp(-E_p/RT) \tag{5.8}$$

Since the overall rate constant is given by

$$k_R = \hat{k}_p\left(k_d/\hat{k}_t\right)^{1/2} \tag{5.9}$$

the dependence of overall rate constant on temperature can be written as

$$k_R = k_{R_0}\exp(-E_R/RT) \tag{5.10}$$

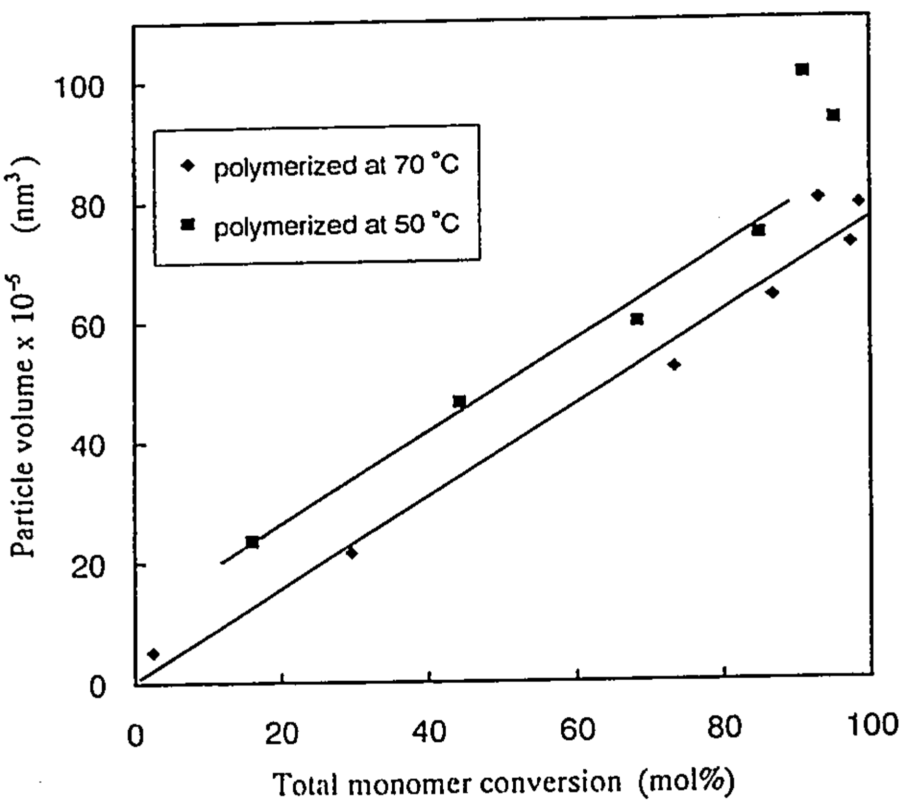

Figure 5.4: Particle volume of poly(NIPAM/BAM) latices (runs LS1, LS6) at 50 °C versus total monomer conversion for two polymerization temperatures

For two runs of polymerization at different temperatures but the same recipe,

$$\frac{R_{p1}}{R_{p2}} = \frac{\exp(-E_R/RT_1)}{\exp(-E_R/RT_2)} = \exp\left(\frac{E_R}{RT_2} - \frac{E_R}{RT_1}\right) \tag{5.11}$$

Taking the logarithm of two sides of Equation (5.11) and rearranging gives:

$$E_R = \frac{\ln(R_{p1}/R_{p2})}{1/RT_2 - 1/RT_1} \tag{5.12}$$

Substituting T_1 = 343.2 °K, T_2 = 323.2 °K, R_{p1} = 1.88 mol/L.min, R_{p2} = 0.363 mol/L.min, the value of the activation energy for overall polymerization is estimated to be: E_R = 18±0.2 kcal/mol. This value is close to that for the homopolymerization of acrylamide found by Thomson et al. (17.8 ± 0.21 kcal/mol).[9] The activation energy of decomposition of KPS, E_d, is about 32 kcal/mol,[7,10] so the difference between the activation energy of polymerization and half that of termination E_t is:

$$(E_p - \frac{1}{2}E_t) = (E_R - \frac{1}{2}E_d) = 2.0 \qquad \text{(kcal/mol)} \tag{5.13}$$

This value is in good agreement with that found for acrylamide by Kim and Hamielec (2.002 kcal/mol).[11]

5.3.2 Influence of BAM Level in Recipe

The influence of BAM on the polymerization rate and particle size was investigated. The reactivity ratios of NIPAM and BAM were evaluated from the theoretical calculations based on the data in literature.

(i) Polymerization rate

The polymerization rate and monomer conversion versus time in the presence and absence of BAM are plotted in Figure 5.5. The polymerization rate was slower in the absence of BAM as expected. This may be interpreted as due to the lower reactivity of NIPAM monomer, which is supported by the data in Figure 5.2. The conversion-time curves for NIPAM are lower than those of BAM at both temperatures.

(ii) Particle size

The particle size development during polymerization of NIPAM (initial BAM mole fraction f_{10} = 0) and NIPAM/BAM (f_{10} = 0.068) versus time are shown in Figure 5.6. The particles of poly(NIPAM/BAM) were larger (average diameter at full conversion was ca.15 % greater), and grew faster than those of poly(NIPAM). The faster growth rate can be explained by the observed higher polymerization rate. However, the larger particle size cannot be explained by this.

Possible explanations for larger size of poly(NIPAM/BAM) can be:

(1) Cross-linking reaction aids the polymer particle coagulation. When particles of poly(NIPAM/BAM) collide they can more readily "fuse" forming larger particles by the reaction with pendant double bonds.

(2) Weaker association of poly(NIPAM/BAM) with SDS molecules than poly(NIPAM) since the BAM monomer units are less hydrophobic than NIPAM units at polymerization temperature (> LCST). SDS molecules have long hydrocarbon tails. These tails would readily associate with the hydrophobic isopropyl groups in NIPAM.

(3) Lower volume average surface charge contributed from the initiator for poly(NIPAM/BAM) due to higher molar mass of the copolymer.

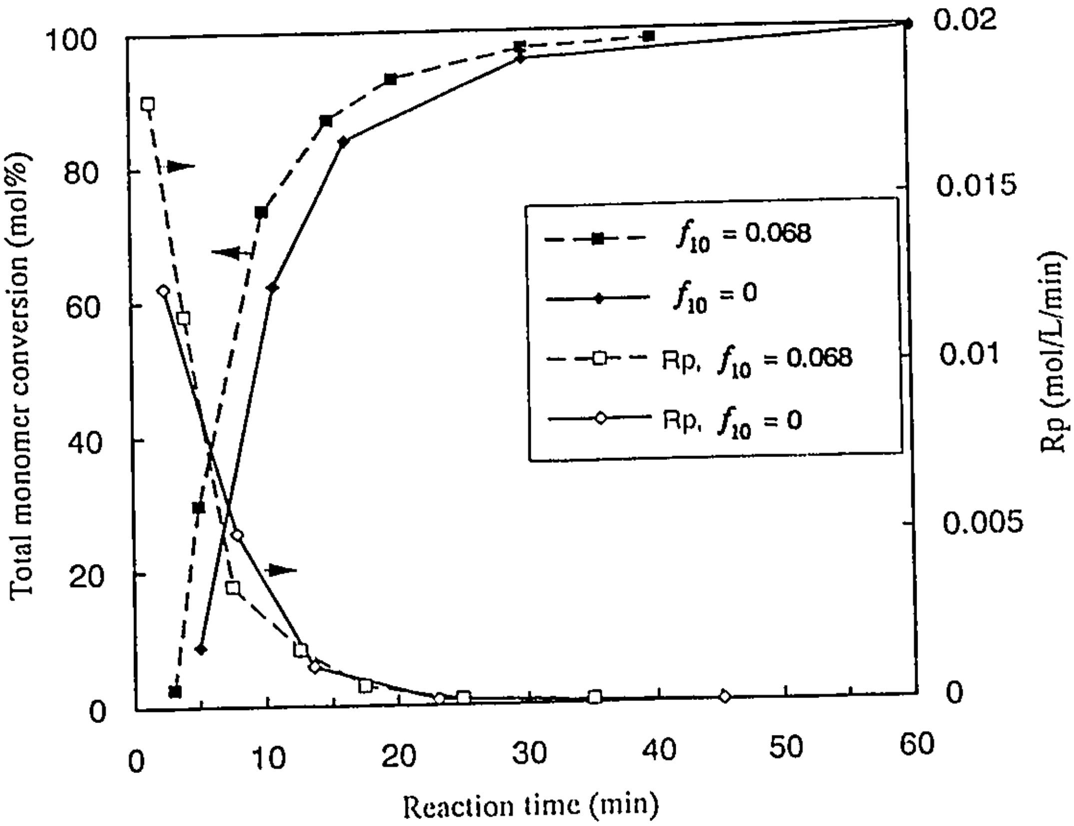

Figure 5.5: Monomer conversion and polymerization rate(Rp) versus reaction time for different BAM levels in recipe (runs LS1, LS8, polymerized at 70 °C)

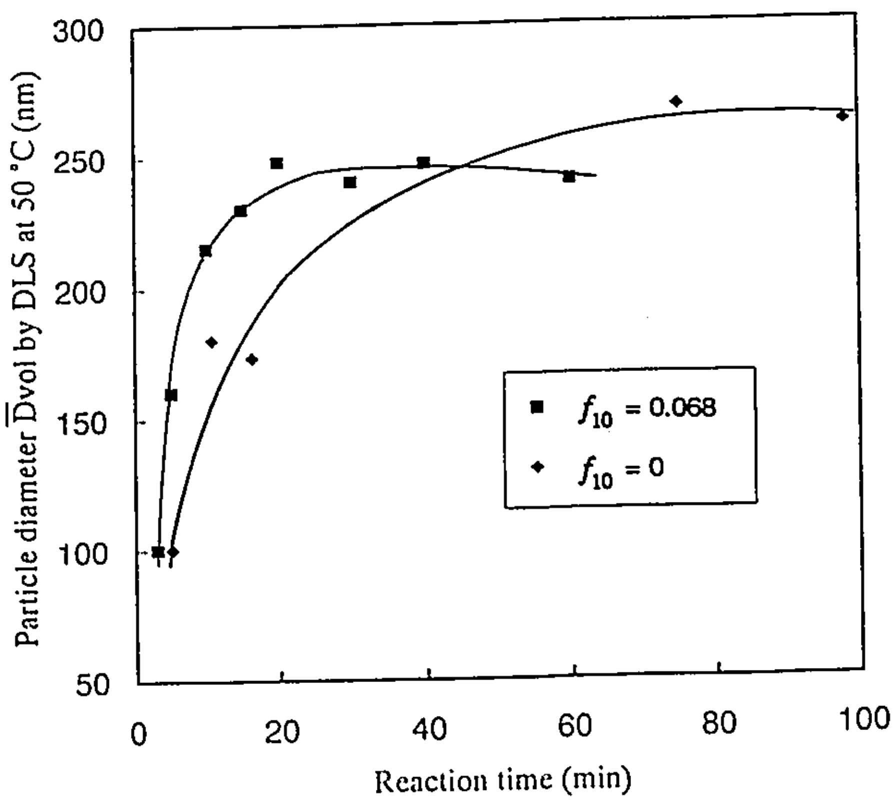

Figure 5.6: Influence of BAM level in recipe on particle growth rate (runs LS1, LS8, polymerized 70 °C)

(iii) Reactivity ratios

The reactivity ratios for NIPAM and BAM in the copolymerization were estimated using the Price-Alfrey method.[12,13] In this method, the polarities of the monomer and its derived radical are assumed to be the same, and the cross-propagation rate constant is defined as

$$k_{ij} = P_i Q_j e^{-e_i e_j} \tag{5.14}$$

and hence the reactivity ratios can be written as

$$r_1 = (Q_1/Q_2)\exp[-e_1(e_1 - e_2)] \tag{5.15}$$

$$r_2 = (Q_2/Q_1)\exp[-e_2(e_2 - e_1)] \tag{5.16}$$

$$r_1 r_2 = \exp[-(e_1 - e_2)^2] \tag{5.17}$$

where P and Q are parameters related to the resonance of the monomers, e_1 and e_2 are the polarities of monomer one and monomer two respectively.

Since there are no data available for direct calculation of r_1 and r_2, an indirect approach was applied: (1) calculating Q and e for BAM from the values of reactivity ratios for the copolymerization of AM with BAM used by Tobita and Hamielec[14] (r_1 = 2.0, r_2 = 0.5); (2) estimating the reactivity ratios of the copolymerization of NIPAM with BAM using the Q and e of BAM obtained in step (1), and of NIPAM from Chiklis and Grasshoff's results[15] of copolymerization of NIPAM with acrylamide (AM). The calculated results, as well as the data from references (ref.14, 15), are listed in Table 5.2.

Table 5.2 Computation of reactivity ratios for copolymerization of NIPAM with BAM

Monomer 1	Monomer 2	r_1	r_2	Q_1	e_1
NIPAM	AM	0.5	1.0[15]	0.40	0.47
BAM	AM	2.0	0.5[14]	2.36	1.3
BAM	NIPAM	2.0	0.25		

Thus, the reactivity ratios, r_1 and r_2, were estimated to be 2.0 and 0.25 respectively. These estimates can be checked by calculating the instantaneous copolymer compositions. The instantaneous copolymer compositions can be calculated using the Mayo-Lewis Equation:

$$F_1 = \frac{r_1 f_1^2 + f_1 f_2}{r_1 f_1^2 + 2 f_1 f_2 + r_2 f_2^2} \tag{5.18}$$

Applying the values $f_{10} = 0.068$, $f_{20} = 0.932$, the copolymer composition for the copolymer LS1 was calculated to be: $F_1 = 0.206$, $F_2 = 0.794$. These values were close to experimental values observed in this study at a reaction time of three minutes, $F_1 = 0.167$, $F_2 = 0.833$ (LS1). Thus, the estimated reactivity ratios seem to be reasonable.

5.3.3 Influence of SDS concentration

The influence of SDS concentration on the polymerization rate, particle size and particle concentration were studied.

(i) Polymerization rate

The monomer conversions at two SDS levels (LS1: 0.409, LS6: 2.46 mmol/L) are plotted against reaction time in Figure 5.7.

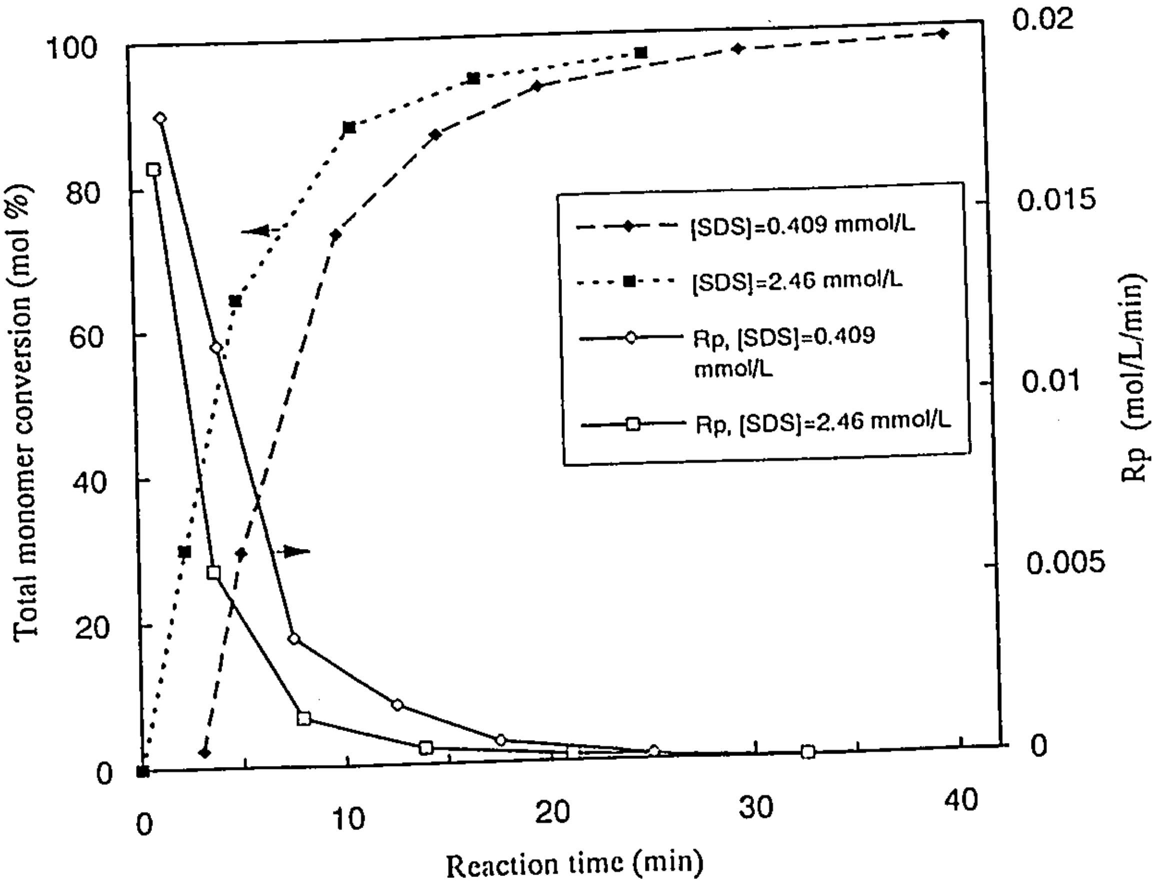

Figure 5.7: Influence of SDS concentration on the reaction rate of copolymerization of NIPAM/BAM (runs LS1 and LS10, f_{10} = 0.068, T=70 °C)

The induction period was shorter at the higher SDS level. The polymerization rate, however, did not depend on the SDS concentration.

(ii) Particle size

(a) Particle formation during polymerization

Figure 5.8 displays the change of particle size with time at two SDS levels. In both cases, the particle nucleation time was short (about a few minutes), and the particle size approached a constant value due to almost complete consumption of monomers. The volume average diameter of the particles prepared with 0.409 mmol/L SDS was ca. 250 nm larger than those prepared with 2.46 mmol/L SDS by about four times. The particle volume is plotted against monomer conversion in Figure 5.9. The two curves at different SDS levels had different slopes. The particle volume increased with monomer conversion linearly in the whole region for SDS at 2.46 mmol/L; while only up to ca. 85 % for SDS at 0.409 mmol/L. For the latter condition, this suggests that the particles coalesce at monomer conversion above 85 % due to insufficient stabilizing agent.

The final diameter (at complete consumption of the monomers) of the particles prepared at various SDS levels as a function of SDS concentration is plotted in Figure 5.10. The logarithm of particle diameter decreased linearly with the increase in the logarithm of SDS concentration. The slope of the regressed data as a straight line is - 0.71, i.e., $\overline{D}_{vol} \propto [SDS]^{-0.71}$.

(b) Particles formed solely by homogeneous nucleation (no free-radicals present)

Homogeneous poly(NIPAM) aqueous solutions were prepared with and without SDS. Poly(NIPAM) precipitated from the solutions and formed particles when the solutions were

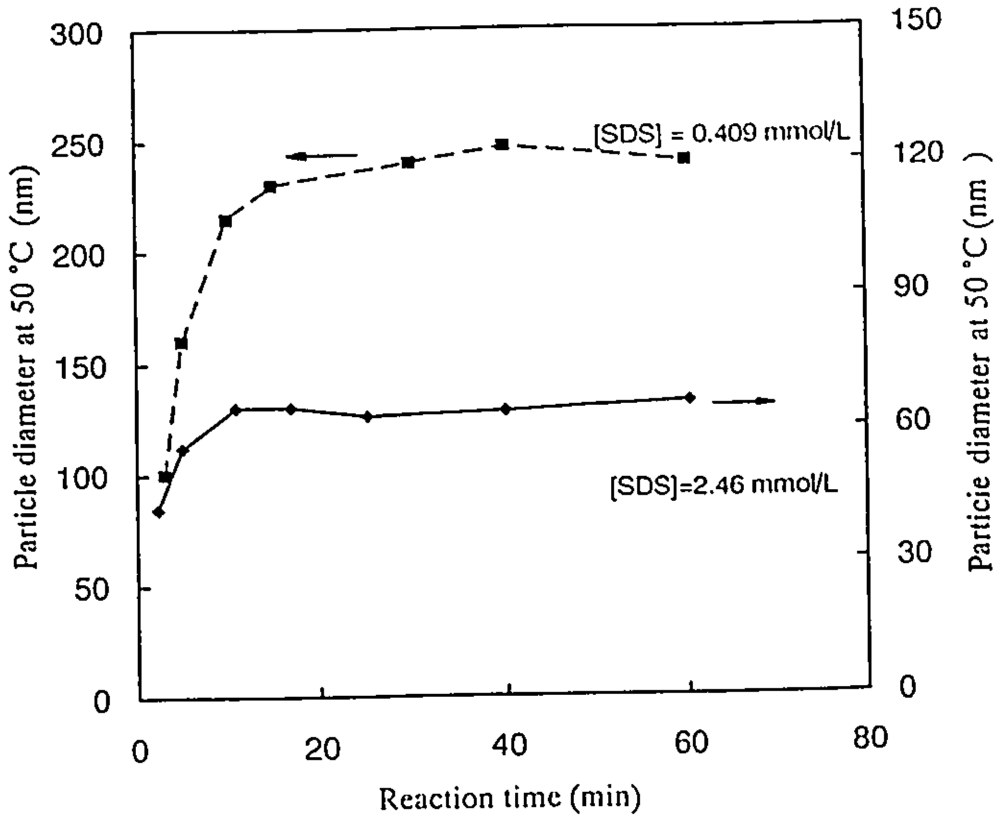

Figure 5.8: Particle size versus reaction time with different SDS level (runs LS1, LS10, polymerized at 70 °C). The particle diameter reported is volume average diameter.

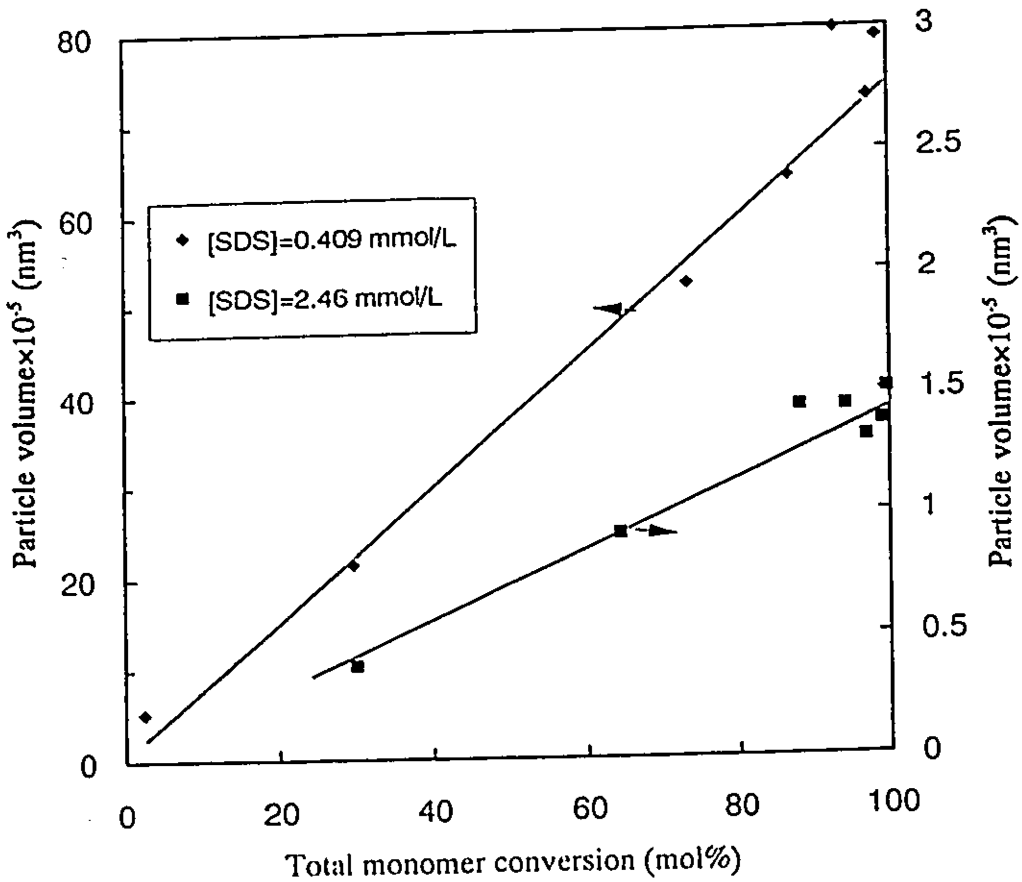

Figure 5.9: Particle volume of poly(NIPAM/BAM) measured by DLS at 50 °C versus total monomer conversion for different SDS levels (runs LS1, LS10, polymerized at 70 °C)

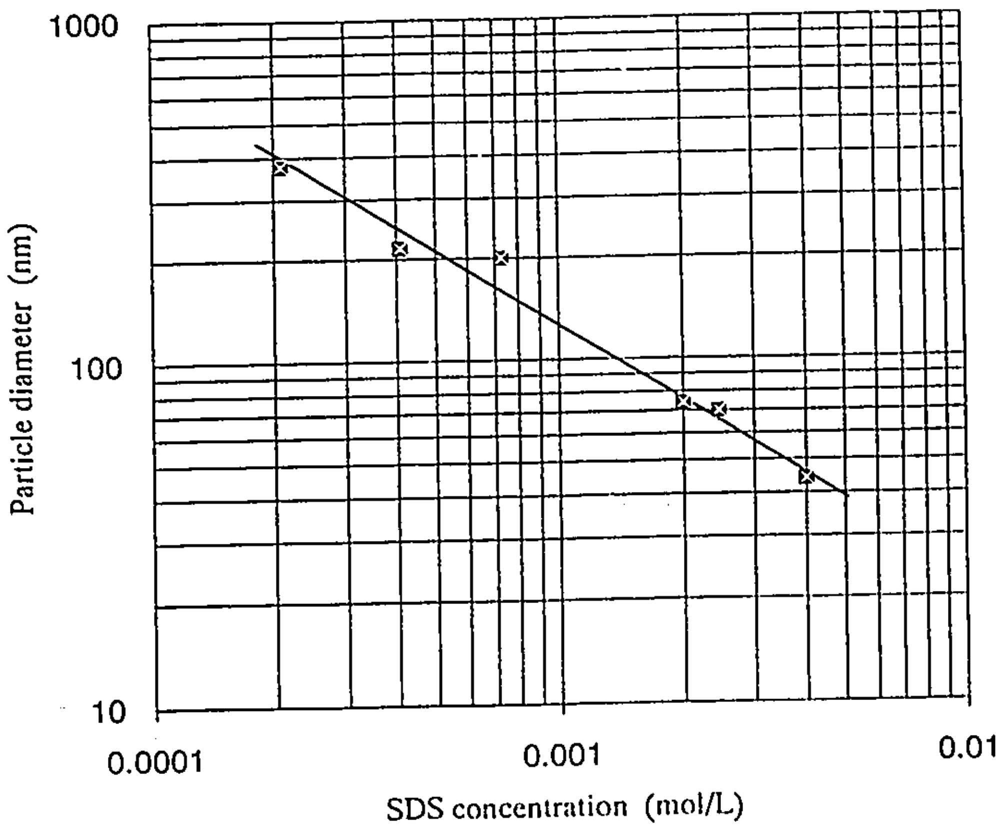

Figure 5.10: Final particle diameter(at complete conversion of monomer) measured by DLS at 50 °C as a function of SDS concentration (runs LS1, LS10, LS2-LS5)

heated to 50 °C (> LCST). The diameters of the particles were determined by DLS at 50 °C. Without SDS, the $\overline{D}_{vol}$ was found to be 80 nm, while with 0.118 g/L SDS (< CMC), the $\overline{D}_{vol}$ was 37 nm. These measurements were done to provide additional data to help in elucidation of the particle nucleation mechanism, because in the absence of free-radical initiator, no micellar nucleation can occur.

(iii) Particle concentration

Measured particle concentrations as a function of SDS level are shown in Figure 5.11. A nearly linear relationship between log N_p and log [SDS] was found with $N_p \propto [SDS]^{2.5}$ from linear regression. There was no dramatic change of particle concentration in the range of SDS levels studied. This suggests that no switch in nucleation mechanism occurred[16,17]. This may have been expected because the SDS level used was lower than the CMC (ca. 8.0 mmol/L) of SDS. Hansen and Ugelstad[8] found that in emulsion polymerization of styrene without seeding, the number of particles per unit volume drastically increased when SDS concentrations were above the CMC. The results by Napper and others, which were quoted by Dunn[16], showed the same trend. The drastic increase in particle concentration with surfactant concentration represents the onset of micellar nucleation of particles.[10,11,18] In classical emulsion polymerization, as will be discussed later, the particle concentration is proportional to $[SDS]^n$. The power n is much higher when [SDS] is lower than the CMC. These data confirm that the mechanism of polymer particle formation is by homogeneous nucleation in this investigation.

5.3.4 Influence of pH and Ionic Strength

The pH and ionic strength in polymerization system influenced the particle size and

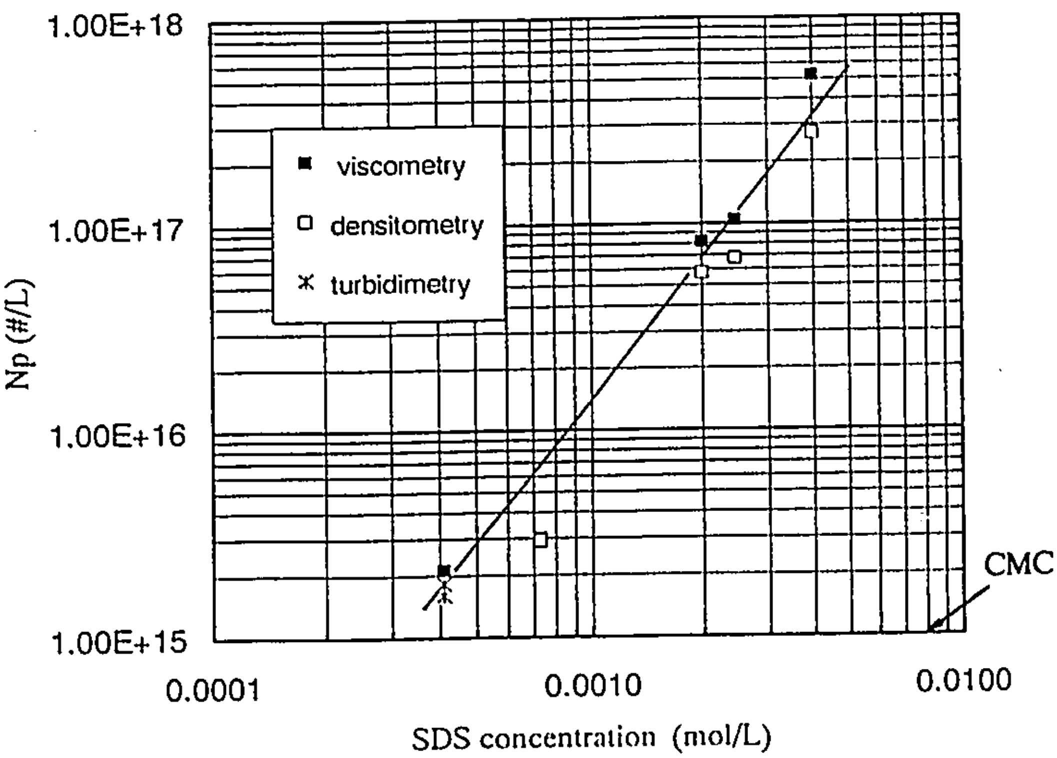

Figure 5.11: Number concentration of particles in poly(NIPAM/BAM) latices versus SDS level (runs LS1, LS2-LS5, LS10)

particle size distribution, as well as polymerization rate.

(i) Particle size and particle size distribution

The decomposition rate of potassium persulfate has been shown to increase with decrease in pH in the range of pH < 4.[10,4] To prevent this complication, buffers are often added. In this work, the influence of pH on polymerization was investigated at pH 6.7 in a buffered solution and at the natural pH of the initiator and monomer solution. The pH, conductivities of the media, salt concentrations, diameter of the particles, and the distribution of the particle size are listed in Table 5.3. The pH of the medium with buffer varied in the range, 6.7 to 6.3 and that without buffer decreased from 4.6 at the beginning of polymerization to 2.6 at the end. The conductivities of the media after reaction were 1002 and 3900 μS/cm respectively at 20 °C. The diameters measured by DLS at 25 °C were 950 nm and 430 nm prepared in buffer solution and prepared without buffer respectively, i.e., the former were more than twice the latter. Again, the particle size distribution from the buffer solution was much broader than that without buffer.

Table 5.3 Effect of pH and Electrolyte Concentration

	pH		Electrolyte concentration mmol/L		Conductivity at End (μS/cm)	$\overline{D}_{vol}$ (nm) DLS (25°C)	Rel. Std deviation $\sigma/\overline{D}_{vol}$*
	Beginning	End					
buffered	6.7	6.3	KPS SDS K_2HPO_4 KH_2PO_4	2.07 0.409 2.50 2.50	1002	950	56 %
"natural"	4.6	2.7	KPS SDS	2.07 0.409	3900	430	17 %

* This is a relative standard deviation (standard deviation divided by mean diameter) based on Gaussian analysis and represents the width of the particle size distribution as

measured by DLS.

Figure 5.12 shows that the turbidity of a 2.8 wt.% poly(NIPAM/BAM) latex prepared at higher, buffered pH and ionic strength reached a higher level than that at lower, "natural" pH and ionic strength. This suggests that larger particles are formed in the buffered solution since turbidity is nearly proportional to about the fourth power of diameter and to the first power of the number of particles.

The pH and electrolyte levels can affect both the radical generation rate (affecting decomposition rate of initiator) and the stability of primary particles newly formed. The effect on radical generation rate is likely small, and therefore the major effect of pH and electrolyte level is on the coagulation of primary particles. It is well known that an increase in electrolyte level can cause polymer particles to coagulate if they are stabilized electrostatically. When the ionic strength is high the electric double layer around the particles is compressed, and thus particles coagulate to obtain enough surface charge density for stabilization. This mechanism was confirmed by Pelton[19] who added NaCl to a polystyrene latex at the early stage of polymerization, and obtained particles with larger size than those without NaCl. The effect of ionic strength on the electrostatic energy of poly(NIPAM/BAM) particles was measured by McPhee[4]: the electrophoretic mobility of the particles at 40 °C dropped from -4 to -2 (10^{-8} m^2/Vs) as the KCl concentration increased from 0.01 to 10 mmol/L.

(ii) Polymerization rate

Monomer conversions with and without buffer are shown as a function of time in Figure 5.13. Unexpectedly, the polymerization rate does not appear to depend significantly on pH and ionic strength. One would expect a higher R_p for small polymer particles (larger particle

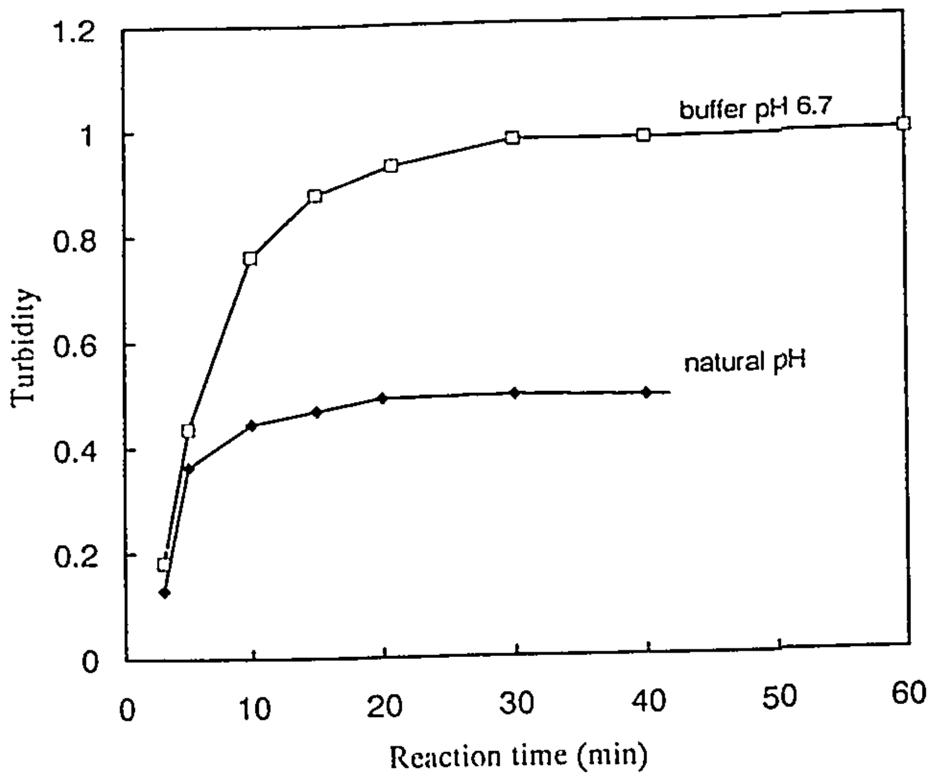

Figure 5.12: Turbidity of 2.8 wt.% poly(NIPAM/BAM) latices (runs LS1, LS7) versus reaction time for different pH and ionic strength of medium

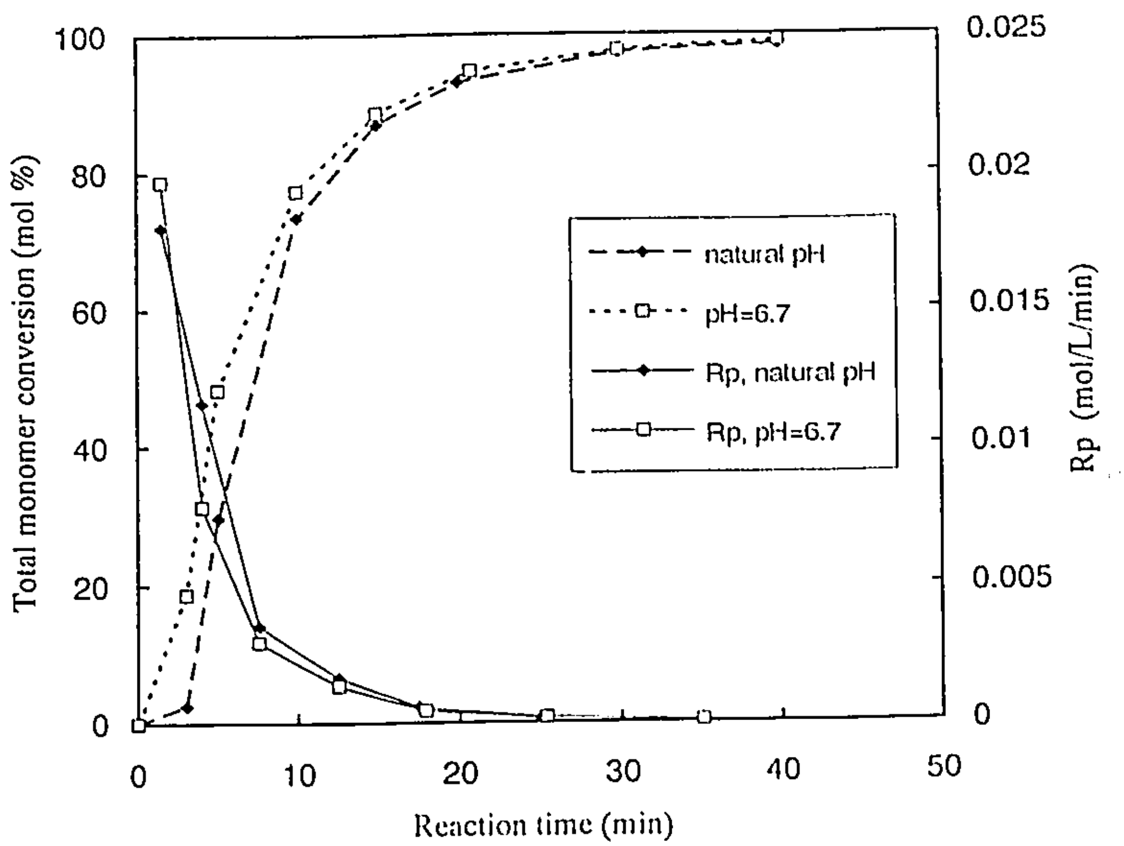

Figure 5.13: Effect of pH on the reaction rate of copolymerization of NIPAM with BAM (runs LS1, LS7, f_{10} = 0.068, [SDS] = 0.409 mmol/L)

concentration) if classical emulsion polymerization kinetics was operative.

5.4 DISCUSSION

This section will discuss the nucleation mechanism of particles, linear dependence of particle volume on monomer conversion, and polymerization mechanism.

5.4.1 Nucleation Mechanism of Particles

It has been found that the presence of SDS can elevate the cloud point of poly(NIPAM),[20,21,22] and it has been suggested that free micelles continuously form beyond the critical aggregation concentration[7]. This observation and interpretation raised questions: Do the poly(NIPAM) chains precipitate from the aqueous solution under the polymerization conditions? Are free micelles present in polymerization system?

The mechanism of particle nucleation during polymerization in aqueous solution will be discussed under three titles: Existence of free SDS micelles; Precipitation of polymer chains; Dependence on surfactant concentrations.

(i) Existence of free SDS micelles

When some kinds of polymers, such as NIPAM polymers, are present, SDS molecules associate with the polymer chains forming clusters, called polymer-bound micelles. To distinguish SDS-alone micelles, the micelles without association with polymer are named free SDS micelles (see Part B Chapter 2 and ref.23). At temperatures 50 - 70 °C (higher than the cloud point), polymer saturation was not observed in the presence of 0.06% poly(NIPAM/BAM) (corresponding to 4% monomer conversion), and the CMC of SDS was almost the same as that of poly(NIPAM/BAM)-free solution. In other words, at 50 - 70 °C, the association of SDS with the polymer may not be in a micellar form. Since the SDS concentration employed in this work was 0.409 ~ 2.46 mmol/L, much lower than the CMC of SDS (8 ~ 11 mmol/L, at temperature 25 ~ 70 °C), no free SDS micelles were present under the polymerization conditions used. Therefore, one can rule out micellar nucleation in this study. The major role of SDS in the polymerization was stabilizing the primary particles or precursors, and minimizing the extent of coagulation.

(ii) Precipitation of poly(NIPAM) chains

Figure 5.14 shows the cloud point of poly(NIPAM) as a function of SDS concentration for various poly(NIPAM) concentrations. For the polymerization conditions used in this study, it is clear that two phases (polymer-rich and water-rich phases) were present. A requirement for homogeneous nucleation is that the polymer precipitate from a homogeneous solution under conditions of polymerization. Figure 5.14 illustrates that all experiments of polymerization were conducted in two phase region. This means that the polymerization conditions used in this work met the requirement of homogeneous nucleation.

In the homogeneous nucleation process, a polymer chain grows in solution until a certain chain length (number of monomer units) is reached and then polymer precipitates. This chain length is called critical chain length which depends on the solubility of a polymer chain in a solvent and thus varies for different polymer/solvent system. For example, the critical chain length for polystyrene to precipitate is about 4 ~ 5 in aqueous solution,[7] for poly(methyl methacrylate) (PMMA) in an organic solvent, 16 ~ 36 when the interfacial tension was 5 ~ 15 dynes/cm.[5] Now the question is what is the critical chain length for poly(NIPAM) chains to precipitate. According to Snyder and Klotz[23], a poly(NIPAM) chain with three monomer units precipitated from aqueous solution, since they observed that the trimer of NIPAM

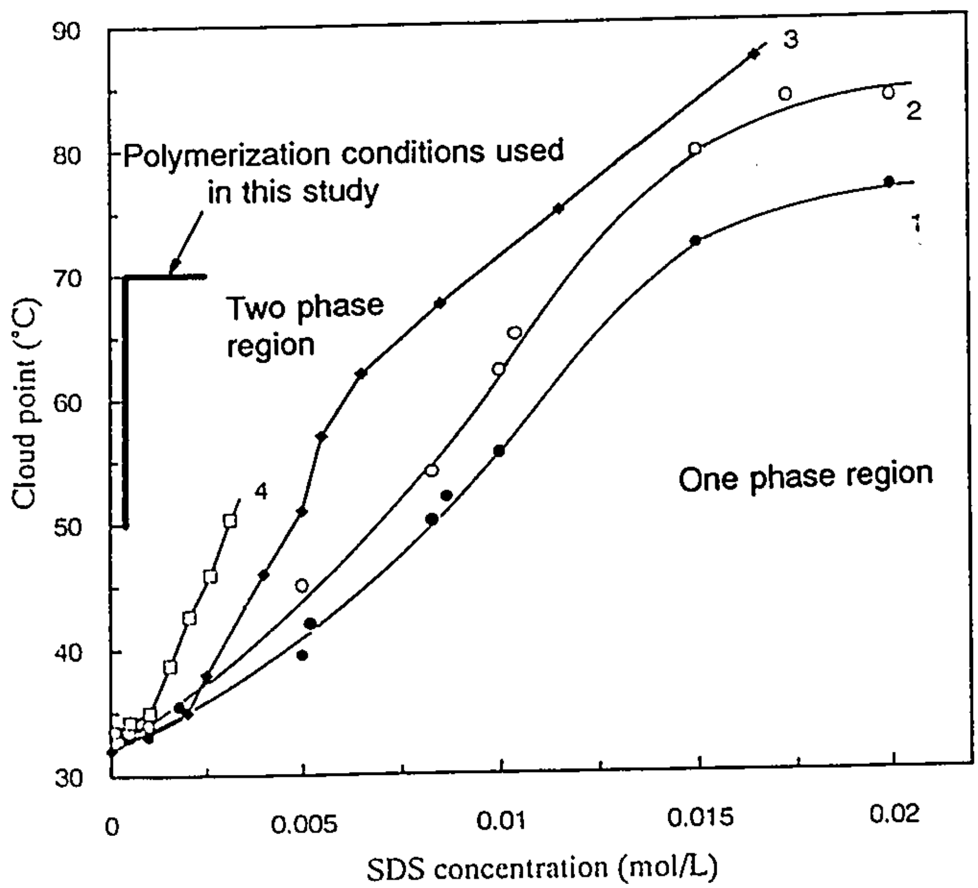

Figure 5.14: Phase diagram of poly(NIPAM) in SDS solution and polymerization conditions

Poly(NIPAM) concentration: Curve 1, this work, 0.5 wt.%; 2, this work, 1.0 wt.%; 3, Schid and Tirrell's data, 0.04 wt.%; 4, Meewes et al.'s data, 0.001 - 0.02 wt.%.

showed a negative temperature coefficient of solubility in water as did the high polymers. This suggests that the oligomer radicals of NIPAM likely precipitate before they have terminated. Similar observations were made by Fujishige[24] who failed to fractionate poly(NIPAM) according to molecular weight by heating the polymer solution towards the LCST. He found that the poly(NIPAM) of $\overline{M}_n$ from 5×10^4 to 8×10^6, precipitated from aqueous solution at the same temperature (~ 31 °C).

(iii) Nucleation mechanism of particles

(a) Models available in the literature

Since the concentration of free micelles were negligible for polymerizations of NIPAM and NIPAM/BAM, since no rapid change in particle number was observed over the range of SDS levels used, and since the NIPAM oligomers precipitated in aqueous solution, as discussed in section (ii), the poly(NIPAM) particles were likely formed by homogeneous nucleation rather than micellar nucleation. However, to distinguish the mechanism of self-nucleation (one oligomer radical gives one polymer particle) from that of aggregative nucleation (many oligomer radicals agglomerate to form a polymer particle), more analysis was needed.

(i) Self-nucleation model

In classical aqueous emulsion polymerization, following the Smith-Ewart theory for case-II kinetics, every free radical formed during polymerization produces a new particle in the presence of sufficient surfactant. With this assumption, together with the assumption that the particle volumetric growth rate is the same for all particles and is constant, then the number of particles, N_p, is predicted to be proportional to the 0.6th power of surfactant concentration

$[S]^{7.8}$

$$N_p \propto [S]^{0.6} \tag{5.19}$$

This model is called "self-nucleation", or "dispersant-limited nucleation".

(ii) Aggregative nucleation model

Frequently, deviation from the above model (much higher power of the surfactant or dispersant concentration) has been observed in both aqueous emulsion polymerization and non-aqueous dispersion polymerization.[6] Therefore, another model has been developed. This model assumes that the particles actually observed are formed by the agglomeration of much smaller, primary particles; Primary particles grow to such size and number that the dispersant is no longer sufficient to cover the surface effectively, and thus the primary particles start to flocculate; The dispersant serves merely to prevent secondary aggregation and plays no role in the formation of primary particles. If in this way, and assuming that the particle size distribution is fairly uniform, There are the following relationships between number of particles, diameter of particles and dispersant concentration:

$$N_p \propto [S]^3 \tag{5.20}$$

$$\overline{D} \propto [S]^{-1} \tag{5.21}$$

This model is called "aggregative nucleation", or "dispersant-limited agglomeration". The above relationships were derived from theory. Practically, the exponents on [S] vary with monomer type. For example, Barrett and Thomas[6] observed exponents - 0.5 in Equation (5.21) for methyl methacrylate (MMA) homopolymerization, and - 0.6 for MMA copolymerization with other monomers in organic media; Fitch and Tsai's[25] data for polymerization of MMA in aqueous solutions gave an exponent 3.87 in Equation (5.20).

In this work, the correlations observed for the polymerization of NIPAM/BAM above the LCST in aqueous solutions at low SDS levels (0.2 - 40 mmol/L) were:

$$N_p \propto [S]^{2.5} \tag{5.22}$$

$$D \propto [S]^{-0.71} \tag{5.23}$$

These results do not agree with the predictions for micellar nucleation nor for dispersant-limited nucleation, but are closer in agreement with the model for dispersant-limited agglomeration. However, the experimental results show that poly(NIPAM) particles formed from homogeneous solutions upon heating beyond the LCST in the absence of SDS (section 5.3.3 (ii) (b)), and that poly(NIPAM) latex was produced in aqueous medium without any surfactant.[2] Therefore it appears that poly(NIPAM) or poly(NIPAM/BAM) particles are formed by a mechanism of homogeneous agglomeration. The agglomeration extent depends on the amount of surfactant. Without surfactant, more agglomeration occurs, and thus the particles were larger. The more the surfactant that is used, the smaller the particles that are generated.

(b) Complementary evidence

The size of poly(NIPAM) and poly(NIPAM/BAM) particles at various monomer conversion measured by DLS at 50 °C are plotted in Figure 5.15. The x-axis is the particle diameter which was measured after the particles were cooled down to about 4 °C and then heated to 50 °C. The y-axis is the diameter of the particles kept hot at the reactor temperature (70 °C) after they were taken from reactor. These particles were then cooled down to 50 °C and measured by DLS (50 °C). The diagonal represents the equal size of the particles

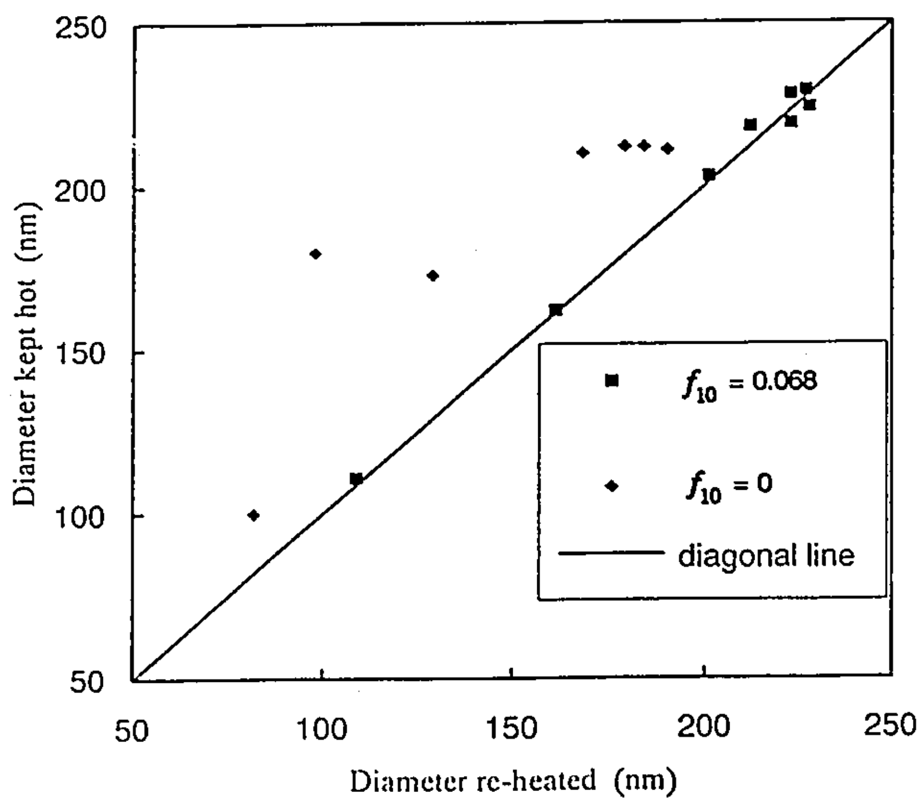

Figure 5.15: Comparison of particle size kept hot and reheated for the polymers (runs LS1, LS8) with and without cross-linking agent BAM

measured in two cases. For the poly(NIPAM/BAM), the data points lie almost on the diagonal. However, the data points of poly(NIPAM) are above the diagonal, that is, the diameters of poly(NIPAM) kept hot were greater than those re-heated. This observation suggests that a non-cross linked and soluble poly(NIPAM) particle (soluble at lower temperature) consists of many polymer chains. The polymer chains dissolve out of polymer particles into the continuous phase at 4 °C. When reheated to 50 °C, new and smaller polymer particles are formed by chain precipitation. The particles of cross-linked poly(NIPAM/BAM) cannot dissolve at the lower temperature, and hence new polymer particles are not formed. This mechanism is schematically illustrated in Figure 5.16.

As the latices were diluted about 10^4 times with distilled water for the measurement by dynamic light scattering, the SDS content in the solution was much lower than in original latices, and thus the particles formed when re-heated might be expected to be fewer in number and greater in size. Contrary to this, the particle size was smaller. A possible reasons for this might be that part of charged end groups on polymer chains were trapped in the original particles, and thus more polymer chains were required to obtain enough surface charge; when the particles formed from the more diluted solutions, fewer charged groups were trapped and thus more effective.

This hypothesis is supported by McPhee's observation.[4] Based on his electrophoresis and titration results, combined with O'Brien and White's theory, McPhee estimated that only about 11 ~ 23 % of the charged groups were on the particle surface with the rest distributed within particles. Also the particle size of poly(NIPAM) at 50 °C was 37 nm in 0.118 g/L SDS, and 80 nm in pure water. This suggests that the particle size is determined by surface charge.

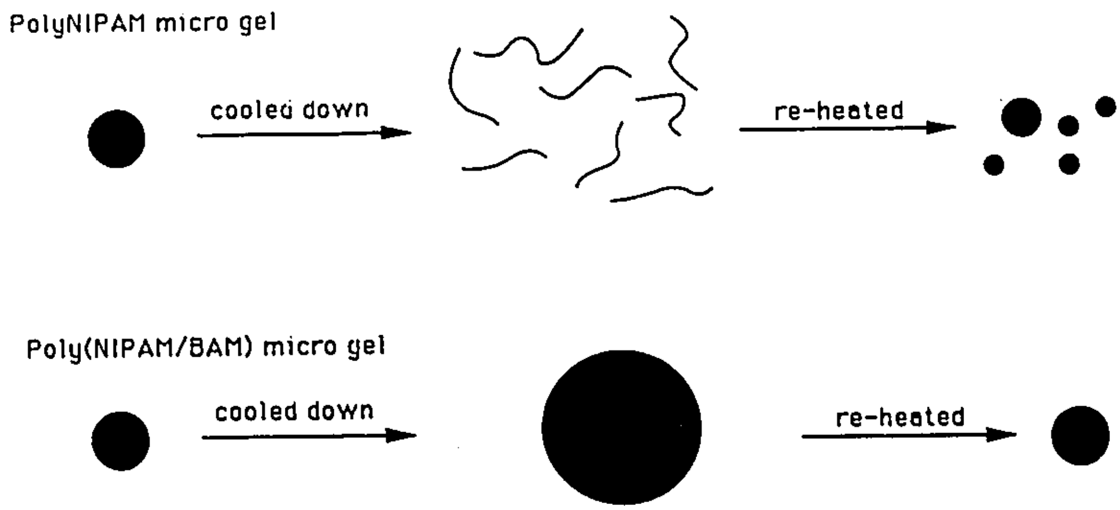

Figure 5.16 Schematic diagram of linear and cross-linked NIPAM polymeric micro gels undergoing cool-heat cycle

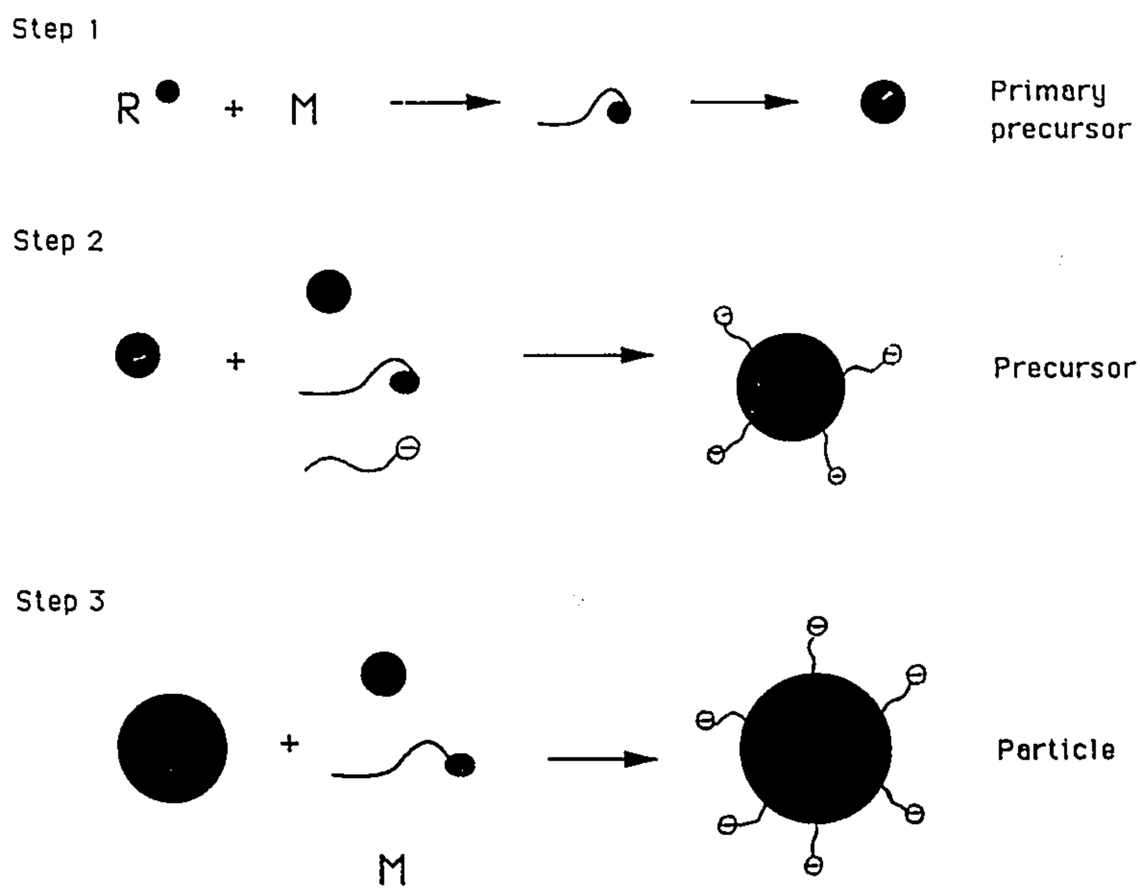

Figure 5.17 Schematic diagram for proposed nucleation mechanism of NIPAM polymeric particles

$R^{\bullet}$ —— initiator radical

M —— monomer

—— polymeric radical or oligomeric radical

—— SDS anionic group

In summary, the particle nucleation likely follows the mechanism illustrated in Figure 5.17, in which the nomenclature is adopted from Feeney, Napper and Gilbert:[26]

Step 1 Primary precursor particles formed by precipitation of poly(NIPAM) or poly(NIPAM/BAM) with chain length longer than some critical chain length;

Step 2 The primary precursor particles agglomerate to form precursor particles which are stabilized by the surface charge provided by initiator and SDS;

Step 3 The precursor particles grow by capturing primary precursors and oligomer radicals, and/or by polymerization of monomers. The nucleation of new particles ceases when the total interfacial area between polymer particles and aqueous phase is sufficiently large that oligomer radicals are captured before growing to critical chain length, and/or, the primary precursors are captured before becoming stable particles due to insufficient surfactant.

5.4.2 Linearity of particle volume vs monomer conversion

In Figures 5.3 and 5.9, linear relationships between $\overline{D}_{vol}$ and monomer conversion, x, are displayed in the range $0 < x < \sim 85\%$. This suggests instantaneous or very rapid particle nucleation followed by a period where particles are colloidally stable and do not agglomerate. This interval would be called stage II in classical emulsion polymerization, and if (1) the weight ratio of monomer to polymer in the particles is constant, and (2) the particle concentration is constant, the average particle volume increases linearly with x, according to Ugelstad and Hansen's derivation:[27]

$$\overline{V} = (xQ_0/N_p)[1/\rho_{pol} + (1/\rho_{mon})(1/x_c - 1)] , \qquad \text{for } x < x_c \qquad (5.24)$$

where N_p is particle concentration, Q_0 is the initial concentration of monomer, x_c is the conversion at the end of stage II, ρ_{pol} and ρ_{mon} are the densities of polymer and monomer respectively.

In classical emulsion polymerization, monomer droplets exist during whole stage II. The droplets supply the monomer to particles and keep the monomer concentration constant in particles. Thus the condition (1) can be often fulfilled. In this work, however, there are no monomer droplets present - all the monomer(s) are dissolved in the aqueous continuous phase, and/or absorbed in polymer particles; and the monomer concentration continuously drops during the whole polymerization period. Therefore, the monomer concentration in the particles cannot be constant. The linear relationship between particle volume and monomer conversion observed may be explained as: (1) relatively constant concentration of NIPAM/BAM polymer particles,[28] and (2) almost constant particle density ρ_p. NIPAM/BAM polymer particles are swollen by water (even at 60 °C, there is more than 10 % water in the particles). The swelling extent of the particles is mainly determined by the water content rather than the monomer content since the monomer concentration in the continuous phase is about 1.5% or less. The particle volume would increase linearly with monomer conversion x as long as the particle concentration and the volume ratio of water to polymer are constant. It is possible to describe the volume-conversion relationship of NIPAM/BAM polymer particles with the following equation derived from mass balance:

$$\overline{V} = \frac{Q_0 x}{\rho_{pol} \phi_p N_p} \tag{5.25}$$

where the small contribution of monomer to the particle volume is neglected and ϕ_p is the volume fraction of polymer in the polymer particles.

5.4.3 Polymerization mechanism

In classical emulsion polymerization, polymerization rate Rp is proportional to particle concentration N_p:[22]

$$R_p = k_p N_p [M]_p \bar{n} / N_A \tag{5.26}$$

while in dispersion polymerization, R_p is proportional to the square root of the volume fraction of particles ϕ (volume of particles / (volume of particles + volume of continuous phase) based on the assumption that the polymerization mainly occurs in particles since polymer radicals initiated in the dilute phase are rapidly captured by existing particles:[6]

$$R_p = k_p (2fk_d/k_t)^{1/2} [M]_p [I]^{1/2} \phi^{1/2} \tag{5.27}$$

where $[I]$ is the total amount of initiator in moles divided by the total volume of the dispersion. Actually, Equation (5.27) is exactly the same as that for classical emulsion polymerization obeying Case III kinetics, which means that the equation describes the special case of dispersion polymerization in which there are many radicals per particle and all the polymerization occurs in the polymer particles.

The polymerization rates of NIPAM/BAM at two SDS levels did not show significant difference, as described in 5.3.3 (i), although the particle concentrations were quite different (2.1×10^{15} and 1.0×10^{17} #/L). This suggests that if the polymerization is emulsion polymerization, it could be either Case III kinetics applied or Case I kinetics with rapid radical desorption .

Table 5.4 compares the characteristics of dispersion polymerization, emulsion polymerization with the results of this work.

Table 5.4 Comparison of dispersion, emulsion polymerization with the results of this work*

Characteristic	Dispersion	Emulsion	This system
Separate monomer phase	×	✓	×
Initiator dissolved in both phases	✓, ×	×	✓
Particles formed in diluent phase	✓	✓	✓
Particle concentration dependent on stabilizer concentration	✓	✓	✓
Polymerization rate proportional to particle concentration	×	✓	?

* ✓ means "yes", × "no".

In dispersion polymerization, or emulsion polymerization (Case III kinetics) the polymerization rate is proportional to the square root of volume fraction of particles according to Equation (5.27), or proportional to the volume fraction of particles.[29] However, the polymerization rate (runs LS1 and LS10) found in this work hardly depends on the particle size and particle concentration. The polymerization may take place inside the particles, and in the aqueous phase. In the latter case, primary particles grow by the precipitation of polymer radicals and are captured by existing particles.[5]

5.5 SUMMARY

The kinetic aspects and the mechanism of heterogeneous polymerization of NIPAM/BAM in aqueous media were investigated. Several factors including temperature, ionic strength, concentrations of cross-linking agent and surfactant were studied. It was found that: (1) increasing temperature by 20 °C elevated the polymerization rate by a factor of five; (2) the

BAM raised the polymerization rate as well as the particle size, so did the higher ionic strength; (4) increasing SDS concentration reduced the induction period but hardly changed the polymerization rate; (5) the particle diameter decreased, while the particle number increased, with increasing SDS level: $\overline{D}_{vol} \propto [SDS]^{-0.71}$, $N_p \propto [SDS]^{2.5}$.

The particles are likely nucleated by the mechanism of homogeneous agglomeration, and that, probably, the polymerization followed emulsion polymerization (Case III kinetics) or equivalently a special case of dispersion polymerization (where polymerization occurs only in the polymer particles and the average number of radicals per particle are much greater than 1.0).

Symbols

D — Particle diameter (nm)

e_1, e_2 — Polarity of monomer 1 and 2

E_d, E_p, E_t, E_R — Activation energy of decomposition, propagation, termination, and overall reaction (kcal/mol)

f — Initiation efficiency

f_1, f_2 — Mole fraction of monomer 1 and 2

F_1, F_2 — Mole fraction of monomer 1 and 2 in copolymer

k_d, k_p, k_t, k_R — Rate constant of decomposition (min^{-1}), propagation ($L.mol^{-1}.min^{-1}$), termination ($L.mol^{-1}.min^{-1}$), and overall reaction ($L^{1/2}.mol^{-1/2}.min^{-1}$). Subscript "0" represent constant in Arrhenius equation.

k_{ij} — Rate constant of cross-propagation ($L.mol^{-1}.min^{-1}$). i, j equal 1 and 2 representing monomer 1 and 2.

$\hat{k}_p$, $\hat{k}_t$ — Pseudo rate constant of propagation ($L.mol^{-1}.min^{-1}$) and termination ($L.mol^{-1}.min^{-1}$) in copolymerization. Subscript "0" represent constant in Arrhenius equation.

k_{td}, k_{tc} — Rate constant of termination ($L.mol^{-1}.min^{-1}$) by disproportionation and combination. Subscript "1", "2" represent monomer 1 and 2.

[M], [I] — Monomer and initiator concentration respectively (mol/L). Subscript "0" represents initial values. Subscript "p" represents the concentration in the particles.

$\bar{n}$ — Average number of radical per particle

N_A — Avogadro's number

N_p — Particle concentration (#/L)

P_i, Q_j — Parameters related to resonance of monomers

Q_0 — Initial charge of monomer

r_1, r_2 — Reactivity ratio of monomer 1 and 2

R — Gas constant

R_p — Polymerization rate ($mol.L^{-1}.min^{-1}$). Subscripts "1" and "2" represent different temperatures.

$[S]$ — Surfactant concentration (mol/L)

t — Reaction time (min)

T — Temperature (°C) or (°K) specified in equations

$\bar{V}$ — Average particle volume (nm^3)

x — Monomer conversion

x_c — Monomer conversion at which stage II of emulsion polymerization ends

Z — Ionic strength (mol/L)

ρ_{pol}, ρ_{mon} — Density of polymer and monomer respectively (g/cm^3)

ϕ — Volume fraction of particles in suspension

ϕ_p — Volume fraction of polymer

φ_1, φ_2 — Mole fraction of radicals with terminal monomer unit 1 and 2

φ_{td} — Fraction of termination by disproportionation

References

1. W.C. Wooten, R.B. Blanton, and H.W. Coover,Jr., J. Polymer Science, Vol.xxv, 403-12 (1957)

2. R.H. Pelton and P. Chibante, Colloid and Surfaces, **20**, 247-56 (1986)

3. R.H. Pelton, H.M. Pelton, A. Morphesis, and R.L. Rowell, Langmuir, **5**(3), 816-8 (1989)

4. W. McPhee, *Poly(N-isopropylacrylamide) Microgel Latexes*, Masters Thesis, McMaster University, Canada, 1991

5. *Free Radical Polymerization*, Ed. by Z.R. Pan and Z.Z. Yu, Polymer Chemistry Series Book (Chinese), Chemical Industry Publisher, 1983

6. K.E.J. Barrett and H.R. Thomas, Kinetics and Mechanism of Dispersion Polymerization, in *Dispersion Polymerization in Organic Media*, Ed. by K.E.J Barrett, John wiley & Sons, Toronto, 1975

7. J.W. Goodwin, R.H. Ottewill, R. Pelton, G. Vianello, and D.E. Yates, Brit. Polym. J. **10**, 173 (1978)

8. A.E. Hamielec, Course Notes for Chem. Eng. 6B3, Department of Chemical Engineering, McMaster University, Hamilton, Canada, 1987

9. R.A.M. Thomson, C.K. Ong, C.M. Rosser and J.M. Holt, Makromol. Chem. **184**, 1885 (1983)

10. D.C. Blackley, Initiation and Initiator Systems, in *Emulsion Polymerization*, John Wiley & Sons, New York-Toronto, 1975

11. C.J. Kim and A.E. Hamielec, Polymer, **25**, 845, (1984)

12. T. Alfrey, Jr., and C.C. Price, J. Polym. Sci. **2**, 101 (1947)

13. P.J. Flory, *Principles of Polymer Chemistry*, Cornel University, Ithaca, 1953

14. H. Tobita, *Cross-linking Kinetics for Free Radical Polymerization*, Ph.D. Thesis, McMaster University, Hamilton, Canada (1991)

15. C.K. Chiklis and J.M. Grasshoff, J. Polym. Sci. A2, **8**, 1617-26 (1970)

16. F.K. Hansen and J. Ugelstad, Particle Formation Mechanism, in *Emulsion Polymerization*, Ed. by D.C. Blackley, Academic Press, Inc., 1982

17. A.S. Dunn, Absorption of Emulsifier and Its Effects on Kinetics of Polymerization, in *Sci. & Tech. Polym. Coll.*, Vol.2, p314-334 Ed. by G.W. Poehlein, R.H. Ottewill and J.W. Goodwin, Martinus Nijhoff Publisher, 1983

18. B.S. Casey, I.A. Maxwell, B.R. Morrison and R.G. Gilbert, Makromol. Chem., Makromol. Symp. **31**, 1-10 (1990)

19. R.H. Pelton, *Studies on Cationic Polystyrene Latices*, Ph.D Thesis, University of Bristol, Great Britain, 1976

20. H. G. Schild and A. Tirrell, Polymer Preprints (ACS Div. Poly. Chem.) **30**(2), 350-51 (1989)

21. J. Rička, M. Meewes, R. Nyffenegger, and T. Binkert, Physical Review Letters **65**(5), 657-60 (1990)

22. X.Y. Wu, R.H. Pelton, K.C. Tam, D.R. Woods and A.E. Hamielec, Poly(N-isopropylacrylamide) 1. Interaction with sodium dodecyl sulfate measured by conductometry, J. Polym. Sci., in press

23. W.D. Snyder and I.M. Klotz, J. Am. Chem. Soc. **97**(17), 4999 - 5003 (1975)

24. S. Fujishige, Polymer J. **19**(3), 297-300, (1987)

25. R.M. Fitch and C.H. Tsai, in *Polymer Colloids*, Ed. by R.M. Fitch, Plenum Press, New York, 1979

26. P.J. Feeney, D.H. Napper and R.G. Gilbert, Macromolecules, **20**(11), 2922-30 (1987)

27. J. Ugelstad and F.K. Hansen, Kinetics and Mechanism of Emulsion Polymerization, Rubber Chem. Tech. **49**, 536 (1976)

28. J.L. Gardon, Interfacial, Colloidal, and Kinetic Aspects of Emulsion Polymerization, in *Interfacial Synthesis*, Vol.1, Eds. F. Millich and C.E. Carraher, Jr., Marcel Dekker, 1977

29. K.H. Reichert, Hamilton, Canada, personal communication (1991)

APPENDIX B-1

Aqueous Solution Polymerization of NIPAM Initiated by Redox System

In aqueous solution NIPAM polymer precipitates when the temperature was raised above ~ 31 °C. Therefore, the aqueous solution polymerization must be carried out below 31 °C and hence requires a redox initiator pair to generate radicals. In the literature, some authors performed the aquecus solution polymerization of NIPAM with redox systems. Table B-1.1 gives some example recipes and conditions.

Table B-1.1 Examples of published aqueous solution polymerization with redox initiators

Author	Initiators	$[M]_0$	Temperature	Rate
Wooten[1]	$NaHSO_3/NH_4S_2O_8$	5 %	25 ~ 32 °C	t=16 min x=1.0
Priest[2]	$TEMED/NH_4S_2O_8$	1 %	R.T.	t=10 min x=0.87

In this work, two redox initiator pairs at different levels were used to conduct the solution polymerization of NIPAM under various conditions. The recipes and conditions are summarised in Table B-1.2

[1] W.C. Wooten, R.B. Blanton, and H.W. Coover, Jr., J. Polym. Sci. vol.xxv, 403-412, (1957)

[2] J.H. Priest, S.L. Murry, R.J. Nelson, and A.S. Hoffman, in *Reversible Polymeric Gels and Related Systems* (ACS Symposium Series 350, 255-64, 1987)

Table B-1.2 Recipes and conditions for aqueous solution polymerization of NIPAM with redox initiators

Run	Initiators 1 / 2	$[I]_0$ mmol/L 1 / 2	$[M]_0$ mol/L	T (°C)
RS1	$NaHSO_3$ / $Fe_2(SO_4)_3.5H_2O$	0.442 / 0.094	0.177	18.4 ~ 20.3
RS2	$NaHSO_3$ / $Fe_2(SO_4)_3.5H_2O$	0.961 / 0.204	0.177	18.5 ~ 19.9
RS3	$NaHSO_3$ / $K_2S_2O_8$	0.961 / 0.407	0.177	18.4 ~ 21.2
RS4	$NaHSO_3$ / $K_2S_2O_8$	2.36 / 1.00	0.177	18.4 ~ 20.5
RS5	$NaHSO_3$ / $K_2S_2O_8$	2.36 / 2.36	0.177	25
RS6	$NaHSO_3$ / $Fe_2(SO_4)_3.5H_2O$	0.961 / 0.204	0.177	10

The monomer conversion was determined with HPLC (see Part B Chapter 5 for details). Figure B-1.1 is the plot of monomer conversion vs. reaction time. The polymerizations initiated by $NaHSO_3$ / $K_2S_2O_8$ were slower than those by $NaHSO_3$ / $Fe_2(SO_4)_3.5H_2O$ although the concentration of the former was higher. The slower reaction rates are likely caused by the slower generation rate of radicals from $NaHSO_3$ / $K_2S_2O_8$. Interestingly, the polymerization carried out at room temperature ceased at monomer conversion of 14.3% and 66.3 % for RS1 and RS2 respectively, while at 10 °C, the polymerization approached completion. The curves for RS1 and RS2 are similar to "dead end" polymerizations — the polymerizations which stop before all the monomer has been consumed due to complete consumption of initiator. Probably, at room temperature the initiators were consumed so fast that many of the radicals experienced recombination before they could initiate the monomer polymerization.

The "dead end" polymerization and limiting conversion can be used to estimate the ratio f/k_d where f is the initiation efficiency and k_d is the rate constant of the first-order decomposition of the initiator for initiators which decompose thermally.[3,4] For the polymerization initiated by thermally-decomposed initiators, the polymerization rate is given by (for the derivation see reference[5]):

$$-\frac{d[M]}{dt} = k_p\left(\frac{fk_d}{k_t}\right)^{1/2}[I]^{1/2}[M] \tag{1}$$

where k_d, k_p, k_t are rate constants for initiator decomposition, polymer propagation and termination, respectively; $[I]$, $[M]$ are the concentrations of initiator and monomer.

Substituting the expression[5] of $[I] = [I]_0 e^{-k_d t}$ into Equation (1) and integrating it, one can obtain the following equation at time t (or monomer conversion x)

$$-\ln\frac{[M]}{[M]_0} = -\ln(1-x) = 2k_p\left(\frac{f[I]_0}{k_d k_t}\right)^{1/2}(1-e^{-k_d t/2}) \tag{2}$$

At long times, the monomer conversion no longer changes, i.e., $x \to x_\infty$, $[M] \to [M]_\infty$

$$-\ln\frac{[M]_\infty}{[M]_0} = -\ln(1-x_\infty) = 2k_p\left(\frac{f[I]_0}{k_d k_t}\right)^{1/2} \tag{3}$$

Dividing (2) by (3), gives:

---

3 Zuren Pang and Zaizhang Yu, *Free Radical Polymerization*, Chemical Industry Publisher (China, 1983), pp 98-99

4 A.V. Tobolsky, C.E. Rodgers and R.D. Brickman, J. Am. Chem. Soc. 82, 1277 (1960)

5 A.E. Hamielec, Course Notes of Chem. Eng. 6B3, McMaster University, Hamilton, Canada (1987)

$$\ln\left[1 - \frac{\ln(1 - x)}{\ln(1 - x_{\infty})}\right] = -\frac{k_d t}{2} \tag{4}$$

Plotting the left hand side of Equation (4) against time t, one can find k_d from the slope.

For polymerization initiated by a redox pair, the reactions are as follows:

$$I_1 + I_2 \xrightarrow{k_1} R^{\bullet} \qquad R_r = k_1[I_1][I_2] \tag{5}$$

$$R^{\bullet} + M \xrightarrow{k_i} M^{\bullet} \qquad R_i = f\, k_i[R^{\bullet}][M] \tag{6}$$

$$M^{\bullet} + M \xrightarrow{k_p} MM^{\bullet} \qquad R_p = k_p[M^{\bullet}][M] \tag{7}$$

$$M_n^{\bullet} + M_m^{\bullet} \xrightarrow{k_t} P \qquad R_t = k_t[M^{\bullet}]^2 \tag{8}$$

where $[I_1]$, $[I_2]$ are the concentrations of reducing and oxidizing agent; k_1 is the rate constant for the reaction generating radicals; $[R^{\bullet}]$, $[M^{\bullet}]$ are the concentrations of initiator radicals and monomer radicals.

At stationary state, the generation rate of initiator radicals almost equals to the consumption rate of them, that is,

$$R_r \approx R_i, \qquad k_1[I_1][I_2] \approx k_i[R^{\bullet}][M] \tag{9}$$

$$[R^\cdot] \approx \frac{k_1[I_1][I_2]}{k_i[M]} \qquad (10)$$

Also, the producing rate of monomer radicals approximately equals to the consumption rate:

$$R_i \approx R_t, \qquad fk_i[R^\cdot][M] \approx k_t[M^\cdot]^2 \qquad (11)$$

$$[M^\cdot] = \left(\frac{fk_i[R^\cdot][M]}{k_t}\right)^{1/2} \qquad (12)$$

Substituting (10) into (12), one obtains:

$$[M^\cdot] = \left(\frac{fk_i(k_1[I_1][I_2]/k_i[M])[M]}{k_t}\right)^{1/2} = \left(\frac{fk_1[I_1][I_2]}{k_t}\right)^{1/2} \qquad (13)$$

Substituting (13) into (7) gives the following equation for the polymerization rate when a redox initiator pair is used:

$$R_p = -\frac{d[M]}{dt} = k_p\left(\frac{fk_1}{k_t}\right)^{1/2}[I_1]^{1/2}[I_2]^{1/2}[M] \qquad (14)$$

If the initial concentration of I_1 is $[I_1]_0$, and that of I_2 is $[I_2]_0$, then at time t, I_1 is consumed $([I_1]_0 - [I_1])$ thus the concentration of I_2 is:

$$[I_2] = [I_2]_0 - ([I_1]_0 - [I_1]) = [I_2]_0 - [I_1]_0 + [I_1] \qquad (15)$$

Substituting Equation (15) into (5), one gets:

$$R_r = -\frac{d[I_1]}{dt} = -\frac{d[I_2]}{dt} = k_1[I_1][I_2] = k_1[I_1]([I_2]_0 - [I_1]_0 + [I_1]) \qquad (16)$$

Integrating both sides of Equation (16) gives:

$$\frac{-\ln([I_2]_0 - [I_1]_0 + [I_1]) + \ln([I_1]) + \ln([I_2]_0) - \ln([I_1]_0)}{([I_2]_0 - [I_1]_0)} = -k_1 t \tag{17}$$

The concentration of I_1 is then solved from Equation (17) to be:

$$[I_1] = \frac{[I_2]_0 - [I_1]_0}{[I_2]_0/[I_1]_0 \text{ep } [k_1 t([I_2]_0 - [I_1]_0)] - 1} \tag{18}$$

Substituting (18) into (15) and rearranging give:

$$[I_2] = ([I_2]_0 - [I_1]_0)\left[1 + \frac{1}{[I_2]_0/[I_1]_0 \exp[k_1 t([I_2]_0 - [I_1]_0)] - 1}\right] \tag{19}$$

Substituting (18) and (19) into (14) and rearranging, one obtains:

$$\begin{aligned} -\frac{d[M]}{dt} = k_p\left(\frac{fk_1}{k_t}\right)^{1/2}[M]\,([I_2]_0-[I_1]_0)&\left(\frac{1}{\frac{[I_2]_0}{[I_1]_0}\exp[k_1 t([I_2]_0-[I_1]_0)]-1}\right)^{1/2} \\ &\times\left(1+\frac{1}{\frac{[I_2]_0}{[I_1]_0}\exp[k_1 t([I_2]_0-[I_1]_0]-1}\right)^{1/2} \end{aligned} \tag{20}$$

Rearranging right side of (20) and separating the variables gives:

$$-\int\frac{d[M]}{[M]} = k_p\left(\frac{fk_1}{k_t}\right)^{1/2}([I_2]_0-[I_1]_0)\int\frac{\{[I_2]_0/[I_1]_0\exp[-k_1 t([I_1]_0-[I_2]_0)]\}^{1/2}}{[I_2]_0/[I_1]_0\exp[-k_1 t([I_1]_0-[I_2]_0)]-1}\,dt \tag{21}$$

Integrating both sides of (21) for time from 0 to t ($[M]_0$ to $[M]$), gives:

Simplifying (22), one obtains:

$$
\begin{aligned}
-\ln\frac{[M]}{[M]_0} = k_p\left(\frac{fk_1}{k_t}\right)^{1/2}([I_2]_0-[I_1]_0)\left(\frac{[I_2]_0}{[I_1]_0}\right)^{1/2}\left(\frac{[I_1]_0}{[I_2]_0}\right)^{1/2}\frac{1}{k_1([I_2]_0-[I_1]_0)}\\
\times\left[\ln\frac{(-[I_1]_0\exp(k_1t[I_1]_0-[I_2]_0\exp(k_1t[I_2]_0)}{([I_2]_0\exp(k_1t[I_2]_0)-[I_1]_0\exp(k_1t[I_1]_0))}\right.\\
\left.+2([I_2]_0[I_1]_0)^{1/2}\exp[\frac{1}{2}k_1t(I_2]_0+[I_1]_0)]+\ln\frac{([I_2]_0-[I_1]_0)}{-[I_1]_0-[I_2]_0+2([I_1]_0[I_2]_0)^{1/2}}\right]
\end{aligned}
\tag{22}
$$

$$
\begin{aligned}
-\ln\frac{[M]}{[M]_0} = k_p\left(\frac{f}{k_1k_t}\right)^{1/2}\left[\ln\frac{[I_2]_0-[I_1]_0}{-[I_1]_0-[I_2]_0+2([I_1]_0[I_2]_0)^{1/2}}\right.\\
\left.+\ln\frac{-[I_1]_0\exp(k_1t[I_1]_0-[I_2]_0\exp(k_1t[I_2]_0}{[I_2]_0\exp(k_1t[I_2]_0)-[I_1]_0\exp(k_1t[I_1]_0)}+2([I_1]_0[I_2]_0)^{1/2}\exp[\frac{1}{2}k_1t([I_2]_0+[I_1]_0)]\right]
\end{aligned}
\tag{23}
$$

Let Term A, Term B and Term C represent the three terms in the bracket of right hand side of (23):

$$\text{Term A} = \ln\frac{[I_2]_0-[I_1]_0}{-[I_1]_0-[I_2]_0+2([I_1]_0[I_2]_0)^{1/2}} \tag{24}$$

$$\text{Term B} = \ln\frac{-[I_1]_0\exp(k_1t[I_1]_0-[I_2]_0\exp(k_1t[I_2]_0}{[I_2]_0\exp(k_1t[I_2]_0)-[I_1]_0\exp(k_1t[I_1]_0)} \tag{25}$$

$$\text{Term C} = 2([I_1]_0[I_2]_0)^{1/2}\exp[\frac{1}{2}k_1t([I_2]_0+[I_1]_0)] \tag{26}$$

where Term C is constant for a given initial concentration of redox pair.

To investigate the effects of the three terms on the right side of (23), an example calculation was conducted using the recipe of run RS1 in Table 2. In the calculation of the three terms, a guess of k_1 value was made from the first-order approximation of the reaction rate of initiator pair: the second-order reaction rate of the initiator pair was approximated by the product of two individual rate of first-order reaction; and the individual rates are given by:

$$[I_1] = [I_1]_0 \, e^{-k_1 t} \tag{27}$$

$$[I_2] = [I_2]_0 \, e^{-k_1 t} \tag{28}$$

Substituting (27) and (28) into (14), one obtains:

$$-\frac{d[M]}{dt} = k_p \left(\frac{f k_1}{k_t}\right)^{1/2} ([I_1]_0 [I_2]_0)^{1/2} \left(e^{-k_1 t}\right)^{1/2} [M] \tag{29}$$

Integrating the above equation gives:

$$-\ln \frac{[M]}{[M]_0} = -\ln(1-x) = 2k_p \left(\frac{f}{k_1 k_t}\right)^{1/2} ([I_1]_0 [I_2]_0)^{1/2} \left(1 - e^{-k_1 t/2}\right) \tag{30}$$

At long times, the monomer conversion approaches a constant value x_∞, the above equation becomes:

$$-\ln \frac{[M]_\infty}{[M]_0} = -\ln(1-x_\infty) = 2k_p \left(\frac{f}{k_1 k_t}\right)^{1/2} ([I_1]_0 [I_2]_0)^{1/2} \tag{31}$$

Dividing Equation (30) by (31), gives:

$$\ln\left[1 - \frac{\ln(1-x)}{\ln(1-x_\infty)}\right] = -\frac{k_1 t}{2} \tag{32}$$

This equation is the same as Equation (4). Thus, the k_1 value was guessed by the plot of the L.H.S. of (32) versus time t. Figure B-1.2 is an example of the plot which was produced using the data of runs RS1 and RS2. Both data sets displayed linear relationships between the L.H.S. and t, although some scattering was observed. The slopes S and correlation coefficients γ^2 for two runs were: RS1, S = - 0.072, γ^2 = 0.96; RS2, S = - 0.48, γ^2 = 0.99. Thus, k_1 = 0.144 for RS1 and 0.96 for RS2.

By using 0.144 as an initial guess of k_1, the values of three terms in Equation (23) and the summation of them were calculated based on the data of RS1. These values are plotted against reaction time in Figure B-1.3. It is seen from the figure that at the beginning of the reaction, Term A is dominant; Term B decreases but Term C increases with the time; After long times (e.g. about 30 min), Term B becomes negligible. Therefore, at long times, Equation (23) can be written as:

$$-\ln(1-x) = k_p\left(\frac{f}{k_1k_t}\right)^{1/2}\Bigg[\ln\frac{[I_2]_0-[I_1]_0}{-[I_1]_0-[I_2]_0+2([I_1]_0[I_2]_0)^{1/2}} + 2([I_1]_0[I_2]_0)^{1/2}\exp[\frac{1}{2}k_1t([I_2]_0+[I_1]_0)]\Bigg] \tag{33}$$

Rearranging and taking logarithm of both sides give:

$$\ln\left[-\ln(1-x)-k_p\left(\frac{f}{k_1k_t}\right)^{1/2}\ln\frac{[I_2]_0-[I_1]_0}{-[I_1]_0-[I_2]_0+2([I_1]_0[I_2]_0)^{1/2}}\right] = \ln\left[2k_p\left(\frac{f}{k_1k_t}\right)^{1/2}([I_1]_0[I_2]_0)^{1/2}\right]+\frac{1}{2}([I_2]_0+[I_1]_0)k_1t \tag{34}$$

Plotting the left hand side of (34) against the reaction time t, one can get the rate constant of reaction between redox pair k_1. To get k_1, however, constant group, $k_p(f/k_1k_t)^{1/2}$, must be known. The following equation, which is derived from (23), can be used for this purpose:

$$k_p\left(\frac{f}{k_1k_t}\right)^{1/2} - \frac{-\ln(1-x)}{\text{Term A}+\text{Term }B+\text{Term }C} \tag{35}$$

By applying the kinetics data of run RS1, the value of the group was estimated to be in the range of 0.034 to 0.084. Figure B-1.4 shows that the constant group is a function of the reaction time. It increased first and then decreased with time after about 15 minutes.

By using the results of $k_p(f/k_1k_t)^{1/2}$ from Equation (35) and run RS1, the left hand side (L.H.S.) of Equation (34) was computed. Figure B-1.5 is the plot of L.H.S. of (34) versus time. It shows a linear relationship between L.H.S. and t. The slope of the line was found to be 0.0098 with a correlation coefficient 0.98. The value of the k_1 was then estimated from the slope, to be 0.0367. The calculation of L.H.S. of (34) and then the evaluation of k_1 were repeated using the new value of k_1 until the new k_1 value no longer changed. After four times of iteration, the value of k_1 = 0.00317 (min^{-1}) was obtained. The curve used to find this k_1 value is also plotted in Figure b-1.5 as curve 2.

The constant group, $k_p(f/k_1k_t)^{1/2}$, was re-calculated using k_1 = 0.00317. The trend of this group is shown in Figure B-1.4 as curve 2. Unlike curve 1 (k_1 = 0.144), no decrease of $k_p(f/k_1k_t)^{1/2}$ with time was observed in this case. If assuming f = 0.8 as usually used, one can estimate the value of $k_p/k_t^{1/2}$ by: $k_p/k_t^{1/2} = [k_p(f/k_1k_t)^{1/2}]\times[(k_1/f)^{1/2}]$. The value of $k_p/k_t^{1/2}$ was computed to be 0.0021 to 0.0053 ($L^{1/2}.mol^{-1/2}.min^{-1/2}$) based on the data of RS1. The change of $k_p/k_t^{1/2}$ with time is given in Figure B-1.6.

Figure B-1.1 NIPAM monomer conversion versus time for aqueous polymerization initiated by redox system

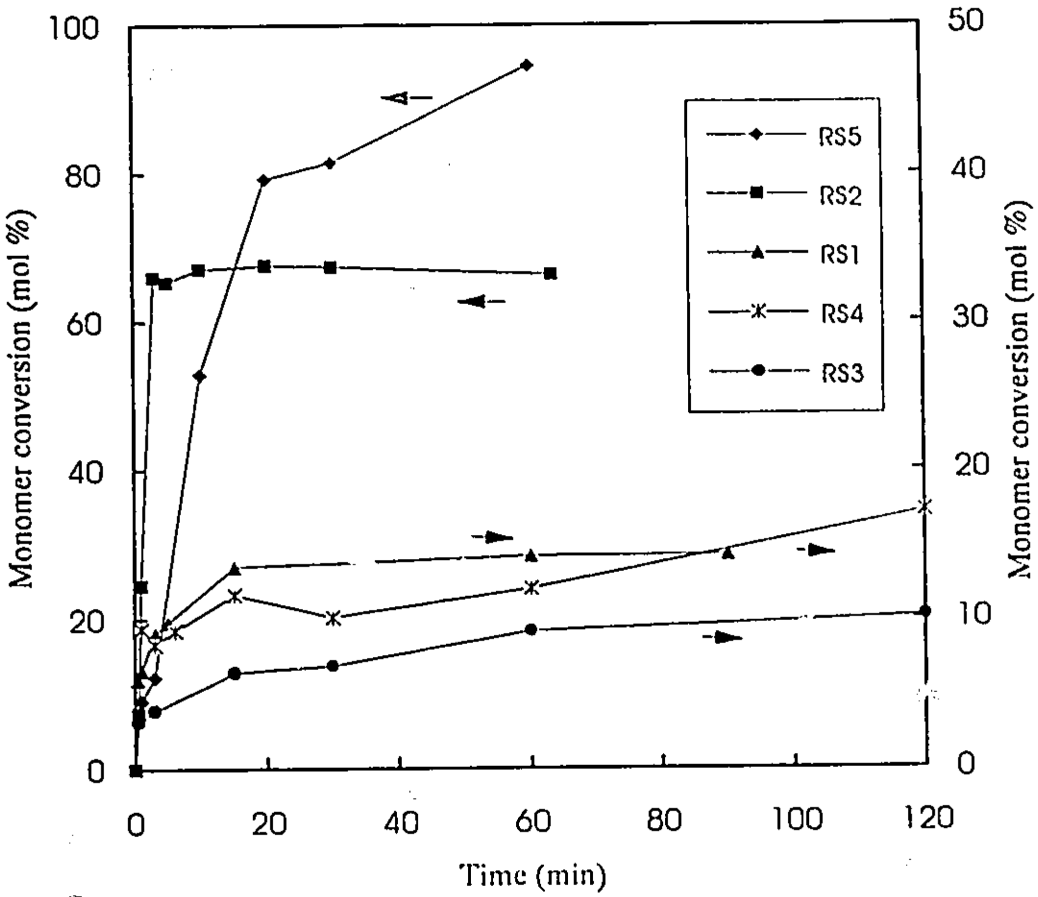

Figure B-1.2 $\ln [1 - \ln(1 - x) / \ln(1 - x_\infty)]$ versus reaction time

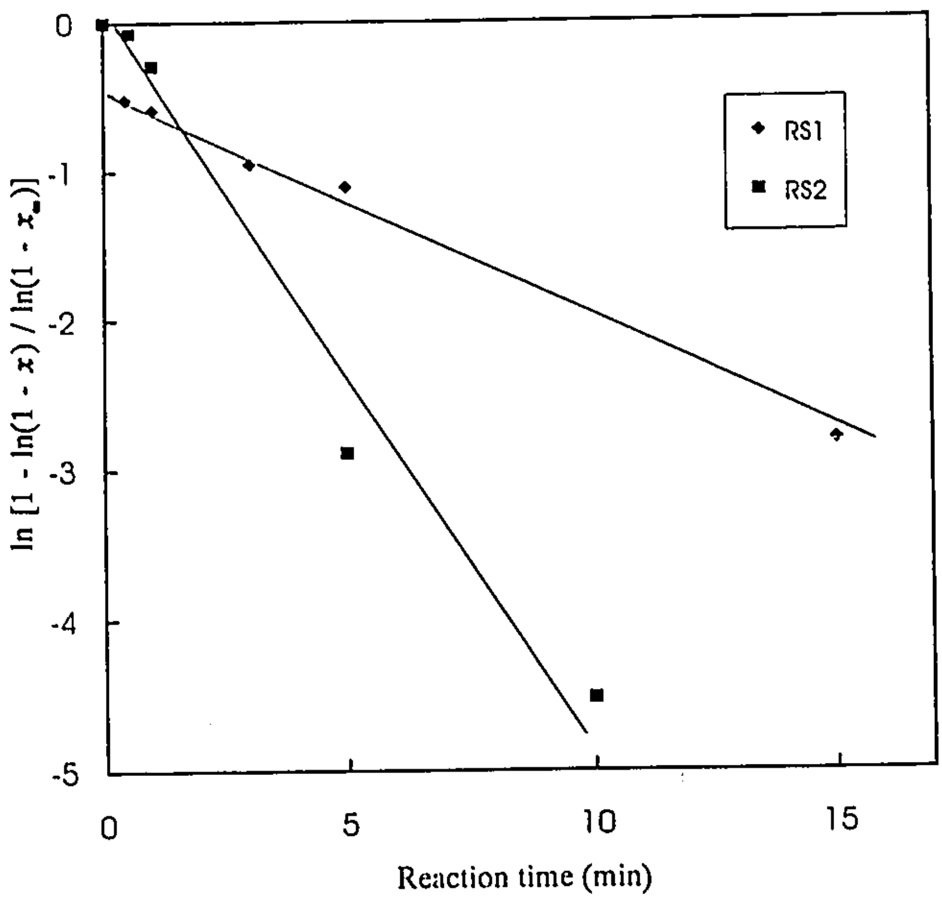

Figure B-1.3 Evaluation of each term and summation of the terms in Equation (23)

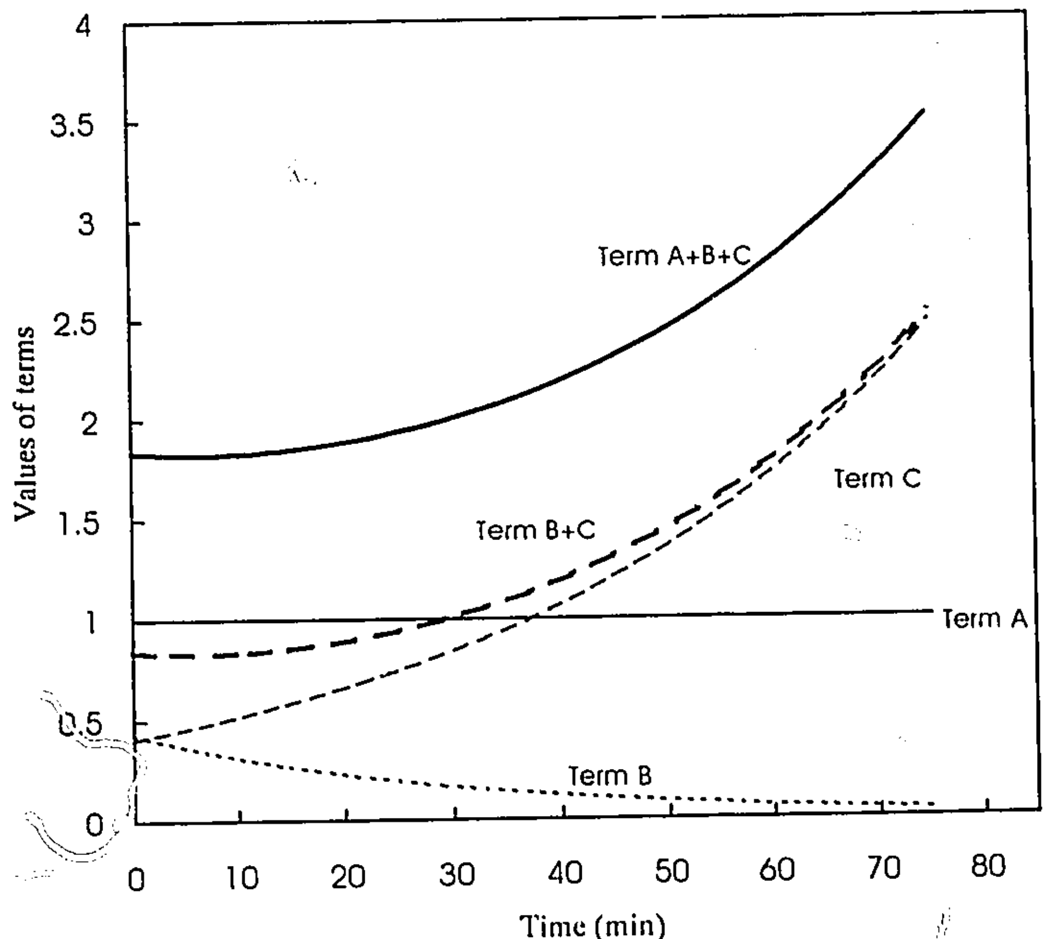

Figure B-1.4 Dependence of constant group $k_p(f/k_1k_t)^{1/2}$ on reaction time

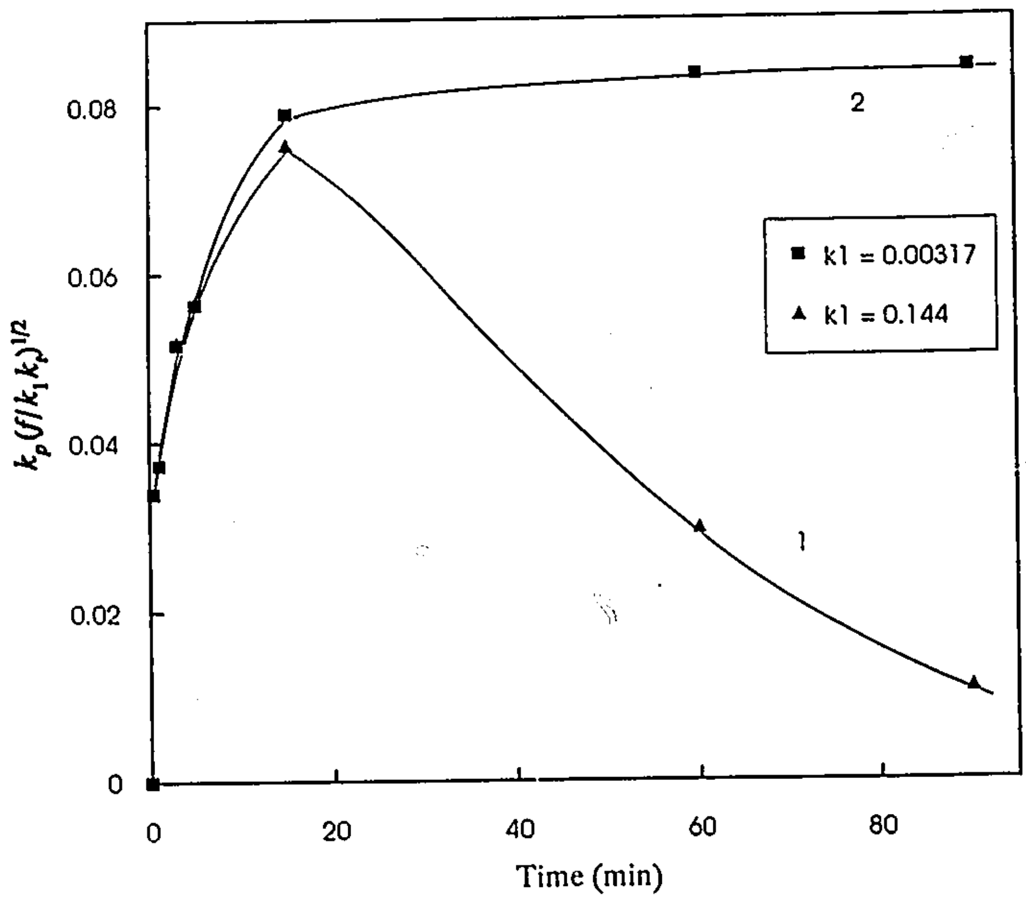

Figure B-1.5 Left hand side of Equation (34) versus reaction time

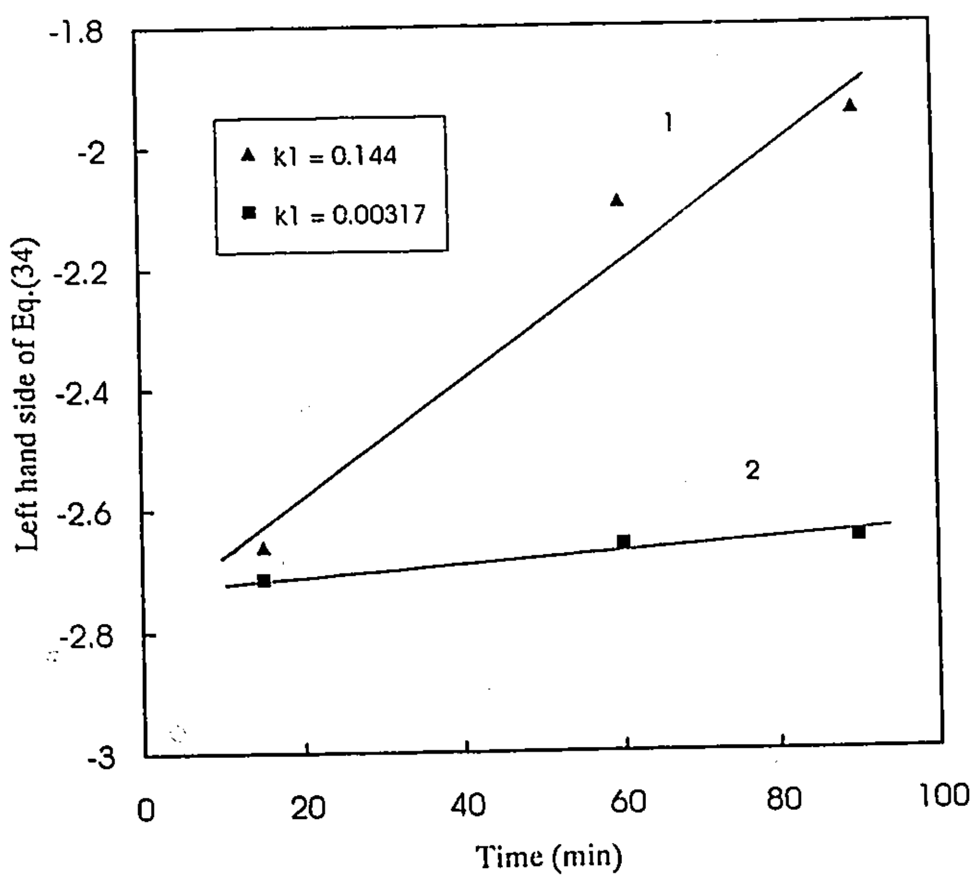

Figure B-1.6 $k_p/k_t^{1/2}$ versus reaction time for NIPAM solution polymerization at room temperature (run RS1) initiated by redox system

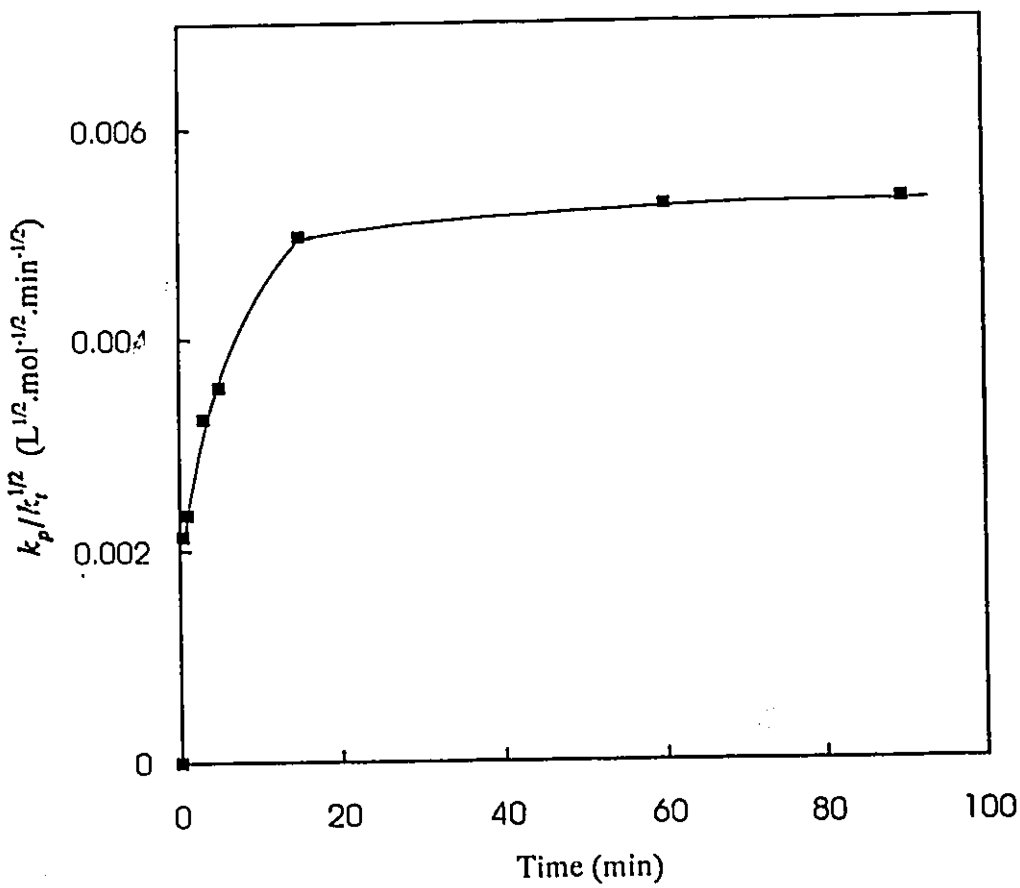

APPENDIX B-2

The Age of SDS Solution and the CMC of SDS

It is usually believed that SDS hydrolyses to alcohol in aqueous solution, and therefore the surface activity changes.[1] In order to ensure that the SDS solution used for titration has the same effective concentration, a study on the age of SDS solution was performed. The solutions prepared for 2 days, 40 days were compared with "just-prepared" solution to determine the CMC in 10^{-3} M KCl. The solutions prepared for 1 day, 30 days and 74 days were used to determine the CMC in 10^{-4} M KCl. In two cases, the CMC values were both reproduced up to four significant figures. Figure B-2.1 is the one of the examples, differential conductivity versus SDS concentration in 10^{-4} M KCl. It is seen that the curves overlap in the transition region although they do not at the beginning. Therefore, a conclusion was drown that the age of SDS solution did not influence the determination of the critical concentration of SDS by conductometry.

1 R.H. Pelton, Course Notes for Chem. Eng. 704-I, McMaster University, Hamilton, Canada, 1989

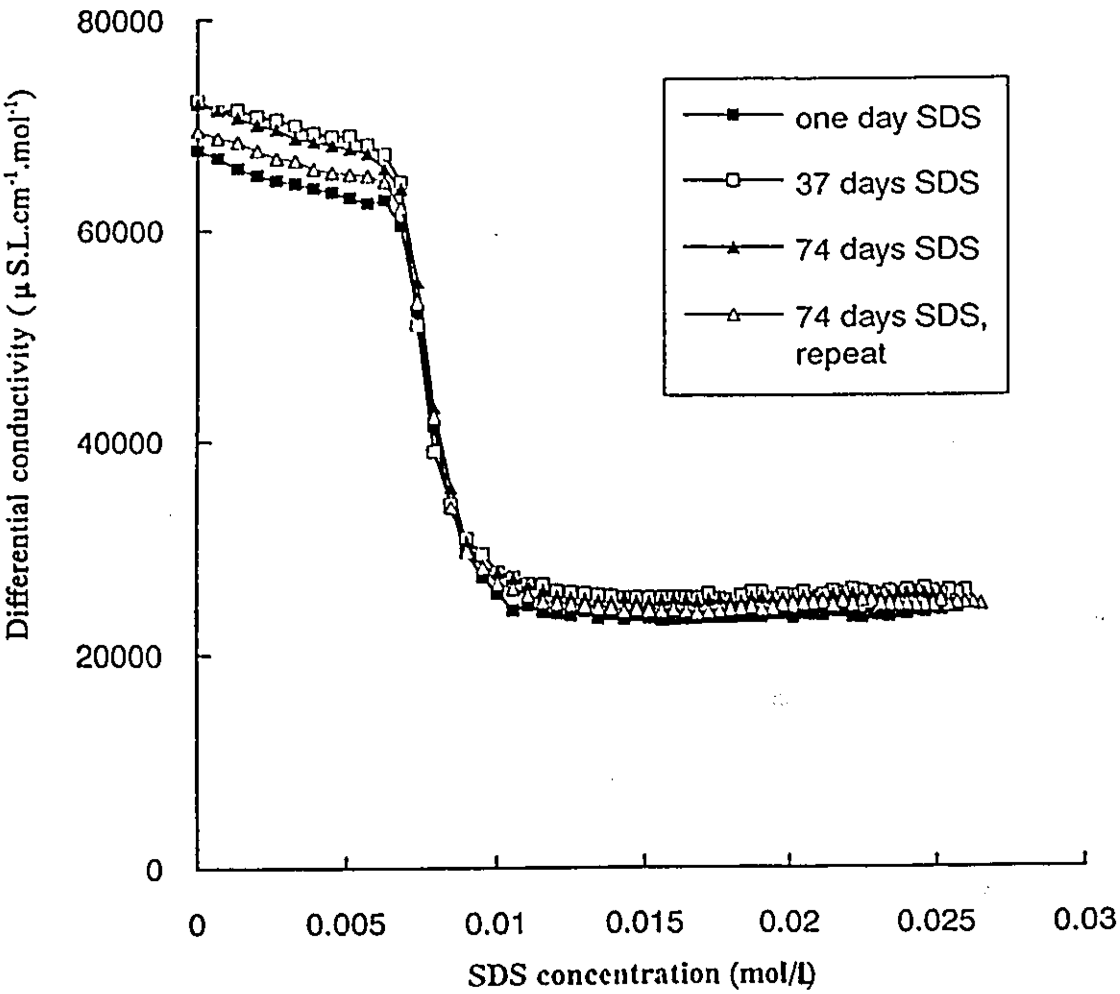

Figure B-2.1 Differential conductivity of 10^{-4} M KCl versus SDS concentration for SDS solutions of various age at 25 °C

APPENDIX B-3

Influence of Monomers on the CMC of SDS

To study the nucleation mechanism of poly(NIPAM/BAM) particles, the effects of monomers (NIPAM and BAM), in addition to the effect of polymer (see Part B Chapter 2) on the CMC of SDS, were investigated. A monomer solution was prepared at the same concentrations as that for polymerization: 1.54 g monomers (1.4 g NIPAM and 0.14 g BAM) in 100 ml 10^{-3} M KCl. A 2% SDS solution was added to the monomer solution by the method described in Part B Chapter 2. The conductivity of the solution versus SDS concentration at 25 and 70 °C is plotted in Figure B-3.1. In the presence of monomers, the titration curves were less sharp, and some deviation from the SDS-alone curves was observed. The CMC of SDS with monomer was slightly higher than that without monomers. These observations suggest that there is interaction between NIPAM, BAM and SDS. But this interaction would not reduce the CMC of SDS.

Figure B-3.1 Conductivity of 10^{-3} M KCl with and without monomers versus SDS concentration at 25 and 70 °C
(---) with 1.54 wt.% monomers; (——) without monomers

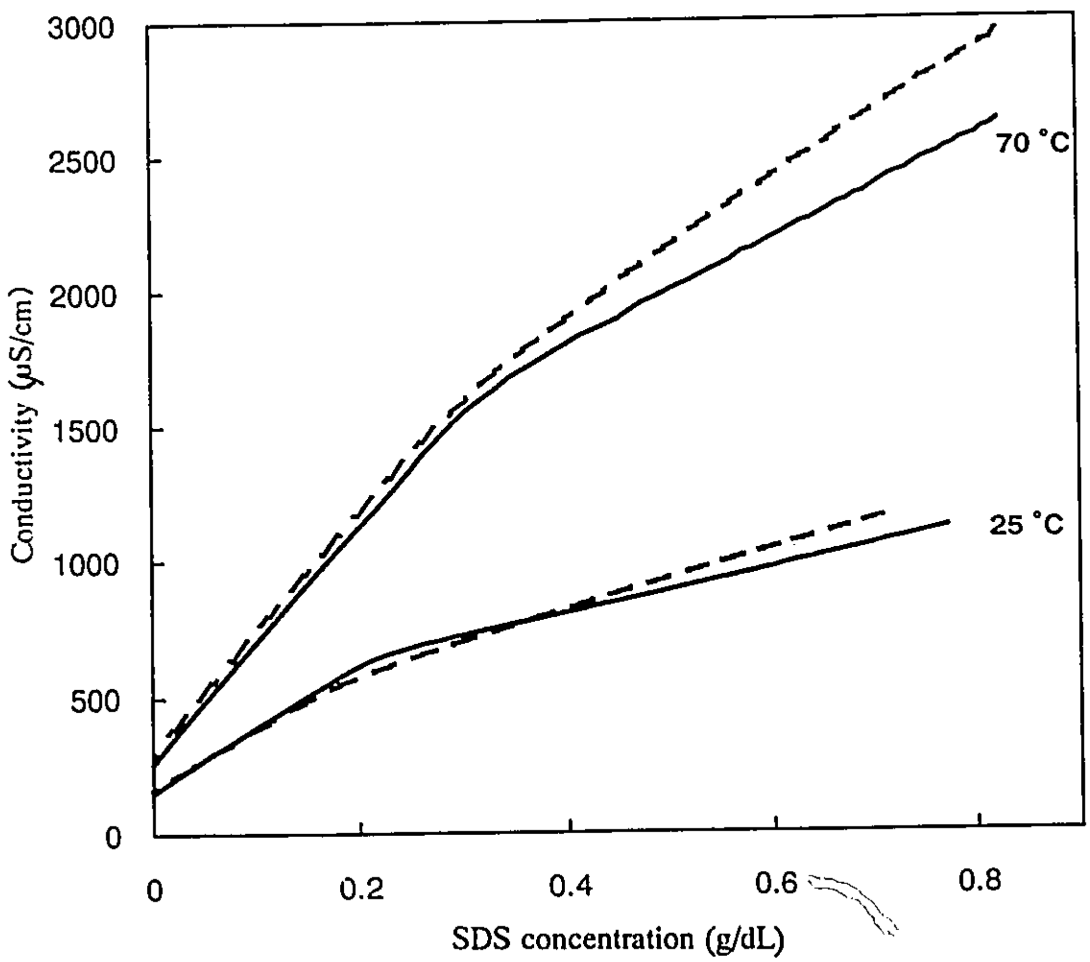

APPENDIX B-4

Preliminary Study on the Rheological Properties of Poly(NIPAM/BAM) Latex

The volume of poly(NIPAM/BAM) latex particles changes with temperature, which gives the latex interesting rheological properties. On the other hand, rheology can provide useful information about the thermal response of the particles, about the interaction among the particles or between the particles and solute (e.g., salt, surfactant), and about the stabilization mechanism of the particles.

In this preliminary study, the viscosity of poly(NIPAM/BAM) latex at temperature 25 - 45 °C was measured with a Bohlin Rheometer, at a shear rate 14.7 1/s, and a heating rate 0.1 °C / 12 s. The latex samples were 100% wet latex and 50% diluted wet latex (diluted with DDI water). The wet latex was obtained by ultracentrifuging the original latex LS6. Figure B-4.1 shows that the viscosity of 100% latex bed decreases with increase in temperature until ~ 35 °C (LCST of poly(NIPAM/BAM)), and then increases slightly. This increase may be caused by the coagulation of latex particles above the LCST because the coagulation was observed after the rheology experiment. Figure B-4.2 displays the viscosity change during a cycle of heating and cooling of 50% latex bed. In the first half of the cycle (heating process), the viscosity decreases with increase in temperature and suddenly drops at about 33 °C, and then remains constant. In the second half of the cycle (cooling process), the viscosity increases with decrease in temperature faster at the beginning, and then is almost constant in the range of about 38 - 32 °C, and finally increases again with temperature. Two curves have different shapes but cross at the point corresponding to the volume transition temperature (~ 33 °C).

The difference between the heating and cooling process may suggest relaxation of the latex particles upon cooling.

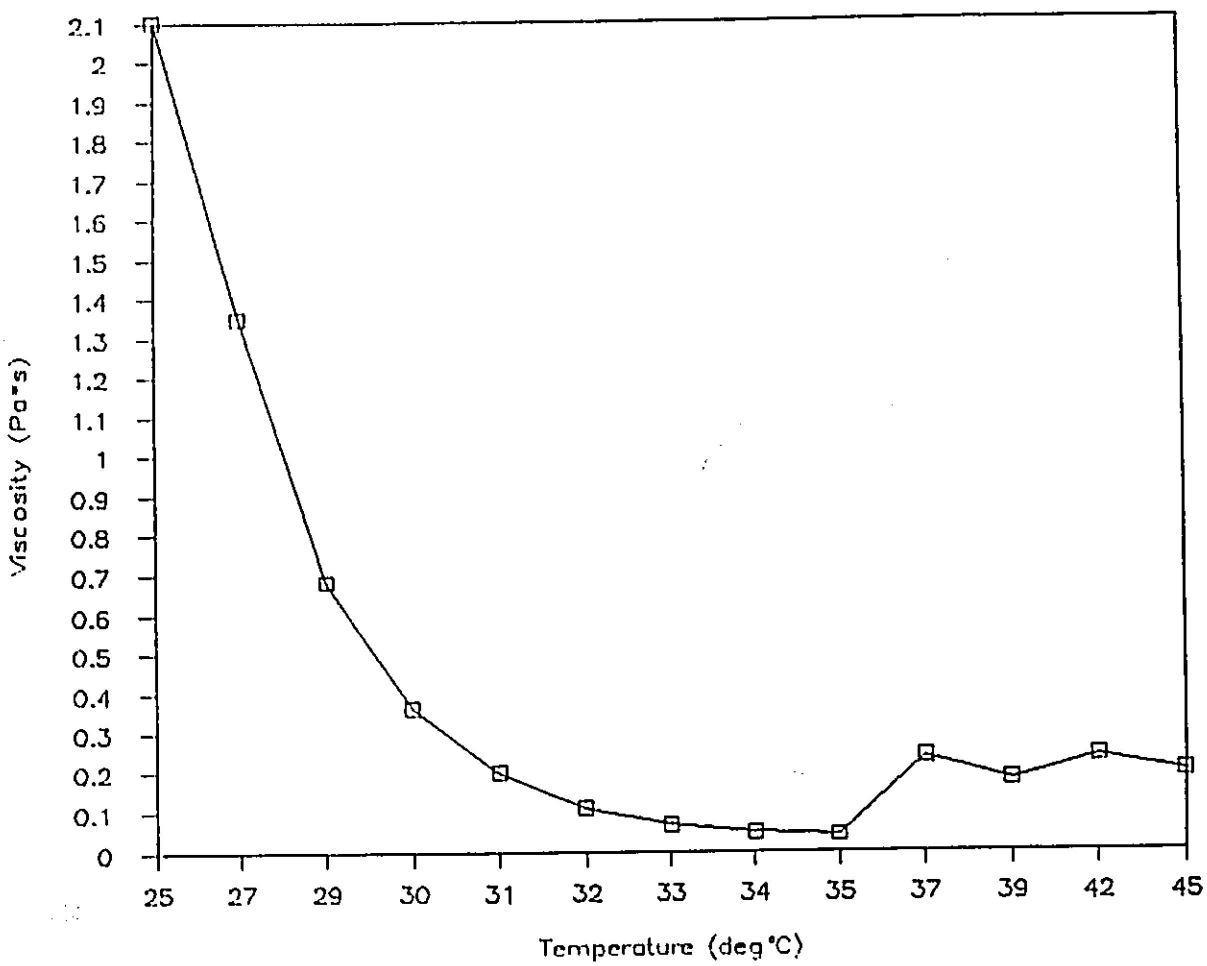

Figure B-4.1 Viscosity of 100% wet latex of LS6 versus temperature

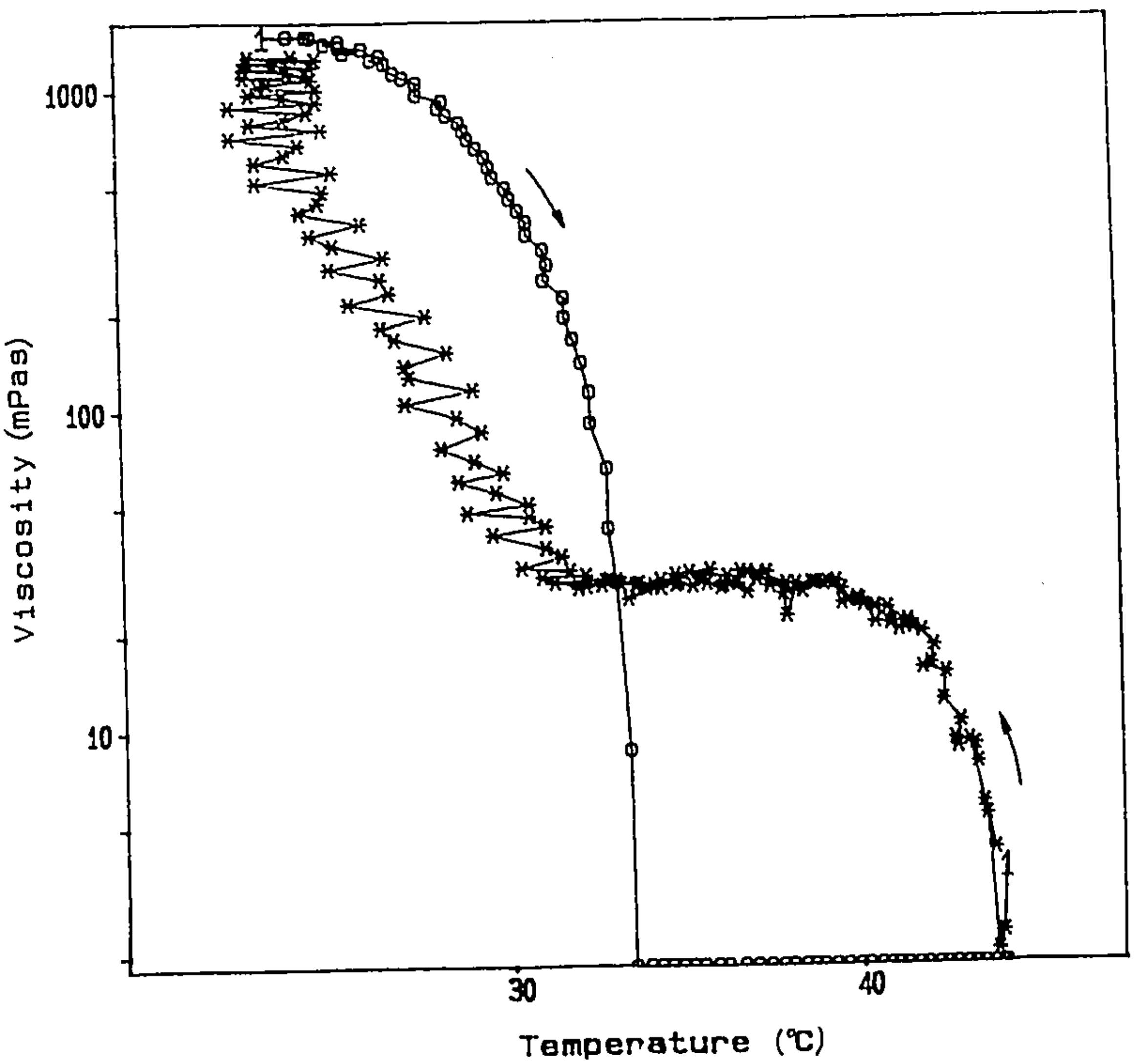

Figure B-4.2 Viscosity of 50% diluted wet latex of LS6 versus temperature

APPENDIX C

Software for Data Analysis in This Thesis

Both UWHAUS subroutine (Department of Chemical Engineering, McMaster University, Canada) and EXCEL FOR WINDOWS (Microsoft Company) were used for most of the data computations and parameter estimations. The parameters in Part A Chapter 2 were determined in 1988 - 1989 using UWHAUS. The parameters in Part A Chapter 3 and in Part B were evaluated using EXCEL ver. 3.0 in 1989 - 1991. In Part B Chapter 2, the regression of the conductivity titration curves and the calculation of the first and second derivatives of the conductivity were conducted using TURBLE PASCLE NUMERICAL TOOL BOX ver.

The scattering coefficient K in Eq.(4.8) of Part B Chapter 4 was calculated using a subroutine provided by Dr. Th. Kourti (Ph. D. Thesis, McMaster University, Canada, 1989).